THE UNIVERSITY OF QUEENSLAND

AUSTRALIA

The fate of atmospheric metal pollutants in the landscape, Snowy Mountains, south-eastern Australia

Nicola Stromsoe

Bachelor of Science (Hons)

A thesis submitted for the degree of Doctor of Philosophy at

The University of Queensland in 2015

School of Geography, Planning and Environmental Management

Abstract

Industrial metals, emitted to the atmosphere by human activity, have been transported and deposited to almost every location on Earth, including Antarctica and Greenland. This is demonstrated by an increasing body of literature in which many atmospheric industrial metals (e.g. Pb, Hg, Cd and Cu) have been shown to be significantly enriched in environmental archives. Studies have largely focussed on peat mires and ice cores, which receive high rates of atmospheric deposition relative to terrestrial inputs. By contrast, few studies have examined the extent of atmospherically derived metals across the wider landscape, where processes such as pedogenesis, erosion and sedimentation affect the spatial extent and magnitude of metal enrichment. In the Snowy Mountains, Australia, atmospheric pollutant metals have previously been identified in alpine peat mires, although their impact on the wider environment has not been assessed. Interest in the fate of atmospheric pollutants in the Snowy Mountains has increased due to the operation of a cloud seeding program in which, silver iodide, AgI, is released to the atmosphere, leading to concerns that silver, Ag, contamination may be accumulating in this ecologically important region. This thesis examines the spatial extent and magnitude of atmospherically derived metals in the Snowy Mountains by investigating patterns of enrichment in a range of geomorphic settings and catchment positions, including in soils, peat mires, lakes and reservoirs. The potential movement of metals through the landscape was also assessed by examining rates of geomorphic processes, including rates of pedogenesis and erosion, determined via radionuclides. The thesis was undertaken in three parts which are summarised below.

The long-term (from c.200 BCE to 2011 CE) history of surface contamination by atmospheric industrial metals in the Snowy Mountains was examined in the first part of this thesis. The chronology and magnitude of metal contamination was reconstructed using sediment cores extracted from an alpine tarn. Industrial metal enrichment in the lake was minimal throughout the industrial period (in Australia, c.1890 to present), e.g. enrichment factors were Ag: 1.3, Pb: 1.3, Zn: 1.1 and Cu: 1.2. This contrasts with previously demonstrated enrichment in a proximal peat mire of Ag: 2.2, Pb: 3.3, Zn: 2.1 and Cu: 4.1. The discrepancy between the peat and lake records was shown to be a function of substantial natural catchment-derived flux of lithogenic metals to the lake, i.e. approximately 92-97 % of total metal accumulation was catchment derived. This had the effect of diluting the significance of atmospheric pollution. The results of this chapter imply that the concentration of atmospheric metal contamination in surface sediments is heterogeneous across the

landscape and may be reduced where rates of sediment generation and transport are high relative to atmospheric flux.

The significance of atmospheric industrial metals across the wider environment was investigated in the second part of the thesis. The concentrations of metals in various surface environments were compared to metal enrichment in aerosols and their rates of deposition from the atmosphere. Results showed industrial metals, including Pb, Sb, Cr and Mo, were enriched in the atmosphere of the remote Snowy Mountains by 3.5 (Pb) – 48 (Sb) times natural concentrations. In surface sedimentary environments, industrial metals showed varying degrees of enrichment, depending on the relative significance of atmospheric input, the natural concentration of metals, catchment size and metal behaviour. In areas dominated by atmospheric deposition (ombrotrophic peat mires in the upper parts of catchments), the order and magnitude of metal enrichment most closely resembled that of collected aerosols, however, on average enrichment was 5-7 fold lower than in the aerosols. Metals most sensitive to enrichment, i.e., those with low natural abundance in local sediments (Cd, Ag, Sb, Mo), were enriched in all environments including the most geomorphically active settings (tarn lake sediments). In reservoirs, located lower in catchments, patterns of metal enrichment largely reflected concentrations in catchment soils but metals were additionally enriched or depleted depending on their relative particle reactivity. For those metals which are most sensitive to enrichment (Ag, Cd, Sb), the increase in excess flux required to reach trigger value concentrations is lowest in the reservoir sediments (Ag: 13-18, Cd: 7-10 and Sb: 17-61 times the current flux) and highest in the tarn lake (Ag: 60, Cd: 15, Sb: 27 times the current flux) and the peat mire (Ag: 74, Cd: 15, Sb: 18 times the current flux).

In part three of this thesis, rates of soil production and soil erosion were quantified using radiocarbon dating, fallout radionuclides and sediment yields in lakes and reservoirs in order to assess the stability of landscape metal stores. Although equivocal, the soil production rates determined in this study are (20-220 t/km^2/y) amongst the highest rates reported in Australia. They are, however, comparable to soil production rates reported from other alpine areas, worldwide, adding to the global dataset demonstrating rapid soil production rates in alpine areas where precipitation and vegetation productivity promote chemical weathering. Average erosion rates over the past 100 years, determined from $^{210}Pb_{ex}$ inventories, were 60 t/km^2/y with an estimated uncertainty range of 10-90 t/km^2/yr. Thus Snowy Mountain soil erosion rates are low, even in an Australian context. Low erosion and high soil production relative to the rest of Australia is explained by high vegetation cover and by the formation of organic

soils, which rapidly accumulate mass by comparison to other soil types. This suggests that metals deposited from the atmosphere are largely incorporated into the developing soil profile at the present time. This is supported by the maximum and minimum soil production rates which have exceeded comparative erosion rates over the mid-late Holocene. However, soil basal ages (2500 cal. y. BP) and historical accounts of rapid soil erosion following grazing by sheep and cattle imply that the landscape is subject to soil stripping and increased sediment transport if the protective vegetation cover is maintained. Thus anthropogenic or climatic disturbance may result in the transformation of hillslope soils from a net sink to a source of metal pollutants.

In summary, this study has demonstrated that a range of metals are enriched in the atmosphere and surface sediments of the remote-from-source Snowy Mountains by up to 48 (Sb) and 6.8 (Cd) times natural concentrations, respectively. This includes a range of potentially toxic metals, including Cr, Co, Ni, Cu, As, Mo, Ag, Cd, and Sb, for which there has, to date, been a relative lack of enrichment data. Thus, this research has provided further evidence that atmospheric metals contaminants are ubiquitous in the Earth's surface environment. The concentration of atmospherically derived metal contaminants in surface sediments was shown to vary across the landscape and between archive types. The incorporation of atmospheric metals into different parts of the environment was controlled by the relative rates of atmospheric deposition and terrigenous sediment inputs; the natural background concentrations of metals in local soils and sediments; catchment area, and; characteristics of individual metals, such as their relative particle reactivity. Assessing the spatial scale and magnitude of atmospherically derived contamination in surface environments requires that enrichment be understood at a landscape scale and within a geomorphic process context.

Declaration by author

This thesis *is composed of my original work, and contains* no material previously published or written by another person except where due reference has been made in the text. I have clearly stated the contribution by others to jointly-authored works that I have included in my thesis.

I have clearly stated the contribution of others to my thesis as a whole, including statistical assistance, survey design, data analysis, significant technical procedures, professional editorial advice, and any other original research work used or reported in my thesis. The content of my thesis is the result of work I have carried out since the commencement of my research higher degree candidature and does not include a substantial part of work that has been submitted *to qualify for the award of any* other degree or diploma in any university or other tertiary institution. I have clearly stated which parts of my thesis, if any, have been submitted to qualify for another award.

I acknowledge that an electronic copy of my thesis must be lodged with the University Library and, subject to the policy and procedures of The University of Queensland, the thesis be made available for research and study in accordance with the Copyright Act 1968 unless a period of embargo has been approved by the Dean of the Graduate School.

I acknowledge that copyright of all material contained in my thesis resides with the copyright holder(s) of that material. Where appropriate I have obtained copyright permission from the copyright holder to reproduce material in this thesis.

Publications during candidature

Peer-reviewed papers

Marx, S.K., Rashid, S., **Stromsoe, N.** 2015. The global extent of Pb contamination within the Earth's environment. *Environmental Pollution.* (submitted) (this paper does not form part of this thesis)

Stromsoe, N., Marx, S.K., Callow, N., McGowan, H.A., Heijnis, H., 2015. Late Holocene estimates of soil production and erosion in the Snowy Mountains, Australia. *Earth Surface Processes and Landforms.* (submitted)

Stromsoe, N., Marx, S.K., McGowan, H.A., Callow, N., Heijnis, H., Zawadzki, A., 2015. A landscape-scale approach to examining the fate of atmospherically derived industrial metals in the surficial environment. *Science of The Total Environment* 505, 962-980.

Stromsoe, N., Callow, J.N., McGowan, H.A., Marx, S.K., 2013. Attribution of sources to metal accumulation in an alpine tarn, the Snowy Mountains, Australia. *Environmental Pollution* 181, 133-143.

Conference presentations

Stromsoe, N., Marx, S.K., Callow, J.N., McGowan, H.A., 2014. *Landscape scale variability of atmospherically derived metal enrichment in surface environments*. American Geophysical Unions (AGU) Fall Meeting, 15-19 December 2014, San Francisco, USA.

Stromsoe, N., Callow, J.N., Marx, S.K., McGowan, H.A., 2014. *Holocene soil production and erosion in the Snowy Mountains*. Australian and New Zealand Geomorphology Group (ANZGG) 16th Conference, 30 November-3 December 2014, Mt Tambourine, Australia.

Stromsoe, N., Callow, J.N., McGowan, H.A., Marx, S.K., 2013. *Sediment sources, yield and connectivity in a low relief alpine environmetn, Snowy Moutnains, New South Wales, Australia*. 8th International Conference on Geomorphology (IAG), 27-31 August 2013, Paris, France

Stromsoe, N., McGowan, H.A., Callow, J.N., Marx, S.K., 2012. *Attribution of sources to metal contribution in an alpine tarn, Club Lake, Snowy Mountains, NSW, Australia.* Australian and New Zealand Geomorphology Group (ANZGG) 15th Conference, 2-7th December 2012, Bundanoon, Australia.

Publications included in this thesis

Publication 1: Included as Chapter 3.

Stromsoe, N., Callow, J.N., McGowan, H.A., Marx, S.K., 2013. Attribution of sources to metal accumulation in an alpine tarn, the Snowy Mountains, Australia. *Environmental Pollution* 181, 133-143.

Contributor	Statement of contribution
N. Stromsoe (Candidate)	Research design, implementation (80%) Data analysis (100%) Wrote the paper (90%)
J.N. Callow	Research design, implementation (10%) Edited the paper (40%)
H.A. McGowan	Research design, implementation (10%) Edited the paper (40%)
S.K. Marx	Advice on analysis of geochemical data Production and interpretation of previously published peat results Edited the paper (20%)

Publication 2: Included as Chapter 4.

Stromsoe, N., Marx, S.K., McGowan, H.A., Callow, N., Heijnis, H., Zawadzki, A., 2015. A landscape-scale approach to examining the fate of atmospherically derived industrial metals in the surficial environment. *Science of The Total Environment* 505, 962-980.

Contributor	Statement of contribution
N. Stromsoe (Candidate)	Research design, implementation (85%) Data analysis (90%) Wrote the paper (85%)
S.K. Marx	Research design and implementation (5%)

	Data analysis (10%) Wrote and edited paper (15%)
J.N. Callow	Research design, implementation (5%) Edited the paper (50%)
H.A. McGowan	Research design, implementation (5%) Edited the paper (50%)
H. Heijnis	Research design, interpretation of dating results, edited the paper
A. Zawadski	Research design, interpretation of dating results, edited the paper

Publication 3: Included as Chapter 5.

Stromsoe, N., Marx, S.K., Callow, N., McGowan, H.A., Heijnis, H., 2015. Estimates of Late Holocene soil production and erosion in the Snowy Mountains, Australia. *Catena.* (submitted)

Contributor	Statement of contribution
N. Stromsoe (Candidate)	Research design, implementation (85%) Data analysis (90%) Wrote the paper (90%)
S.K. Marx	Research design (5%) Data analysis (10%) Wrote and edited paper (10%)
J.N. Callow	Research design, implementation (5%) Edited the paper (50%)
H.A. McGowan	Research design (5%) Edited the paper (50%)

H. Heijnis	Research design, interpretation of dating results, edited the paper

Contributions by others to the thesis

Supervision team Nik Callow and Hamish McGowan made standard contributions to this thesis. This includes shared experimental design, revision and editing of this work. Sam Marx assisted with revision and editing of this work and made contributions to manuscripts as outlined above.

Statement of parts of the thesis submitted to qualify for the award of another degree

None

Acknowledgements

This research would not have been possible without the support of my supervisors Dr. Nik Callow and Professor Hamish McGowan. To Nik, my principle supervisor, thank you for your dedication and skill as a teacher over the last 7 years, for being perpetually good humoured and for editing drafts with impressive speed. I am grateful that your enthusiasm for geomorphology helped spark my interest all those years ago. To Hamish, thank you overseeing this project, your ability to see practicalities and your sense of humour in the field. Your high expectations have pushed me to always improve. I hope I have acquired at least some of your ability to read landscapes along the way. Also to Sam Marx, who helped me swim through a sea of trace element data and has been a hard-working and genuine collaborator. Thank you for geochemistry and generosity.

This project was funded by Snowy Hydro Ltd. I would like to thank the numerous staff who were unfailing professional in providing supplementary data, logistical and field work support, in particular, John Denholm, Loredana Warren, Karen Kemsley, Johanna Speirs, Andrew Peace, Shane Bilish, Lizzie Pope and the entire hydrography department.

The radionuclide analyses were funded by an Australian Institute of Nuclear Science and Engineering Post Graduate Research Award and Engineering Post Graduate Research Award (PGRA No. 10085). This grant provided access to facilities and allowed me to spend time at Environmental Radioactivity Measurement Centre (Australian Nuclear Science and Technology Organisation (ANSTO)) learning the principles and applications of nuclear techniques in environmental science. Thank you to my ANSTO supervisor Professor Henk Heijnis and to Atun Zawadzki for being generous and knowledgeable collaborators and for helping me to interpret radiochemical data. Thank you also to Patricia Gadd, Daniella Fierro and Jack Goralewski for teaching me the techniques of gamma and alpha spectrometry and ITRAX and for expert analysis of numerous soil and sediment samples.

Thanks also to Dr. Alan Greig at the University of Melbourne for providing expert ICP-MS analysis. To Dr. Adrian Chappell for providing advice, being so generous with time, and providing a valuable perspective on the complexities of using radionuclides as erosion tracers. I would also like to thank Colin de Pagter for piloting par-excellence, generously imparting his astounding knowledge of the Snowy Mountains and for assistance with sample collection. Thanks also to the Alan, Clwedd, Michael and the professional staff at GPEM

who are unfailingly considerate and always go out of their way to help. And to Josh, Michael and Alison, thank you for being such good office-mates.

And to Andrew, my family, and all my friends who have cooked for me and put up with me being distracted for 4 years. I could not have done it without you.

Keywords

metals, contamination, atmospheric, pollution, peat, lake, soil, geomorphology, sediment, holocene

Australian and New Zealand Standard Research Classifications (ANZSRC)

039901 Environmental Chemistry (incl. Atmospheric Chemistry (60%)

040601 Geomorphology and Regolith and Landscape Evolution (35%)

040202 Inorganic Geochemistry (5%)

Fields of Research (FoR) Classification

0399 Other Chemical Sciences (50%)

0406 Physical Geography and Environmental Geoscience (30%)

0502 Environmental Science and Management (20%)

Table of Contents

CHAPTER 1. INTRODUCTION 1

1.1 ATMOSPHERIC INDUSTRIAL METALS IN THE EARTH'S ENVIRONMENT 1

1.2 THE STATE OF KNOWLEDGE AND KEY KNOWLEDGE GAPS IN THE FATE OF ATMOSPHERIC INDUSTRIAL METALS 2

1.3 AIM AND OBJECTIVES 5

1.4 THESIS STRUCTURE 8

CHAPTER 2. ATMOSPHERIC METAL AND METALLOID CONTAMINATION IN SURFACE SEDIMENTS 10

2.1 SOURCES OF INDUSTRIAL METALS TO THE ENVIRONMENT 10

2.1.1 Atmospheric emission sources and volumes 10

2.1.2 Atmospheric transport of metal contaminants 12

2.3 IDENTIFYING ATMOSPHERIC INDUSTRIAL METALS IN THE ENVIRONMENT 14

2.3.1 Introduction 14

2.3.2 Importance of remote sites 14

2.3.3 Environmental archives 15

2.3.4 Enrichment factors 16

2.4 PEAT AND ICE RECORDS OF THE ATMOSPHERIC DEPOSITION 17

2.5 MOBILITY OF ATMOSPHERICALLY DERIVED METALS IN THE SURFICIAL ENVIRONMENT 20

2.6 LAKE SEDIMENTS AND SOILS AS ARCHIVES OF METAL CONTAMINANTS 22

2.6.1 Lake sediments 23

2.6.2 SOILS 24

2.7 REGIONAL SETTING 25

2.7.1 Metal production and metal contaminants in Australia 25

2.7.2 Existing research from the Snowy Mountains 27

2.7.3 Cloud seeding by AgI 29

2.7.4 Conceptual model of cloud seeding AgI fate 31

2.7.5 Summary 33

CHAPTER 3. ATTRIBUTION OF SOURCES TO METAL ACCUMULATION IN AN ALPINE TARN, SNOWY MOUNTAINS, SOUTH-EASTERN AUSTRALIA 37

ABSTRACT 37

3.1 INTRODUCTION 38

3.2 METHODS 40
3.2.1 Study site *40*
3.2.2 Core collection *40*
3.2.3 Core processing and sedimentological analysis *41*
3.2.4 Trace element analysis *42*
3.2.5 Dating *42*
3.3 RESULTS 43
3.3.1 Dating results and age model *43*
3.3.2 Sediment characteristics *45*
3.3.3 Anthropogenic trace metal enrichment *46*
3.4 DISCUSSION 57
3.4.1 Moderating processes which influence the relationship between atmospheric emissions and environmental concentrations in the Snowy Mountains *58*
3.5 CONCLUSION 64
CHAPTER 4. A LANDSCAPE-SCALE APPROACH TO EXAMINING THE FATE OF ATMOSPHERICALLY DERIVED INDUSTRIAL METALS IN THE SURFICIAL ENVIRONMENT 66
ABSTRACT 66
4.1. INTRODUCTION 67
4.2. PHYSICAL SETTING 68
4.3 ANTHROPOGENIC DISTURBANCE AND SOURCES OF METALS 70
4.4 METHODS 71
4.4.1 Conceptual approach and sampling *71*
4.4.2 Aerosol sampling *72*
4.4.3 Estimation of aerosol/metal deposition flux *75*
4.4.4 Peat and lake cores *77*
4.4.5 Soil samples *78*
4.4.6 Reservoir cores and sample processing *78*
4.4.7 Trace element analysis *79*
4.4.8 Dating of sediment cores *79*
4.5. RESULTS 80
4.5.1 Atmospheric aerosol concentrations and industrial metal enrichment *80*
4.5.2 Aerosol and industrial metal deposition *85*
4.5.3 Industrial metal accumulation in peats and lakes *87*
4.5.4 Industrial metals in soils *90*

4.5.5 Age structure of the reservoir cores *93*
4.5.6 Industrial metal accumulation in reservoirs *95*
4.6 Discussion 96
4.6.1 Metal enrichment in aerosols; contributing sources and comparisons *96*
4.6.2 The atmospheric contribution of industrial metals *97*
4.6.3 Metals concentrations in peat mires *98*
4.6.4 Industrial metals in Club Lake *100*
4.6.5 Industrial metals in soils *102*
4.6.6 Industrial metal enrichment in reservoirs *104*
4.6.7 Summary and implications *107*
Supplementary material 112
Estimation of aerosol/metal deposition flux *112*
Wet deposition *113*
Trace element analysis *114*

CHAPTER 5. ESTIMATES OF LATE HOLOCENE SOIL PRODUCTION AND EROSION IN THE SNOWY MOUNTAINS, AUSTRALIA 122

Abstract 122
5.1 Introduction 123
5.2. Regional setting 125
5.3. Methods 126
5.3.1 Study locations *126*
5.3.2 Measurement of soil development rates 127
5.3.3 Estimating hillslope erosion rates 129
5.3.4 Estimating sedimentation rates *131*
5.5 Results 132
5.5.1 Radiocarbon ages *132*
5.5.2 Hillslope erosion rates 134
5.5.2.1 Radionuclide reference inventories *134*
5.5.2.2 Hillslope radionuclide inventories *138*
5.5.2.3 Modelled erosion rates *138*
5.5.3 Sedimentation rates 141
5.6 Discussion 142

5.6.1 The age of alpine and subalpine soils in the Snowy Mountains and its implications for sediment production *142*
Maximum possible ages for the onset of soil development in the Snowy Mountains *144*
Evidence for late Holocene onset of soil development *147*
5.6.2 Soil production rates 149
5.6.3 Erosion rates 151
5.7. Soil development, erosion and sedimentation – Summary and implications 154
Implications of Chapter 5 for metal transport in the Snowy Mountains 156
CHAPTER 6. SYNTHESIS AND CONCLUSION 160
6.1 Introduction 160
6.2 Research findings 160
6.2.1 Objective 1 ..... *160*
6.1.2 Objective 2 ..... *162*
6.1.3 Objective 3 ..... *165*
6.3 Study significance 167
6.3.1 Introduction *167*
6.3.2 Discussion *168*
Metal enrichment in different landscape and geomorphic settings. *168*
Atmospheric metal enrichment and how changes are recorded in different archives. *169*
Metals other than Pb. *171*
Metal enrichment records from the Southern Hemisphere *172*
Other emerging themes from this work *173*
6.4 Priorities for future research 175
6.4 Summary 177
REFERENCES 179
APPENDIX 1. TRACE ELEMENT CONCENTRATION OF SAMPLES 215

List of Figures and Tables

Figures

CHAPTER 1. INTRODUCTION

Figure 1.1 Thesis structure..... 9

CHAPTER 2. ATMOSPHERIC METAL AND METALLOID CONTAMINATION IN SURFACE SEDIMENTS

Figure 2.1 Global Pb production between 1998 and 2011..... 12

Figure 2.2 Global Ag mine production between 1998 and 2011..... 12

Figure 2.3 Documented pollution transport pathways..... 12

Figure 2.4 Emissions to the atmosphere from anthropogenic sources..... 26

Figure 2.5 The Snowy Mountains, showing important emission sources and transporting winds..... 28

Figure 2.6 Australian silver production 1970-2012..... 30

Figure 2.7 Revised conceptual model of cloud seeding Ag fate..... 32

CHAPTER 3. ATTRIBUTION OF SOURCES TO METAL CONTAMINATION IN AN ALPINE TARN, SNOWY MOUNTAINS, SOUTH-EASTERN AUSTRALIA

Figure 3.1 Study site location a) location of Club Lake and Upper Snowy peat bog within the Snowy Mountains, Australia (inset) b) Club Lake and its catchment..... 41

Figure 3.2 Age model constructed for the CL3 core..... 44

Figure 3.3 CL3 core: Particle size D_{10}, D_{90}, % organic (LOI) matter and sedimentation rate..... 45

Figure 3.4 Metal age profiles for CL3..... 47

Figure 3.5 Metal enrichment profiles for CL3..... 54

Figure 3.6 Metal enrichment profile for CL3 and CL4..... 55

Figure 3.7 Metal enrichment profiles for USC..... 56

Figure 3.8 Ba/Lu vs Tm/Li mixing plot for sediments from Murray-Darling Basin (MDB) dust source areas and pre/post-industrial sediments in CL3 and the USC..... 59

Figure 3.9 Weathering index/Age profiles for CL3..... 61

Figure 3.10 Lake levels for Club Lake March 2010 to November 2011..... 62

CHAPTER 4. A LANDSCAPE-SCALE APPROACH TO EXAMINING THE FATE OF ATMOSPHERICALLY DERIVED METALS IN THE SURFICIAL ENVIRONMENT

Figure 4.1 Locations of sampling sites in the Snowy Mountains..... 70

Figure 4.2 Surface sampling sites..... 72

Figure 4.3 The average trace element composition of aerosols collected during this study normalised against MUQ (MUd from Queensland Kamber et al., 2005)..... 81

Figure 4.4 Antimony (Sb) enrichment (*EF*) and excess metal ($Metal_{ex}$) concentrations in peat mires (USC and DCC panel A) and Club Lake (panel B)..... 83

Figure 4.5 A) Mean enrichment factors (*EF*) for industrial metals in Snowy Mountains aerosols between 2012/2013. B) Mean excess industrial metal ($Metal_{ex}$) concentrations in the same aerosols…… 84

Figure 4.6 Time series of Cr, Pb and Sb enrichment (*EF*) in Snowy Mountains aerosols (September 2012-October 2013)…… 84

Figure 4.7 Time series of excess ($Metal_{ex}$) Cr, Pb and Sb concentrations in Snowy Mountains aerosols (September 2012-October 2013)…….. 85

Figure 4.8 Industrial metal enrichment (*EF*) in peat mires post-1980 plotted beside aerosol enrichment (2012/2013) for comparison..... 88

Figure 4.9 Industrial metal enrichment (*EF*) in Club Lake post-1980 plotted beside aerosol enrichment (2012/2013) for comparison..... 90

Figure 4.10 Industrial metal patterns in Snowy Mountains soils…… 92

Figure 4.11 Unsupported ^{210}Pb activity profiles in cores collected from A) Geehi and B) Guthega reservoirs..... 93

Figure 4.12 Lead (Pb) and Cu enrichment (*EF*); in A) Geehi and B) Guthega reservoirs cores…. 94

Figure 4.13 Industrial metal enrichment (*EF*) in reservoirs (Geehi and Guthega) plotted alongside aerosol enrichment (2012/2013) for comparison. …… 96

Figure 4.14 Industrial metal mass flux and metal enrichment (*EF*) patterns in the Snowy Mountains; shown for Pb (top panel), Cu (middle panel) and Sb (lower panel)…….. 109

CHAPTER 5. ESTIMATES OF LATE HOLOCENE SOIL PRODUCTION AND EROSION IN THE SNOWY MOUNTAINS, AUSTRALIA

Figure 5.1 Location of soil and sediment sampling sites…… 127

Figure 5.2 Radiocarbon soil ages vs depth for soil pits at Guthega Hill A) ridge-crest, B) mid-slope pit, C) toe slope..... 133

Figure 5 .3 Vertical distribution of ^{137}Cs and $^{210}Pb_{xs}$ in Snowy Mountains soil. Plots show mean activity of 3 cores from Guthega reference site…… 135

Figure 5.4 Radionuclide inventories for reference and hillslope at Guthega A) ^{137}Cs B) $^{210}Pb_{ex}$ and Cootapatamba C) ^{137}Cs and D) $^{210}Pb_{ex}$…….. 139

Figure 5.5 Soil production and erosion rates estimated by various methods from this study and by previous studies undertaken during the era of grazing induced erosion..... 153

Tables

CHAPTER 2. ATMOSPHERIC METAL AND METALLOID CONTAMINATION IN SURFACE SEDIMENTS

Table 2.1 Annual flux of seldom studied metals to the atmosphere (natural and anthropogenic)..... 20

CHAPTER 3. ATTRIBUTION OF SOURCES TO METAL CONTAMINATION IN AN ALPINE TARN, SNOWY MOUNTAINS, SOUTH-EASTERN AUSTRALIA

Table 3.1 ^{14}C and ^{210}Pb dates..... 44

Table 3.2 Trace element data for rock standards (based on long-term analyses at University of Melbourne)..... 48

Table 3.3 Trace element data for soil standards (based on long-term analyses at University of Melbourne)..... 52

CHAPTER 4. A LANDSCAPE-SCALE APPROACH TO EXAMINING THE FATE OF ATMOSPHERICALLY DERIVED METALS IN THE SURFICIAL ENVIRONMENT

Table 4.1. Sample details..... 74

Table 4.2. Average atmospheric industrial metal atmospheric concentrations for selected studies 82

Table 4.3. Estimated total and excess metal flux from the atmosphere..... 86

Table 4.4 Relative sensitivity of industrial elements to enrichment..... 102

Table 4.5. Industrial metal enrichment in Geehi and Guthega reservoirs relative to topsoil concentrations..... 106

Table 4.6. Sensitivity of archives to enrichment (increase in industrial flux required to produce sediment concentrations equal to trigger values)..... 111

CHAPTER 4 SUPPLEMENTARY MATERIAL

Supplementary Table 4.1. Parameter values for cloud water deposition..... 116

Supplementary Table 4.2. ^{210}Pb activities and CIC ages for reservoir..... 117

Supplementary Table 3.Trace element data of standards (μg g^{-1})..... 118

CHAPTER 5 ESTIMATES OF LATE HOLOCENE SOIL PRODUCTION AND EROSION IN THE SNOWY MOUNTAINS, AUSTRALIA

Table 5.1 Model parameters describing radioactivity depth distribution..... 131

Table 5.2. Radiocarbon ages for hillslope soils..... 134

Table 5.3. Descriptive statistics for radionuclide inventories at Guthega and Cootapatamba..... 136

Table 5.4. Statistical tests for differences in distribution, mean and median between reference and hillslope radionuclide inventories for ^{137}Cs and $^{210}Pb_{ex}$..... 140

IMPLICATIONS OF CHAPTER 5 FOR METAL TRANSPORT IN THE SNOWY MOUNTAINS

Table 5.6 Mobilisation rate via hillslope erosion for metals enriched in Snowy Mountains soils..... 159

Supplementary Table 1. Trace element concentrations of samples..... 215

Chapter 1. Introduction

1.1 Atmospheric industrial metals in the Earth's environment

This thesis presents an investigation of the fate of atmospherically derived metals, including Ag used for cloud seeding, in the surface environment of the remote-from-source alpine setting, Snowy Mountains, south-eastern Australia.

Beginning in prehistoric times, human activities have modified the flux of metals to the extent that anthropogenic metals can now be considered ubiquitous in the Earth's environment (Bindler, 2011; Murozumi et al., 1969; Shotyk, 1996a). Patterson et al. (1965) demonstrated the scale of their impact when they showed in the 1960s that blood Pb concentrations in the United States of America had reached approximately 100 times natural levels. Industrial activities, such as metal production and fossil fuel combustion, release large volumes of metals to the global atmosphere, accounting for between 10 and 150% of all emissions for metals including Cu, Zn, Cr, Ni, Pb and Ag (Nriagu and Pacyna, 1988; Rauch and Pacyna, 2009).

Metals emitted to the atmosphere may be transported thousands of kilometres from their sources in urban and industrial centres before being deposited to terrestrial and aquatic environments (Brännvall et al., 1999; Burn-Nunes et al., 2011; Erel et al., 2007; Hong et al., 1996; Marx et al., 2008; Osterberg et al., 2008; Outridge et al., 2005; Settle and Patterson, 1982). As a result, contamination of the atmosphere by anthropogenic metals has been documented in almost every setting in which studies have been undertaken including the Arctic (Boutron et al., 1991; Hong et al., 1994; Hong et al., 1996; McConnell, 2002; Osterberg et al., 2008; Rosman et al., 1994; Wolff and Peel, 1988), Antarctica (Dick, 1991; McConnell et al., 2014; Murozumi et al., 1969; Toscano et al., 2005; Vallelonga et al., 2002; Wolff et al., 1999) and the remote oceans (Arimoto et al., 1989; Arimoto et al., 1987a; Duce et al., 1975; Shen and Boyle, 1987; Witt et al., 2006).

The history and scale of atmospheric metal contamination is often studied using environmental archives which preserve a temporal record of atmospheric deposition. Within the wider landscape, these studies have typically selected archives which most directly reflect the state of the atmosphere, such as ice cores and peat mires (Lee and Tallis, 1973; Murozumi et al., 1969). Less well understood are the differences between archive types and the factors

that control metal transport and the relative potential for metal accumulation or concentration across the landscape. This presents a significant challenge in understanding the magnitude and variability of atmospheric metal pollutants in the surface environment. This understanding is important because metal pollutants have been shown to have deleterious effects on human health and ecosystems, even at relatively low concentrations present in locations remote from emission sources (Nriagu, 1990; Van Oostdam et al., 2005). Our understanding of metal pollutants in the surface environment is further limited in areas that lack previous studies or for elements other than Hg or Pb, which have been most commonly investigated.

1.2 The state of knowledge and key knowledge gaps in the fate of atmospheric industrial metals

Although the onset of metal contamination in the Earth's environment can be traced into prehistory (e.g. Brännvall et al., 1999; Klaminder et al., 2003; Lee et al., 2008; Martínez-Cortizas et al., 1997a; Mighall et al., 2009; Monna et al., 2004; Pompeani et al., 2013; Renberg et al., 2000; Shotyk et al., 1998), active monitoring of metal contamination extends back only a few decades (Pacyna and Pacyna, 2001). Much of our knowledge of the magnitude of anthropogenic metal fluxes is therefore derived from records of metal contamination in stable environmental archives (e.g. ice cores, peat mires and lake sediments). These archives incorporate atmospherically deposited metals in sequentially accumulating layers and thus preserve a temporal record of atmospheric deposition. This approach also has the advantage of allowing metal contamination to be quantified relative to natural background concentrations by analysing the composition of the pre-contamination (older) section of the archive (e.g. Lee and Tallis, 1973; Murozumi et al., 1969; Shirahata et al., 1980; Shotyk, 1996b).

As they seek to understand the changing rate of atmospheric metal deposition, studies have primarily focussed on archives which: 1) receive high rates of atmospheric deposition relative to terrestrial inputs, and; 2) in which metals are efficiently retained. This typically includes peat mires and ice (e.g. Glooschenko et al., 1986; Hong et al., 1994; Le Roux et al., 2004; Lee and Tallis, 1973; Livett et al., 1979; Martínez-Cortizas et al., 1997a; Murozumi et al., 1969; Renberg et al., 2002; Shotyk et al., 1996; Vallelonga et al., 2002; Weiss et al., 1997).

An increasing body of literature has demonstrated that archives of this type can be used to identify subtle changes in the source, transport and deposition of metals (e.g. Brännvall et al.,

1999; Hong et al., 1994; Le Roux et al., 2005; Lee et al., 2011; Martínez-Cortizas et al., 1997a; Marx et al., 2010; McConnell et al., 2014; Mighall et al., 2009; Osterberg et al., 2008; Shotyk et al., 1996; Shotyk et al., 2001; Uglietti et al., 2015; Vallelonga et al., 2002; Weiss et al., 1997; Zheng et al., 2007). Records of metal pollutants in environmental archives have the advantage over mass balance style approaches in that they; 1) provide potentially continuous long-term temporal records, and; 2) allow anthropogenic changes to be quantified relative to the full range of natural variability. Accordingly, they have been instrumental in highlighting the scale of metal contamination in the Earth's environment (e.g. Murozumi et al., 1969). In addition, although Pb contamination can be identified based on changes in Pb isotopic composition, this is not possible for many other pollutant metals where either the isotopic variability is less well understood, measurement is more complex, or isotope ratios are not amenable to fingerprinting sources. For these metals, the concentration/inventory change within environmental archives remains the best method for quantifying the magnitude of metal contamination.

Measuring enrichment in archives where metal flux is dominated by atmospheric deposition allows the rate of deposition and atmospheric metal load to be quantified. At a landscape scale, however, the distribution and abundance of anthropogenic metals in the terrestrial environment is known to be moderated by post-depositional processes which can remobilise metals originally derived from the atmosphere or cause metals to become more concentrated or diluted within surface sediments (Bacardit et al., 2012; Balogh et al., 2000; Brännvall et al., 2001b; Foster and Charlesworth, 1996; Klaminder et al., 2006b; Kober et al., 1999; Landre et al., 2010; Lidman et al., 2014; Lindberg and Turner, 1988; Salomons and Förstner, 1984a; Salomons and Förstner, 1984b; Starr et al., 2003; Steinnes and Friedland, 2006; Sutherland, 2000; Swain et al., 1992; Watmough and Dillon, 2007; Yang and Rose, 2005; Young, 2013). These processes are important because they control the degree to which atmospheric metals are incorporated into the environment and therefore determine their ecological impact (Kabata-Pendias and Mukherjee, 2007).

Thus, the concentration of anthropogenic metals in singular archives (e.g. peat and ice or atmospherically dominated lake sediment records) does not necessarily provide an indication of their impact and variability across the wider landscape. In addition, records derived from proximal archives reflecting different landscape processes (e.g. peat mires and lakes) are not often directly compared (exceptions include Bindler et al., 1999; Brännvall et al., 2001c; Klaminder et al., 2010; Koinig et al., 2003; Liu et al., 2012; Norton and Kahl, 1987; Shotyk

and Krachler, 2010; Yang et al., 2007). As a result, the degree to which atmospherically dominated archives represent concentrations in different landscape settings is not well understood. The focus on atmospherically dominated archives, therefore, means that the concentration and variability of atmospheric metals across the wider environment remains a key knowledge gap.

To date, archive investigations have primarily focussed on Pb (e.g. Murozumi et al., 1969) and Hg (e.g. Boutron et al., 1998). For other metals, the extent and magnitude of enrichment relative to natural background concentrations is less well understood. There is, however, growing evidence that a range of metals are present in the Earth's environment at concentrations sufficient to deleteriously affect human health and ecosystems (Dietz et al., 2000; Nriagu, 1990; Van Oostdam et al., 2005). In the context of continuing increases in global metal emissions (Pacyna and Pacyna, 2001) and growing concern over the consequences of chronic low-level exposure (Martinez-Zamudio and Ha, 2011; Satarug et al., 2010), further investigation into the concentrations and variability of these metal contaminants in the environment is warranted.

In addition, our understanding of metal contamination in the surface environment is limited by a relative scarcity of records for large areas of the Earth's surface. While there is a concentration of metal enrichment records within Europe and to a lesser extent North America (see Hong et al., 1994; Le Roux et al., 2004; Lee and Tallis, 1973; Livett et al., 1979; Martínez-Cortizas et al., 1997b; McConnell et al., 2002; Mighall et al., 2009; Monna et al., 2004; Murozumi et al., 1969; Norton and Kahl, 1987; Shotyk et al., 1998; Shotyk et al., 2005b; Weiss et al., 1997; Yang et al., 2002; Zheng et al., 2007), elsewhere the chronology and scale of metal enrichment is less well understood and relies on only a few studies. This is particularly so in the Southern Hemisphere where the few existing studies are largely confined to South America and Antarctica (Cooke et al., 2007; De Vleeschouwer et al., 2014; Marx et al., 2010; McConnell et al., 2014; Vallelonga et al., 2002).

In Australia, only one previous study has comprehensively documented the impact of human activity on the regional environment by examining long-travelled metals in a remote-from-source setting, a study by Marx et al. (2010) in the Snowy Mountains Australia (Marx et al., 2010). That study investigated metal enrichment in ombrogenous alpine peat mires, demonstrating that atmospheric metal contamination of the Snowy Mountains dated to the onset of industrialisation in south-eastern Australia (Marx et al., 2010). It calculated that industrial metals are presently being deposited to the Snowy Mountains at approximately five

times natural rates (Marx et al., 2010). However, the study did not explore the fate of atmospheric metals across the wider landscape.

The scale of the atmospheric metal contamination in Australia and the Snowy Mountains is of interest because:

- In Australia, the volume of metal production and emissions to the atmosphere is has increased in recent years (Marx et al., 2010). This contrasts with the situation in parts of Europe and North America where the rise of post-industrial economies and the introduction of cleaner production methods has decreased emissions over recent decades (e.g. Pacyna et al., 2009).
- Since 2004, a cloud seeding program which releases Ag in the form of AgI (and from 2004-2011 In in the form of In_2O_3) to the atmosphere has operated within the Snowy Mountains, representing an independent source of metals to the environment, in addition to emissions from regional industrial sources.

In summary, there exist a series of key knowledge gaps in the understanding of atmospheric metal contaminants in the Earth's environment. These gaps can be summarised as:

1) A limited understanding of variability in atmospherically derived metal enrichment in different parts of the landscape that are affected by different geomorphic processes.
2) A correspondingly limited understanding of where atmospheric metal enrichment occurs in landscapes and how changes in atmospheric deposition are recorded in different environmental archives.
3) A historic focus on the environmental enrichment of Hg and Pb, with correspondingly limited understanding of the accumulation of other potentially deleterious metals in the landscape.
4) A paucity of metal enrichment records from the Southern Hemisphere and from Australia in particular.

These key gaps in understanding have been used to formulate the following research objective of this thesis.

1.3 Aim and objectives

The main aim of this thesis is to quantify the contribution of atmospherically derived industrial metals to the surface environment of a remote-from-source setting, the Snowy

Mountains, south-eastern Australia and to assess the magnitude of atmospheric metal contamination in different parts of the landscape. The specific objectives of this thesis are:

Objective 1: Construct a temporal record of metal enrichment in tarn lake sediments, in order to place previous metal contamination records constructed in the Snowy Mountains in a wider landscape context. Assess the response of lake sediment metal concentrations to changing atmospheric metal deposition. Identify the processes that control the timing, magnitude and pattern of metal enrichment in the tarn.

The outcomes of this objective are presented in Chapter 3 of this thesis. This objective as achieved by analysing the trace element contents of a dated sediment core extracted from a tarn lake located within a short distance of the peat mire record of Marx et al. (2010), in the Snowy Mountains, south-eastern Australia. This existing record demonstrated that metal contaminants are enriched in peat mires by approximately five times pre-industrial levels (Marx et al., 2014b). In the current study, the chronology and magnitude of metal enrichment in the tarn was compared to the peat mire record in order to investigate the variability of metal enrichment across the landscape and to assess the differences in how atmospheric metal contamination is recorded in different archives. Trace element signatures were used to identify the respective sources of metals to the peat mire and to the tarn lake and to investigate factors controlling metal accumulation and enrichment in tarn sediments. The temporal pattern of Ag enrichment and accumulation was examined to determine whether the release of AgI during cloud seeding had resulted in a detectable increase in Ag within the tarn sediments.

A second aim of Chapter 3 is to improve the limited understanding of how atmospheric metal contamination varies across the landscape and how changes in atmospheric deposition are manifest in different archives. This will be achieved by a direct comparison between proximal lake and peat record and through identifying the factors which control relative metal enrichment and accumulation in the peat mire and lake sediment. A third aim of Chapter 3 is to fill the gap in records for Australia and more generally for the Southern Hemisphere by producing a high resolution lake sediment record for the Snowy Mountains. A fourth and final aim of this chapter is to improve the, to date, limited understanding of environmental contamination by metals other than Pb and Hg by providing new enrichment data for additional metals including Cu, Zn and Ag.

Objective 2: Examine the response of a variety of different surface archives to increased atmospheric metal deposition in a remote-from-source setting. Assess how the magnitude of contamination varies across the landscape. Identify the factors which control metal enrichment in different parts of the landscape.

The outcomes of this objective are presented in Chapter 4 of this thesis. This objective was achieved by quantifying metal concentrations, enrichment and accumulation in a range of key identified receptors in the Snowy Mountains to investigate the variability of atmospheric metal contamination at the landscape scale, examine how changes in atmospheric deposition are recorded in different archives and to identify factors controlling enrichment in different parts of the landscape. Aerosols were also sampled using a network of high-volume samplers. Aerosol samples were analysed for trace elements to quantify the enrichment of industrial metals in the atmosphere and to provide a snapshot estimate of atmospheric metal deposition to the Snowy Mountains.

This aim of this chapter is to contribute to improving the understanding of how atmospheric metal contamination varies across the landscape and how different archives respond to changes in atmospheric metal deposition. A second aim is to identify factors controlling the variability of metal enrichment across the landscape. This chapter also aims to contribute to filling the gap in records for Australia by building on the previous peat mires record of Marx et al. (2010) and the tarn lake record of Stromsoe et al. (2013) by producing additional temporal records of metal enrichment in reservoir sediments from the Snowy Mountains. A third aim is to quantify the impact of industrial activity within south-eastern Australia on *metal* concentrations in Snowy Mountains soils and, in doing so, improve the understanding of contamination by metals other than Pb and Hg by quantifying concentrations for a suite of metals measurable by the multi-trace element method of Eggins et al. (1997) and Kamber (2009). This included metals and metalloids associated with agriculture, coal combustion and metal production i.e., Cr, Co, Ni, Cu, Sn, As, Mo, Ag, Cd, In, Sn, Cs, Tl, Pb, Th and U.

Objective 3: Quantify soil production and soil erosion rates to assess landscape stability in the Snowy Mountains over recent timescales (millennia to decades), with the aim of understanding soil erosion as a key surficial process that may influence the transport or accumulation of metals in the landscape.

The outcomes of this objective are presented in Chapter 5 of this thesis. This objective was achieved by quantifying soil production and erosion rates using radiocarbon analysis,

geomorphic evidence, fallout radionuclides as well as published records of paleoclimate impacts and historical accounts of erosion events. Landscape stability was assessed by examining the balance between soil production and erosion under anthropogenic and climatic forcing conditions. This provided a qualitative assessment of the stability of landscape metal stores under a range of boundary conditions. A quantitative, time integrated estimate of the quantity of atmospheric metal mobilised from hillslopes by the process of soil erosion was produced from the calculated soil erosion rates and soil excess metal concentrations.

The aim of this chapter aim is to improve the understanding how atmospheric metal contaminants accumulate in the environment by assessing the function and stability of primary metal stores and by quantifying the rate at which metals are translocated through the environment by soil erosion and transport.

1.4 Thesis structure

This thesis is comprised of series of published papers (Chapter 3 and 4) or manuscripts in review (Chapter 5). These Chapters are preceded by a literature review and background chapter (Chapter 2) and followed by a synthesis and summary of the key research outcomes of the thesis (Chapter 6).

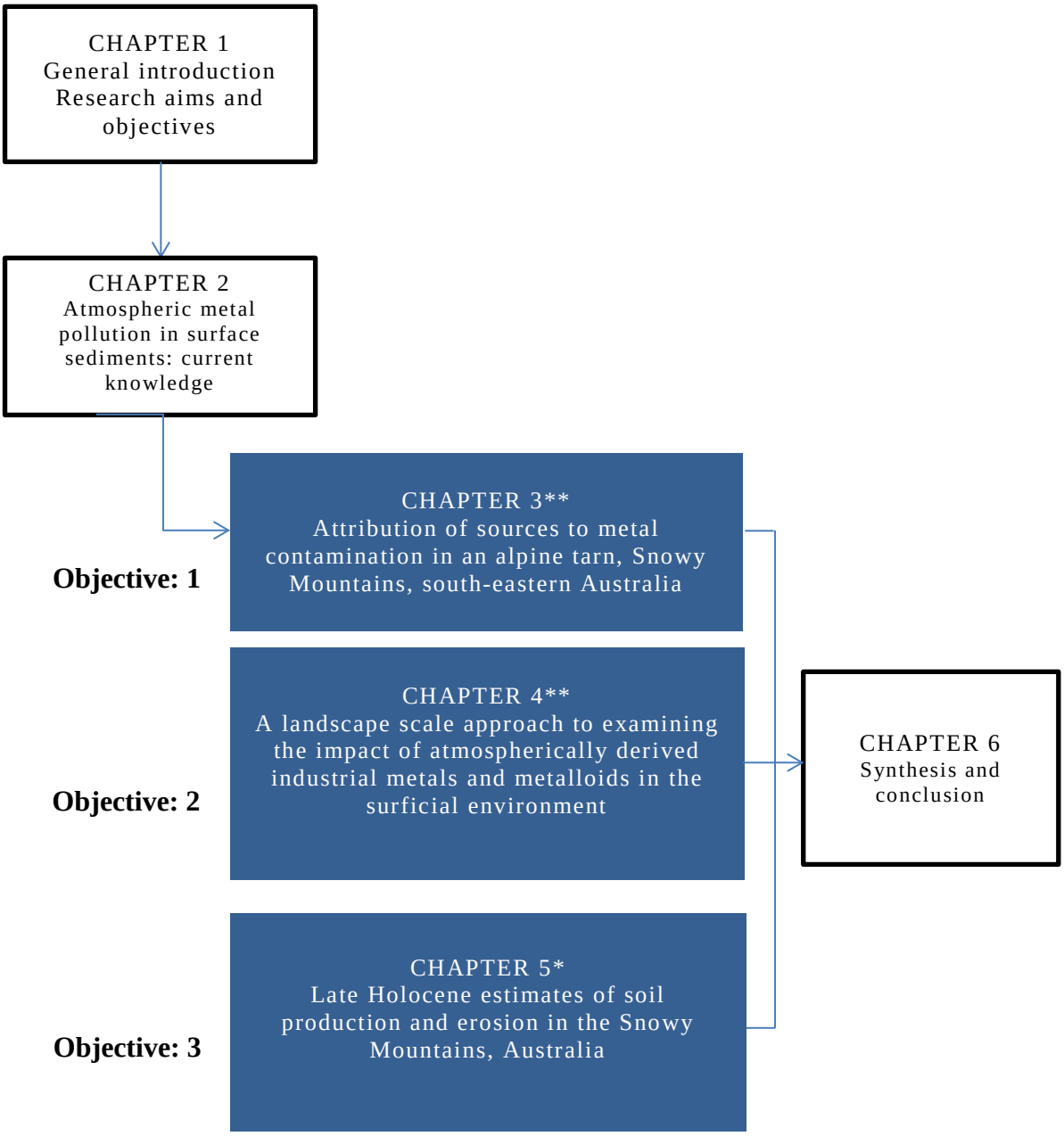

Figure 1.1 Thesis structure ** published papers, * submitted manuscript

Chapter 2. Atmospheric metal and metalloid contamination in surface sediments

This chapter provides a summary of existing knowledge on metal contamination to form a background and framework for the study objectives, approach and design. It identifies the sources of industrial metals to the atmosphere, reviews the methods by which anthropogenic metals are identified, the extent and magnitude of contamination in surface sediments, and the current state of knowledge regarding the processes controlling the transport and accumulation of metals across the wider landscape (following deposition from the atmosphere). Finally, the study setting and research approach taken by this thesis are outlined.

2.1 Sources of industrial metals to the environment

2.1.1 Atmospheric emission sources and volumes

Metals are emitted to the atmosphere primarily from mining, metal production and stationary fossil fuel combustion (Nriagu and Pacyna, 1988). Other sources include agriculture (fertilizer and pesticide application), cement production, waste incineration and transport (Nriagu and Pacyna, 1988). While fossil fuel combustion, including by mobile petroleum sources, is the most important source of emissions to the atmosphere for Pb, emissions from metal production are the primary sources for Ag, Cr, Cu, Ni, and Zn (Rauch and Pacyna, 2009). In addition, the recycling of metals between environmental compartments, e.g. from previously contaminated soils to the atmosphere has been shown to be important for some metals (e.g. Pb (e.g. Pb; Erel et al., 2007)).

The scale of metal use by humans results in very large quantities of metals being released to the environment each year. In 2000 CE, global mine production for the most highly exploited trace metals totalled 13.2 x 10^6 t for Cu, 8 x 10^6 t for Zn, 13.7 x 10^6 t for Cr, and 1.2 x 10^6 t for Ni (USGS, 2015). Rauch and Pacyna (2009) assessed global emissions for the same year and calculated atmospheric emissions from production, fabrication and fossil fuel combustion to be 42 000 t for Cu, 91 000 t for Zn, 15 500 for Cr, 116 000 t for Pb and 31 000 for Ni. The latest global emissions data for Ag dates from 1997. In that year total global silver production totalled 16 400 t (USGS, 2001), with emissions to the atmosphere estimated at 400 t (Rauch and Pacyna, 2009).

Thus, metal use by humans has resulted in a transformation of the flow of metals through the environment. By collating industry data on production and emission volumes, Rauch and Pacyna (2009) estimated that anthropogenic emissions to the global atmosphere in 2000 CE reached approximately 150 % of the natural flux for Pb, 50% for Cu and Ni, 30% for Zn, 15% for Ag and 10% for Cr (Rauch and Pacyna, 2009). Studies using peat bog archives have demonstrated that Pb deposition rates in parts of the Northern Hemisphere are currently 50-200 times natural the natural background (Le Roux et al., 2005) and reached more than 1000 times natural rates at the height of 20th century (c. 1970s) (Klaminder et al., 2003; Shotyk et al., 1998).

In Europe and North America, metal emissions including Pb, Cd, As, Cu and Zn have decreased over the last 40 years (Harmens et al., 2007; McConnell and Edwards, 2008). This has been attributed to the decline in industrial activity in Europe and North America, and to the introduction of emission controls standards and cleaner production measures in response to concerns over the likely health impacts of metal pollution (McConnell and Edwards, 2008; Pacyna and Pacyna, 2001). The observed decline, however, has not been globally consistent. For example, rapid growth in the rate of coal combustion and metal production combined with less stringent environmental controls in Asia are considered to explain increasing Pb concentrations in the atmosphere of the North Pacific (Osterberg et al., 2008). Examined globally, metal production has continued to increase from the late 1990s through to present. Global production of secondary refined Pb, for example, increased from 2.87 x 10^6 t in 1998 to 5.27 x 10^6 t in 2011 (USGS, 2015) (Fig. 2.1). With regard to Ag, world mine production increased from 17 100 tonnes in 1998 to 23 200 tonnes in 2011 (USGS, 2015) (Fig. 2.2). In many parts of the world anthropogenic metal contamination, therefore, poses an increasing threat to ecosystems and to human health.

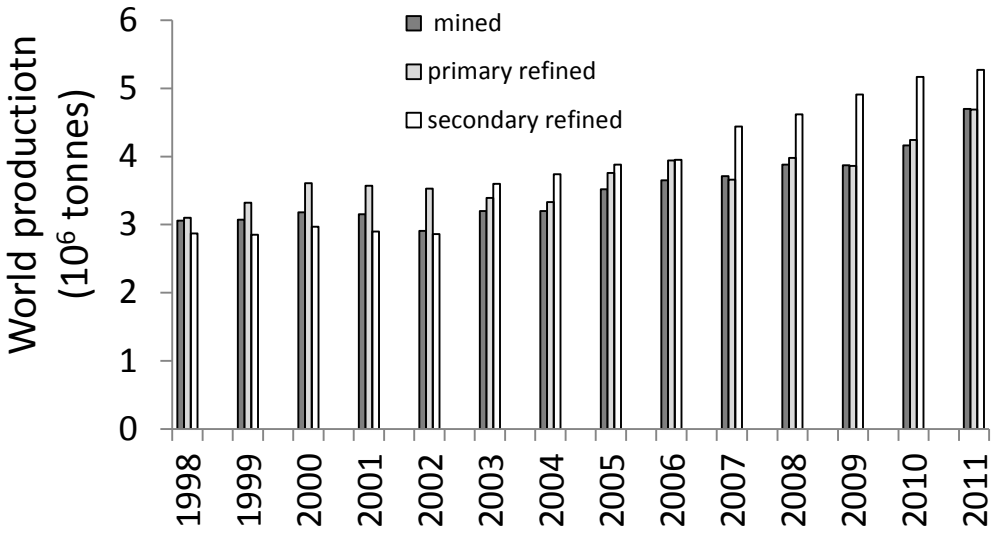

Figure 2.1 Global Pb production between 1998 and 2011 (data source USGS, 2015)

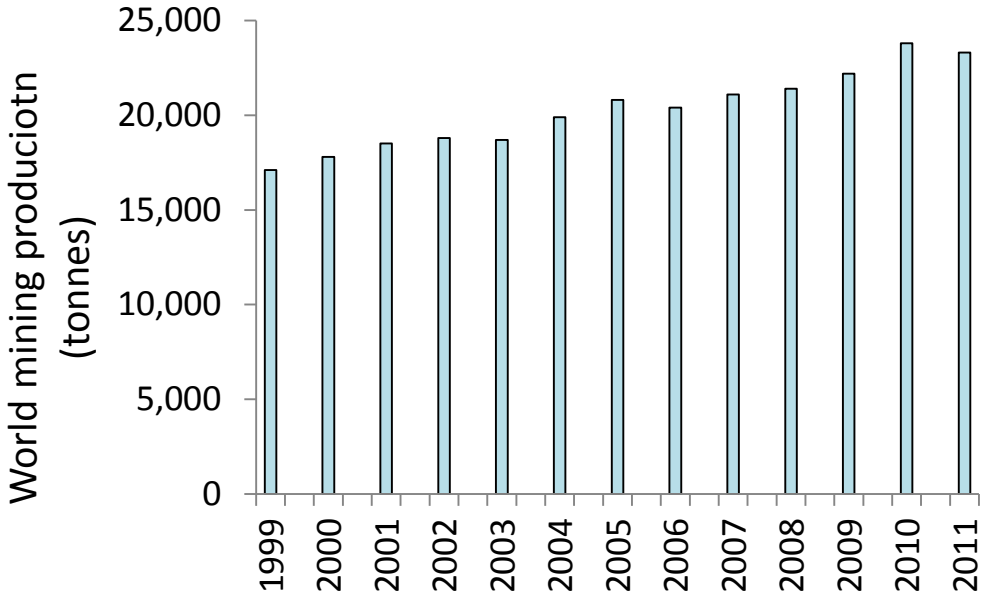

Figure 2.2 Global Ag mine production between 1998 and 2011 (data source USGS, 2015)

2.1.2 Atmospheric transport of metal contaminants

With the exception of Hg, toxic metals in the atmosphere are found primarily in the particulate phase. Combustion sources produce large volumes of fine particles which are resistant to fallout under gravitational settling. This is particularly so for particles in the accumulation mode (0.05 – 2 μm) (Mason, 2013). Consequently, the characteristic residence time of industrial metals in the atmosphere ranges from 1-2 months, during which they may be transported thousands of kilometres from their source (Marx et al., 2008; Mason, 2013).

Equally, mineral dust can scavenge gas phase species and fine metal particulates to serve as a vector for metal transport (Marx et al., 2008). Known transport corridors for atmospheric contaminants include from northern and central Europe to the Arctic Circle; Europe to the Middle East; Asia to the remote central and north Pacific; North America to the Arctic Circle, the Atlantic and Pacific Oceans and from Australia to New Zealand and Antarctica (Arimoto et al., 1989; Brännvall et al., 1999; Burn-Nunes et al., 2011; Erel et al., 2007; Hamelin et al., 1997; Hong et al., 1996; Marx et al., 2008; McConnell et al., 2002; McConnell et al., 2014; Osterberg et al., 2008; Planchon et al., 2003; Settle and Patterson, 1982; Vallelonga et al., 2002; Witt et al., 2006) (Fig. 2.3).

Eventually, these contaminants are transferred from the atmosphere to terrestrial and aquatic environments, either by wet or dry deposition, with wet deposition becoming dominant with increasing distance from the site of emission (Mason, 2013). As a result, anthropogenic metals have been detected in almost every setting where studies have been undertaken including remote locations such as Antarctica (Dick, 1991; McConnell et al., 2014; Murozumi et al., 1969; Planchon et al., 2003; Vallelonga et al., 2002; Wolff and Suttie, 1994) and Greenland (Candelone et al., 1995; Hong et al., 1996; McConnell and Edwards, 2008; Murozumi et al., 1969; Osterberg et al., 2008; Rosman et al., 1994; Shotyk et al., 2005b).

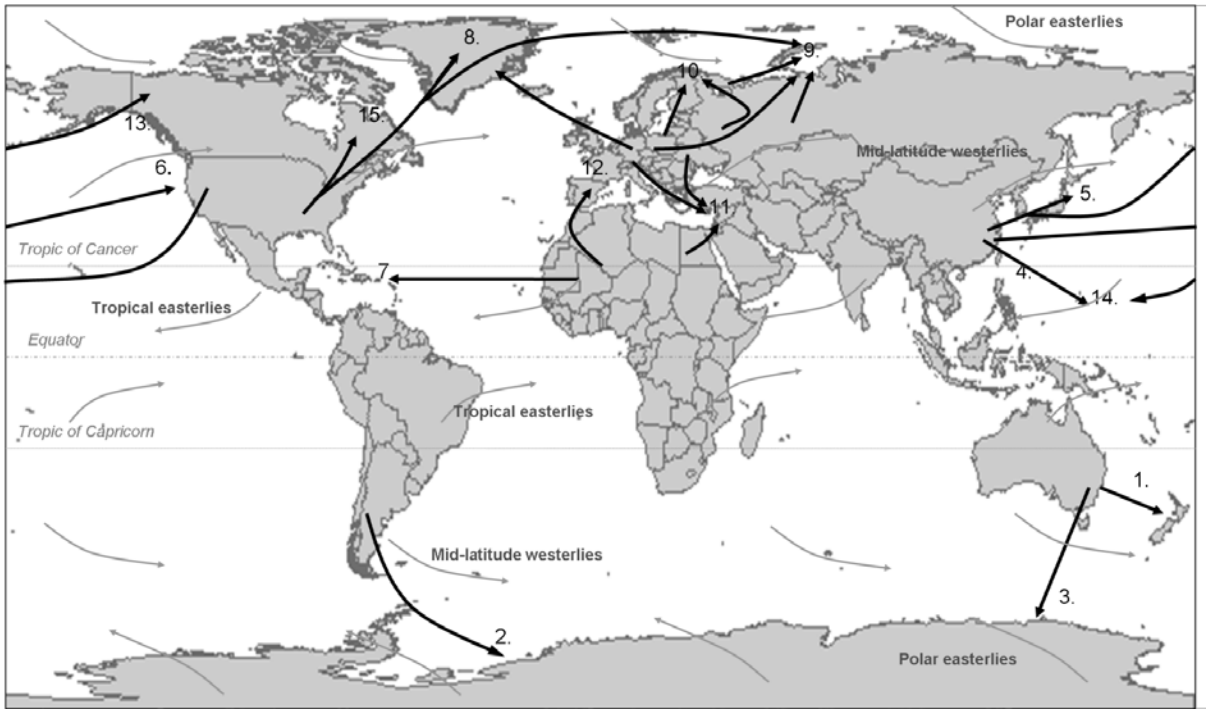

Figure 2.3 Documented pollution transport pathways (Marx and McGowan, 2011).

2.3 Identifying atmospheric industrial metals in the environment

2.3.1 Introduction

Estimating the volume of metals emitted to the atmosphere from anthropogenic sources is difficult. Frequently, emission volumes are not directly measured (Nriagu and Pacyna, 1988). Estimation methods (e.g. the use of emission factors) are, in addition, prone to inaccuracy and require large amounts of information (e.g. production volumes, production technology, metal content of raw material, emission controls) which are frequently not readily available (Nriagu and Pacyna, 1988). Moreover, the scale of contamination at any location also depends on mode of emission and changing intensity of transport pathways (e.g. Murozumi et al., 1969), necessitating the direct measurement of pollutant levels in the environment.

2.3.2 Importance of remote sites

To understand the regional to global scale impact of industrial metals in the environment it is necessary to reduce the influence of local contaminant sources which may overwhelm more long distance contamination. For this reason, studies of regional, continental or hemispheric background contamination are generally undertaken in remote locations distant from direct contaminant sources, often in alpine or polar sites (Barbante et al., 2004; Biester et al., 2002; Camarero et al., 2009; De Vleeschouwer et al., 2014; Hong et al., 2004a; Klaminder et al., 2003; Martínez Cortizas et al., 2012; Marx et al., 2010; Shotyk, 1996a; Thevenon et al., 2011). The Arctic has served to characterise contamination from Europe and North America, for example, (Boutron et al., 1991; Candelone et al., 1995; Hermanson, 1991; Klaminder et al., 2010; Liu et al., 2012; Murozumi et al., 1969; Outridge et al., 2002), while studies of contaminants sourced from Australia and other Southern Hemisphere sources have been undertaken on the Antarctic continent (Burn-Nunes et al., 2011; Dick, 1991; McConnell et al., 2014; Planchon et al., 2003; Toscano et al., 2005; Vallelonga et al., 2002; Wolff and Suttie, 1994). To date, the only studies of long distance contamination undertaken within Australia have been carried out in the Snowy Mountains (Marx et al., 2010), which are several hundred kilometres from the nearest major industrial or urban centres (including the cities of Adelaide (~900 km) and Melbourne (~400 km)) and in the Victorian Alps (Smith and Hamilton, 1992), approximately 130 km from the city of Melbourne.

2.3.3 Environmental archives

Atmospheric metals can be sampled in real time using deposition traps or active samplers, such as high volume samplers or cascade impactors (Arimoto et al., 1987a; Arimoto et al., 1990; Barrie and Barrie, 1990; Bridges et al., 2002; Dick, 1991; Duce et al., 1975; Erel et al., 2007; Marx et al., 2014a; Miller and Friedland, 1994; Witt et al., 2006). Active monitoring, however, dates back at most only a few decades. The history of environmental metal contamination, in contrast, has been demonstrated to extend into pre-history (e.g. Brännvall et al., 1999; Klaminder et al., 2003; Lee et al., 2008; Martínez-Cortizas et al., 1997a; Mighall et al., 2009; Monna et al., 2004; Pompeani et al., 2013; Renberg et al., 2000; Shotyk et al., 1998). In this context, environmental archives such as ice, peat and lake sediment, which accumulate and preserve deposited metals can serve to reconstruct the history of metal contamination. This is achieved through radiometric dating and geochemical analysis of layers successively deposited to the archive. The use of environmental archives dates back to the pioneering work of Patterson and others in the 1960'swho demonstrated that Pb transported to the Greenland icecap had reached 4 times natural levels by 2800 yrs BP (Chow and Patterson, 1962; Murozumi et al., 1969).

The utility of peat mires as long term archives of atmospheric deposition was first demonstrated by Lee and Tallis (1973) and Livett (1979) who showed that the distribution of Pb in peat profiles from British peat mires reflected national production trends over approximately 700-800 years. Ombrogenous peat mires may provide some of highest fidelity records of long term atmospheric contamination because they are fed entirely from the atmosphere and because metals are efficiently retained with the peat with minimal (in the case of more intensively researched Pb at least) post depositional mobility (Shotyk, 1996b).

In Europe, in particular, an increasing body of literature has demonstrated the coherence of peat and ice records in recording temporal trends in Pb concentration. Enrichment and accumulation of Pb within peat profiles have been shown to coincide with known events such as Roman mining and smelting and the Industrial Revolution (e.g. Brännvall et al., 1997; Cloy et al., 2008; Hong et al., 1994; Klaminder et al., 2003; Kylander et al., 2009; Le Roux et al., 2004; Martínez Cortizas et al., 2002a; Renberg et al., 2002; Rosman et al., 1994; Shotyk et al., 1996; Shotyk et al., 2005a; Weiss et al., 1997; Zheng et al., 2007). While less numerous and spatially comprehensive by comparison to Europe, peat and ice studies are also providing increasing information on the chronology and magnitude of metal contamination in Asia (e.g. Lee et al., 2011) and in the Southern hemisphere, including in Australia, South America and

Antarctica (e.g. Biester et al., 2002; De Vleeschouwer et al., 2014; Hong et al., 2004a; Marx et al., 2010; Planchon et al., 2003; Uglietti et al., 2015; Vallelonga et al., 2002).

2.3.4 Enrichment factors

At remote sites, the abundance of anthropogenic metals may be orders of magnitude lower than in more polluted areas (Boyle et al., 2015). Consequently examining concentrations alone is not usually sufficient to distinguish anthropogenic contamination from naturally occurring metals. In the case of Pb, the extent of anthropogenic contamination can be identified against natural background sources by the analysis of isotope ratios which can be used to distinguish Pb derived from various individual ore bodies from Pb produced by weathering of country rock (Chow et al., 1975; Shirahata et al., 1980). For other contaminants, including Zn, Cu and Cd, identifying a definitely anthropogenic isotopic signature has, to date, been less successful (e.g. Chrastný et al., 2015; Fekiacova et al., 2015).

Therefore, to quantify the magnitude of the contamination relative to natural levels, raw concentrations are commonly normalised both to the representative background concentrations of the element of interest and to a conservative reference element which controls for variability of sediment properties such as particle size and organic concentration (Abrahim and Parker, 2008; Duce et al., 1975; Kemp and Thomas, 1976; Pompeani et al., 2013; Schütz and Rahn, 1982; Shotyk, 1996a; Zoller et al., 1974). This double normalisation method produces a ratio describing the magnitude of anthropogenic pollution termed the Enrichment Factor (EF) (Duce et al., 1975; Shotyk, 1996b; Sinex and Helz, 1981; Zoller et al., 1974).

Background concentrations for pollutant elements can be difficult to identify given the long history of human metal use and the global extent of metal contamination, which means that completely uncontaminated sites are essentially non-existent (Shotyk, 1996b). In addition, normalisation to mean values in Upper Continental Crust (UCC) (e.g. Wedepohl, 1995) may fail to account for the natural spatial variability of bedrock compositions so that local enrichment is either over or underestimated (Abrahim and Parker, 2008). Therefore, background concentrations are often determined by analysing the elemental composition of local sediments which pre-date the emission of metals to the environment by human activity (Abrahim and Parker, 2008; Blaser et al., 2000; Pompeani et al., 2013). In the Northern Hemisphere the very long history of human metal use mean that sediments younger than c. 5000 years will most likely contain some anthropogenically derived component (Shotyk,

1996b). In Australia, by contrast, coal combustion and metal production did not occur until mid to late 19th Century, following the colonisation of the continent by the English in 1788 CE. Australia's first mine opened at Glen Osmond in South Australia in 1841 CE (Mudd, 2007). Marx et al. (2010) analysed Pb isotopes and industrial metal/conservative element ratios in peat cores dating to approximately 6500 y. cal. BP and found no evidence of metal enrichment prior to c. 1850 CE.

2.4 Peat and ice records of the atmospheric deposition

As metals emitted by past human activities are retained within the environment, understanding the timing and magnitude of past emissions is essential for understanding the magnitude of contamination in the present. Already from the earliest sedimentary reconstructions, it was apparent that the contamination of the environment by humans extended back at least several thousand years (Murozumi et al., 1969) and, since then, an increasing number of peat, lake and ice core reconstructions have provided evidence of metal contamination extending into prehistory (e.g. Brännvall et al., 1999; Klaminder et al., 2003; Lee et al., 2008; Martínez-Cortizas et al., 1997a; Mighall et al., 2009; Monna et al., 2004; Pompeani et al., 2013; Renberg et al., 2000; Shotyk et al., 1998). This section provides an overview of the evidence on the spatial scale, magnitude and temporal pattern of global metal contamination. The majority of studies have examined Pb contamination due to its known effects on human health (Patterson, 1965), long history of industrial use and the availability of historical production records (Nriagu, 1983; Settle and Patterson, 1980), the ability to provenance Pb sources based on its isotopic signature (Chow et al., 1975) and the immobility of Pb in environmental archives (Shotyk, 1996a).

The first significant emissions of anthropogenic metals to the environment occurred as a by-product early copper smelting (Bindler, 2011). Evidence of associated contamination is found as early as 8000 yrs BP in the sediments of Lake Manganese and Copper Falls Lake on Michigan's Keweenaw Peninsula (Pompeani et al., 2013). These reconstructions provide the first record of environmental contamination by humans and document the atmospheric emission and deposition of Pb from the annealing of copper for tool production by Old Copper Complex societies of the Great Lakes region (Pompeani et al., 2013). The chronology of environmental metal contamination is, in general, best constrained within Europe, due to the number of reconstructions which have been produced for this region. Environmental metal contamination from as early the as Bronze Age, 2500-4000 years BP is well documented by peat and lake archives in Sweden (Brännvall et al., 1999; Klaminder et al.,

2003; Renberg et al., 2000), Spain (Martínez-Cortizas et al., 1997a), Britain (Le Roux et al., 2004; Mighall et al., 2009), France (Monna et al., 2004) and Switzerland (Weiss et al., 1997). While some early records reflect localised impacts (Le Roux et al., 2004; Mighall et al., 2009), others provide evidence of long range transport from early Cu and Pb mining centres in Britain, Germany and the Mediterranean (Brännvall et al., 1999; Klaminder et al., 2003; Renberg et al., 2000; Weiss et al., 1997; Zheng et al., 2007).

The expansion of the Roman Empire and the opening up of Pb mines, particularly in the areas which are now Spain, Germany and Britain has been detected in a number of peat and ice reconstructions as a peak in Pb enrichment at c.2000 years BP (Brännvall et al., 1999; Klaminder et al., 2003; Le Roux et al., 2004; Renberg et al., 2000; Zheng et al., 2007). This is followed by declining Pb enrichment which tracks the fall of the Roman Empire (Brännvall et al., 1999; Klaminder et al., 2003; Le Roux et al., 2004; Renberg et al., 2000; Zheng et al., 2007) and a rise after c.1000 CE following the discovery of major silver deposits in Germany and the economic, population and social expansion of the Late Middle Ages (Brännvall et al., 1999; Klaminder et al., 2003; Renberg et al., 2000; Zheng et al., 2007). Therefore, in Europe at least, contamination of the environment by anthropogenic metal emissions significantly preceded the Industrial Revolution.

In Europe and North America, further rapid increases in metal emissions to the environment followed the introduction of industrial methods of mining and manufacturing from c.1750 CE (the Industrial Revolution) and subsequent technological innovations which occurred in the following years (Settle and Patterson, 1980). The impact of the Industrial Revolution is recorded in rapidly increasing Pb enrichment beginning from c. 1750 to c. 1880 CE in ice and peat cores from various locations in Europe and in Canada and Greenland (Brännvall et al., 1999; Cloy et al., 2008; Hong et al., 1994; Kylander et al., 2009; Le Roux et al., 2004; Martínez-Cortizas et al., 1997a; Pratte et al., 2013; Renberg et al., 2000; Shotyk et al., 1998). Enrichment of Pb in European and North American archives peaked in the late mid-late 20th century (centred around 1950-1970), after which contamination declined in association with the phase-out of leaded petrol and the introduction of more effective emissions controls (Brännvall et al., 1999; Cloy et al., 2008; Kylander et al., 2009; Martínez-Cortizas et al., 1997a; Renberg et al., 2000; Shotyk et al., 1998).

Outside of Europe, fewer records exist to constrain the timing and magnitude of anthropogenic metal contamination. However, pre-industrial enrichment associated with early metallurgy is recorded for North (Pompeani et al., 2013) and South America (Barbante et al.,

2004; Cooke et al., 2007; De Vleeschouwer et al., 2014; Ferrari et al., 2001; Hong et al., 2004a) and East Asia (Lee et al., 2008). In Southern Hemisphere studies (Australia and South America) the major increase in Pb enrichment by industrial emissions did not occur until after 1850-1890 CE (De Vleeschouwer et al., 2014; Marx et al., 2010; Vallelonga et al., 2002), reflecting the later adoption of large-scale industrial manufacturing and mining following the stabilisation of post-independence economies in South America and European colonisation in Australia. In Australia and Asia anthropogenic Pb enrichment in remote-from-source, atmospherically dominated archives does not show the post-1970s CE decrease apparent for North America and Europe, but continues to increase towards the present (Lee et al., 2011; Marx et al., 2010; Osterberg et al., 2008).

The magnitude of contamination is asymmetrical between Europe and the rest of the globe. Currently, the evidence from peat, lake and ice records indicates that Pb is being deposited to western Europe at 100 x the pre-anthropogenic rate (Bindler, 2011). In Sweden, the Pb burden from all emissions to present stands at 2-5 g/m^2 in the south and 1 g/m^2 in the more remote north (Bindler, 2011). For the Southern Hemisphere, enrichment is less well constrained but is presently lower due to lower volume of industrial emissions. Antarctic ice cores imply that the current rate of Pb deposition to Antarctic ice is approximately double the pre-industrial rate (McConnell et al., 2014). Since the onset of Pb and Ag mining and smelting in Australia 130 years ago, approximately 660 t (0.05 mg/m^2) has been deposited to the Antarctic continent (McConnell et al., 2014).

It is noteworthy that academic interest in environmental metal enrichment has focussed primarily on Pb and Hg (e.g. Hong et al., 1994; McConnell et al., 2014; Rosman et al., 1994). This is despite potentially toxic metals such as Cd, Sb, As, Zn and Cr being emitted to the atmosphere in quantities which equal or exceed natural fluxes (Table 2.1). It is clear that, like Pb, these metals are now present in the surface environment at concentrations which exceed natural concentrations, even in remote locations. Enrichment of atmospheric As and Sb extending back to Roman times has been documented in Swiss peat bogs (Shotyk, 1996a), while recent Ag and Sb contamination has been detected in Swedish lake sediments (Grahn et al., 2006). Greater than natural concentrations of metals including Cu, Zn, Ag and Cd, have also been found to occur in ice from the Bolivian Andes (Hong et al., 2004a), Antarctica (Planchon et al., 2002) and Greenland (Candelone et al., 1995). In the remote Arctic, atmospherically derived Cd is present in the food chain at levels considered harmful to higher level predators and humans (Dietz et al., 2000; Van Oostdam et al., 2005). In general,

however, the history, magnitude and global extent of atmospheric contamination by many potential toxic metals remains poorly understood (Nriagu, 1990).

Table 2.1 Annual flux of seldom-studied metals to the atmosphere (natural and anthropogenic)

	Natural (t/yr)[a]	Anthropogenic (t/yr)
Cd	1 440	2 983[b]
Sb	2 400	1 904[c]
As	12 000	28 070[d]
Zn	45 000	99 000[e]
Cr	44 000	47 000[e]

Data sources [a](Nriagu, 1989), [b](Pacyna et al., 2009), [c](Tian et al., 2014), [d](Matschullat, 2011), [e](Rauch and Pacyna, 2009)

The precise timing and especially the magnitude of apparent enrichment varies between records and between regions, depending on the location and nature of the archive and the combination of local and distant contaminant sources (Bindler, 2011; Brännvall et al., 2001a; Harmens et al., 2008; Novák et al., 2003; Osterberg et al., 2008). In many cases, however, the chronology of Pb contamination reconstructed from peat and ice archives has been shown to match regional production volumes (Hong et al., 1994; Le Roux et al., 2004; Marx et al., 2010; Renberg et al., 2000; Shotyk et al., 1998; Weiss et al., 1997) and is also in agreement with archaeological evidence (Martínez-Cortizas et al., 1997a), demonstrating the fidelity of peat and ice records for recording temporal trends in atmospheric contamination.

2.5 Mobility of atmospherically derived metals in the surficial environment

Peat and ice studies highlight the considerable mass of metal contaminants that have been deposited to the Earth's ecosystems. Beyond these relatively stable archives, atmospherically deposited metals are stored in large quantities throughout the Earth's environment, including within soils (e.g. Bindler et al., 1999; Friedland et al., 1992). Following deposition, industrial metals bind to soil mineral particles and organic matter by a variety of mechanisms including adsorption, chemisorption and ion exchange (Salomons and Förstner, 1984a; Young, 2013). This process can serve to immobilise metals within the soil compartment (Klaminder et al.,

2006b). Erel and Patterson (1994) showed that the concentration of Pb in water flowing over soil was reduced from 0.2 ng/g to 0.01 ng/g in as little as 50-500 m, lowering, by more than an order of magnitude, the amount of Pb transferred from fallen snow to the stream.

On the other hand, the accumulation of metals in soils also makes them a potentially significant source of metals to other environmental compartments. This is evidenced, for example, by the delayed transport of previously deposited Pb to streams and lakes, in areas where primary deposition has been reduced by the implementation of stricter emission controls and the phase out of leaded gasoline (e.g. Bindler et al., 2008; Rose et al., 2012). Metals may be mobilised from the soil stores either by leaching (e.g. translocation in porewater) of metals through the soil to groundwater (e.g. Erel and Patterson, 1994; Johnson et al., 1995), or by erosion and transport of soil particles carrying bound metals (e.g. Rose et al., 2012). Soils, therefore, represent both a sink and a secondary source of atmospheric industrial metals (e.g. Klaminder et al., 2006b).

Sediments are acknowledged as important carriers of metals in the environment (Foster and Charlesworth, 1996; Salomons and Förstner, 1984b). The impact of soil erosion and sediment transport on the mobilisation and accumulation of metal contaminants across landscapes has been investigated by real time sampling of suspended particulate metal concentrations in stream water (e.g. Rothwell et al., 2008), sediment core studies which document the contribution of eroding contaminated soils to metal accumulation in lakes (e.g. Rose et al., 2012) and by resampling of previously contaminated sites (Gundermann and Hutchinson, 1995). However, these approaches may be limited by the challenges of upscaling snapshot measurements of continuous processes, the complications of delayed transport and temporary storage of metals within intermediate catchment sinks and issues of data availability and time investment, respectively.

Alternatively, the affinity of atmospherically derived metals for soil particles has been exploited by geomorphologists and soil scientists to quantify rates of soil erosion and soil loss and to investigate sediment transport pathways within landscapes (Blake et al., 2009; Porto et al., 2009; Walling et al., 2003). The radionuclide ^{137}Cs, released to the atmosphere by atomic testing from the c.1950s CE, and the naturally derived nuclide $^{210}Pb_{ex}$ are assumed by this method to effectively bind to soil particles following deposition from the atmosphere (Walling, 2003) (although both ^{137}Cs and to a lesser extent ^{210}Pb may be mobile within the soil profile (MacKenzie et al., 1997; Olid et al., 2016). By assuming that their transport thereafter occurs only the movement of soil particles by wind and water erosion,

geomorphologists have been able to use the relative loss or gain of ^{137}Cs and $^{210}Pb_{ex}$ at different points on the hillslope as a proxy for the volume of soil eroded or deposited since the radionuclide was initially deposited from the atmosphere (Ritchie et al., 1974; Walling, 2003). The radionuclide method can provide a time-integrated estimate of total soil loss over a period of approximately 60 (^{137}Cs) – 100 ($^{210}Pb_{ex}$) years (Ritchie et al., 1974; Walling, 2003). The similarity between the behaviour and transport pathways of ^{137}Cs, $^{210}Pb_{ex}$ and common metal contaminants suggests that they have potential applications for quantifying the transport of metals by soil erosion.

The mobilisation and transport of metals from their original site of deposition may result in metals being concentrated or diluted relative to their initial concentration in some archives, e.g. soils. This is controlled by: 1) metal solubility, i.e. the ease by which an element dissolved in the soil solution to be leached from soil, and/or re-precipitated in the soil itself or in another environment (this is influenced by redox potential and soil pH); 2) size fractionation of sediment during transport leading to either concentration or dilution of pollutant metals depending on the transport regime, due to the preferential association of industrial metals with clay and silt sized grains or; 3) concentration/dilution due to early diagenesis or the transport of matrix minerals, causing post-depositional enrichment/depletion within the profile (Boyle et al., 2015). Thus, the concentration of metals in some archives may not directly reflect the rate of atmospheric deposition.

This is demonstrated for example, by Meili et al. (2003) who, in a regional scale assessment of catchments in southern Sweden, found that within a decade Hg in precipitation had increased by a factor of 10, but Hg in lake sediment had only increased 2-6 fold. The limited response of lake sediments was attributed to buffering of deposited Hg by catchment soils (Meili et al., 2003). Examining enrichment in multiple archives types is, therefore, important to understanding the spatial extent and magnitude of atmospheric metal contamination across the Earth's ecosystems. It is also apparent that there is a need to consider the sediment transport pathways and behaviour of the metals in relation to the post-atmospheric depositional movement of metals in any landscape.

2.6 Lake sediments and soils as archives of metal contaminants

Despite the potential post-depositional transport of metals outlined in the previous section, both lake sediment (Abbott and Wolfe, 2003; Bindler et al., 2001; Brännvall et al., 2001a; Camarero et al., 2009; Cooke et al., 2007; Dillon and Evans, 1982; Evans, 1986; Foster et al.,

1991; Kemp and Thomas, 1976; Klaminder et al., 2010; Norton and Kahl, 1987; Outridge et al., 2002; Pompeani et al., 2013; Renberg et al., 2002; Renberg et al., 1994; Yang et al., 2007) and soils (Brännvall et al., 2001b; Friedland et al., 1992; Fujikawa et al., 2000; Nickel et al., 2015; Reiners et al., 1975; Steinnes et al., 1997) have been used as archives of atmospheric metal deposition.

2.6.1 Lake sediments

As for peat and ice records, lake sediments have been instrumental in demonstrating both the length and magnitude of the impact of human activity on environmental metal flows. The Pb isotope record of Shirahata et al. (1980), demonstrated that industrial Pb flux to a remote subalpine pond of the American High Sierra was 20 times natural inputs and was instrumental in highlighting the contamination of remote areas by gasoline-derived Pb. Lake core reconstructions of atmospheric deposition have extended the knowledge of human metal use and its impact beyond that provided by the historical and archaeological records, providing the earliest evidence of anthropogenic metal contamination (at c.8000 yrs the Great Lakes region of North America; Pompeani et al., 2013).

Lake core records have also demonstrated that long-range transport from central Europe to Sweden occurred as early as 4000 yrs BP (Renberg et al., 1994), provided evidence of Pb enrichment from 400 CE in association with pre-Incan silver smelting in the Peruvian and Bolivian Andes (Cooke et al., 2007) and shown increased environmental concentrations of Cu, Pb, Ni and Zn from the start of the Bronze Age (c. 5000 years BP) in China (Lee et al., 2008). Because lakes respond to changes occurring within their catchment, they can also provide information on the effects of environmental processes such as climate change on the distribution of contaminants in the environment (Liu et al., 2012; Rose et al., 2012).

The use of lake sediments to reconstruct past rates of regional atmospheric deposition is predicated on the assumption that metals are incorporated into sediments in direct proportion to atmospheric emissions (Boyle et al., 2015). This is more likely to be the case in lakes where the overall rate and background variability of metal transport from the catchment is low (e.g. Brännvall et al., 1999; Brännvall et al., 2001a; Renberg et al., 1994), but is difficult to show conclusively where the history of atmospheric deposition is unknown. The reliability of lake sediment records has perhaps been demonstrated most effectively for the small, boreal forest lakes of Sweden, where the existence of historical production data and numerous lake and peat records allow the fidelity between lake sediment records and atmospheric emissions

to be assessed. By comparing the isotopic composition ($^{206}Pb/^{207}Pb$) of Pb in recent and background sediments to that of airborne contaminants, Brännvall et al. (2001c) calculated that 71-95% of Pb is the surface sediments of these lakes is ultimately derived from atmospheric deposition (cf. 100% for peat). The lake sediment Pb records have, furthermore, been shown to match temporal trends in metal production volumes and reconstructions from atmospherically dominated ice and peat archives (Renberg et al., 1994).

In other cases, the atmospheric deposition record of metals in lake sediments can be obscured by catchment inputs, especially where the atmospheric signal is low relative to catchment fluxes (Augustsson et al., 2010; Boyle et al., 2004; Koinig et al., 2003; Meili et al., 2003; Outridge et al., 2005). While comparisons between lake sediment and atmospherically dominated archives (ice and peat) are relatively rare, several studies have shown no, or limited , up core increase in excess metal concentration in lake sediments despite definitive evidence of increased atmospheric deposition (Augustsson et al., 2010; Boyle et al., 2004; Koinig et al., 2003). Conversely, the mobilisation of metals from previously contaminated soils has been shown to delay the recovery of lake sediment Pb concentrations following emission reductions the UK (Rose et al., 2012), northern Sweden (Klaminder et al., 2010) and the Canadian Arctic (Outridge et al., 2002).

2.6.2 Soils

There is compelling evidence that soils in areas distant from industrial and population centres are, like peats and ice, contaminated by industrial metals. The presence of atmospheric contaminants in soils was demonstrated as early as the 1970s in the mountains of New Hampshire, where Pb abundance was higher than expected for a remote area and was shown to be increasing with time (as shown by measurements of soil Pb concentration undertaken over multiple years) (Friedland et al., 1984; Reiners et al., 1975; Siccama and Smith, 1978).

The anthropic origin of metals, including Pb, Hg, Cu, Zn and Cd, in surface soils in Europe and North America is supported by a number of lines of evidence. High metal concentrations have been demonstrated for topsoils relative to underlying parent material (Blaser et al., 2000; Hernandez et al., 2003; Wiener et al., 2006). In addition, soil metal concentrations have been shown to correspond with atmospheric transport pathways (Steinnes et al., 1997). Furthermore, metal topsoil concentrations display geographical trends that are not apparent in the C horizon, indicating that excess metals have an atmospheric rather than a geologic origin (e.g. Steinnes et al., 1997; Wiener et al., 2006).

The anthropogenic origin of metals in soils has been further confirmed by Pb isotopic analysis. In this case, the Pb isotopes ratios in topsoils were found to be skewed towards those of less radiogenic contaminant sources and away from natural ratios in deeper horizons (Bindler et al., 1999; Erel et al., 1997; Gulson et al., 1981; Lindqvist, 1991). Simple isotope mixing models imply that atmospheric deposition from diffuse pollutant sources, in some cases, dominates metal inputs to soils (Bindler et al., 1999; Gulson et al., 1981; Hernandez et al., 2003; Lindqvist, 1991). In Sweden, for example, atmospheric pollution Pb has been estimated to account for most of the total Pb in both the organic horizon of forest soils (>99%) and in ombrotrophic peats (100%) (Bindler, 2008; Brännvall et al., 2001c). In other cases, natural sources, e.g. weathering release from bedrock, may be more important, however, some contaminant component is usually detectable in even the most remote locations (Blaser et al., 2000; Erel et al., 1997; Hansmann and Köppel, 2000; Hernandez et al., 2003).

Atmospherically deposited metals are retained with varying efficiency in the surface horizons of different soils types (Hansmann and Köppel, 2000; Hernandez et al., 2003; Klaminder et al., 2008). In some soils, the rate of leaching of metals from soils is low, particularly for example in the organic rich soils of the Northern Hemisphere temperate zone (Hernandez et al., 2003; Klaminder et al., 2008). Under these conditions, soil concentration profiles may provide insight into the chronology of atmospheric deposition (termed a semi-archive by Klaminder et al., 2008). In general, however, metals are transported both laterally and vertically within the soil profile (Klaminder et al., 2006b; Miller and Friedland, 1994) and incorporated by bioturbation and the plant ‘vascular pump’ (Steinnes and Njastad, 1995). Metal contaminants may also be released from soil stores by water (Liu et al., 2012) or wind erosion (Marx et al., 2014b). In addition, the use of soils as high resolution temporal archives is restricted by the difficulty of accurately determining soil age.

2.7 Regional setting

2.7.1 Metal production and metal contaminants in Australia

In the Southern Hemisphere, the earliest records of anthropogenic metal production date from 1400 BCE and are associated with Hg mining by pre-Chavin societies of the Peruvian Andes (Cooke et al., 2009). Hemispheric metal emissions increased significantly following industrialisation but, for Pb at least, were substantially lower than quantities emitted to the atmosphere of the Northern Hemisphere (Patterson and Settle, 1987; Vallelonga et al., 2002).

At the height of global Pb emissions 90% of emitted Pb was released to the Northern Hemisphere, with the remaining 10% coming from Australia, South Africa, Peru and Argentina (Patterson and Settle, 1987). Australia was the last continent (with the exception of Antarctica) to undergo industrialisation, with small scale mining, coal combustion and agriculture being established shortly after European colonisation in the late 1700s CE (Mudd, 2007).

By the late 1800s Australia had become one of the largest metal producing countries in the world, especially of Pb, Ag and Zn (Mudd, 2007) and Australian domestic consumption of coal was 1.11×10^8 t (BREE, 2014). Due the concentration of emission sources, including fossil fuel combustion in the Europe, North America and Asia, Australia, as a single country, accounts for a relatively small proportion of global emissions to the atmosphere (typically < 5%) (Pacyna and Pacyna, 2001) (Fig 2.4). The volume of metals released to the atmosphere by Australian industry is nonetheless substantial, with Pb emissions in 2013/2014 totalling 330 t (NPI, 2014). In 2013/2014 electricity generation resulted in the emission of an estimated 520 kg of As, 590 kg of Cd, 6340 kg of Cr, 520 kg of Co, 3030 kg of Cu, 12 180 of Pb, 9 100 kg of Ni, 4 kg of Sb and 35 080 of kg Zn and their compounds to the Australian atmosphere (NPI, 2014).

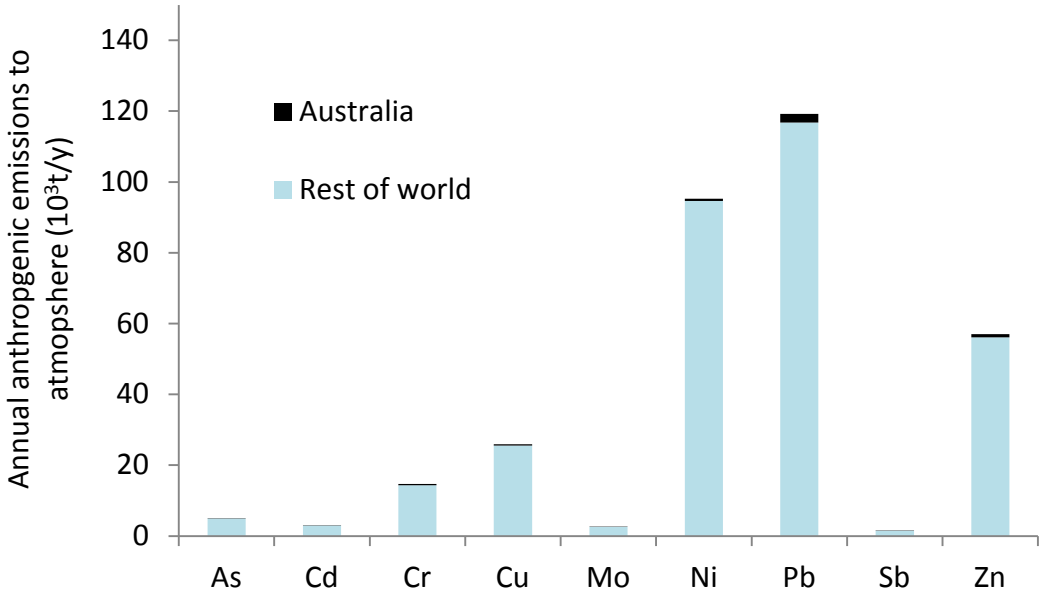

Figure 2.4 Emissions of metals to the atmosphere from anthropogenic sources globally and in Australia (data from Pacyna and Pacyna, 2001)

In comparison to the well constrained history of far-travelled metals contaminants which has been developed for parts of the Northern Hemisphere, there are relatively few studies examining the extent and magnitude of contamination in the Australian region. The history of Australian metal emissions is, to some extent, represented in the ice core records from Antarctica. For example, Pb isotope fingerprinting has demonstrated that Australia is a significant source of anthropogenic Pb to Antarctic ice cores, with rapid Pb increases in Antarctic occurring almost immediately following the establishment of the Broken Hill Pb-Zn-Ag mine in 1885 and the opening of the smelter at Port Pirie in 1889 (McConnell et al., 2014; Vallelonga et al., 2002). Antarctic ice cores also imply levels of Cr, Cu, Zn, Ag, Pb, Bi, and U in the Southern Hemisphere environment have increased substantially since the late 18th century (Barbante et al., 1997; Boutron et al., 1994; Boutron and Patterson, 1983; McConnell et al., 2014; Planchon et al., 2002; Planchon et al., 2003; Rosman et al., 1998; Vallelonga et al., 2002; Wolff and Suttie, 1994; Wolff et al., 1999). Currently Pb concentrations in Antarctic snow remain 4-5 fold greater than the natural background (McConnell et al., 2014).

On the Australian mainland, soil and sediment metal concentrations of anthropogenically derived metals have been primarily undertaken in areas directly surrounding mines or smelters, or in urban areas where local emissions are likely to overwhelm the regional contaminant signal (Alyazichi et al., 2015; Batley, 1987; Birch and Taylor, 1999; Birch et al., 2011; Cartwright et al., 1977; Chenhall, 2004; Chenhall et al., 1995; Chiaradia et al., 1997; Connor and Thomas, 2003; Gillis and Birch, 2006; Hollins et al., 2011; Kachenko and Singh, 2006; Kilby and Batley, 1993; Martley et al., 2004; Roach, 2005; Schneider et al., 2015; Taylor, 2007; Taylor et al., 2010). The only previous studies of long-travelled contaminants undertaken in remote areas within Australia include a study of a single lake located on the Baw Baw Plateau, Victoria (Smith and Hamilton, 1992) and a study examining two peat mires in the Snowy Mountains, New South Wales (Marx et al., 2010). The record of Marx et al. (2010) is the only record where contemporary metal enrichment is quantified relative to natural background concentrations which existed prior to the industrialisation of Australia.

2.7.2 Existing research from the Snowy Mountains

The Snowy Mountains are located several hundred to a thousand kilometres downwind from the industrial or urban centres including coal fired power stations surrounding the cities of Melbourne (˜400 km) and Adelaide (˜900 km) and the globally significant Pb-Zn-Ag mines at Broken Hill (˜800 km) and the associated Pb, Ag, Zn, Cu, Au smelters at Port Pire, South

Australia (˜1000 km) (Fig. 2.5; Marx et al., 2010). Historically, Broken Hill and Port Pirie dominated metal production in Australia with Broken Hill producing approximately 20 x 10^6 t Pb, 19 x 10^6 t Zn and, 28 000 t Ag since its discovery in 1883 (Mudd, 2007). Most of the output of Broken Hill was refined at the the Port Pirie smelter near Adelaide, which was established by the original major Broken Hill mining company, BHP Ltd., in 1889. Port Pirie remains Australia's most important producer of refined Ag and the 3rd largest Ag smelter in the world, outputting almost 557 t Ag in 2013 (Nyrstar, 2013). The Snowy Mountains lie within the pathway of prevailing westerly weather systems which have been shown to be important in the inter-regional transport of contaminants beyond the Australian continent (Marx et al., 2008; Marx et al., 2014a). The origin of air parcels arriving at 500 m AGL over Blue Cow (36.39°S, 148.3°E) has been shown by trajectory analysis to be predominantly from the southwest with a secondary pathway from the north (Chubb et al., 2011). Consequently, the Snowy Mountains are well placed to examine the regional significance of industrial metal contaminants in the south-eastern Australian atmosphere and their impact on the surface environment.

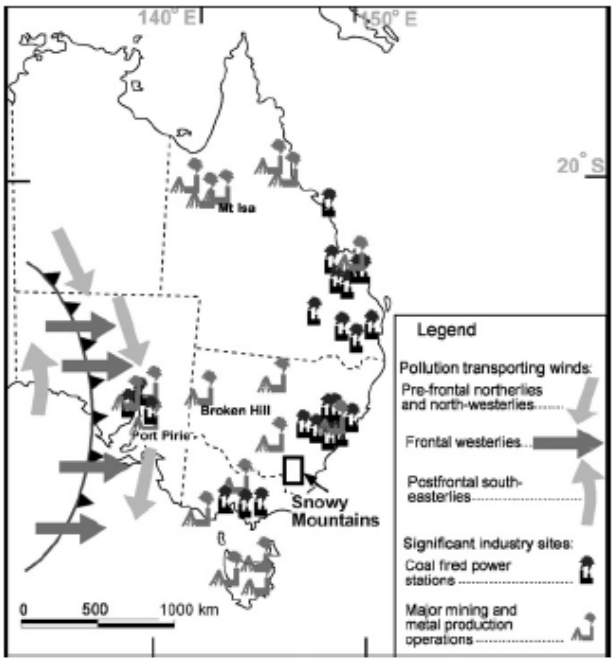

Figure 2.5 The Snowy Mountains, showing important emission sources and transporting winds (Marx et al., 2010)

The transport of industrial metals to the Snowy Mountains was previously investigated by Marx et al. (2010) who examined the chronology of metal enrichment in two alpine/subalpine ombrogenous peat mires in Kosciusko National Park. The peat mires were shown to record a detailed, high resolution chronology of atmospheric metal deposition with temporal trends reflecting the timing of mining, industrial and agricultural developments at upwind sites within south-eastern Australia. Enrichment of metals, including Pb, Cu, Mo, Ag, Zn, was shown to have begun in c.1850 CE and with enrichment increasing towards the present (Marx et al., 2014b). Pb enrichment in the mires almost immediately began followed the establishment of small mining operations in New South Wales and Western Australia in the 1850s and increased significantly following the onset of mining at Broken Hill in the 1890s, with Pb isotopic ratios implying that up to 70% of contaminant Pb was sourced from Broken Hill ore either via primary emission or by secondary emission from Pb in gasoline (Marx et al., 2010). It was estimated that metals are currently being deposited to the Snowy Mountains at approximately five times their natural rates (Marx et al., 2010). Significantly, these records showed no evidence of recent decreases in the rate of metal flux to peat mires, suggesting that atmospheric deposition may continue to be an important source of metals to the Snowy Mountains in the future. In addition, the demonstrated enrichment of peat mires raised questions as to the impact of atmospherically derived metals on the wider landscape, including how metals are transported through the surface environment following deposition from the atmosphere and how geomorphic processes such as sediment transport control the significance of atmospheric metals in key environmental receptors.

2.7.3 Cloud seeding by AgI

In 2004, Snowy Hydro Ltd. established a cloud seeding program to increase snow precipitation and, therefore, water inflows (following snow melt) to the dams of the Snowy Mountains Hydro Electric Scheme. This program uses AgI to increase ice nucleation and therefore snow precipitation to the high elevation catchments of the scheme. Thus AgI released during the cloud seeding program represents an additional Ag source, over and above more distant industrial activities (e.g. smelting at Port Pirie). AgI is released as an aerosol from 23 ground-based propane burners located on the western (upwind) side of the range during weather conditions suitable for generating snow fall, i.e. the passage of westerly cold-fronts when cloud seeding operation criteria are met. The AgI aerosol is carried into the atmosphere over the cloud seeding target area by prevailing westerly winds. Each generator releases approximately 20 g of AgI to the atmosphere for each hour of operation

(Manton et al., 2011). Between 2004 and 2013 (inclusive) the program released a total of 228.5 kg AgI which (Snowy Hydro Ltd, pers. comm., 2015) was dispersed to the atmosphere over the 2110 km^2 target area. Understanding the impact of cloud seeding Ag against more distantly sourced industrial inputs is considered especially important given recent sustained increases in Australian Ag production, including at sites upwind of the Snowy Mountains (Fig. 2.6).

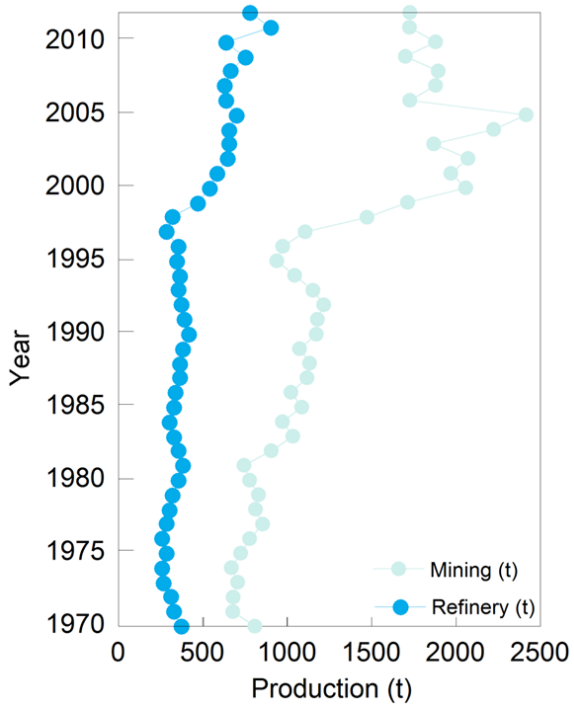

Figure 2.6 Australian silver production 1970-2012 (data from BREE, 2013)

As part of the cloud seeding program, Snowy Hydro Ltd, under the regulation of the New South Wales Government, established an environmental monitoring program which measured, annually, the concentration of Ag in the environment of Kosciusko National Park, by analysing Ag concentrations in surface soil, sediment, water and moss. The program used a statistical approach to detect temporal trends through repeated measurement of Ag concentrations in the target area versus those in a representative control area, also in the Snowy Mountains, but upwind of the cloud seeding generators and target area. The environmental monitoring samples are analysed by external laboratories and reported by Snowy Hydro Ltd to the New South Wales Government on an annual basis. The information contained in Snowy Hydro's 2010 report indicated that Ag and In concentrations measured in soil, sediment and potable water samples: 1) were present at variable but detectable levels

prior to the commencement of cloud seeding; 2) remained low compared to the Guideline Trigger Values (GTV) over each year of the trial to that date. For example the 2010 mean Ag concentrations in soils surrounding the cloud seeding generators were 5.4% of the GTV, while mean In concentrations in 2009 and 2010 were 3% of the GTV (Snowy Hydro Ltd, 2011). In a review of the cloud seeding program, the Natural Resources Commission (NRC), concluded that there was no evidence of the trial having any adverse environmental impacts (NRC 2010). Nevertheless, the NRC identified that uncertainty relating to the ultimate fate of the cloud seeding agents remained, and recommended that *"Snowy Hydro take a more investigative approach to the fate of these chemicals"* (NRC 2010 p.3).

As a result of this recommendation, this PhD was established as an independent project to investigate the fate of cloud seeding Ag in the Snowy Mountains environment, in addition to the main thesis aim of investigating the fate and variability of industrial metal more generally. To this end, the work presented in this thesis sought to uncover the history and magnitude of industrial metal enrichment in the Snowy Mountains environment, including how the significance of atmospheric metals varies across the landscape and to identify the processes controlling metal enrichment within key environmental receptors of the cloud seeding target zone.

2.7.4 Conceptual model of cloud seeding AgI fate

In planning the cloud seeding environmental monitoring program, Snowy Hydro engaged the Commonwealth Scientific and Industrial Research Organisation (CSIRO) to develop a conceptual model of the fate of the cloud seeding agents (AgI) (Kearns, 2003). This model identified that Ag deposited in snow would, likely bind to the soil surface (due to the affinity Ag and AgI for mineral and organic particles), where it would remain until sediment was mobilised by erosion, triggered by events such as spring snow melt, rain storms/floods and bushfires. In addition to organic substrates in peat mires, sediment sinks such as tarn lakes and reservoirs were identified as areas where Ag might accumulate at increased rates due to the transport and deposition of sediment-bound Ag.

In the initial stages of this PhD project, the conceptual model of Kearns (2003) was reviewed through examining the literature on metal behaviour and transport. The process found the Kearns Model (2003) represented a reasonable explanation of cloud seeding agent fate and provided a useful framework for investigating the transport and accumulation of atmospheric metals in the landscape. Based on the Kearns Model and literature review a revised

conceptual model was developed (shown in Fig. 2.7. Few previous studies have examined the environmental chemistry of the AgI compound specifically. AgI falling out to the soil surface is expected to be relatively immobile due to the high insolubility of the AgI molecule. Tsiuoris et al. (2003) demonstrated that the addition of 0.2 g of AgI to the surface of soil in pots produced concentrations of < 1 ug L^{-1} Ag in leachate after 2 years. The free Ag ion is readily reduced to insoluble compounds, or adsorbed to soil organic and mineral particles (Cooper and Jolly, 1970; Howe and Dobson, 2002; Kabata-Pendias and Mukherjee, 2007; Kabata-Pendias and Pendias, 2001; Purcell and Peters, 1998; Smith and Carson, 1977). As a consequence of its affinity for organic and mineral particles previous studies have demonstrated Ag to be relatively immobile within the soil profile (Alloway, 1990; Jones et al., 1986; Kabata-Pendias and Pendias, 2001; Tsiouris et al., 2003). For example, in controlled experiments Jones et al. (1986) added Ag (as highly soluble AgNO3) to the surface of soil cores and found that that 90% was retained in the top 40 mm after one year of leaching. For peat the percentage of silver retained was higher at >98%.

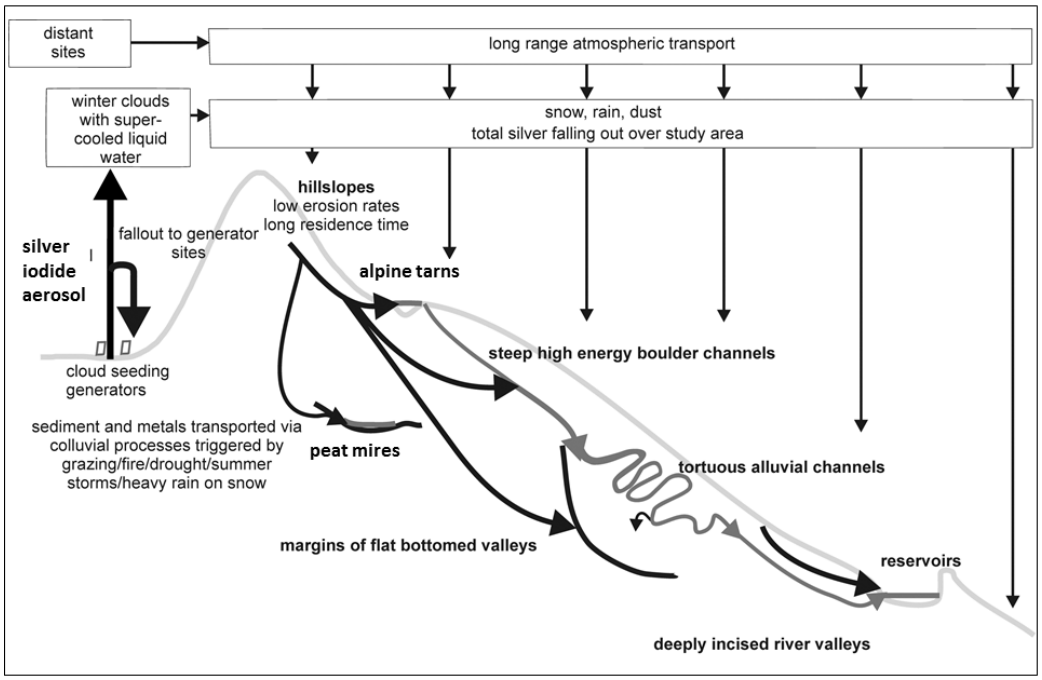

Figure 2.7 Revised conceptual model of cloud seeding Ag fate

This revised model suggests that the hillslope soils of the Snowy Mountains are likely the most spatially extensive primary receptor for cloud seeding Ag and industrial metals initially deposited from the atmosphere and may be both an important store and potential source of

metals to other landscape compartments. Metals may also be sequestered at relatively high concentrations in ombrogenous peat mires which receive and retain metals exclusively from the atmosphere. Based on a qualitative classification of hydrologic and geomorphic process zones in the Snowy Mountains landscape, landscape units identified as potential secondary sinks for metals mobilised from hillslope soils include colluvial deposits at the base of hillslopes, alpine tarn sediments and the reservoirs of the Snowy Mountains Hydro-electric scheme.

A need to understand the longer term history of metal accumulation and transport, as a result of natural processes and increased industrial emissions over the past c 150 years, in order to predict the likely future fate of cloud seeding Ag was also identified. The current study, therefore, targeted the key receptors identified by the conceptual model (soils, peat mires, tarn lake and reservoir sediments) to investigate the chronology and magnitude of metal enrichment across the Snowy Mountains landscape.

2.7.5 Summary

The key outcomes of this literature review for this thesis are that metals released to the atmosphere by industrial activity can be found accumulating in the surficial environment, often in concentrations which exceed natural background levels by many times. This includes locations far from emission sources (Brännvall et al., 2001a; Cooke et al., 2007; Le Roux et al., 2005; McConnell et al., 2014; Murozumi et al., 1969; Shotyk and Krachler, 2004; Wolff et al., 1999). To date, most reconstructions of atmospheric metal contamination include only one archive type. As these studies are primarily interested in quantifying temporal trends and rates of atmospheric deposition, they tend to focus on archives which are dominated by atmospheric deposition (peat mires, ice and atmospherically dominated lake sediments). This literature review has identified that, across the wider landscape, the concentration and enrichment of atmospherically derived metals may be moderated by processes which transport both metals and matrix materials such as soil and sediment. Despite this, few studies directly compare the history and magnitude of metal contamination in a range of different archive types.

Thus, our understanding of 1) the magnitude and extent of atmospheric metal contamination in surface sediments and its variability across the wider landscape, 2) how changes in atmospheric metal deposition are recorded in different archives and 3) the degree to which atmospherically dominated archives such as peat mires represent the general state of

contamination across the wider landscape is incomplete. Accordingly, there is a clear need to quantify the variability of atmospheric metals across wider landscape and between different archives and to investigate the processes which control the significance of atmospheric metals within different environmental archives. Related to this is the need to more clearly understand the impact of geomorphic processes such as soil erosion and sediment transport on the stability of environmental metals stores and on the transport of metals from primary sinks to secondary receiving environments.

While there are numerous studies documenting metal contamination accumulation in the environment in Europe, there are few studies from much of the rest of the globe. This is especially true for Australia where there are only two previous records of atmospheric metal accumulation from a remote setting (Marx et al., 2010; Smith and Hamilton, 1992). Considering Australia's position as a globally significant producer of metals and source of contamination to areas beyond the Australian continent, including New Zealand and Antarctica (Arimoto et al., 1990; Marx et al., 2014a; McConnell et al., 2014) there is a clear need for more records to quantify the impact of Australia's industrialisation on the regional environment and to fill the spatial gap in our understanding of global scale metal contamination. This is particularly the case for the Snowy Mountains, where it is necessary to understand the impact of cloud seeding in the context of industrial background emissions to what is considered a relatively pristine environment.

In addition, there are relatively few reconstructions which include metals other than Pb. Given that human activities emit potentially toxic metals, including Cd, As, Sb, Zn, to the atmosphere at rates which equal or exceed natural fluxes (Pacyna and Pacyna, 2001) this constitutes an important gap in our understanding of humanity's impact on the flows and impact of metals in the global environment. Accordingly, there is a need for more studies which quantify of deposition and enrichment rates for metals, including Cu, Zn, Sb, As and Cd.

These themes and the three specific research objectives outlined in Chapter 1 are explored in the following three chapters, presented as papers that are published or in review. Chapter 3 focusses on research objective 1. It aims to better investigate the temporal record of metal enrichment in tarn lake sediments relative to previous work on peat mires in the Snowy Mountains and to identify the processes that control the timing, magnitude and pattern of metal enrichment in the tarn. This chapter is published as Stromsoe et al. (2013), also see Appendix 1. Chapter 4 examines the response of different surface archives to assess how the

magnitude of contamination varies across the landscape and to identify factors which control metal enrichment, and is published as Stromsoe et al. (2015), also see Appendix 2. Chapter 5 quantifies soil production and erosion rates to assess landscape stability (over timescales of millennia to decades) to understanding how soil erosion may influence the transport or accumulation of metals in the landscape, and has been submitted for publication in Catena.

Chapter 3

Attribution of sources to metal accumulation in an alpine tarn, Snowy Mountains, south-eastern Australia

Chapter 3 is reproduced from the following published paper

Stromsoe, N., Callow, J.N., McGowan, H.A., Marx, S.K., 2013. Attribution of sources to metal accumulation in an alpine tarn, the Snowy Mountains, Australia. Environmental Pollution 181, 133-143.

Chapter 3. Attribution of sources to metal accumulation in an alpine tarn, Snowy Mountains, south-eastern Australia

Abstract

This study analyses 1800 years of heavy metal accumulation in a remote alpine lake experiencing long-range atmospheric contamination and additional inputs of Ag from cloud seeding. In comparison to previous work undertaken on peats, lake sediments show limited post-industrial metal enrichment with enrichment factors of Ag 1.3, Pb 1.3, Zn 1.1, Cu 1.2 compared to Ag: 2.2, Pb: 3.3, Zn 2.1, Cu 4.1 for peat. We show this to be the result of substantial fluvial lithogenic flux of metals (92-97% of total metal flux) to the lake. Total annual metal flux to the lake ranges from: Ag: 4-12 ng/cm^2/yr to Zn: 3380-11 310 ng/cm^2/yr. As a result, any contribution of cloud seeding to additional enrichment of Ag in lake sediments is considered negligible. Results show that metal enrichment is not necessarily ubiquitous through a landscape. This has implications for predicting the impacts of atmospheric metal contaminants on complex environmental systems.

3.1 Introduction

It is widely acknowledged that emissions from anthropogenic sources have substantially altered the global atmospheric flux of metals (Hong et al., 1994; Murozumi et al., 1969; Settle and Patterson, 1980). Typically released to the atmosphere during high temperature combustion of hydrocarbons or the smelting of metal ores, metals exist primarily as gases and fine particulates which may be transported thousands of kilometres from their source (Macdonald et al., 2000; Marx et al., 2008). Thus, atmospheric deposition is the primary mode of metal contamination for remote ecosystems distant from local contaminant sources (Liu et al., 2012; Stankwitz et al., 2012). Consequently, metals have been found to be enriched within the Greenland ice cap and within numerous remote lakes and peats (Brännvall et al., 2001a; Dillon and Evans, 1982; García-Alix et al., 2013; Renberg et al., 1994; Shotyk et al., 2001; Yang et al., 2002).

These environmental archives are valuable for understanding metal enrichment relative to natural background levels and for distinguishing changes arising from natural processes, such as weathering, from anthropogenic influences. Different substrates (e.g., lakes, mires, mosses or soils), however, may differ in their specific response to increased atmospheric loadings of metals (Meili et al., 2003). Understanding the behaviour of metals within these different environments is important as preferential accumulation in particular environments, e.g. lakes, has implications for the biota which inhabit them (Kabata-Pendias and Mukherjee, 2007).

By comparison to Europe and North America, there are very few studies examining the levels of enrichment of atmospheric metals in the Australian environment. A study from the Snowy Mountains, demonstrated that the region's ombrotrophic peat bogs have accumulated substantial quantities of anthropogenic metals since industrialisation approximately 150 years ago (Marx et al., 2010), implying that other environments in the same region, such as lakes and soils may be similarly enriched. However, until now these environments have not been examined. Their enrichment cannot necessarily be predicted from the peat records because, in addition to atmospheric deposition, catchment processes such as erosion and runoff often have a dominant influence on trace metal accumulation in lakes (Han et al., 2007; Shotyk and Krachler, 2010; Tornimbeni and Rogora, 2012). Metal accumulation in the lakes of the Snowy Mountains, therefore, warrants further attention.

The fate of anthropogenic metals in the Snowy Mountains is of particular interest because of the existence of cloud seeding operations to increase snowfall and ultimately runoff in the

catchments (Manton et al., 2011). This program follows an earlier clouding seeding trial from 1955 to 1959 (Smith et al., 1963) and uses AgI as a nucleating agent to enhance the formation of ice crystals (Manton et al., 2011). In the current cloud seeding program In_2O_3 was used as an inert tracer from 2004 to 2012. At the time the cores described in the paper were collected, the program had been operating for almost 8 years, releasing 20.4 kg of AgI on average per year.

Based on the very high particle affinity of the Ag ion (Cooper and Jolly, 1970; Kabata-Pendias and Mukherjee, 2007; Purcell and Peters, 1998), it is assumed that Ag preferentially bind to soil when released into the environment where it may remain immobilised on slopes until soil is eroded. In a report to guide the cloud seeding environmental monitoring program Kearns (2003) hypothesised that lakes and other alluvial and colluvial deposition sites in the Snowy Mountains were areas in which the accumulation of Ag may be enhanced.

Understanding how Ag accumulates in sites such as alpine lakes is important because they may be especially sensitive to contamination by atmospheric metals. This is due to high precipitation and often efficient runoff processes from catchments which are dominated by exposed rock and therefore have limited capacity to buffer lakes from contaminant inputs (Lafrenière and Sinclair, 2011). Relatively low sedimentation rates in some alpine lakes (Rose et al., 2011) may also limit dilution of the atmospheric metal component by local fluvial inputs (Lafrenière and Sinclair, 2011). In addition, in some circumstances, lakes will be additionally enriched due to concentration of metals in the finer sediment fractions mobilised during runoff (Foster et al., 1991).

Previously published records of metal contamination from the analysis of peat cores from the Snowy Mountains (Marx et al., 2010) provide a good opportunity to investigate these physical process against a sediment core collected from an alpine lake within the same region Accordingly, the objective of this paper is to present a record of metal accumulation from an alpine tarn within a region exposed to cloud seeding for within-core comparison against historical and natural background rates, and to the peat bog record presented by Marx et al. (2010). Importantly, this study provides the first insight into natural (i.e. pre-industrialisation), pre cloud-seeding and contemporary metal accumulation histories in lakes in the Australian Alps.

3.2 Methods

3.2.1 Study site

The Snowy Mountains are located within the Lachlan Fold Belt in south-eastern Australia and form part of the Great Dividing Range, which runs for >3500 km along Australia's east coast. Although the highest region of Australia, with peaks above 2000 m, compared to most alpine areas, relief in the Snowy Mountains is subdued, denudation rates are low and soils are well developed (Bishop and Goldrick, 2000; Costin, 1954) This is the result of the region's limited glaciation during the Pleistocene, general tectonic stability and their continental margin setting (Bishop and Goldrick, 2000; Costin, 1954). Consequently, sediment yield from the Snowy Mountains is low, e.g. suspended sediment yields of 2.4-23 t/km^2/yr (Yu and Neil, 1994) are an order of magnitude lower than alpine zones in Europe, i.e., 451 t/km^2/yr (Vanmaercke et al., 2011).

The climate is cool/montane. Westerly winds prevail in all seasons while annual precipitation above 1700 m exceeds 1900 mm (Bureau of Meteorology2012), with snow present for between 3-6 months of the year. Much of the Snowy Mountains is now protected within National Parks, however, it was used for grazing from the late 1800s to the mid-1900s.

The Snowy Mountains are located downwind of the Murray-Darling Basin, Australia's main agricultural region, as well as a number of major mining operations and metal processing plants, most notably the Port Pirie smelter in South Australia. They are also downwind of the major cities of Melbourne and Adelaide (Marx et al., 2010). Long-range contaminants from these sources have been documented to have been transported as far as New Zealand (Marx et al., 2008). Consequently, the Snowy Mountains are well placed to receive long-range contaminants.

3.2.2 Core collection

Two cores (Club Lake 3 (CL3) and Club Lake 4 (CL4)) were collected from Club Lake, a small (0.015 km^2), shallow (< 2m deep) tarn, located on the south-eastern side of the Main Range (36.414°, 148.291°, 1950 m), in February and November 2011. Club Lake is within 5 km and 50 m elevation of the Upper Snowy peat core (USC) described in Marx et al. (2010) (-36.463^{0}S, 148.200^{0}E, 1940 m) (Fig. 3.1). The lake catchment consists of an extensive cover of alpine humus soil stabilised by alpine herbfield vegetation, outcrops of Ordovician aged metamorphic rock (Tex, 1955) and associated talus.

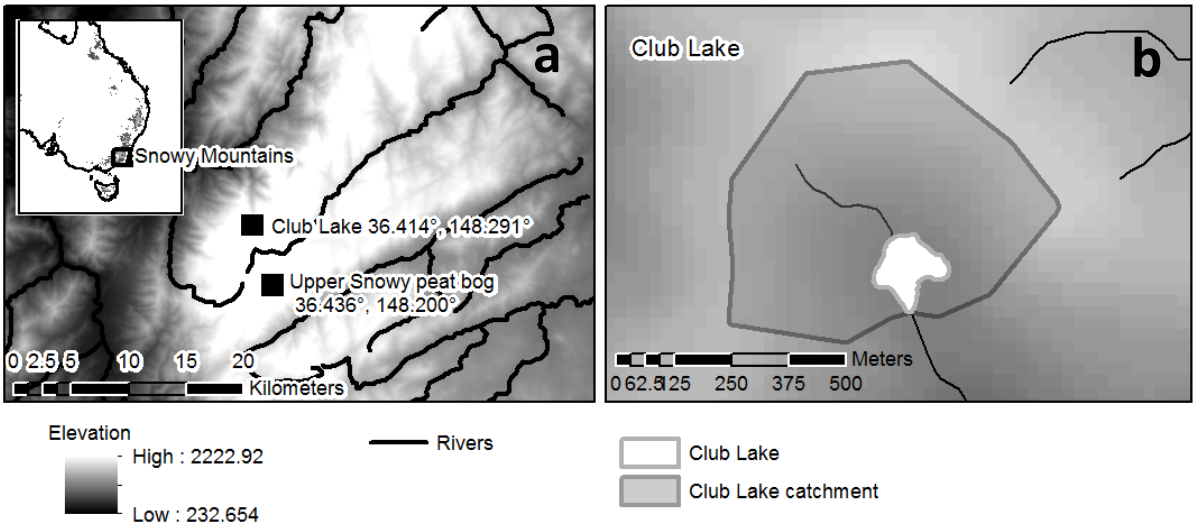

Figure 3.1 Study site location a) location of Club Lake and Upper Snowy peat bog within the Snowy Mountains, Australia (inset) b) Club Lake and its catchment

The two lake cores (CL3 and CL4) were collected by inserting a 70 mm diameter polyvinylchloride pipe into the sediments, then capping the pipe and extracting the sediment from the lake bed. Both were collected from the deepest part of the lake within approximately 1 m from each other. The cores were then sealed completely for return to the laboratory.

Research elsewhere has found positive correlations between lake pollutant loads and physical characteristics, such as the catchment to lake area ratio and catchment position (Berg et al., 2005; Evans, 1986; Gantner et al., 2010). Club Lake's relatively small catchment to lake area ratio (0.3/0.015 km^2) and its position in the catchment headwaters suggest that atmospheric flux should form a significant and, therefore, detectable proportion of total sedimentary metal concentration.

3.2.3 Core processing and sedimentological analysis

In the laboratory, the cores were frozen to preserve their stratigraphy and shaved into 2 mm sub-samples with a stainless steel scalpel. The outermost 3 mm of each core was discarded to prevent contamination by smearing of material down the sides of the PVC pipe during core collection.

Samples were dried at 60°C for 36 hours then lightly crushed with a mortar and pestle to remove large aggregates. Following drying, organic content was measured by loss on ignition (LOI) at 400°C for 12 hours. The mass change following LOI is assumed to be proportional to weight of the organic material contained in the sediment. We acknowledge that in some

instances organic content can be affected clay dewatering, especially in this case where sample organic content is low (Heiri et al., 2001). Consistency in grain size throughout the CL3 core, however, implies uniformity of clay contents. LOI results are therefore considered to be internally consistent. Particle size was determined on 29 samples from CL3 using a Coulter Multisizer according to the procedure of McTainsh (1989). Bulk density was estimated using the formula *mass/volume*, where mass is the mass of the sediment dried at 60°C to standard weight and volume is the volume of the wet sample.

3.2.4 Trace element analysis

Trace element analysis (including heavy metals) was performed by solution quadrupole inductively coupled plasma mass spectrometry (ICP-MS) on a Varian 810 instrument at the Universityof Melbourne, Australia. Forty three samples were analysed from CL3 and 14 from CL4. Prior to analysis samples were digested in Teflon beakers on a hotplate at 150°C using HF-HNO_3 as described in Marx et al. (2010). The ICP-MS protocol of Eggins et al. (1997) with modifications according to Kamber (2009) was employed. The rock standard W2 was used as the calibration standard, while external precision was assessed by analysis of the rock standards BHVO-2, JB-3 JA-2, AGV-2. The soil standards JSo-1 and GSSS-1 which were also analysed alongside the samples in this study were used to assess external precision of Ag and In, which are of interest to this study but have not been routinely analysed within the rock standards. Internal precision was maintained by the addition of enriched isotopes and pure elemental solutions to correct for internal drift, while external drift was corrected for by repeat analysis of a reference solution every 5-8 samples (Eggins et al., 1997).

3.2.5 Dating

The CL3 core was dated using ^{210}Pb (n=6) at the Institute for Environmental Research, Australian Nuclear Science and Technology Organisation (ANSTO) and by ^{14}C (n=4) Accelerator Mass Spectrometry at the Waikato Radiocarbon Dating Laboratory, New Zealand.

Total ^{210}Pb activity was determined by measuring its granddaughter, ^{210}Po, with which it is assumed to be in secular equilibrium, using alpha spectrometry. Unsupported ^{210}Pb was determined by subtracting ^{210}Pb activity from that of ^{226}Ra, where ^{226}Ra activity represents the in-situ production of supported ^{210}Pb. Lead-210 dates were calculated using the Constant Rate of Supply model (Appleby and Oldfield, 1978) assuming constant deposition between

samples which were spaced approximately 10-20 mm apart. Errors in returned ^{210}Pb dates are estimated from counting uncertainty.

Radiocarbon dating was performed on pollen concentrate extracted using the modified method of Faegri and Iverson (2013). Dates were calibrated using the OxCal program v 4.17 (Bronk-Ramsey, 2009) and the ShCal04 Southern Hemisphere atmospheric calibration curve (McCormac et al., 2004). The uppermost sample (Wk-32019) contained carbon from atomic testing and was calibrated using the Wellington ^{14}C dataset (Manning and Meilhuish, 1994).

3.3 Results

3.3.1 Dating results and age model

The dating and age model development for the USC core is described in Marx et al. (2010). The accuracy of the USC age model is supported by the close correlation between the timing of metal enrichment in the core calculated from the age model and, the actual timing of mining and agricultural developments in Australia (Marx et al., 2010).

For both the CL3 and USC cores, unsupported ^{210}Pb activity shows a constant exponential decay profile with depth, indicating the suitability of these cores for ^{210}Pb dating (Table 3.1). For CL3, the uppermost ^{14}C date (Wk-32019), from 20 mm depth, was consistent with the ^{210}Pb derived age/depth structure (Table 3.1).

An age model was developed for the CL3 core using the ^{210}Pb and ^{14}C dates (Table 3.1) using two separate linear equations for the sections of the core above and below the limits of the ^{210}Pb dating (Fig. 3.2). Older ^{14}C dates result in a steepening of the age model below the limit of the ^{210}Pb method. Subtle changes in the concentration of some lithogenic elements occur at approximately this depth (these are outlined in the discussion), however the consistency of sediment particle size and organic matter across this boundary do not support a major change in sedimentation processes at this time. The older ^{14}C dates may be explained by the dating of pollen concentrate which has been shown in some instances, including in the Snowy Mountains to return an older age than other material due to pollen being stored within the catchment for significant periods before being remobilised and deposited (Marx et al., 2010; Vandergoes and Prior, 2003).

Table 3.1. ^{14}C and ^{210}Pb dates. Lead-210 samples are relative to November 2011.

Lab code	Dating method	Material	Depth (mm)	Radiocarbon age (years BP)	Supported ^{210}Pb (Bq/kg)	Unsupported ^{210}Pb (Bq/kg)	Age (cal. years BP) (^{14}C calibrated and ^{210}Pb)*	Age model residuals
N103	^{210}Pb	sediment	0-2	-	48.0 ± 3.9	1135 ± 50	1±1	0
N221	^{210}Pb	sediment	10-14	-	64.8 ± 5.8	720 ± 35	17±4	-6.8
Wk-32019	^{14}C AMS	pollen concentrate	20-22	107.7+-0.4	-	-	53±0.23	-32.7
N222	^{210}Pb	sediment	30-32	-	54.7 ± 4.3	225 ± 15	38±6	-7.5
N104	^{210}Pb	sediment	50-56	-	44.5 ± 3.5	92 ± 7	51±7	-0.2
N223	^{210}Pb	sediment	70-76	-	42.7 ± 3.2	75 ± 6	64±8	7.1
N105	^{210}Pb	sediment	100-104	-	42.1 ± 3.3	52 ± 5	97±10	4.6
Wk-32020	^{14}C AMS	pollen concentrate	120-122	508+-25	-	-	512.5±22.5	-233
N224	^{210}Pb	sediment	150-152	-	45.7 ± 3.5	0.3 ± 4	-	-
N225	^{210}Pb	sediment	198-206	-	43.2 ± 3.2	not detected	-	-
Wk-32021	^{14}C AMS	pollen concentrate	250-252	961+-25	-	-	840±75	190
N226	^{210}Pb	sediment	252-256	-	40.2 ± 3.0	not detected	-	-
Wk-32022	^{14}C AMS	pollen concentrate	382-386	2009+-25	-	-	1907.5±832.5	-84

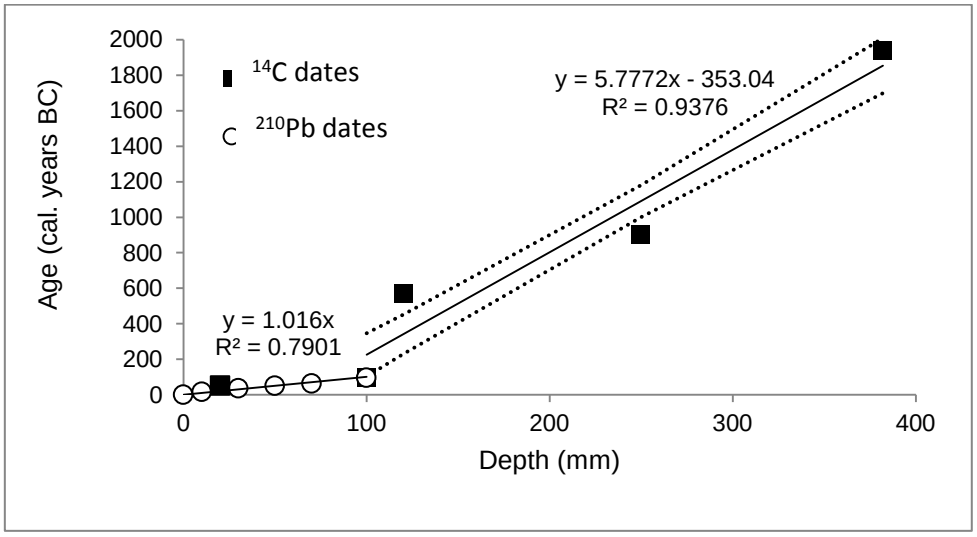

Figure 3.2 Age model constructed for the CL3 core. Two separate linear fits are applied to the sections of the core above and below 100 mm depth. Dashed lines are 95% confidence intervals of the fit of the age model to the dates below 100 mm.

3.3.2 Sediment characteristics

Based on the ^{210}Pb and ^{14}C dates (Table 3.1), sedimentation rates in Club Lake vary from 30 to 840 g/m^2/yr over the past 1800 years (Fig. 3.3). The analysed cores consist of dark grey brown clayey silts of consistent organic content and particle size. Organic content in the CL3 core is low, varying between only 1% and 3% and showing no systematic variation with depth (Fig. 3.3). Particle size analyses show less variability than LOI data (Fig. 3.3). D_{10} (where 10% of the particle size distribution is below this diameter) and D_{90} (where 90% of the particle size distribution is above this diameter) are selected to characterise changes in the proportion of smaller particles, which will likely have the greatest effect on trace metal concentration due to their relatively large surface area for adsorption of metals. For the CL3 core there is no apparent trend in D_{10} (Fig. 3) and only a very minor variation in D_{90} above 70 mm depth (Fig. 3.3).

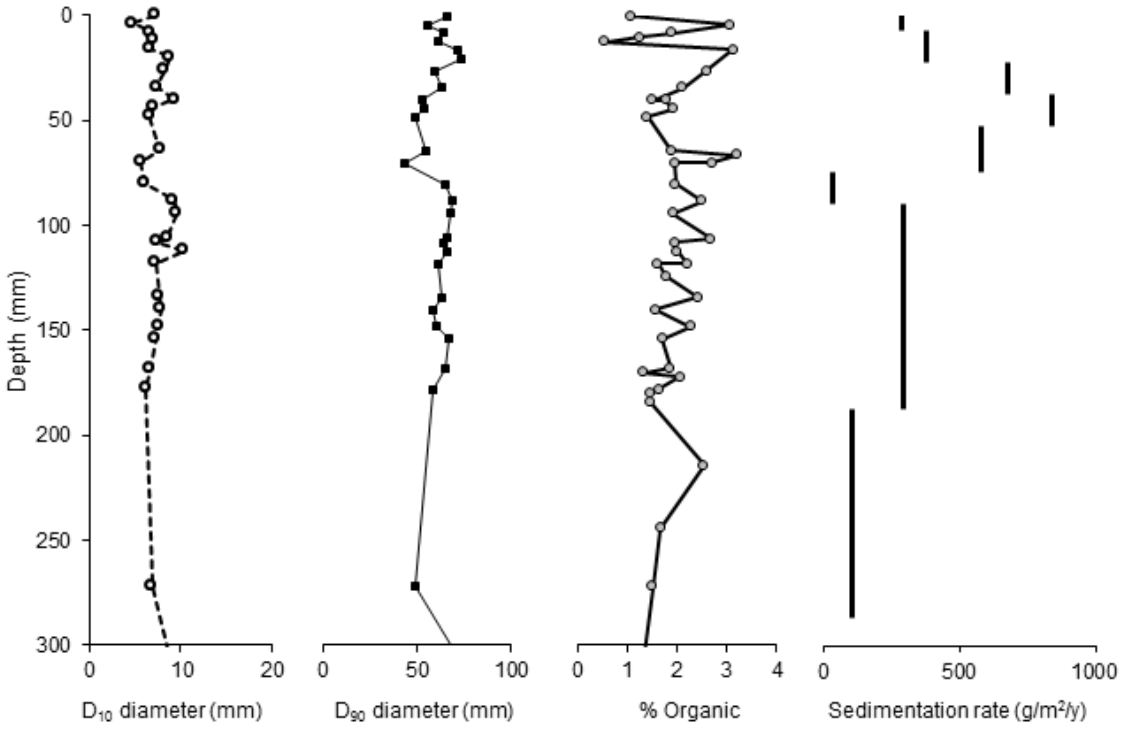

Figure 3.3 CL3 core: Particle size D_{10} (where 10% of the particle size distribution is below this diameter), D_{90} (where 90% of the particle size distribution is above this diameter), % organic (LOI) matter and sedimentation rate

3.3.3 Anthropogenic trace metal enrichment

Accuracy and precision of the trace metal analyses is demonstrated by very low relative standard deviations (RSD) (<2%) for 40 of the 47 elements analysed in the rock standards JA-2 and BHVO-2 and for 44 of the 47 elements analysed in AGV-2 (Table 3.2). For JSo-1 and GSS-1, RSD of Ag and In was <3%. For the elements discussed in this paper, results are in good agreement with certified values for analysed standards (Table 3.3).

The key metals of interest to this study are those which are typically enriched in the environment from anthropogenic activities. These commonly include Ag, As, Cd, Cr, Cu, Hg, Mn, Mo, Ni, Pb, Sb, Se, V and Zn (Nriagu and Pacyna, 1988). In this paper Pb, Cu, Ag and Zn are presented. For metal concentrations in CL3, variability across the entire 1800 year record is low (Fig. 3.4, note that for ease of interpretation, only the most recent 500 years of the core is plotted, however the concentration beyond 200 years BP is relatively consistent until 1800 years BP, all analyses are performed on the full data set). Mean concentrations during this period are: Ag 0.01 ± <0.01 µg/g, Pb 4.53 ± 0.06 µg/g, Cu 2.9 ± 0.05 µg/g and Zn 13.50 ± 0.15 µg/g (mean ± standard error).

The section of the Club Lake cores corresponding with the pre-industrial age in Australia (prior to 120-150 years BP) is presumed to represent natural background metal concentrations in the lake. While anthropogenic enrichment of metals occurs from as early as 4000 years BP in Europe (Brännvall et al., 2001a; García-Alix et al., 2013; Martínez Cortizas et al., 2002a; Rosman et al., 1997; Shotyk et al., 1998), 5000 years BP (Lee et al., 2008) in China and 3400 years BP in South America (Cooke et al., 2009) in Australia it appears to date only from the 1850s (~ 160 years BP) (Marx et al., 2010). This much later date is explained by Australia's relatively late industrialization combined with the apparently negligible transport of particulate metals from the Northern Hemisphere (Flegal et al., 1993). Lead enrichment attributed to the onset of mining at Broken Hill and smelting at Port Pirie and Cockle Creek is coincident within Antarctic ice cores (Vallelonga et al., 2002), and the Snowy peat records (Marx et al., 2010).

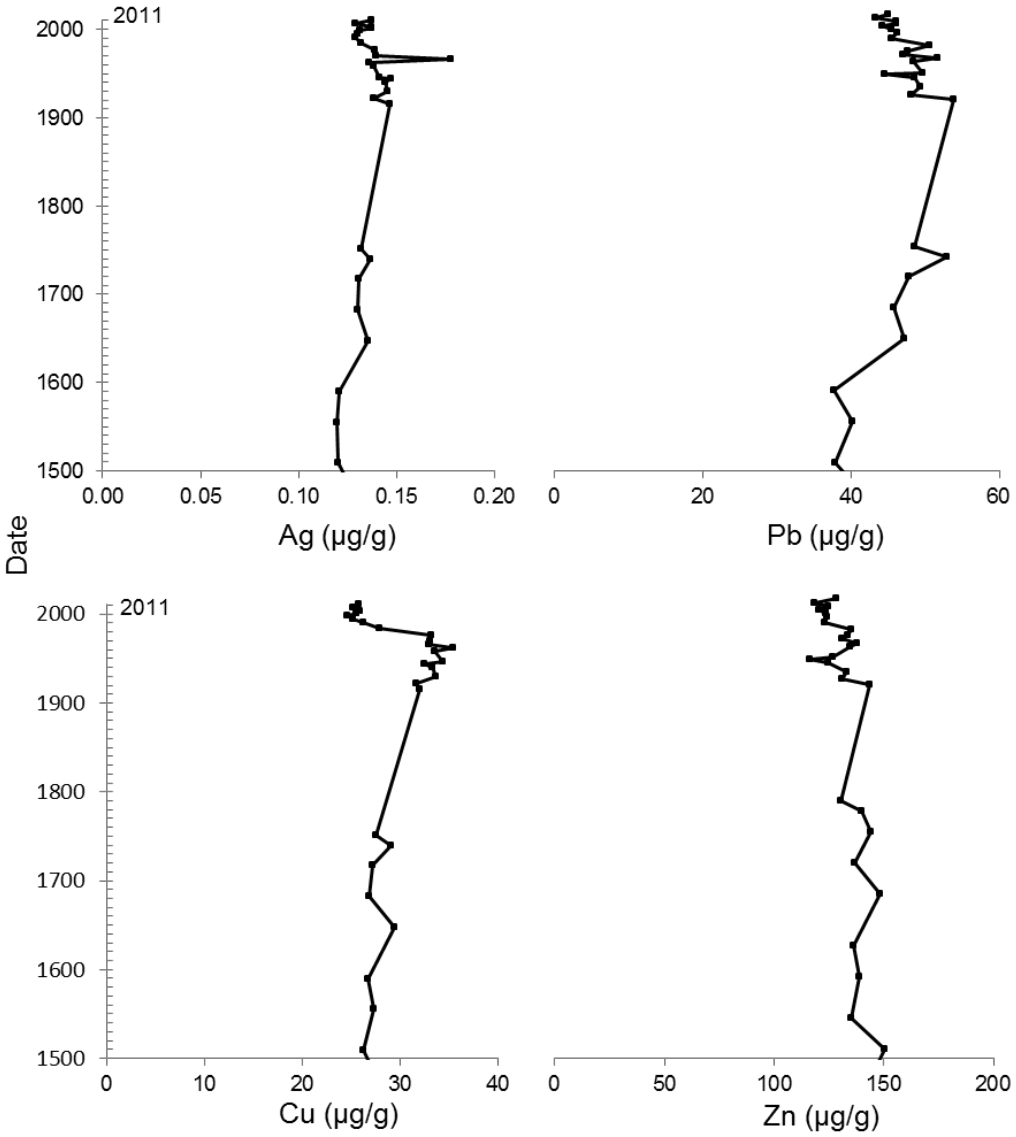

Figure 3.4 Metal concentration/age profiles for CL3

Table 3.2. Trace element data for rock standards (based on long-term analyses at University of Melbourne)

Standard	JA-2				BHVO-2				AGV-2			
	Mean (µg/g)	RSD (%)	Certified values (µg/g)[a]	laboratory deviation from certified values (%)	Mean (µg/g)	RSD (%)	Certified values (µg/g)[b]	laboratory deviation from certified values (%)	Mean (µg/g)	RSD (%)	Certified values (µg/g)[c]	laboratory deviation from certified values (%)
Li	29.2	0.67	27.3	-7.1	5	1	nv	-	11	<0.5	nv	-
Be	2.10	1.10	2.05	-2.39	1.02	1.58	nv	-	2.14	0.81	nv	-
Ca	45900	2	45000	-21	82400	1	81700	-1	37000	<0.5	37200	1
Sc	19.6	1.4	19.6	0.2	32	1	32	-1	13	1	13	2
Ti	4031	2	4200	4	16500	1	16300	-1	6100	1	6300	3
V	121	2	169	28	316	1	317	<0.05	114	<0.5	120	5
Cr	438	2	436	-1	301	1	280	-8	16	1	17	5
Co	29.9	1.1	29.5	-1.4	46	1	45	-1	16	1	16	2
Ni	139	1	130	-7	119	1	119	<0.5	18	1	nv	-
Cu	27.5	1.1	29.7	7.5	126	1	127	1	19	1	53	8
Zn	63.3	2.2	64.7	2.1	102	1	103	1	88	1	86	-2
Ga	16.5	0.8	16.9	2.7	21.10	0.61	21.7	2.8	20	1	20	0
As	0.37	15.14	0.85	56.00	0.42	15.27	nv	-	0.51	2.87	nv	-

Standard	**JA-2**				**BHVO-2**				**AGV-2**			
	Mean (µg/g)	RSD (%)	Certified values (µg/g)[a]	laboratory deviation from certified values (%)	Mean (µg/g)	RSD (%)	Certified values (µg/g)[b]	laboratory deviation from certified values (%)	Mean (µg/g)	RSD (%)	Certified values (µg/g)[c]	laboratory deviation from certified values (%)
Rb	70.0	0.5	72.9	4.0	9.2	0.51	9.8	-	67.8	0.3	68.6	1.2
Sr	243	<0.5	248	2	394	<0.5	389	-	656	<0.5	658	<0.5
Y	15.8	1	18.3	13.8	24	1	26	-	18	<0.5	20	9
Zr	111	1	116	4	173	2	172	-	236	<0.5	230	2
Nb	9.00	0.55	9.47	4.92	18	1	nv	-	14	<0.5	15	8
Mo	0.54	1.59	0.60	10.83	3.35	6.67	nv	-	1.97	0.28	nv	-
Cd	0.06	3.00	0.08	19.23	0.09	2.25	nv	-	0.07	2.68	nv	-
In	0.04	1.17	nv	-	0.09	1.25	nv	-	0.05	2.72	nv	-
Sn	1.74	2.06	1.68	-3.51	1.96	6.51	nv	-	2.34	0.48	nv	-
Sb	0.12	5.57	0.14	16.43	0.08	5.90	nv	-	0.42	0.42	nv	-
Cs	4.78	0.60	4.63	-3.20	0.10	1.25	nv	-	1.17	0.60	nv	-
Ba	310	1	321	3	131	1	130	1	1141	<0.5	1140	<0.5
La	15.6	0.4	15.8	1.6	15	1	15	1	38	<0.5	38	1
Ce	32.7	0.4	32.7	0.1	38	<0.5	38	1	70	<0.5	68	-2

Standard	JA-2				BHVO-2				AGV-2			
	Mean (µg/g)	RSD (%)	Certified values (µg/g)[a]	laboratory deviation from certified values (%)	Mean (µg/g)	RSD (%)	Certified values (µg/g)[b]	laboratory deviation from certified values (%)	Mean (µg/g)	RSD (%)	Certified values (µg/g)[c]	laboratory deviation from certified values (%)
Pr	3.70	0.33	3.84	3.54	5.38	0.45	nv		8.2	0.13	8.3	0.94
Nd	14.1	0.6	13.9	-1.2	24.4	0.41	25.0	2.30	30	<0.5	30	-1
Sm	3.02	0.54	3.11	2.96	6.07	0.67	nv	-	5.5	0.38	nv	-
Eu	0.88	0.49	0.93	5.27	2.05	0.44	nv	-	1.53	0.23	nv	-
Gd	2.99	0.36	3.06	2.39	6.22	0.46	nv	-	4.49	0.38	nv	-
Tb	0.48	0.74	0.44	-7.95	0.94	0.73	nv	-	0.63	0.46	nv	-
Dy	2.88	0.62	2.80	-2.68	5.25	0.57	nv	-	3.5	0.16	3.6	4.08
Ho	0.61	0.61	0.50	-21.80	1.00	0.60	nv	-	0.68	0.46	nv	-
Er	1.71	0.50	1.48	-15.74	2.51	0.68	nv	-	1.80	0.54	nv	-
Tm	0.26	0.62	0.28	7.86	0.34	0.81	nv	-	0.26	0.97	nv	-
Yb	1.66	0.79	1.62	-2.59	1.99	0.76	nv	-	1.6	0.90	1.6	-2.75
Lu	0.25	0.97	0.27	8.15	0.27	0.68	nv	-	0.25	0.39	nv	-
Hf	2.86	0.81	2.86	0.17	4.4	1.1	4.1	-	5.21	0.65	nv	-
Ta	0.65	0.74	0.80	19.38	1.14	0.54	nv	-	0.83	0.14	nv	-
W	1.16	1.26	0.99	-17.07	0.19	1.17	nv	-	0.44	0.64	nv	-

Standard	**JA-2**				**BHVO-2**				**AGV-2**			
	Mean (µg/g)	RSD (%)	Certified values (µg/g)[a]	laboratory deviation from certified values (%)	Mean (µg/g)	RSD (%)	Certified values (µg/g)[b]	laboratory deviation from certified values (%)	Mean (µg/g)	RSD (%)	Certified values (µg/g)[c]	laboratory deviation from certified values (%)
Tl	0.33	0.80	0.32	-2.81	0.02	1.77	nv	-	0.27	0.31	nv	-
Pb	18.5	1.6	19.2	3.7	1.45	5.16	nv	-	13	<0.5	13	2
Bi	0.09	2.17	0.07	-22.86	0.01	2.83	nv	-	0.04	2.00	nv	-
Th	4.67	0.54	5.03	7.10	1.18	0.70	nv	-	5.9	0.46	6.1	-
U	2.24	1.06	2.21	-1.54	0.42	0.93	nv	-	1.89	0.46	nv	-

[a] (Imai et al., 1995), [b] (Wilson, 1998b), [c] (Wilson, 1998a), nv denotes no certified reference value available

Table 3.3 Trace element data for soil standards (based on long-term analyses at University of Melbourne)

	JSo-1				GSS-1			
	Mean (µg/g)	RSD (%)	Certified values (µg/g)*[4]	laboratory deviation from certified values (%)	Mean (µg/g)	RSD (%)	Certified values (µg/g)*[5]	laboratory deviation from certified values (%)
Ag	0.11	2.10	nv	-	0.36	2.70	0.35	2.86
In	0.09	1.90	0.09	0	0.08	2.60	0.08	4.94

*[4] (Terashima et al., 2002), *[5] (Xie et al., 1989), nv denotes no certified reference value available

In CL3, the actual differences between mean pre and post-industrial concentrations of anthropogenic metals are small, increasing by approximately 7% for Ag, 11% for Pb and 5% for Cu. In contrast post-industrial zinc concentrations decrease by 9% (Fig. 3.4). The increase in mean post-industrial concentrations from natural background is statistically significant for Ag (two-sample $t_{(41)} = -2.93$, $p < 0.05$) and Pb ($t_{(41)} = -7.01$, $p < 0.05$) only. To distinguish anthropogenic changes from natural variability it is common practice to normalise metal concentrations against conservative, lithogenic elements which have no significant anthropogenic source (Arimoto et al., 1989; Shotyk, 1996a). As the choice of normalising element can impact the interpretation of metal perturbation or lack thereof (Boës et al., 2011), multiple normalising elements which span a range of mineral association and element behaviours were utilised. These included two rare earth elements (REE), Sc and La, which are known to exhibit conservative behaviour, Ga, a group 13 metal with behaviour analogous to Al and therefore an indicator of changes in allochthonous dust input through time, and Zr, which is hosted primarily in Zircon and is therefore indicative of the behaviour of heavy minerals (which are subject to density sorting in sedimentary deposits).

The formula used for normalisation was:

$$EF = (M_s/Ec_s)/(M_{nat}/Ec_{nat}) \quad (3.1)$$

where *EF* is the enrichment factor, (M_s/Ec_s) is the ratio of a metal of interest to a conservative element in a sample from the post-industrial section of the core (post-1850) and (M_{nat}/Ec_{nat}) its mean ratio in the pre-industrial portion of the core.

Prior to the 20th Century, enrichment factors are relatively constant (EF 0.9-1.1) for Ag, Cu, Zn. In the case of Pb, pre-20th century enrichment displays some variability (EF 0.9-1.2). Averaged across the four normalising elements (Sc, La, Ga and Zr) Pb EF steadily increases from 0.9 at approximately 1590 to 1.2 by c.1790. Following this peak Pb EF decreases to 1.1. by c.1940 before increasing again in the latter half of the 20th Century. When enrichment factors were averaged using the four normalising elements (Sc, La, Ga and Zr), very small enrichments in Ag begin at approximately 25 years, BP, Pb from approximately 40 years BP and Cu from approximately 90 years BP (Fig. 3.5). Maximum enrichment in the post-industrial part of CL3 is 1.3 for Ag (1966), 1.3 for Pb (2011), 1.2 for Cu (1945) and 1.1 for Zn (2011) (Fig. 3.5). The 1.3 value for Ag is based one sample (from 1966) which is not consistent with the general trend in that section of the core. If this sample is excluded the maximum Ag enrichment is 1.2 (Fig. 3.5).

The consistency of the pattern within Club Lake is supported by the results from the CL4 core which was correlated with CL3 by depth. Similarly to CL3, maximum post-industrial increases based on the mean of all metal/lithogenic element ratios in CL4 were 1.5 for Ag and 1.2 for Pb (Fig. 3.6). While we acknowledge that there may be subtle differences between these cores, including in the age-depth relationship, it is significant that neither core records the same magnitude of increase apparent in the peat core of Marx et al (2010).

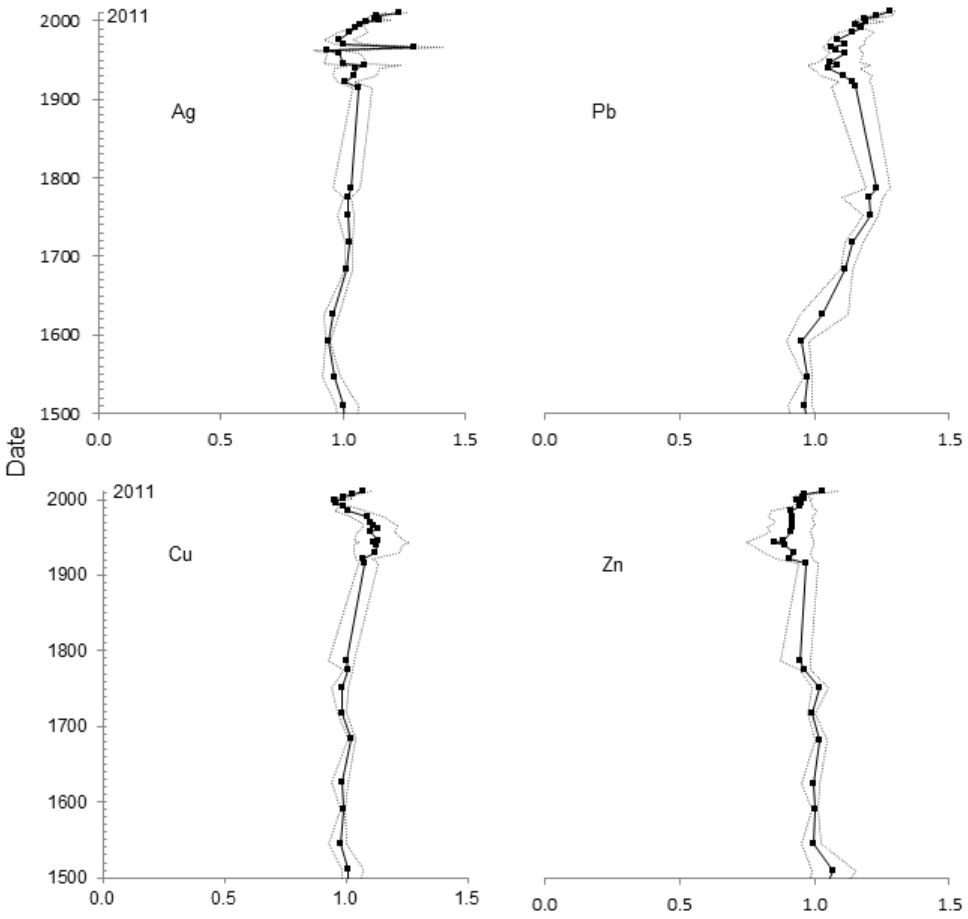

Figure 3.5 Metal enrichment profiles for CL3. Profiles are the mean (solid line), maximum and minimum enrichments (dotted lines) calculated from 4 metal/lithogenic element ratios (Ga, La, Zr, Sc).

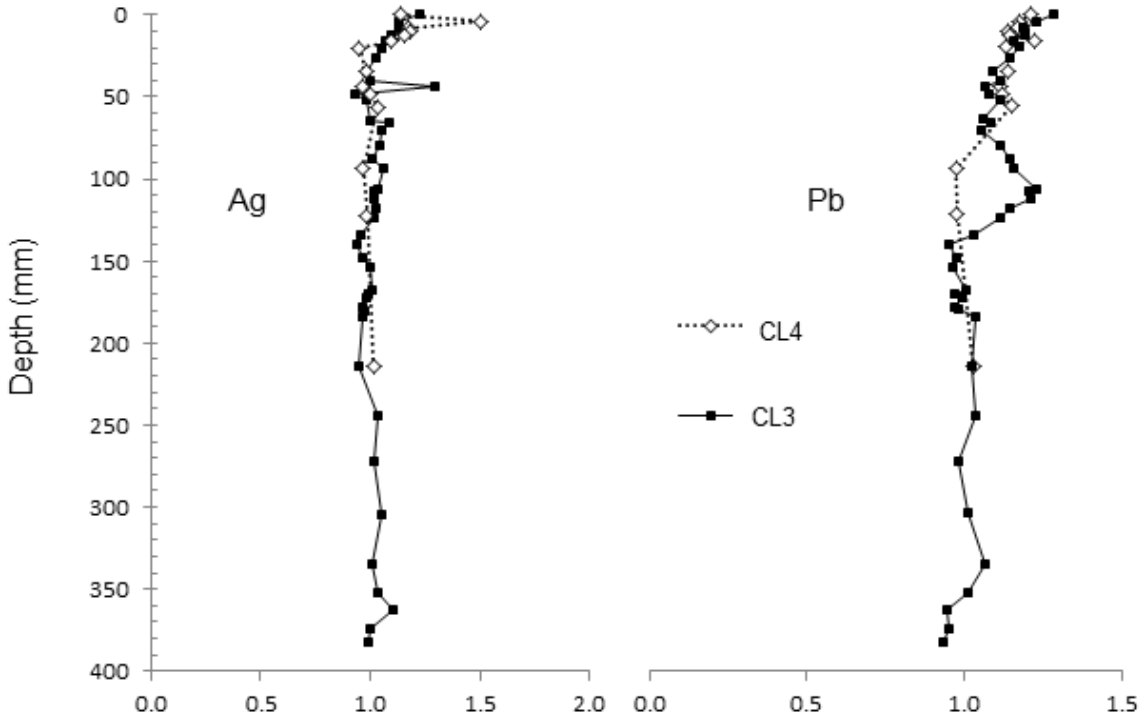

Figure 3.6 Metal enrichment profile for CL3 and CL4. Profiles are the mean enrichment calculated from 4 metal/lithogenic element ratios (Ga, La, Zr, Sc)

Enrichment of CL3 generally occurs later than in the USC (Marx et al., 2010). Additionally enrichment factors in the post-industrial sections of CL3 are approximately half those in the USC peat core. Maximum post-industrial enrichments in the USC averaged across all normalising elements are 2.2 for Ag, 3.2 for Pb, 4.2 for Cu and 2.1 for Zn (Fig. 3.7).

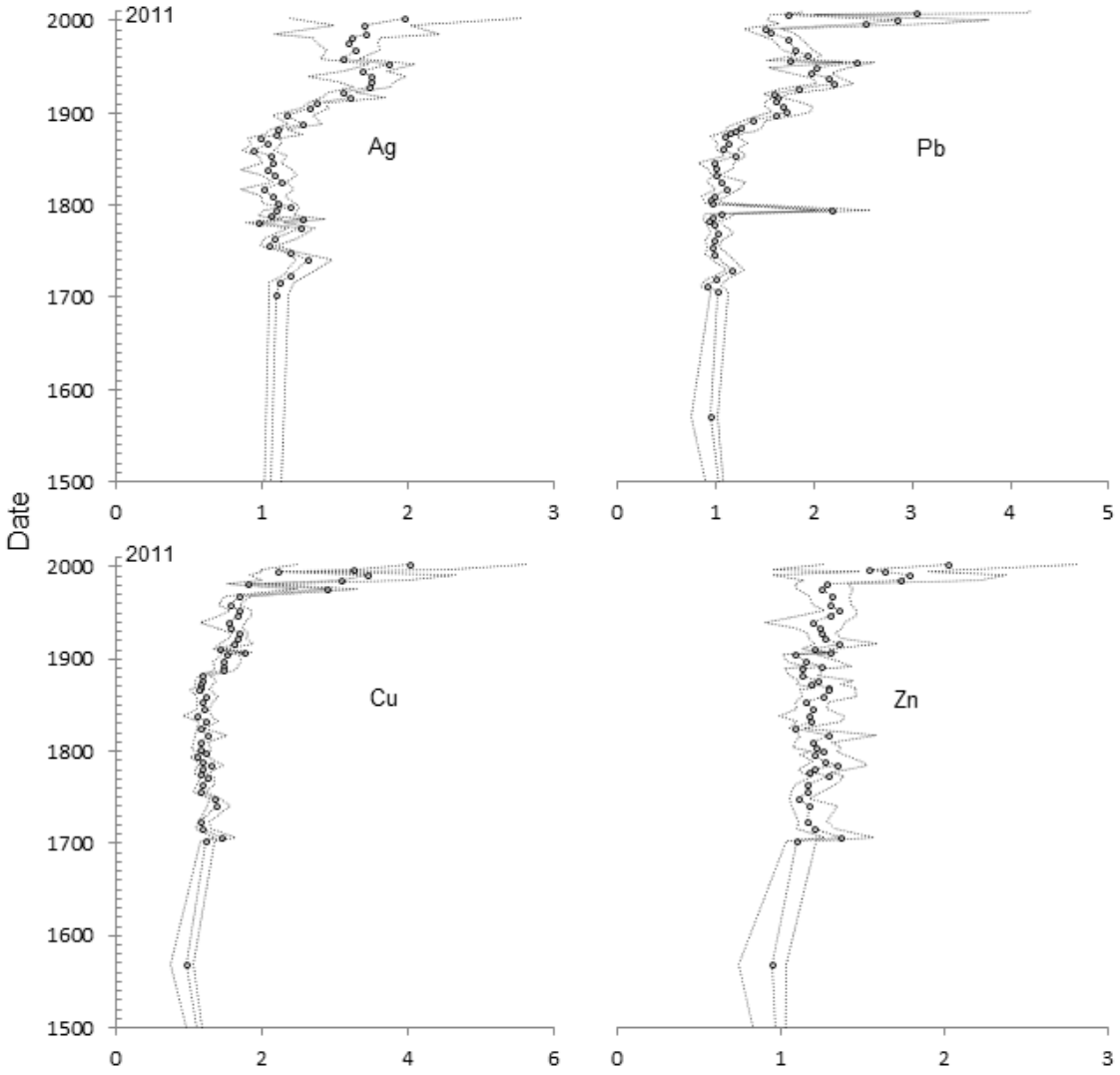

Figure 3.7 Metal enrichment profiles for USC. Profiles are the mean (solid line), maximum and minimum enrichments (dotted lines) calculated from 4 metal/lithogenic element ratios (Ga, La, Zr, Sc)

Based on the CL3 age model, the top two samples in CL3 and CL4 (spanning ~ 6 years or 4 mm) represent the period since current cloud seeding operations commenced in the study area and have been exposed to both cloud seeding and to long-range industrial metals. While Ag enrichment in two of the four samples is amongst the highest in the cores (Ag enrichment factors: 1.1-1.5), the other two contain levels of Ag similar to the previous 5 year period before cloud seeding (Ag enrichment ~1.2) (Fig. 3.5 and 3.6). The outlier from around 1966 post-dates the cloud seeding experiments in the 1950s by about 6 years, although the uncertainty in

modelled ages (with residuals of up to 7.5 years in this part of the core) makes the precise date at which these samples were deposited uncertain. Considering none of the earlier samples below (dated 1958 and 1962) were not similarly enriched, this spike is not likely related to cloud seeding.

A similar pattern of increasing enrichment in the top 4 mm is also observed for metals that are not associated with cloud seeding (e.g. Pb and Cu, Fig. 3.6). In some cases, enrichment in the top 5 -15 mm of lacustrine sediment columns as seen in CL3 and CL4 has been demonstrated to reflect the complex array of processes operating at the water-sediment-interface including redox and adsorption/desorption with the overlying water column. As a result, the increase in metal concentration in the very top of the CL3 and CL4 cores is not necessarily indicative of increased atmospheric deposition over short timescales (McKee et al., 1989; Rasmussen, 1998).

3.4 Discussion

Here we have investigated the sensitivity of alpine lakes and peat bogs to increases in the atmospheric loading of anthropogenic trace metals with the aim of understanding how metals, including those released from cloud seeding, are incorporated into the environment following atmospheric deposition. The lake and peat cores from the Snowy Mountains, which are subject to the same level of regional contamination, provide a good opportunity to investigate how physical processes operating within the lake catchment affect trace metal enrichment.

Results show that metals in peat bogs are enriched by 2-4 times pre-industrial levels (Fig. 3.7). These enrichments are of a similar scale to other estimates from the Southern Hemisphere including Australian dust deposited in New Zealand (enrichment = Pb: 5.1, Cu: 5.4, Zn: 3.5) (Marx et al., 2008) and recent Antarctic snow (where Pb is enriched 4 times over natural background concentrations in the ice cap) (Wolff and Suttie, 1994). This supports the assumption that these ombrotrophic peats closely reflect the actual regional atmospheric flux. By comparison, lake sediment enrichments are relatively subdued (approximately 1.1-1.3 x pre-industrial concentrations), indicating a dampened response relative to atmospheric increases (Fig. 3.5).

Previous studies suggest that the sensitivity of lakes to increasing atmospheric metal emissions may depend strongly on local conditions and that, under different circumstances, lakes may either subdue (Martínez Cortizas et al., 2002b; Shotyk and Krachler, 2010), amplify (Swain et

al., 1992) or faithfully reflect (Dillon and Evans, 1982) the direct atmospheric flux. In the absence of long term direct measurements, some indication of the variability in the relationship between atmospheric deposition and lake enrichment can be obtained by comparing enrichments estimated from peat bogs and lakes within the same catchment or region, assuming that peats clearly reflect atmospheric flux (Shotyk et al., 1996). The few examples where the appropriate enrichment factors can be extracted from the published data indicate that the relative sensitivity of lakes may be approximately half (Shotyk, 1996a) to 2 times that of peats (Brännvall et al., 1997).

Such variability between different lake sediment records suggests that post-depositional processes such as connectivity between contaminated catchment sources and the lake, patterns of sediment storage, runoff regimes and the degree to which metals are concentrated or diluted during transport are significant controls on the record of metal accumulation relative to input. That the response of Club Lake appears relatively subdued is significant given catchment characteristics which would normally suggest a substantial contribution from the atmospheric component to total sediment and metal input (e.g. relatively high precipitation, its headwater position and small catchment to lake area ratio) (Berg et al., 2005; Evans, 1986; Gantner et al., 2010).

3.4.1 Moderating processes which influence the relationship between atmospheric emissions and environmental concentrations in the Snowy Mountains

The importance of the atmospheric metal flux relative to local fluvial input can be determined by examining differences in the concentration of elements in local Snowy Mountains sediment relative to dust source areas. Using a geochemical fingerprinting approach, Marx et al. (2011) demonstrated that the southern Murray Darling Basin (MDB) is the most important source area of aeolian sediment (dust) deposited in the Snowy Mountains. Locally generated Snowy Mountains sediments were found to have different concentrations of a number of trace elements (e.g., Ba and Li) relative to sediment from lower in the MDB. In the case of Ba and Li, lower concentrations down catchment were attributed to increased weathering, leading to relative depletion of these mobile elements. Figure 3.8 shows Ba/Lu ratios plotted against Tm/Li ratios (where Lu and Tm are both conservative elements) for sediments from CL3, USC and for a

selection of sediments collected from within potential dust source regions lower in the MDB (Marx et al., 2011).

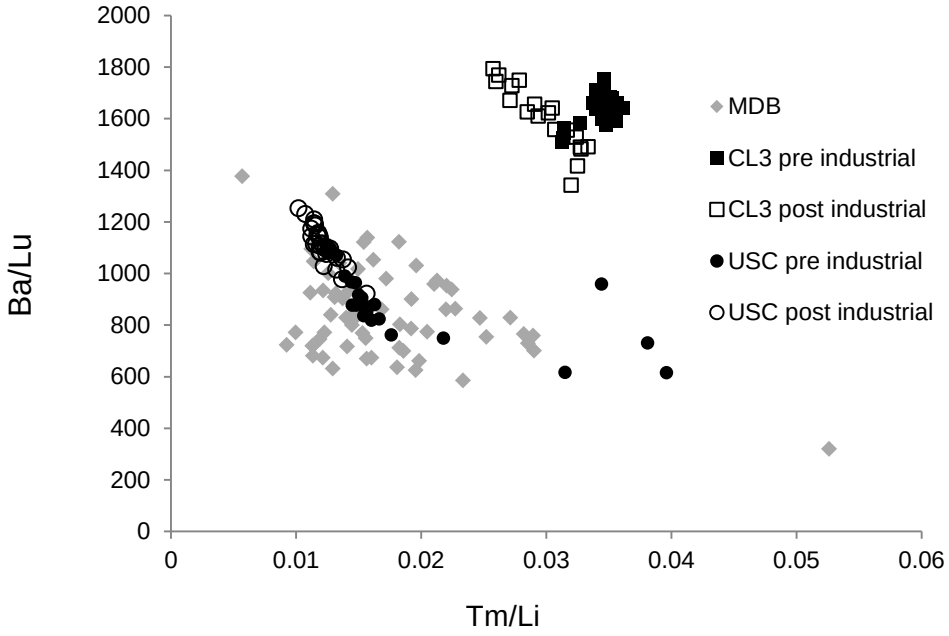

Figure 3.8 Ba/Lu vs Tm/Li mixing plot for sediments from Murray-Darling Basin (MDB) dust source areas (Marx and Kamber, 2011), and pre/post-industrial sediments in CL3 and the USC (Marx et al., 2010).

This plot shows a clear separation of CL3 sediments from those of the USC and MDB. The overlap between MDB and USC ratios in Ba/Lu and Tm/Li space implies that the mineral fraction of the USC is derived primarily from aeolian dust transported from the lower MDB, as previously demonstrated in Marx et al. (2011). By contrast, sediment from CL3 plots with higher Ba/Lu ratios and lower Tm/Li ratios. This implies either that dust deposited to Club Lake undergoes substantial post-depositional modification or that these sediments are largely locally derived and contain relatively little dust. The post-industrial CL3 sediments plot closer to the MDB sediments, possibly reflecting an increase in dust flux to the lake following the introduction of agriculture in the basin which resulted in increased dust emissions (Marx et al., 2011). Nevertheless, even these sediments remain distinctly different from MDB dust.

This suggests the relatively small atmospheric contamination signal in Club Lake is being swamped by the much larger contribution of sediment from the lake catchment. This effect is further enhanced by relatively high natural concentrations of heavy metals in local Club Lake

sediment relative to aeolian dusts. This is evidenced by high pre-industrial metal/Sc ratios in CL3 (Pb 2.7, Cu: 1.8 and Zn: 9.0) compared to USC peat core (Pb: 1.8, Cu: 0.9 and Zn: 3.6) (we note, however, this is not the case for Ag, with pre-industrial Ag/Sc ratios equal in both the lake and peat cores, i.e. Ag: 0.01).

Historical patterns of trace metal enrichment may be complicated by short-term changes in physical and chemical weathering within lake catchments. Elsewhere, rapid reductions in metal concentrations have been associated with increased delivery of coarser sediment fraction to lakes (Thevenon et al., 2011). Conversely, increased runoff from previously contaminated catchments has, in some lakes, accelerated the delivery of anthropogenic metals to lakes independently of direct atmospheric flux (Klaminder et al., 2010). To investigate whether anthropogenic metal enrichment in Club Lake is influenced by such short-term variability we compare mobile element concentrations to the equivalent immobile element with the closest magmatic compatibility on the understanding that mobile elements such as Sr, Ba, Ca, Sr are depleted during weathering (Gaillardet et al., 1999).

In CL3, Rb/Sr, Th/Ba, Ti/Ca, and Nd/Sr ratios show different temporal patterns but all suggest some level of disturbance to erosion or weathering processes which overlaps with the industrial era in Australia (Fig. 3.9). Increasing then steadying or decreasing Rb/Sr, Th/Ba, Ti/Ca, and Nd/Sr ratios in the upper sections of the core indicate increasing then steadying or decreasing delivery of more highly weathered material to the lake within the last 150 years. This may be associated with the introduction then elimination of grazing from the Snowy Mountains. These indices, however, are not correlated with anthropogenic enrichment. The correlation between Pb enrichment and the various indices, for example, varies between -0.3 and +0.7, indicating that such short term variations in weathering or erosion do not unduly influence the interpretation of the metal-age profiles.

Outflow losses from Club Lake may also contribute to the incomplete retention of deposited metals. Relatively rapid through-flow of water in Club Lake could result in significant portions of the trace metals preferentially adsorbed to the finer colloids being transported downstream before they settle out of suspension in the lake. This explanation is supported by the water level data obtained from Club Lake over an almost 2 year period from March 2010 to November 2011. These data imply a maximum water height beyond which outflow occurs. The fact that

lake levels remain close to this threshold for much of the year suggests that through-flow of water and, by implication, metals in Club Lake is relatively high (Fig. 3.10).

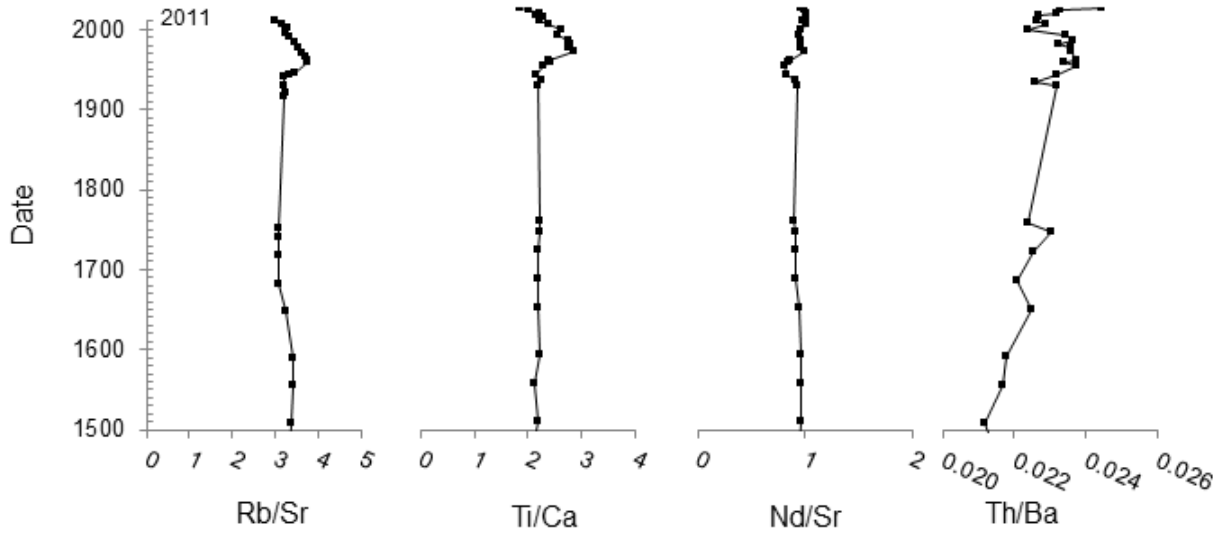

Figure 3.9 Weathering index/Age profiles for CL3. Mobile elements (Ca, Sr and Ba) are depleted during weathering.

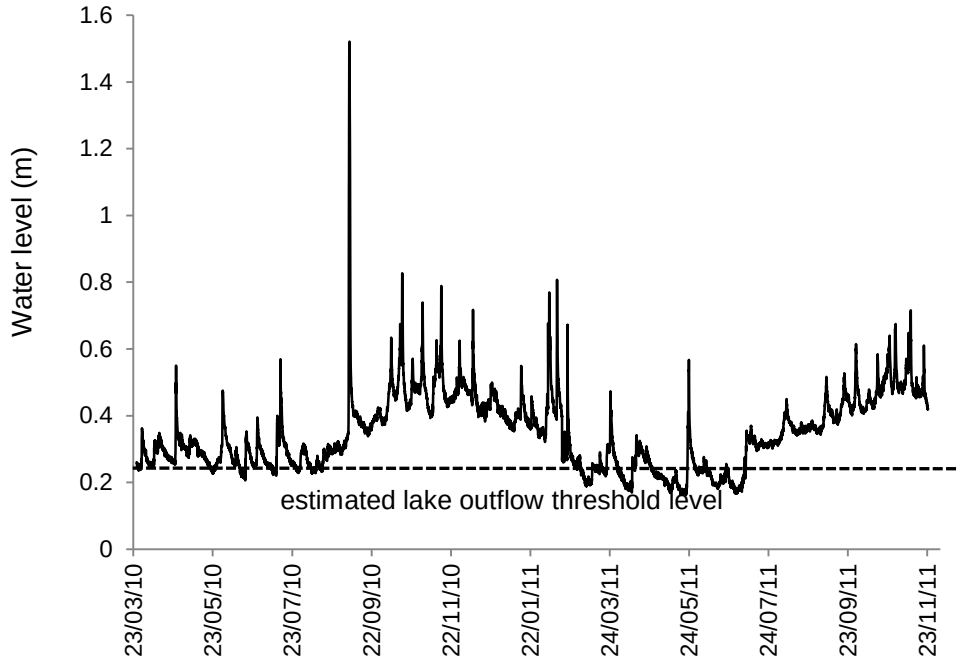

Figure 3.10 Lake levels for Club Lake March 2010 to November 2011. The dotted line represents the estimated lake outflow threshold level

The relative insensitivity of Club Lake to atmospheric deposition has implications for the behaviour of silver released during cloud seeding and for the way other new metal emissions are likely to impact the lakes of the Snowy Mountains. To provide some quantitative assessment of the potential for any new atmospheric inputs to increased concentrations in lake sediments over and above current post-industrial levels we attempted to estimate the relative contributions of aeolian and locally sourced terrigenous metals to total metal flux. If the peat bog reported by Marx et al. (2010) is presumed to receive almost all inputs from direct deposition (Shotyk, 1996a), the relative importance of locally sourced vs aeolian input can be estimated by comparing the total annual flux of metals to the lake with that to the USC peat bog.

Total metal flux was estimated using the equation:

$$Flux = concentration_{metal} \; X \; accumulation\ rate_{dust\ or\ sediment}$$

Where $concentration_{metal}$ is the concentration in a given sample and $accumulation\ rate_{dust\ or\ sediment}$ is the sediment accumulation rate at the equivalent interval. For CL3, sediment accumulation rates were estimated by multiplying the depth of sediment accumulated between dated samples

by the associated bulk density. Metal flux calculations for the peat bog were performed for the mineral component remaining after ashing of the peat (see Marx et al., 2010 for details).

Based on these calculations, the estimated current metal flux to Club Lake from both atmospheric deposition and catchment inputs ranges from: Pb: 1.23 x 10^3-4.17 x 10^3, Ag: 4 x 10^0-1 x 10^1, Cu: 7.2 x 10^2-2.89 x 10^3 and Zn: 3.4 x 10^3-11.3 x10^3 ng/cm^2/yr. Metal flux to Club Lake is controlled primarily by the variation in sedimentation rate rather than by metal concentration, which remains relatively consistent with depth (Fig. 3.3 and 3.4), highlighting the importance of local terrigenous inputs.

By comparison, the atmospheric flux to Club Lake, estimated from the inputs to the USC core, is almost negligible, accounting for only 4-8 % of total annual metal input to the lake. While any inaccuracies in the respective age models will impact the estimated difference between the peat and lake cores, any error is likely to be small relative to the large differences between the atmospheric and fluvial fluxes to the lake.

The peat bog fluxes themselves provide a measure of the importance of regional industrial activity to metal accumulation in the region. For example, Pb flux to the USC peat bog (1.56 x 10^2 – 2.47 x10^2 ng/cm^2/y) is an order of magnitude greater than that reported for the more remote-from-source Magellanic Moorelands in Chile, (2.29 ng/cm^2/y) (Biester et al., 2002). In contrast, it is 5 times less than the 1010 ng/cm^2/y estimated by Shotyk et al. (1998) for the Etang de la Gruere peat bog in the Jura Mountains Switzerland, reflecting the significantly higher population and level of development surrounding the Jura Mountains.

In Club Lake the overwhelming importance of lithogenic sources over atmospheric anthropogenic contamination suggests that any new atmospheric input, unless very substantial, would likely be overwhelmed by much larger background inputs from the lake catchment. To produce an enrichment signal equivalent to the current 90th percentile of Ag concentration in each annually accumulating interval would require an annual atmospheric flux 15 x current levels. In the context of cloud seeding, to produce an enrichment equivalent to the 90th percentile of current sediment concentration would require 19 x the current annual cloud seeding emissions each year (assuming all Ag released during cloud seeding is deposited to the surface and dispersed evenly over the 2150 km^2 seeding target area). This implies that cloud seeding related enrichment of Ag in lakes is extremely unlikely.

3.5 Conclusion

The results of this study have significant implications for predicting the long term impact of atmospheric trace metals on alpine lakes in Australia and elsewhere. Benchmarked against long term deposition rates obtained from peat cores, lake sediments show very little response in metal concentrations to at least 100 years of enhanced atmospheric deposition to both the lake and its catchment. Geomorphic and hydrological processes appear to be diluting, rather than amplifying, any increase in atmospheric loading. As such, the subdued lake response may largely be explained by the overwhelming dominance of natural lithogenic trace metals over atmospheric inputs and the natural enrichment of local sediment relative to aeolian dust.

From an environmental impact perspective, these results suggest that increased atmospheric loading will not result in metal concentrations in Snowy Mountains lakes over and above that of the surrounding landscape. However, over the long term, lakes, being significant sediment traps, may act as a long term store for metals in low concentrations. The differences between Club Lake and previous peat core results highlight the heterogeneity of metal accumulation across different functional geomorphic zones. As a result, predicting the long-term impact of atmospheric metal contamination on natural systems requires that accumulation be considered at the landscape scale and within a process context.

Chapter 4

A landscape-scale approach to examining the fate of atmospherically derived industrial metals in the surficial environment

Chapter 4 is reproduced from the following published paper

Stromsoe, N., Marx, S.K., McGowan, H.A., Callow, N., Heijnis, H., Zawadzki, A., 2015. A landscape-scale approach to examining the fate of atmospherically derived industrial metals in the surficial environment. Science of The Total Environment 505, 962-980.

Chapter 4. A landscape-scale approach to examining the fate of atmospherically derived industrial metals in the surficial environment

Abstract

Industrial metals are now ubiquitous within the atmosphere and their deposition represents a potential source of contamination to surficial environments. Few studies, however, have examined the environmental fate of atmospheric industrial metals within different surface environments. In this study, patterns of accumulation of atmospherically transported industrial metals were investigated within the surface environments of the Snowy Mountains, Australia. Metals, including Pb, Sb, Cr and Mo, were enriched in aerosols collected in the Snowy Mountains by 3.5-50 times pre-industrial concentrations. In sedimentary environments (soils, lakes and reservoirs) they showed varying degrees of enrichment. Differences were attributed to the *relative* degree of atmospheric input, metal sensitivity to enrichment, catchment area and metal behaviour following deposition. In settings where atmospheric deposition dominated (ombrotrophic peat mires in the upper parts of catchments), metal enrichment patterns most closely resembled those in collected aerosols. However, even in these environments significant dilution (by 5-7 times) occurred. The most sensitive industrial metals (those with the lowest natural concentration; Cd, Ag, Sb and Mo) were enriched throughout the studied environments. However, in alpine tarn-lakes no other metals were enriched, due to the dilution of pollutant-metals by catchment derived sediment. In reservoirs, which were located lower within catchments, industrial metals exhibited more complex patterns. Particle reactive metals (e.g. Pb) displayed little enrichment, implying they were retained up catchment, whereas more soluble metals (e.g., Cu and Zn) showed evidence of concentration. These same metals (Cu and Zn) were depleted in soils, implying they are preferentially transported through catchments. Enrichment of other metals (e.g. Cd) varied between reservoirs as a function of contributing catchment area. Overall this study showed that the fate of atmospherically derived metals is complex, and depends upon metal behaviour and geomorphic processes at landscape scales.

4.1. Introduction

Industrial metals, which include Pb, Cu, Ni, Cd, Cr, Zn, Ag, Sb and Mo, can now generally be considered a ubiquitous part of the Earth's atmospheric environment. Even in remote locations such as Enewetak Atoll in the central western Pacific (Arimoto et al., 1985) and southern New Zealand (Marx et al., 2014a), enrichment of industrial metals occurs persistently within collected aerosol samples. These metals are typically released to the atmosphere during industrial processes including metal production and mining, combustion of fossil fuels, cement production and waste incineration (Pacyna and Pacyna, 2001). They are thereafter, transported by the wind to be deposited to terrestrial and aquatic environments (Pacyna and Pacyna, 2001).

As a consequence, industrial metals have been found accumulating in the remote-from-source locations such as Antarctica (Vallelonga et al., 2002) and Greenland (Hong et al., 1996). Typically, however, these studies have focussed on those parts of the landscape which receive high relative rates of atmospheric input such as peat mires (Marx et al., 2010; Shotyk et al., 2002) and snow and ice (Hong et al., 2004b; McConnell and Edwards, 2008). Enrichment has also been demonstrated in soil (Brännvall et al., 2001b; Klaminder et al., 2006a) and lake sediments (Brännvall et al., 1999; Stromsoe et al., 2013; Wong et al., 1984; Yang et al., 2007) although these records maybe more complex due to the influence of catchment and *in situ* soil processes (e.g. Augustsson et al., 2010; Shotyk and Krachler, 2010). Over the last 20 years, an increasing body of literature has documented metal enrichment in such settings (peat mires and ice) where, in many cases, temporal patterns in metal enrichment directly reflect regional industrial histories (e.g. Brännvall et al., 1999; Cooke et al., 2007; Le Roux et al., 2004; Lee et al., 2008; Marx et al., 2010). These studies demonstrate the pronounced perturbation of these metals that has occurred globally since the Industrial Revolution, while also recording pre-industrial metal contamination dating from the Bronze Age in Europe and Asia (Brännvall et al., 1999; Hong et al., 1996; Lee et al., 2008).

Atmospherically dominated archives tend to record the state of the atmosphere and do not necessarily reflect the general extent of industrial metal contamination throughout the wider landscape. The significance of atmospheric industrial metals across the wider landscape is likely to be more complex, reflecting rates of atmospheric deposition relative to sediment generation (by physical, biological and chemical weathering) and sediment transport rates (by aeolian,

fluvial and colluvial processes). A substantial body of literature has focussed on quantifying the inputs, flows and retention of atmospherically derived industrial metals through watersheds using a mass balance approach, often in areas experiencing relatively high rates of industrial metal enrichment (Landre et al., 2010; Lindberg and Turner, 1988; Watmough and Dillon, 2007). However, despite collected aerosol samples universally recording industrial metal enrichment (e.g. Arimoto et al., 1995; Huang et al., 2001; Marx et al., 2014a; Witt et al., 2006) there are few studies which examine the relative significance of the deposition of industrial metals across a variety of environmental archives (e.g. Landre et al., 2010; Rose et al., 2012; Starr et al., 2003; Watmough and Dillon, 2007), where they may potentially concentrate or dilute depending on the behaviour of individual metals (e.g. their particle reactivity) and hydrological and geomorphic processes.

This paper adopts a landscape-scale approach to examine patterns of industrial metal enrichment in the surface environments of the Snowy Mountains Australia. It aims to investigate the significance of atmospherically derived industrial metals in different parts of the landscape, using enrichment factors to assess the degree of contamination. This study builds on the results of two previous studies which examined metal accumulation in peat mires (Marx et al., 2010) and tarn-lakes (Stromsoe et al., 2013). However, whereas those studies focused on the chronology (historical variability) and source apportionment of industrial metals, this study compares atmospheric enrichment of metals and their accumulation in various environmental archives (peats, lakes, reservoirs and soils) to investigate patterns of dilution and concentration across the landscape. Together these provide a perspective on the environmental significance of atmospheric pollutants in this region and on the fate of atmospheric pollutants in the surficial environment more broadly.

4.2. Physical setting

The Snowy Mountains are located in southeast Australia (Fig. 4.1) and, rising to 2228 m (Australian Height Datum - AHD), are the highest region in Australia. They form part of the Palaeozoic Lachlan Fold Belt, consisting primarily of granitic and sedimentary rocks with minor metamorphics and volcanics also present. The Lachlan Fold Belt forms part of the eastern boundary of the Murray-Darling Basin (MDB), a large sedimentary basin (~1 million km^2) covering approximately 1/7 of the Australian continent. Much of the MDB is classified as semi-

arid, with rainfall decreasing westward. The basin is Australia's most important agricultural region, with extensive livestock grazing and cropping, and contains significant mineral resources; including the globally important Pb-Zn-Ag mines at Broken Hill (Fig. 4.1).

The Snowy Mountains experience a cool montane climate. Annual temperatures vary from 18° C (summer) to -7° C (winter), with annual precipitation ~2000 mm and prevailing westerly quarter winds (BOM, 2012). Snow is generally present on the peaks for between 3-6 months of the year. Despite their alpine setting, the Snowy Mountains can be considered relatively stable in a geomorphic context, a result of the intraplate setting of the Australian continent combined with a relative lack of recent glacial activity (Barrows et al., 2001). The Snowy Mountains therefore experience low denudation rates (Bishop and Goldrick, 2000; Young and McDougall, 1993) and sediment yields that are approximately 1-2 orders of magnitude lower than European alpine areas (Stromsoe et al., 2013; Yu and Neil, 1994).

Alpine soils of the Snowy Mountains are classed as Chernic Tenosols and are characterised by a high organic content and consisting of an A horizon overlying a BC horizon (McKenzie et al., 2004). The soils are also noteworthy in that they contain a high proportion of dust transported from the MDB (Costin et al., 1952; Johnston, 2001; Marx et al., 2011). This is of significance in the context of this study because industrial metals are enriched in dusts (Marx et al., 2008; Marx et al., 2014a), implying that high concentrations of industrial metals may be present in the soils of the Snowy Mountains. Vegetation above the tree line consists of alpine herb fields and heath, with ombrotrophic *Sphagmun* peat mires blanketing extensive areas (Costin, 1972; Martin, 1999). Below the treeline vegetation consists largely of Snowgum (*Eucalyptus pauciflora)* woodland with peat mires common as valley fills.

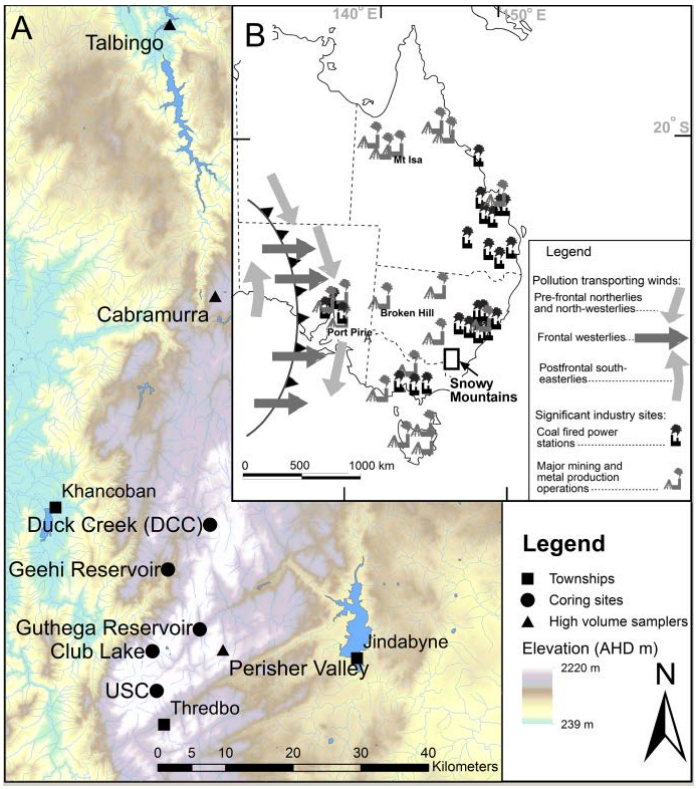

Figure 4.1 Locations of sampling sites in the Snowy Mountains. Aerosol samples (triangles) were collected from Talbingo, Cabramurra and Perisher. Sediment cores (circles) were collected from peat mires (DCC and USC), Club Lake and Geehi and Guthega reservoirs. Soils were sampled along a catena near Guthega Reservoir (see Fig. 4.2). The inset shows the position of the Snowy Mountains in eastern Australian, major industrial sites in eastern Australia and likely contaminant transporting winds (after Marx et al., 2010).

4.3 Anthropogenic disturbance and sources of metals

The study region is located within Kosciusko National Park from which farming and resource extraction are currently excluded; however, alpine areas were used for grazing from the 1860s until the mid-1900s. In addition, minor local mining, mainly comprising small-scale alluvial Au workings occurred during the mid to late 1800s. Sporadic Ag, Cu and Sn mining continued up until the early 1900s but quantities produced were generally too small to be commercially viable. A major hydro-electric power generation scheme (The Snowy Mountains Scheme) was constructed in the Snowy Mountains from 1949. This involved construction of a series of hydroelectric dams and associated infrastructure. A significant skiing industry also occurs within the Snowy Mountains. While it is possible that these activities may result in minor additions of

metals to the environment, previous studies of metal accumulation in sedimentary archives have not overtly recorded metals from these sources (Marx et al., 2010).

Since 2004 a cloud seeding operation has been undertaken in the Snowy Mountains in which AgI is released into the atmosphere to promote the formation of snow crystals during favourable conditions. Between 2004 and 2013 the operation released on average 10.5 kg of elemental Ag annually. This represents a potential additional source of Ag to the Snowy Mountains environment. Ag is presented along with the other metals in the current study but will be examined further in a subsequent paper.

Marx et al. (2010) found that the major sources of metal pollutants to the Snowy Mountains environment were remote sources upwind (west) of the range. These include a number of significant mining and metal production operations, most notably the Broken Hill mines and the smelters at Port Pirie; coal combustion (coal fired power stations are located around major cities upwind of the Snowy Mountains including Melbourne and Adelaide) and agriculture (Fig. 4.1).

4.4 Methods

4.4.1 Conceptual approach and sampling

The sampling strategy followed a multi-archive approach in order to examine the extent of industrial metal enrichment in the Snowy Mountains. This involved collecting and dating sediment cores from a range of geomorphic and hydrologic settings in the alpine and subalpine zone. These included from atmospherically-fed (ombrogenous) peat mires, which in the Snowy Mountains are located in upper catchments of the alpine zone, alpine lakes with small catchments, which are fed by both direct atmospheric deposition, but also by significant terrestrial runoff, and subalpine reservoirs with larger catchments fed overwhelmingly from runoff (Fig. 4.1 and 4.2 and Table 4.1). In addition, soil pits were sampled from a range of geomorphic positions. Together, these sedimentary archives serve to demonstrate the relative significance of atmospheric industrial metals in settings influenced by a range of additional processes including weathering, pedogenic processes and alluvial and colluvial sediment transport. In addition, a snapshot of industrial metal enrichment in the atmosphere of the Snowy Mountains was provided by sampling contemporary aerosols using a network of continuously operating high volume particulate samplers (Fig. 4.1 and 4.2 and Table 4.1). These were used to

examine the partitioning of industrial metals between the atmosphere and the surface environments sampled and to provide an estimate of metal deposition to the surface.

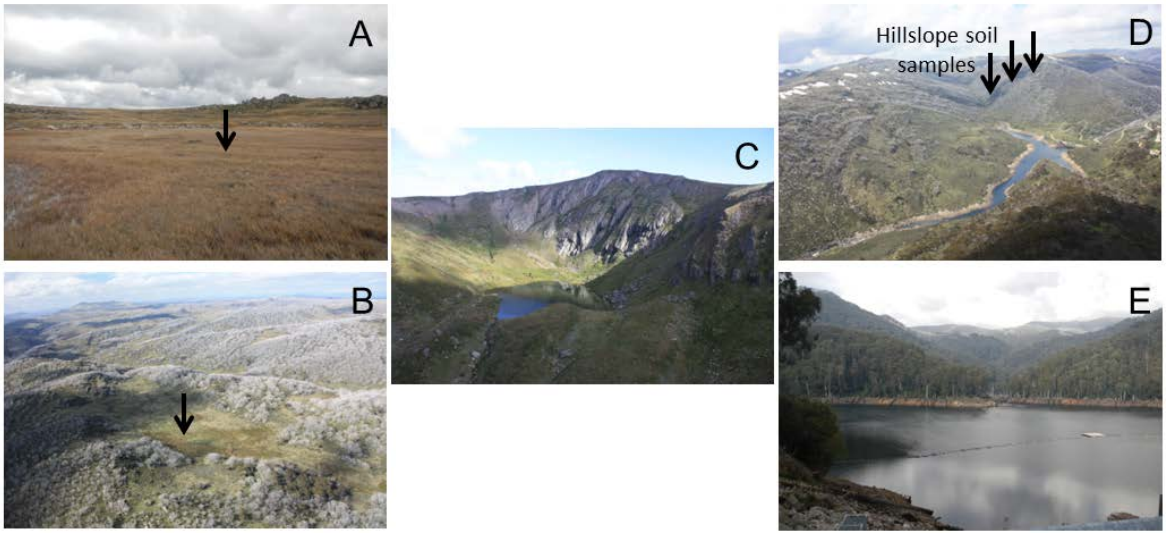

Figure 4.2 Surface sampling sites; A) Upper Snowy (USC) peat mire, B) Duck Creek (DCC) peat mire (arrows show location of cores), C) Club Lake, D) Guthega Reservoir (arrows show location of soil sampling sites within the catchment) and E) Geehi Reservoir.

4.4.2 Aerosol sampling

Aerosols were sampled continuously over one year (October 2012-October 2013) at three locations (near Talbingo and Cabramurra Townships and near Perisher) across the Snowy Mountains using Total Suspended Particulate high volume particulate samplers (Flow Set, Lear Siegler Australasia) loaded with polycarbonate membrane filters (nominal 3 µm pore size, Sterlitech) (Fig. 4.1). Filters were replaced at 1-4 week intervals and kept in chemically inert plastic bags prior to and following collection. Prior to use, filters were dried at 40^0 C degrees for 20 hrs and weighed on a 4 decimal place analytical balance. Following collection, filters were re-dried and weighed in order to determine dust mass. A sub-sample of dust was then gently scraped from the filter using a stainless steel spatula from where it was prepared for trace element analysis. A total of 50 aerosol samples were collected across the three sites during this study and analysed by Inductively Coupled Plasma Mass Spectrometry (ICP-MS).

Industrial aerosols are often submicron in size, however, these are typically scavenged from the atmosphere with larger particulates with which they are transported and deposited (Han et al., 2004; Jaffe et al., 1999; Marx et al., 2008). Membrane pore filters are also known to efficiently collect particles substantially smaller than the nominal pore size with efficiency increasing substantially with increased filter loading, including over significantly shorter sampling intervals than those used here (Kemp and Kownacka, 1987; Yamamoto et al., 2004). In addition, previous field experiments obtained with using these same filters yielded largely identical results to those obtained on a cascade impactor (Marx et al., 2014a), implying use of these filters is appropriate in this context.

Table 4.1. Sample details

Name	Sample type	Environment	Location	Altitude (m AHD)	Catchment	Core/pit depth (m)	Sampling date	Sampling resolution	Number of analysed samples
USC	Sediment core	Peat mire	-36.463°, 148.299°	1940	Guthega	1	2006	2-5 mm	79
DCC	Sediment core	Peat mire	-36.247°, 148.372°	1790	Geehi	0.66	2006	2-5 mm	81
Club Lake (CL3)	Sediment core	Lake	-36.414°, 148.291°	1950	Guthega	0.38	2011	2-5 mm	43
Geehi Reservoir	Sediment core	Reservoir	-36.379°, 148.371°	1578	Geehi	0.27	2012	2-5 mm	32
Guthega Reservoir	Sediment core	Reservoir	-36.305°, 148.316°	1100	Guthega	0.26	2012	2-5 mm	20
Guthega ridge	Soil pit	hill slope	-36.360°, 148.373°	1866	Guthega	0.6	2013	100 mm	6
Guthega mid-slope	Soil pit	hill slope	-36.360°, 148.370°	1804	Guthega	0.67	2013	100 mm	5
Guthega toe-slope	Soil pit	hill slope	-36.360°, 148.366°	1665	Guthega	0.46	2013	100 mm	3
Talbingo	Aerosols	Atmosphere	-35.583°, 148.293°	396	Jounama		Oct 2012-Oct 2013	1-4 wks	20
Cabramurra	Aerosols	Atmosphere	-35.939°, 148.379°	1484	Tumut		Oct 2012-Oct 2014	1-4 wks	12
Perisher	Aerosols	Atmosphere	-35.394°, 148.394°	1904	Jindabyne		Oct 2012-Oct 2015	1-4 wks	24

4.4.3 Estimation of aerosol/metal deposition flux

To assess the relative importance of atmospheric industrial metal fluxes to each archive, deposition rates were estimated from the atmospheric concentrations using simple models of wet and dry deposition (Jacobson, 2005; Jickells and Spokes, 2001). We note that, as with any inferential method, there are likely to be considerable uncertainties inherent in these estimates. They should therefore be considered as an estimate of the relative significance of atmospheric deposition by comparison to surface geomorphic inputs rather than an absolute measure of trace element flux.

Dry Deposition

Dry deposition was estimated from the aerosol concentration and estimated dry deposition velocities for individual aerosol particle sizes according to equation 4.1.

$$F_d = \sum_{i=1}^{n} V_{d,i} * C_i \qquad (4.1)$$

where F_d is the dry deposition flux ($\mu g\, m^{-2}\, s^{1}$), V_d the particle size specific deposition velocity ($m\, s^{-1}$) and C is concentration of that size-class in the atmosphere ($\mu g\, m^{-3}$).

Deposition velocities were determined from particle size/mass distribution and mean atmospheric conditions during the sampling intervals using Stokes Law according to Jacobson (2005). The dry deposition flux for individual industrial metals was then estimated from the aerosol deposition rates and the individual trace metal aerosol concentrations. A detailed description of the estimation method and equations is provided in the supplementary material to this chapter.

Wet Deposition

Precipitation

Due to the lack of data with which to parameterise more complex processes-based micrometeorological models, wet deposition (precipitation deposition + cloud water deposition) was estimated from simple empirical relationships relating aerosol concentration at ground level to cloud water and precipitation concentrations. Precipitation deposition was calculated by estimating the concentration of metals in precipitation from their concentration in the atmosphere using a scavenging ratio (Z), defined by the equation (Duce et al., 1991):

$$Z = C_p/C_a \quad (4.2)$$

where C_p is the concentration of the metal in precipitation and C_a its concentration in the atmosphere. A detailed description of the process and a full set of equations is provided in the supplementary material to this chapter.

We note the limitations of this approach, including in the assumption that concentrations at ground level are representative of the concentration in the air from which the pollutant is being scavenged (e.g. in the precipitating cloud) (Barrie, 1985). Thus, scavenging ratios are subject to considerable uncertainty and values may vary up to ˜4-6 fold between locations and between trace elements (Arimoto et al., 1985; Gao et al., 2003). Previously measured scavenging ratio values for pollutant aerosols range most frequently from ˜ 100 – 500 (Arimoto et al., 1985; Duce et al., 1991; Kane et al., 1994; Mason, 2013), with extreme values of between 30 (Zn, Cu) (Mason, 2013) and 1500 (also Cu) (Arimoto et al., 1985). In this study the value of Z is taken as the mean of previously published values for pollutant elements, including Cu, Ni, Zn, As, Pb and Cd (Z = 380) (Arimoto et al., 1985; Kane et al., 1994; Mason, 2013). We note that there is a substantial degree of uncertainty surrounding the selection of this value. Therefore the calculation of wet deposition is repeated using upper and lower values of the mean ± the standard error of previously published values for Z (Z = 460 and 305 respectively), providing an estimated range for the flux of pollutant elements from the atmosphere to the surface. As the relative scavenging efficiency of snow is largely unknown (Wang et al., 2014a), a single Z value is applied to the total precipitation amount. Likewise, the application of a single mean value to all trace elements is necessitated by the dearth of available data for many of the pollutants considered in this study. These assumptions should be noted as a potential source of error in the deposition estimates.

Cloud water deposition

Cloud water interception is an important mechanism of trace element deposition to high-elevation ecosystems where it may account for ≥ 50% of the total wet deposition flux (Herckes et al., 2002). In this study cloud water deposition was estimated from the concentration of metals in the atmosphere, the scavenging efficiency of cloud water for aerosols, and the deposition velocity of cloud water drops according to equation 4.3.

$$F_{i,cw} = F_{cw} * C_{i,cw} \quad (4.3)$$

where $F_{i,cw}$ is the annual cloud water flux of element *i* (ug m^{-2} y^{-1}), F_{cw} is the annual cloud water hydrologic input (g m^{-2} y^{-1}), and $C_{i,cw}$ (ug g^{-1}) is the mean annual concentration of the element in cloud droplets. The hydrologic flux (F_{cw}) was determined from the estimated mean liquid water content of the cloud (*LWC*), the deposition velocity of cloud water droplets ($V_{c,d}$) and the time the site spends below the cloud base each year (*t*). The air equivalent concentration of each element in cloud water ($C_{i,cw}$) was estimated from the concentration in the element in interstitial aerosols (i.e. from the TSP samplers) and the scavenging efficiency of cloud water drops for aerosols (*E*). This approach is outlined in detail in the supplementary material to this chapter.

The measurement of *E* (scavenging efficiency), *LWC* (liquid water content) and *t* (time below the cloud base) was beyond the scope of this study. Values are therefore estimated from previously published values for mountain environments elsewhere (*E*), from limited empirical data available for the Snowy Mountains (*LWC*) and from observation (*t*). To provide an estimate of uncertainty associated with the selection of these values the deposition flux calculations were performed using mid, low and high estimates for *E, LWC* and *t*.

4.4.4 Peat and lake cores

Two peat cores were collected from two mires in the Snowy Mountains in 2006. A 1 m core (named USC) was collected from the headwaters of the Snowy River (-36.463°, 148.299° 1940 m AHD) in the southern Snowy Mountains, while a 0.66 m core was collected from Duck Creek (DCC) in the central Southern Snowy Mountains (-36.247°, 148.372°, 1790 m AHD) (Fig. 4.1 and 2). A 0.38 m core (CL3) was collected from a Club Lake (-36.414°, 148.291°, 1950 m AHD), a tarn in the central southern Snowy Mountains (Fig.4.1 and 4.2) in 2011. Each core was sectioned into sub-samples and dated using ^{210}Pb and ^{14}C. Metals and trace elements were then analysed by ICP-MS on individual sub-samples through each core (n = 79, 81 and 43 for USC, DCC and the Club Lake core, respectively). Full details of the peat core collection, processing and dating was described in Marx et al., (2010), while the Club Lake core was described in Chapter 3 and in Stromsoe et al. (2013).

4.4.5 Soil samples

Samples were collected from within three soil pits excavated along a hillslope catena in the catchment of Guthega Reservoir in 2012 (Fig 4.1 and 4.2). The hillslope had a westerly aspect, an average slope >20° and measured approximately 0.5 km in length. Three soil profiles were excavated at 1) the top of the hill slope close to the ridge crest (-36.360°, 148.373°, 1866 m AHD), 2), the mid-slope (-36.360°, 148.370°, 1804 m AHD) and 3) the toe slope (-36.360°, 148.366°, 1665 m AHD) respectively, in each case until the saprolite was reached (at approximately 0.6 m). Samples were collected at 100 mm depth intervals in each soil pit. They were then dried, crushed in a mortar and pestle to homogenise and their trace element composition analysed by ICP-MS.

4.4.6 Reservoir cores and sample processing

In 2011 cores were collected from the Guthega (-36.379°, 148.371°, 1578 m AHD) and Geehi (-36.305°, 148.316°, 1100 m AHD) reservoirs, located in the southern and central Snowy Mountains, respectively, using a gravity corer (Fig. 4.1 and 4.2). Guthega reservoir was constructed in 1955 and has a contributing catchment of 91 km^2, which is largely within the alpine zone and includes Club Lake, the mire from where the USC was collected, and the hillslope from where the soil samples were collected. The reservoir has an area of 0.26 km^2 while its depth varies as a function of precipitation and hydro-electric power generation. Geehi reservoir was constructed in 1967 and has a contributing catchment area of 148 km^2, which includes the Duck Creek (DCC) mire. Approximately 2/3 of the catchment is within the alpine zone with the reservoir having an area of 0.66 km^2 while again its depth is variable in time. A 0.27 m core was extracted from Guthega Reservoir and a 0.26 m core from Geehi Reservoir. Cores were extracted from approximately the middle of each reservoir.

In the laboratory the cores were sliced into 2 to 5 mm samples using a stainless steel scalpel. The outermost 3 mm of each core was discarded to prevent contamination by smearing of material during core collection. Each sample was dried at 60°C for 36 hours then lightly crushed with a mortar and pestle to remove large aggregates. The metal concentration of 32 samples from Guthega and 20 samples from Geehi were analysed by ICP-MS. Subsamples from each core were dated using ^{210}Pb.

4.4.7 Trace element analysis

The analysis of trace elements (including industrial metals) in the aerosol samples, sediment samples extracted from the reservoirs cores, soils and samples from the Club Lake core (previously presented in Stromsoe et al., 2013) was performed by solution quadrupole ICP-MS on a Agilent 7700x instrument at the Department of Earth Sciences University of Melbourne, Australia. Sediment samples from the peat cores were analysed at Laurentian University, Ontario, Canada on a Varian 810 instrument using the same approach (Marx et al., 2010). Analytical details and presentation of rock and soil standards are provided in the supporting material and Supplementary Table 4.2.

4.4.8 Dating of sediment cores

Lake and peat cores were dated using ^{210}Pb and ^{14}C accelerator mass spectrometry. Results and age model construction was previously discussed in Chapter 3 and in Stromsoe (2013) and Marx et al., (2010), respectively. Sediment samples from both the Guthega and Geehi reservoirs were dated using ^{210}Pb at the Institute for Environmental Research, Australian Nuclear Science and Technology Organisation (ANSTO) by Alpha spectrometry. Dating by ^{210}Pb was performed by measuring ^{210}Po activity, the granddaughter of ^{210}Pb, with which it is assumed to be in secular equilibrium. Supported ^{210}Pb was determined by measuring ^{226}Ra, with unsupported ^{210}Pb calculated from the difference between supported and total ^{210}Pb activity (Harrison et al., 2003).

Unsupported ^{210}Pb activities in both Geehi and Guthega reservoirs cores were relatively high (supplementary Table 4.3 and Fig. 4.11). Unfortunately, the coring equipment was not able to collect more than 0.26 m length core at Geehi and 0.27 m at Guthega, therefore unsupported ^{210}Pb activities could not be determined below these depths. Five samples between 0 and 155 mm depth were analysed from the Geehi core while seven samples between 0 and 200 mm depth were analysed from the Guthega core (^{210}Pb activities are presented in supplementary Table 4.3).

4.5. Results

4.5.1 Atmospheric aerosol concentrations and industrial metal enrichment

Mean aerosol concentrations over the Snowy Mountains, as measured by the three high volume particulate samplers during 2012-2013, were 8 ± 1µg m^{-3}. Concentrations were lower during the austral winter (June-August) (5 ± 0 µg m^{-3}) relative to the rest of the year (9 ± 1µg m^{-3}). These aerosols included industrial metals, natural dust and organics.

To identify which metals are perturbed within the atmosphere of the Snowy Mountains, i.e., have concentrations higher than would be expected naturally, the average trace element concentrations of all aerosol samples were plotted normalised against MUQ (MUd from Queensland; Kamber et al., 2005) (Fig. 4.3). MUQ is a compilation of alluvial sediment samples from 25 Queensland Rivers draining the major geologic units of eastern Australia. It is therefore representative of the average background (unpolluted) chemistry of rocks and sediments in eastern Australia in addition to average global composition of Upper Continental Crust. Thus it is also broadly representative of the composition of mineral dust in eastern Australia. A number of metals exhibited high concentrations with respect to continental crust, implying their concentration has been influenced by industrial activity. These were Cr, Ni, Cu, Zn, As, Mo, Ag, Cd, Sn, Sb and Pb. We note, however, the surface sediments which constitute MUQ may also be enriched in some industrial metals (see Kamber et al., 2010). Normalisation of aerosols against MUQ may therefore mask enrichment in some metals, although it still serves to show that a number of metals are enriched even with respect to the general perturbation of surface sediment geochemistry by industrial activity.

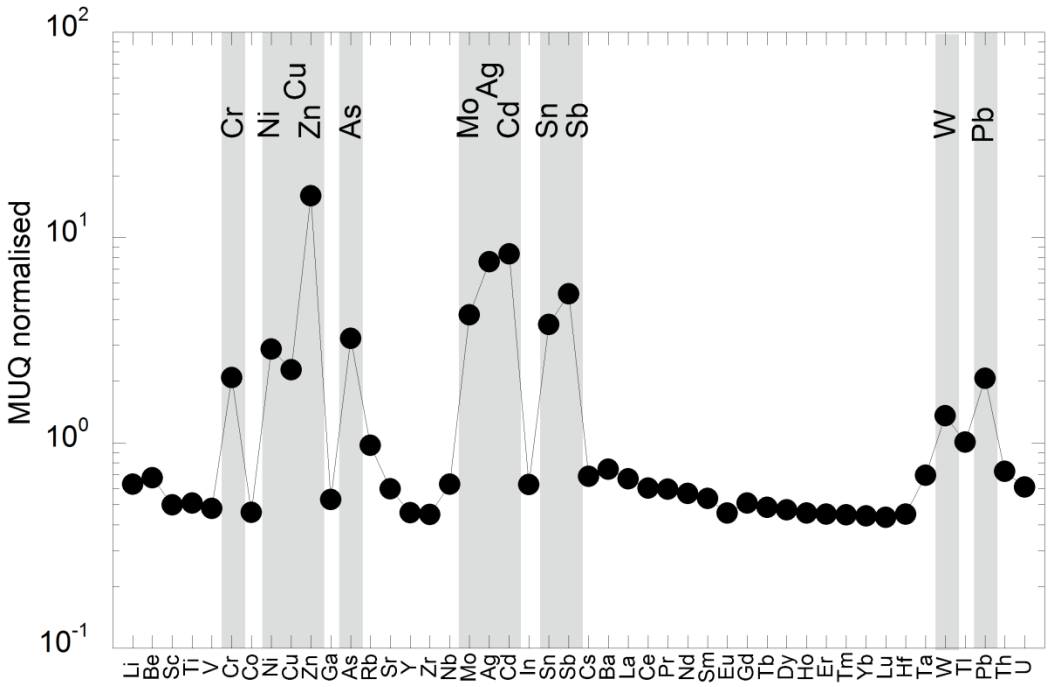

Figure 4.3 The average trace element composition of aerosols collected during this study normalised against MUQ (MUd from Queensland Kamber et al., 2005). Note As, Mo, Cd and Sb data are from Marx and Kamber (2010); Ag and In data from the Perisher core which predates industrial activity and is considered of local sediment chemistry (see Marx et al., 2011). The abundance of metals with concentrations significantly greater than MUQ are indicated in grey.

The atmospheric concentrations of individual metals were estimated from the product of the total aerosol mass per unit atmosphere and the elemental composition of sampled dust. Average atmospheric concentrations of known pollutant metals were generally < 1000 pg m^{-3} and ranged from 1 pg m^{-3} (Ag) to >3500 pg m^{-3} (Zn) (Table 4.2). Zinc, however, was present in high concentrations in blank analyses of the polycarbonate membrane filters (Marx et al., 2014a). Consequently, some of the total Zn concentration in this context is likely to be derived from the filter itself. Other metals present in concentrations >100 pg m^{-3} include Cr, Ni, Cu and Pb (Table 4.2).

Table 4.2. Average atmospheric industrial metal atmospheric concentrations for selected studies (pg m^{-3})

Location	This study[ab]	Alpine New Zealand[ab]	Antarctica[ab]	Samoa[ae]
Cr	900 ± 900	-	-	-
Co	70 ± 70	30.7 ±23.9	-	0.37 ±3.0
Ni	500 ± 900	371.4 ± 313.9	-	-
Cu	400 ± 200	192 ± 203.7	1 ± 5.6	13 ± 2.6
Zn	3500 ± 3500	-	6.1 ± 4.8	64 ± 2.2
As	120 ± 80	5.6 ± 7.0	-	-
Mo	14 ± 8	14.6 ± 13.2	-	-
Ag	1 ± 1	4.2 ± 6.8	-	11 ± 3
Cd	5 ± 7	17.8 ± 19.9	0.06 ± 0.06	-
Sn	80 ± 170	-	-	-
Sb	17 ± 10	53.2 ± 23.4	-	0.19 ± 1.1
W	17 ± 15	-	-	-
Pb	200 ± 100	163 ± 136.6	4.7 ± 3.2	16 ± 2.4

[a]Mean and standard deviation

[b]mean experimental error in the flux calculations is approximately 5% due the variation in repeated filter mass measurements, values quoted in this column are rounded accordingly)

[b]Marx et al., (2014)

[c]Dick et al., (1991)

[d]Arimoto et al., (1987)

Given the potential enrichment of MUQ surface sediments, a more accurate approach for calculating metal enrichment in the aerosols is to use mineral dust sediments which were buried prior to the onset of industrial activity in Australia in the USC core, i.e. prior to ~1850 CE (Marx et al., 2011 and Fig. 4.4). The enrichment factor can then be calculated from equation 4.4 (Arimoto et al., 1990; Shotyk, 2002):

$$EF = (Cm/Cc_{ex})/(Cm/Cc_{natavg}) \quad (4.4)$$

where *EF* is the enrichment factor, Cm/Cc_{ex} is the ratio of a metal whose concentration is suspected of being perturbed (*Cm*) in the aerosol samples to that of a conservative element (*Cc*), and Cm/Cc_{natavg} is the average ratio of *Cm* to *Cc* in the pre-contamination (pre-1850) section of

the USC core. To reduce the possibility that the behaviour of the conservative element may influence the metal *EF*, the average *EF* values using four conservative elements (Ta, Ga, Sc and Ti) were calculated (see Marx et al., 2014b).

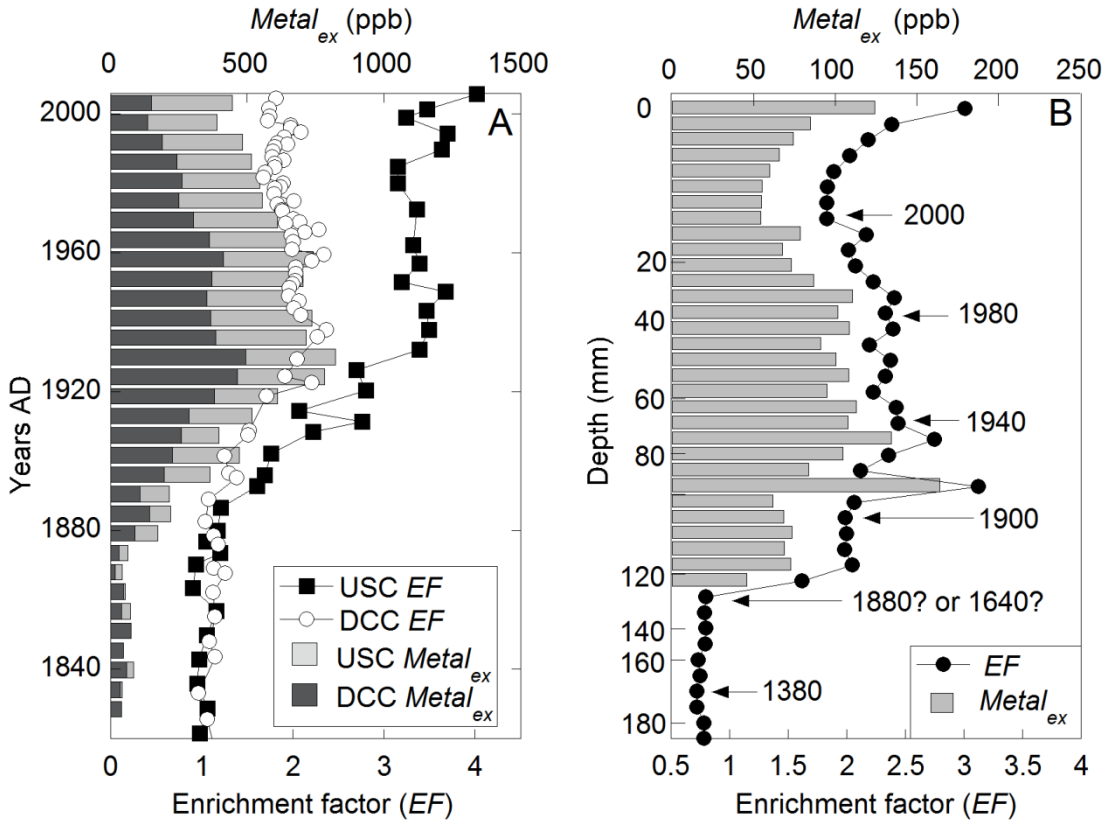

Figure 4.4 Antimony (Sb) enrichment (*EF*) and excess metal ($Metal_{ex}$) concentrations in peat mires (USC and DCC panel A) and Club Lake (panel B). Note for plotting convenience excess Sb in DCC is shown converted to the same number of data points as in USC (by averaging). In panel B, depth is plotted as a non-linear timescale and dates (AD) are indicated.

The average *EF* for metals in aerosols is shown in Figure 4.5a. Metals were enriched in aerosols in the order Ni (2.6) < Pb (3.5) < Co (3.6) < Cr (4.8) < Ag (12) < Mo (12) < Cu (13) < Sn (16) < As (24) < Cd (27) < Sb (48). *EF* in the aerosols varied seasonally, increasing during the austral winter and early spring (illustrated for Cr, Pb and Sb in Fig. 4.6). Wintertime *EF* were on average 3 times those of summer and coincided with reduced atmospheric dust concentrations. This pattern is consistent with the regional climatology (Chubb et al., 2011). During the austral

winter southern Australia experiences an increase of west to south westerly winds resulting in increased precipitation and reduced dust entrainment (McTainsh et al., 1998). The implication of this is increased *relative* transport of industrial metals over naturally derived metals and crustal elements contained in dust occurs during the winter, i.e. there is less atmospheric dust.

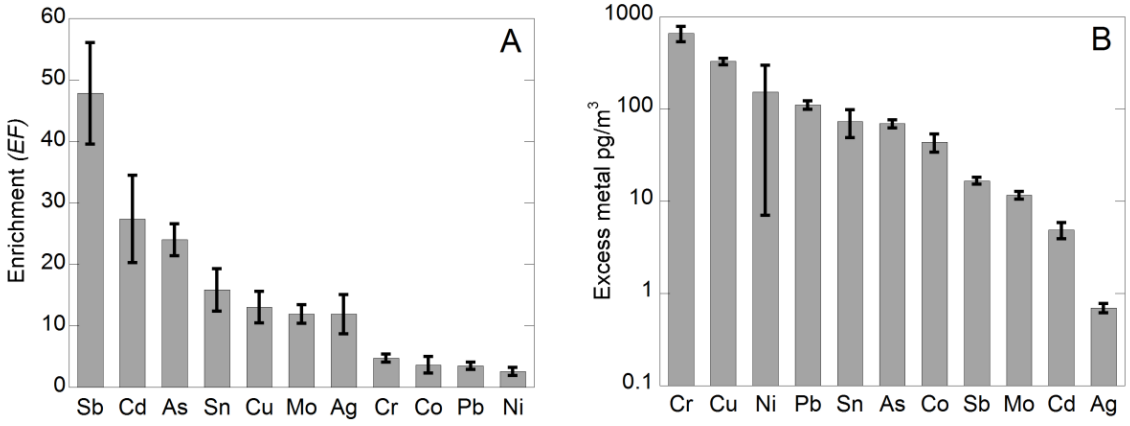

Figure 4.5 A) Mean enrichment factors (*EF*) for industrial metals in Snowy Mountains aerosols between 2012/2013. B) Mean excess industrial metal ($Metal_{ex}$) concentrations in the same aerosols. In both panels bars indicate standard errors.

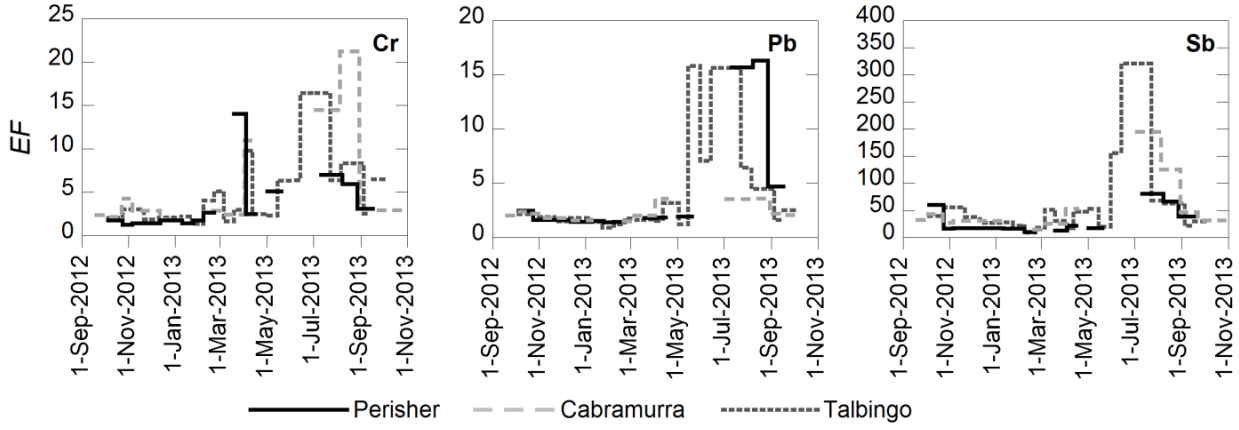

Figure 4.6 Time series of Cr, Pb and Sb enrichment (*EF*) in Snowy Mountains aerosols (September 2012-October 2013).

Excess atmospheric metal concentrations, i.e. the contaminant derived component, were calculated from equation 4.5:

$$Metal_{ex} = Cm-(Cm/EF) \quad (4.5)$$

The $Metal_{ex}$ concentrations range from (mean ± standard error) <1 pg m^{-3} ± < 1 (Ag) to 660 ± 125 pg m^{-3} (Cr) (Fig. 4.5b). The difference between *EF* and $Metal_{ex}$ reflects the relative natural concentration of each metal in the atmosphere, i.e. its relative concentration in upper continental crust. Consequently, for example Sb, which was highly enriched (*EF* = 48) was present at < 20 pg m^{-3}, 7 times less than the concentration of Pb (110 pg m^{-3}) with an *EF* of 3.5 (Fig. 4.5a and b). This is an important distinction in this context because the potential for contamination of the surficial environment by atmospheric contamination may be determined not only by the degree of enrichment, but also by the mass of industrial metal deposited to the surface.

In contrast to *EF*, $Metal_{ex}$ did not display a clear seasonal pattern (illustrated for Cr, Pb and Sb in Fig. 4.7) (although some wintertime enrichment is still apparent). This is explained by variability in atmospheric concentrations of industrial metals *relative* to natural dust.

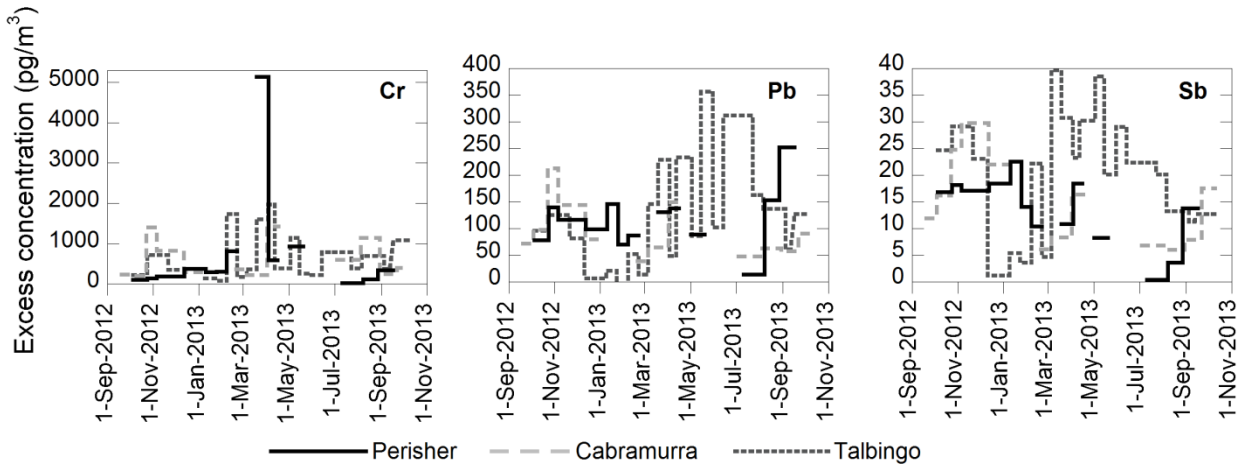

Figure 4.7 Time series of excess ($Metal_{ex}$) Cr, Pb and Sb concentrations in Snowy Mountains aerosols (September 2012-October 2013).

4.5.2 Aerosol and industrial metal deposition

The estimated average aerosol deposition rate during the sampling period (2012-2013) was ˜30 g m^{-2} y^{-1}. The flux for individual industrial metals, i.e. those enriched relative to MUQ (Fig. 4.4), varied by two orders of magnitude (Table 4.3), the range of enrichment being controlled by a

combination of the industrial emission load for a particular metal and its natural concentration within upper continental crust. Estimated deposition flux of enriched industrial metals (mid estimate and (range)) ranged from 5 (5-10) µg m^{-2} y^{-1} for Ag to a maximum of 4000 (3600-7900) µg m^{-2} y^{-1} for Cr (Table 4.3). Notably, several potentially toxic metals are estimated to be deposited to the soils, lakes and peats of the Snowy Mountains at rates greater than 1,000 µg m^{-2} y^{-1}, including Cr, Cu, Ni and Pb (Table 4.3).

Table 4.3. Estimated total and excess metal flux from the atmosphere to the surface of the Snowy Mountains

	Total Flux (µg m^{-2} y^{-1})[a]	Excess Flux (µg m^{-2} y^{-1})[a]
Cr	4000 (3600-7900)	3000 (2500-5500)
Co	300 (300-650)	200 (150-350)
Ni	2500 (2500-5000)	1000 (1000-2000)
Cu	2500 (2000-3500)	2000 (1500-3000)
As	500 (450-1000)	450 (400-950)
Mo	60 (60-120)	60 (50-100)
Ag	5 (5-10)	5 (5-10)
Cd	25 (20-45)	20 (20-40)
Sn	300 (300-650)	300 (250-600)
Sb	80 (70-150)	80 (70-150)
W	70 (60-140)	25 (25-50)
Pb	1100 (1000-2000)	700 (600-1100)

[a]Mid values and range (parentheses)

A proportion of total metal flux is derived from natural sources, i.e. from mineral dust. Therefore, a more accurate assessment of the contribution of industrial pollutants to the Snowy Mountains is provided by the $Metal_{ex}$ flux (equation 4.5). Estimated $Metal_{ex}$ flux to the Snowy Mountains as a proportion of the total flux (i.e. natural + industrial) ranges from 35-45% for Ni (where excess flux is 1000 (1000-2000) µg $m^{-2}y^{-1}$) to 98% for Sb (where excess flux 80 (70-150) µg $m^{-2}y^{-1}$) (Table 4.3). $Metal_{ex}$ fluxes were highly variable between the different industrial metals, ranging from 5 (5-10) (Ag) to 3000 (2500-5500) (Cr) µg m^{-2} y^{-1}. Excess Cr, Cu, Ni and

Pb were estimated to be deposited at rates close to, or greater than, 1000 µg m^{-2} y^{-1} implying *prima facie* that these metals may have the greatest impact on the Snowy Mountains environment (Table 4.3).

4.5.3 Industrial metal accumulation in peats and lakes

The results of metal accumulation and enrichment in the peat mires and Club Lake have been described in detail elsewhere (Marx et al., 2010; Marx et al., 2014b; Stromsoe et al., 2013) and are summarised in brief here only. The peat mires and Club Lake represent different examples of natural sedimentary archives which serve to show how metals are being incorporated into the surficial environment. For both the peat cores and the lake core, *EF* were calculated by comparing the chemistry of the pre-industrial section of each core (pre-1850) with the industrial section of the cores using equation 4.4.

Both peat cores displayed clear temporal trends in metal enrichment that broadly reflected the history of industrial activity in southern Australia, i.e. changing *EFs* through time are primarily a function of changing industrial activity (Marx et al., 2014b). Metal enrichment commenced in the peat cores at approximately 1890, with more significant enrichment occurring after 1980 (shown for Sb by way of example in Fig. 4.4A). In the figure, both peat mires record a sharp rise in Sb enrichment beginning at c.1890. After 1940 the *EF* becomes stabilised at approximately 3.5 in USC and 2 in DCC. The USC mire shows a further increase in *EF* to c. 4 after 1980 which continues to the present. Excess Sb ($metal_{ex}$) in both cores generally reflect these trends, although $metal_{ex}$ in DCC decreases after c. 1960 implying a reduction in industrial Sb deposition at that site.

The pre-1980 section of the core, therefore, reflected historical atmospheric industrial metal concentrations (Marx et al., 2010). By comparison, metal behaviour in the upper most section of the peat cores (post-1980) can be considered broadly comparable with the composition of the contemporary atmosphere (i.e. relatively, though not precisely, contemporaneous with the collected aerosol samples). The same suite of metals that were found enriched in the aerosols samples (Pb, Ag, Cr, Mo, Cd, Co, Cu, Ni, Sb, As, Zn and Sn) were also enriched in ombrotrophic peats (Fig. 4.8).

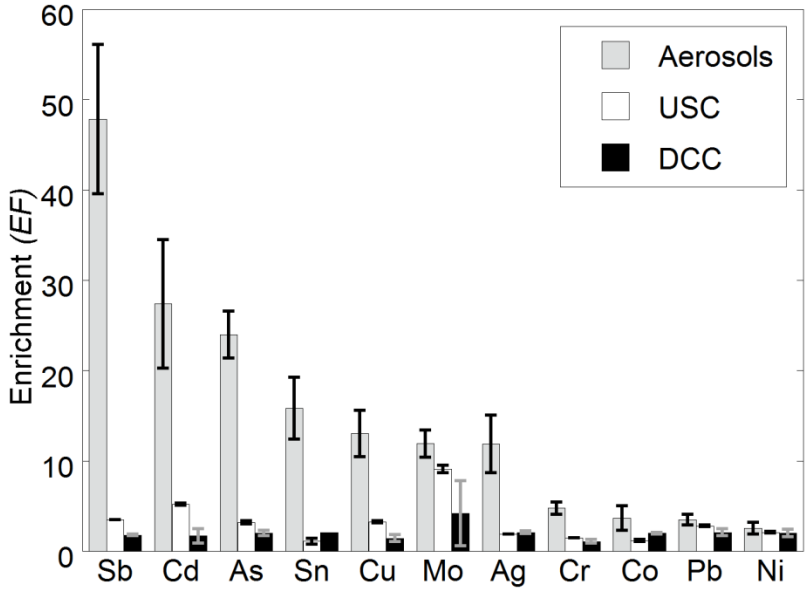

Figure 4.8 Industrial metal enrichment (*EF*) in peat mires post-1980 plotted beside aerosol enrichment (2012/2013) for comparison.

Average industrial (post-1850) *EF* were 2.1 and 1.7 in USC and DCC respectively, while post-1980 *EF* were 3.0 in and 2.2, respectively, meaning industrial metal concentrations have increased toward the present. Metals with average industrial *EF* > 2 in one or both cores were Mo, Cd, Sb, Cu, As, Pb, Ni, Co, Sn and Ag (*EF* are shown in Fig. 4.8). Metals were typically less enriched in post-1980 section of the peat cores by comparison to the collected aerosols by approximately 5 times in the USC and 7 times in the DCC (Fig. 4.8). However, the most highly enriched industrial metals in aerosols samples, i.e. those with *EF* > 10 (Sb, Cd, As, Sn, Cu, Mo, Ag) were generally also the most highly enriched metals in the peat cores.

EF were generally higher in the USC by comparison to the DCC by an average of 1.5 ± 0.3 times. This implies the mire from where the USC was collected receives higher atmospheric input and/or lower input of additional mineral matter (alluvial, colluvial sediment or local dust) than the Duck Creek mire, i.e. there is less dilution of the atmospheric signal. An exception to this general pattern was the behaviour of Ag and Ni where the *EF* were close to unity between the two mires, while Co was typically more enriched in DCC, displaying only minor enrichment

in USC. $Metal_{ex}$ concentrations were similarly typically higher in USC (e.g. Fig. 4.4), although at both sites they were more variable in comparison to *EF* through time. This difference is presumably largely a function of variability in the source(s) of mineral material deposited to the mires, including variability in the sources and relative contributions of long-range dust (e.g. see Marx et al., 2014b) and local sediment input.

By contrast with the studied peat mires, most industrial metals shown to be enriched in aerosols were not enriched within Club Lake sediments (Fig. 4.9). Industrial *EF* were ~1, i.e. there was no enrichment in industrial metals, for Cr, Co, Ni, Cu, Zn and Sn. Although some metals showed a more significant increase post-1980, average enrichment factors for most metals across this period were also ~1. Consequently, *EF* were on average 10 times less than in the aerosol samples. Relatively high rates of local unpolluted sediment generated from the sparsely vegetated cirque walls behind the tarn were concluded to be swamping input of pollutant metals resulting in comparatively low enrichment of lake sediments (Stromsoe et al., 2013).

In exception to the general behaviour of industrial metals, several industrial metals with low natural abundance, including Sb, Mo, As and Cd, displayed more substantial enrichment in Club Lake (mean post-1980 *EF* 2.1, 1.6, 1.3 and 1.4, respectively) (e.g. see Figure 4.4 and 4.9). The behaviour of Sb is shown by way of example in figure 4.4b. Antimony *EF* in Club Lake increases sharply after 1880 CE. They then stabilise at c.1940 CE at *EF*=2, with the uppermost samples exhibiting a further increase in EF. Overall the chronology of Sb *EF* in Club Lake was comparable to that recorded in the peat mires, however $metal_{ex}$ concentrations were significantly lower in Club Lake (Fig. 4.4). Arsenic and Mo displayed similar behaviour to Sb, however Cd showed enrichment in some samples but with greater variability though time. Silver also displayed minor enrichment over this time with *EF* reaching approximately 1.2 in the uppermost samples from the core.

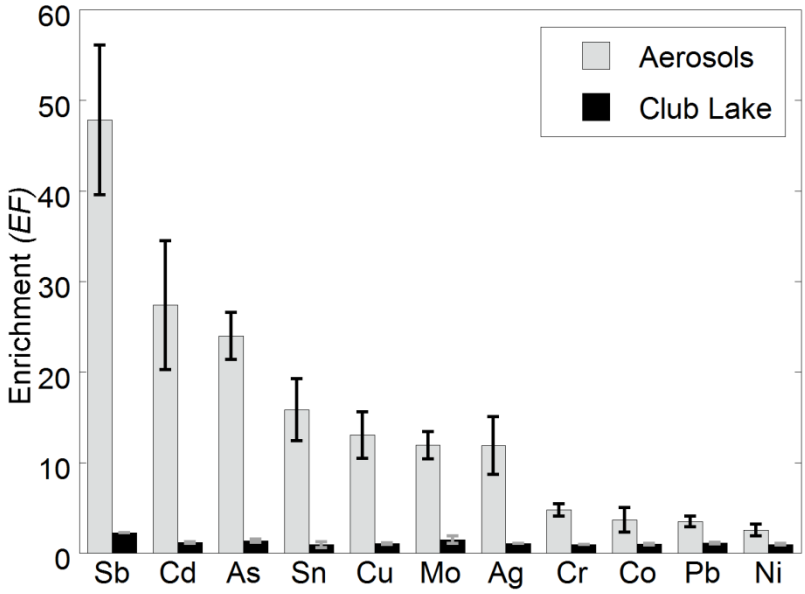

Figure 4.9 Industrial metal enrichment (*EF*) in Club Lake post-1980 plotted beside aerosol enrichment (2012/2013) for comparison.

4.5.4 Industrial metals in soils

Enrichment factors for the three soil profiles were calculated (using equation 4.4) relative to sediment samples from a core extracted in the Perisher Valley (Fig. 4.1). These Perisher sediments predate industrial activity and are considered representative of locally transported and eroded sediment in the Snowy Mountains (Marx et al., 2011). Three main *EF* patterns were apparent in the soil profile:

(i). First, Pb and Zn showed apparent generalised enrichment throughout each profile, with no clear change in *EF* with depth (e.g. Pb in Fig. 4.10A).

(ii) Cu, Ni and Cr showed enrichment at the bottom of each soil profile, however *EF* decreased toward the soil surface (e.g. Cu Fig 4.11A).

(iii) Mo, Cd, Sb and Ag showed no enrichment at the base of each soil profile, but recorded a pronounced up-profile increase in *EF* (e.g. Mo in Fig 4.10A). These metals also recorded the highest maximum *EF*. Arsenic patterns were inconsistent between the three soil profiles.

The age of the soil profiles is unknown. It is very unlikely, however, that the base of each soil profile, post-dates industrialisation in Australia, which accords with the onset of industrial

enrichment in the peat mires (see Fig. 4.4 and Marx et al., 2010). Apparent enrichment of metals in the base of the profiles (Fig. 4.10A) is therefore an artefact of relatively low concentrations of the conservative elements used to calculate the *EF*s (Sc, Ti, Ga, and Ta) in the soils relative to the Perisher sediments, e.g. the raw Pb concentrations in the ridge top soil are actually highest in the surface soil as opposed to the reverse pattern in *EF* shown in Fig. 10A. Calculating *EF* relative to element concentrations in the lower most soil sample for each profile therefore removes this apparent enrichment in the base of the soil profiles (e.g. Fig. 4.10B).

The observed low concentrations of conservative trace elements (e.g. Sc, Ti, Ga and Ta) in the base of the profiles arise from the unusual way alpine soils form in the Snowy Mountains. They are fed, at least in part, by dust deposition (Costin et al., 1952; Marx et al., 2011; McKenzie et al., 2004), the rates of input of which may exceed rates of physical and chemical weathering. Calculation of accurate *EF* relies upon the conservative behaviour of the normalising element(s) (Marx et al., 2008). In this case, however, the concentration of conservative elements varies markedly through the soil profiles, presumably as a function of relative dust input versus weathering loss. Comparing the change in relative industrial metal concentration through the profile may therefore further elucidate metal behaviour in the soils.

When the relative change in metal concentration through the soil is plotted, Mo, Cd, Sb and Ag again increase toward the top of each profile (e.g. shown for Mo Fig. 4.10C). Most of the other elements, however, show variability between the three soil profiles (e.g. as shown for Pb in Fig. 10D, profile locations shown in Fig. 4.2). Industrial metal concentrations in the uppermost (ridge-crest) soil profile increase toward the profile surface. In mid-slope profile, concentrations decline in the middle of the profile before recovering toward the top of the profile (e.g. Fig. 4.10D). However, whereas Cr, Pb and Sn reach unity at the surface, Co, Zn and most significantly Cu show relative concentration depletion (plot not shown). In the toe-slope profile the concentrations of most metals decline toward the surface (with the exception of Mo, Cd, Sb and Ag) (e.g. Pb in Fig. 4.10D).

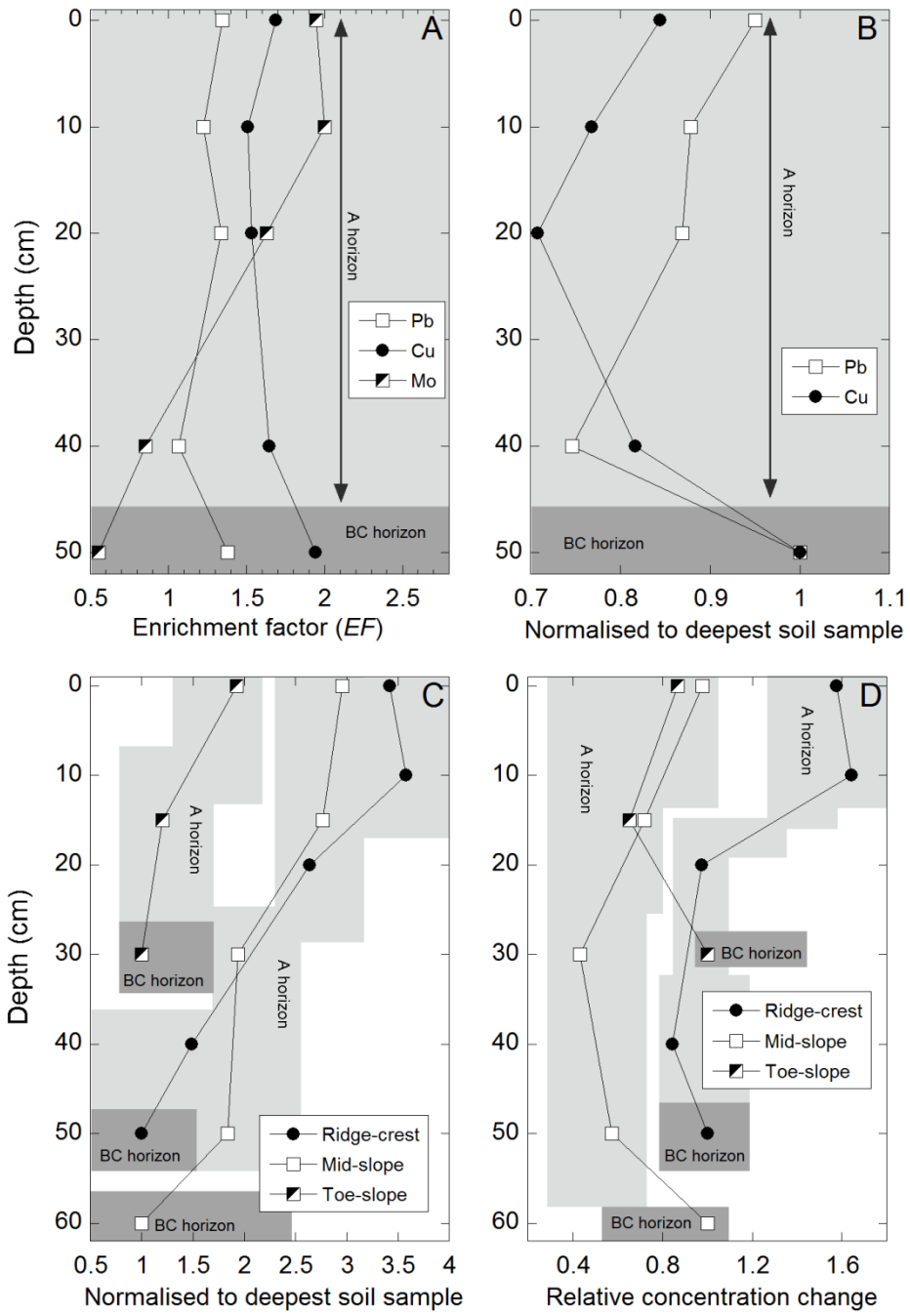

Figure 4.10 Industrial metal patterns in Snowy Mountains soils. A) Lead (Pb), Cu and Mo enrichment (*EF*) in the ridge-crest profile. *EF* was calculated relative to the Perisher core sediments. B) Copper (Cu) and Pb in the ridge-crest profile normalised to the deepest soil profile sample. C) Molybdenum (Mo) enrichment in each soil profile normalized to the deepest soil profile sample. D) Relative change in Pb concentration in each soil profile.

The overall impression, is, Mo, Cd, Sb and Ag show strong evidence of enrichment in the soils. Other industrial metals show some evidence of enrichment in the ridge-crest soil profile, whereas they may be depleted in the mid-slope and toe-slope profiles. Of these metals Cu shows the most significant degree of loss, implying it may be preferentially removed from the soils in this environment.

4.5.5 Age structure of the reservoir cores

Unsupported ^{210}Pb activities in both Geehi and Guthega reservoirs cores were relatively high (Supplementary Table 4.3 and Fig. 4.11). In order to construct robust age models using ^{210}Pb it is necessary that ^{210}Pb activities decrease consistently down core. In the Geehi Reservoir unsupported ^{210}Pb activities did not exhibit a decreasing profile in the top 100 mm. However, ^{210}Pb activity did decrease significantly between the data points at 95 and 155 mm depth from 364 to 215 Bq kg^{-1} (Fig. 4.11A). An estimate of sediment accumulation rates (0.08 g cm^{-2} year^{-1}) was calculated from these two points using the Constant Initial Concentration (CIC) model (Robbins and Edgington, 1975). Applying this mass accumulation rate to the whole core allowed sediment ages to be calculated (Supplementary Table 4.3, Figure 4.11). Due to the lack of reliable ^{210}Pb data, these ages can be considered approximate only.

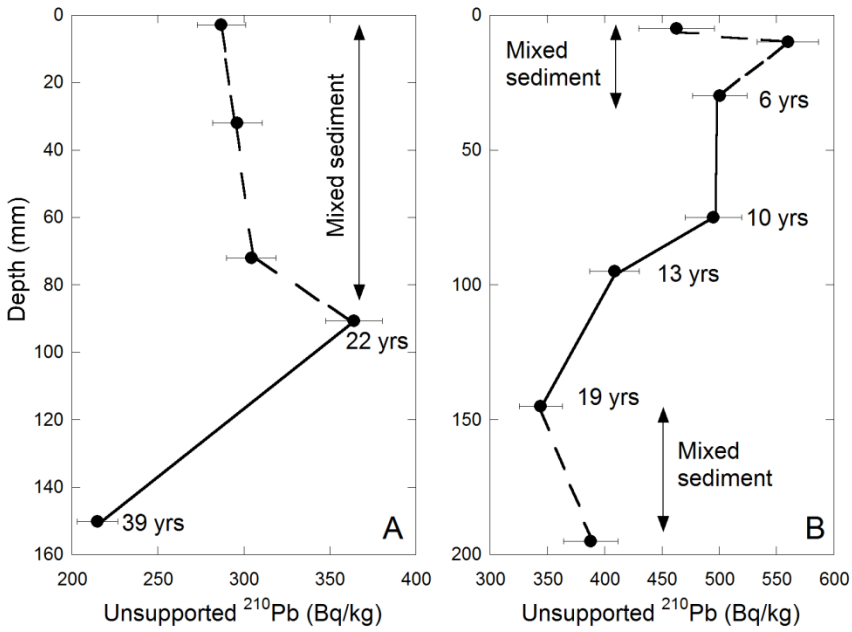

Figure 4.11 Unsupported ^{210}Pb activity profiles in cores collected from A) Geehi and B) Guthega reservoirs. Sediment ages (years) and regions where sediment mixing is likely are indicated on each panel.

In the Guthega Reservoir core unsupported ^{210}Pb activities exhibited a decreasing profile between 30 and 145 mm depth only (Fig. 4.11B). These data were used to estimate a mass accumulation rate for the whole core (0.26 g cm^{-2} y^{-1}), from which sediment ages were calculated (Supplementary Table 4.3, Fig. 4.11).

The unsupported ^{210}Pb depth typology (Fig. 4.11) for both reservoir cores, i.e. unsupported ^{210}Pb concentrations did not consistently decrease with depth, implying that either sediment in the reservoirs has experienced post-depositional mixing, or sediment of differing age/origin (with variable ^{210}Pb activity) has been deposited in the reservoirs at different times. In Geehi Reservoir results indicate sediment mixing and/or a complex origin of sediment, at least above 100 mm depth, while in Guthega Reservoir, these effects have influenced sediment above 30 mm depth and between 145 and 190 mm depth. As a consequence, calculated ages (which are shown in figure 4.12) must be treated with caution. In addition, or alternatively, the ^{210}Pb results also indicate the reservoirs may not record a true temporal deposition history, i.e. based on the basal ^{210}Pb ages Guthega is missing approximately 30 years of sediment.

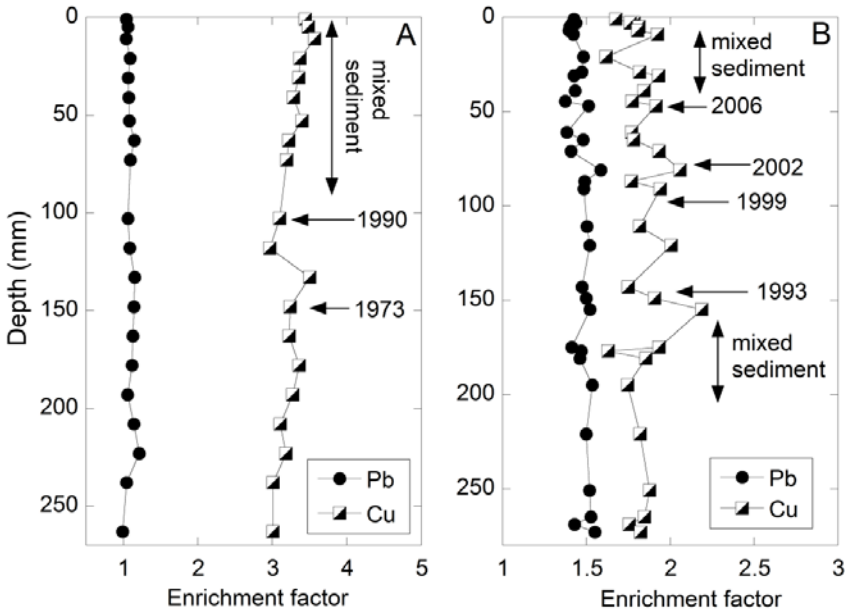

Figure 4.12 Lead (Pb) and Cu enrichment (*EF*); in A) Geehi and B) Guthega reservoirs cores. Ages (years AD) and regions of sediment mixing are indicated in each panel

4.5.6 Industrial metal accumulation in reservoirs

In contrast to the peats mires, which receive predominately atmospheric input, and to Club Lake, which has a small contributing catchment area (0.015 km^2), the reservoirs have significantly larger catchments (91 and 141 km^2 for Guthega and Geehi, respectively). They therefore receive significant catchment input and serve to show how industrial metals are being transported through, and accumulating in the wider surficial environment.

Due to difficulties in establishing the precise age of deposited sediment, *EF* values were calculated from the average enrichment across all samples analysed in the two cores. The reservoirs do not contain pre-industrial sediment (they were constructed after 1850 CE). Therefore metal enrichment was calculated relative to sediment from the core extracted in the Perisher Valley (Marx et al., 2011), using equation 4.4.

Despite uncertainty in the age of the reservoir sediments, calculated *EF* values for both reservoirs clearly demonstrate that many industrial metals found to be enriched in both the aerosol samples and the peat mire sediments (and to a lesser extent the Club Lake sediment) were not enriched in reservoir sediments. These were Pb (e.g. Fig. 4.12A), Ni, Cr and Sn in Geehi reservoir and Ni, Cr and Co in Guthega reservoir (Fig. 4.13). A number of other metals, however, showed more substantial enrichment. In Geehi reservoir As, Cd, Ag, Mo and Cu (e.g. Fig. 4.12A) are enriched by an average of 5.9, 6.4, 4.0, 3.6 and 3.3 times respectively, while in Guthega Reservoir they are enriched by 2.7, 3.8, 3.2, 2.5 and 1.8 times respectively (Figs. 4.12 and 4.13).

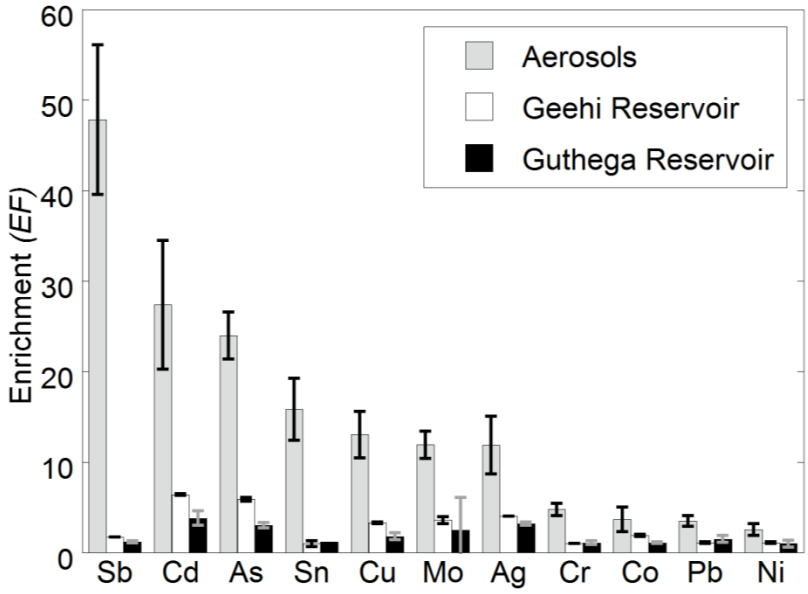

Figure 4.13 Industrial metal enrichment (*EF*) in reservoirs (Geehi and Guthega) plotted alongside aerosol enrichment (2012/2013) for comparison.

4.6 Discussion

In the following sections the results are discussed from the input of industrial metal (via enriched arosols) through the various studied landscape repositories. These include the rainfall fed peat mires and the alpine tarns and soils, located in the upper parts of catchments and soils and reservoirs located lower in the same catchments. Differences in relative enrichment between the source aerosols and each surface repository provides an opportunity to examine how industrial metals are being incorporated into and transported through the environment.

4.6.1 Metal enrichment in aerosols; contributing sources and comparisons

Aerosols in the Snowy Mountains were significantly enriched in pollutant metals known to be perturbed in the global atmosphere due to emissions from stationary fossil fuel combustion, (the primary source of Cr, Sb, Sn, Mo), non-ferrous metal production (the primary source of As, Cd, Cu, Pb, Ni, Zn, Ag) and fertilizer application (an additional source many metals including As, Cd, Cu, Pb, Ni and Zn) (Pacyna and Pacyna, 2001; Rauch and Pacyna, 2009). Patterns in aerosol metal enrichment evident in this study are broadly similar to that previously found within peat mires in the Snowy Mountains, where metal pollutants were shown to derive primarily from mining, metal production and coal combustion within the south-eastern Australian airshed (Marx

et al 2010). The same suite of industrial metals present in the peat mires were enriched in the aerosols samples, although the relative order and magnitude of enrichment differed. The industrial metals most enriched in aerosols were Sb, Cu, As, Cd. These have the highest contemporary emission rates from industrial sources within Australia (NPI, 2003) relative to their natural preindustrial concentrations, again implying that aerosol enrichment in the Snowy Mountains reflects regional industrial contamination.

The concentration of pollutant metals in the atmosphere over the Snowy Mountains is generally within the same order of magnitude as that previously reported for an alpine site in New Zealand (Marx et al., 2014a) but approximately 1-2 orders of magnitude greater than concentrations recorded at more remote Southern Hemisphere sites, including Samoa (Arimoto et al., 1987b) and Antarctica (Dick, 1991) (Table 4.2), reflecting the relative proximity of the Snowy Mountains to industrial emission sources.

4.6.2 The atmospheric contribution of industrial metals

In the absence of local catchment sources, deposition of aerosols enriched in industrial metals represents the most significant source of contamination to the Snowy Mountains. The estimated total aerosol flux to the Snowy Mountains during 2012-2013 was ~30 g m^{-2} y^{-1}. This value is similar, albeit slightly lower, than the 1980-2006 dust deposition rate of 49 g m^{-2} y^{-1} estimated in the USC peat using a mass-balance geochemical model (Marx et al., 2014b). The slightly lower deposition rate reported here may reflect changing dust transport rates in response to changing climate conditions across south eastern Australia. The two years leading up to the 2012/13 sampling periods were among southern Australia's wettest (BOM, 2014a), implying less favourable conditions for dust entrainment, i.e. increased soil moisture and vegetation cover. In addition, average dust deposition in the peat mire was enhanced by prolonged drought in the early to mid-2000s and significant drought during strong El Niño events in 1982-83 and 1987 when large dust storms occurred (Marx et al., 2014b; McTainsh et al., 1989; Raupach et al., 1994).

Deposition flux in the Snowy Mountains is above the global range (1-25 g m^{-2} y^{-1}) shown for sites at intermediate distance (10-1000 km) from significant regional (North America, South Africa, South America and Australia) dust source areas (Lawrence and Neff, 2009). This is consistent with Australia being arguably the largest dust source in the Southern Hemisphere

(Shao et al., 2011) with the lower Murray Darling Basin, upwind of the Snowy Mountains, being one of Australia's major dust producing regions (Hesse and McTainsh, 2003). Dust fluxes are, however, similar to those calculated for other relatively humid, eastern areas of the MDB (31-33 g m^{-2} y^{-1}) (Cattle et al., 2009; McTainsh and Lynch, 1996). The overall similarity between these previously published values and the results of this study (~30 g m^{-2} y^{-1}) supports the appropriateness of the deposition rate estimates. While the exact flux of individual trace elements is uncertain, the estimates appear a reasonable approximation of atmospheric deposition relative to local, surface-derived inputs.

There are few previous estimates of pollutant metal flux within the Australian region. Deposition flux reported for metropolitan areas are substantially higher than those in the Snowy Mountains. For example, the mid-range estimates of Cu and Pb deposition in the Snowy Mountains are 3-60% (Cu) and 3-25% (Pb) of rates reported for metropolitan Sydney (approximately 350 km NW of the Snowy Mountains) (Davis and Birch, 2011). By contrast, fluxes of industrial metals in this study are generally 1-2 orders of magnitude greater than in alpine and remote marine sites in New Zealand (approximately 2,000 km west of the Snowy Mountains) (Arimoto et al., 1990). Thus on one hand, low metal fluxes to the Snowy Mountains, by comparison to metropolitan areas, reflects their remote location and lack of local point sources, while on the other hand, high metal flux by comparison to other remote locations reflects the proximity of significant industrial sources on the Australian continent.

4.6.3 Metals concentrations in peat mires

Of the sedimentary archives examined in this study, the peat mires are generally considered to most accurately reflect rates of atmospheric industrial metal input. This is by virtue of their high *relative* atmospheric input in comparison to the other studied environmental repositories (soils, lakes and reservoirs). In addition, atmospherically deposited metals are likely to be fixed on the organic peat surface due to the availability of numerous exchange sites on which metals can be bound (Steinnes and Friedland, 2006). For this reason, the fidelity with which peat mires record the state of the atmosphere has enabled them to be used widely to examine both the history of atmospheric contamination and natural dust transport and deposition (Le Roux et al., 2012; Marx et al., 2014b; Marx et al., 2009; Shotyk et al., 2002; Weiss et al., 2002). In the Snowy Mountains, the fidelity of peat mires has been previously demonstrated by agreement between the temporal

patterns in metal enrichment recorded in the peat cores with the generalised history of industrial development across south-eastern Australia (Marx et al 2010). The high atmospheric fidelity of the peat mires is demonstrated further by the approximate equivalence in the order of trace metal enrichment between the aerosol samples and the studied peat mires. That is, those metals most enriched in aerosols (Cu, As, Mo, Ag, Cd, Sb) are also those most highly enriched in peat mires (especially in the more ombrotrophic USC).

Despite the fact that metal enrichment patterns are comparable between the aerosols and the peat mires, there are some significant differences. For example, industrial metal *EF* in the peat mires does not reflect the magnitude of atmospheric aerosol enrichment, with *EF* in peats being systematically reduced by an average of 5-7 times. Moreover, averaged across all enriched industrial metals, the measured annual accumulation rate, (that is the total volume of metals in the peat), in the USC peat mire between 1980-2006 CE was only (mid estimate and (range)) 80 (40-90) % of the estimated aerosol deposition rate. While this suggests some possible loss of deposited metals from the peat, these differences may simply reflect the timing and temporal resolution of the peat records by comparison to those of the collected aerosols. As already noted, dust deposition flux estimated by the current study was lower than that measured in USC peat mire between 1980 and 2006. Consequently, part of the relatively low *EF* in the peat mires may arise from relatively higher natural dust loads which dilute the metal contaminant concentrations. Furthermore, incorporation of metals into the peat mires over several years is likely to smooth peaks in atmospheric metal concentration observed in the weekly to monthly aerosol samples. This is supported by the relatively large reduction in *EF* factors between the aerosol samples and the peat mires for the most highly enriched industrial metals (Cu, As, Cd, Sn, and Sb). In addition, higher metal *EF* variability occurred in the aerosols, implying their higher *EF* are relatively more strongly influenced by high contaminant days.

Particle size fractionation effects may additionally contribute to the difference in *EF* between the aerosols and peat mires (Chester et al., 1999). Atmospheric fall-out is dominated by larger particles, which are typically less enriched in industrial metals. This effect has been shown to result in relative depletion during dry deposition by comparison to bulk *in situ* (atmospheric) aerosol by a factor of between 1.8 and 9.9 (Chester et al., 1999). In this study, the *EF* difference between aerosols and peats ranges from 1.2 less times for Ni to 26 times less for Mo, with an average of 6 times less across the two peat mires.

The concentration of individual industrial metals within peat mires may also be controlled by factors specific to individual elements, such as the relative concentration of each element in aerosols compared to locally sourced sediments. For example, the difference in concentration between collected aerosol samples and non-enriched ('natural') local sediments is comparatively greater for Sb by comparison to Mo, i.e. 13 and 9 times, respectively. This implies local non-contaminated sediment delivered to the peat mires will dilute the concentration of industrial Sb more strongly than that of industrial Mo. This effect is likely to contribute to the observed differences in the relative *EF* depletion of Sb and Mo in peat mires compared to aerosols (Sb *EF* is 20 times less in peat mires relative to aerosols samples while Mo is only depleted by a factor of 2 These differences suggest other factors such as efficiency of dust scavenging of individual metal pollutants, pollutant metal phase and oxidation state, particulate size as well as conditions in the peat mires themselves, e.g. moisture content, pH and redox state, may also be important influences on how effectively atmospherically derived industrial metals are incorporated into the peat mires. Despite these differences, in this study industrial metals within peats can be considered broadly representative of atmospheric input.

4.6.4 Industrial metals in Club Lake

By comparison with the peat mires, Club Lake sediments respond far less sensitively to atmospheric input of industrial metals (Stromsoe et al., 2013). Consequently, only those industrial metals which have very low natural sediment concentrations (Sb, Mo, Cd and As) show significant enrichment (maximum *EF* >1.5) in Club Lake. Metals that are highly enriched in aerosols, but present in naturally high concentrations were not found to be enriched. Notably of the elements with the highest excess atmospheric deposition flux (Cr, Ni, Cu, Pb) only Pb displayed possible minor enrichment in Club Lake sediments.

Enrichment factors for even the most highly enriched industrial metals in Club Lake were considerably lower than in the aerosol samples, i.e. 8, 18, and 21 times less for Mo, As and Sb, respectively. This highlights the subdued response of the lake even to relatively high levels of atmospheric enrichment. In addition, metal *EF* in the lake were reduced relative to the peat mires by an average of 2.4 times, suggesting this difference is unlikely to be explained by processes common to both environments such as particle size fractionation during atmospheric deposition.

As discussed in Stromsoe et al., (2013) and Chapter 3, the lack of observed industrial metal enrichment in the Club lake is explained largely by the fact that catchment derived sediment greatly exceeds atmospheric input. Overall the estimated atmospheric deposition of industrial metals (i.e. those enriched in aerosol samples) contributed an average of 35% (or 30-60% depending on the estimation method) of their concentration in the lake sediments. By comparison, atmospheric input is largely the only source of sediment in the peat mires (Marx et al., 2011). The additional 'natural' contribution of these metals is supplied by sediment derived from the lake catchment, which, considering the generally low level of enrichment must be largely free of excess industrial metal. It is therefore likely to be derived from subsurface sediment or freshly weathered material.

The exception to this is the enrichment of a number of industrial metals in Club Lake (e.g. Sb, Mo, Cd and As) which can be attributed, in part, to their enrichment sensitivity. An impression of the *relative* sensitivity of different industrial metals can be provided by comparing the increase in concentration required to produce an *EF* of 2 times background concentrations. This is achieved by dividing the background (natural) concentration of each industrial metal by their mean (background) concentration (equation 4.6).

$$Metal_{sens} = (C_m/C_{mean}) * 100 \quad (4.6)$$

where $Metal_{sens}$ is metal sensitivity, C_m is background concentration of a particular metal in the Perisher (pre-industrial) sediments which also displays enrichment in the aerosol samples and C_{mean} is the mean background concentration of all metals in the Perisher sediments, which are similarly enriched in the aerosol samples.

The relative sensitivity of industrial metals to contamination is shown in Table 4.4. The industrial metals most enriched in the lake sediments (Cd, Sb, Mo and As) are all relatively sensitive to enrichment. This means a small increase in their concentration will result in enrichment. For example, to enrich Sb two times in this context requires an anthropogenic contribution of only 121 µg/kg. Copper by contrast requires environmental concentrations to increase by approximately 28,000 µg/kg and Sn by 9,000 µg/kg. Silver is also relatively sensitive and showed minor enrichment in Club Lake (*EF*<1.5).

Table 4.4 Relative sensitivity of industrial elements to enrichment

	Relative sensitivity* (%)
Ag	0.2
Cd	0.4
Sb	1.1
Mo	1.4
As	8
Co	64
Cu	70
Ni	104
Pb	144
Cr	323
Zn	382

*Relative sensitivity is the concentration increase required to produce an EF of 2

4.6.5 Industrial metals in soils

In contrast to the other environmental archives, calculating *EF* in the soil samples is not straight forward due to variability in the behaviour of conservative elements against which enrichment is compared (Ta, Ti, Sc and Ga). This variability is presumably due to weathering/erosion loss in parts of the soil profile versus input of aeolian dust in the upper profile (Costin et al., 1952; Marx et al., 2011). Despite this difficultly, there is evidence of industrial metal enrichment in the soils. The most obviously enriched metals were Cd (*EF* ~3.4-5), Mo (*EF* ~2-3), Ag (*EF* ~0-4) and Sb (*EF* ~1-2). Enrichment factors in the upper section of the soils profiles are comparable to those of the studied peat mires for Cd and Ag, however Mo and Sb values are lower reflecting their lower relative sensitivity to enrichment (Table 4.4) and implying they are being diluted by additions of natural sediment. Previous studies have demonstrated that, even in areas proximal to emission sources, the identification of industrial metals in soils may be complicated by high background concentrations, or by natural variability within the soil profile (Barbieri et al., 2014). In the Snowy Mountains the obvious enrichment of Cd, Mo, Ag and Sn over other metals with

significant anthropogenic sources reflects their relative sensitivity to enrichment, i.e. low background concentrations in local regolith.

Metals enriched in the aerosols and peat mires, but with relatively low enrichment sensitivity (Pb, Zn, Cu, Ni, Cr), display more complex patterns in the soils. The soil profile closest to the ridge crest contains higher metal *EF* due to its landscape position. Increasing depletion (indicated by $EF < 1$) of these elements downslope is consistent with increasing dilution from 'natural' sediments due weathering, geomorphic processes and/or reduced dust input. There is some evidence of potential eluviation of industrial metals in the soils (Fig. 4.11), i.e. development of a rudimentary E horizon at 200-500 mm depth with an illuvated zone at 500-600 mm depth. While these soils have been previously noted for a distinctive lack of visual evidence of podzolization (Costin et al., 1952; McKenzie et al., 2004), subtle podsolization is however apparent in the ultra-high resolution trace element data presented here.

The concentration of these metals in the A0 and A1 soil horizons (0-10 cm) is approximately 1.5 to 2 times less than in the peat mires. The age of this horizon is unknown. Given the relatively slow rate of vertical accumulation in the peat mires, i.e. 50-150 mm in 120 years, it is likely to integrate the whole history of industrial metal contamination during which metal *EF* in the peat mires has increased from approximately 1 to 5 (Marx et al., 2014b). Consequently, concentrations and *EF* in the A1 soil horizons are diluted by comparison to the post-1980 peat records as they integrate over a longer period including lower industrial metal input (1880-2006 AD; Marx et al., 2010). While it is not possible to reliably correct for this effect, a comparison of the pre and post 1980 *EF* in the peat mires, imply industrial metal input to the top of the soils may be equivalent to that of the peats mires.

There is evidence of loss of some metals from the soil, as shown by the depletion of industrial metals in the upper soil compared to the parent material, most notably for Cu, and to a lesser extent Ni and Zn and possibly Pb, Cr and As in the toe slope soil profile. This is approximately in accordance with the relative geochemical mobility of these elements in soils, which increases in the order Pb < Cr < As < Ni < Zn < Cu (Allison and Allison, 2005). Depletion of this same suite of metals was reported for Swiss forest soils (Blaser et al., 2000). Blaser et al. (2000) describe this as the net outcome of the opposing forces of depletion due to leaching and

enrichment due to deposition and it is proposed this is similarly occurring in the Snowy Mountains.

4.6.6 Industrial metal enrichment in reservoirs

The reservoirs examined in this study are located down catchment from the other archives. Because of their relatively large catchment to lake area ratios they receive relatively little direct atmospheric input, i.e. 7 (5-10) and 15% (10-25%) of total accumulation in Guthega Reservoir and Geehi Reservoir, respectively. Total sediment accumulation rates are relatively high at 700 and 2600 g m^{-2} y^{-1} for Geehi and Guthega Reservoirs, respectively. By comparison, total accumulation in Club Lake is 330 g m^{-2} y^{-1} and < 50 g m^{-2} y^{-1} in the peat mires. As a result, direct atmospheric deposition is only a minor source of industrial metals to the reservoirs, explaining the lack of fidelity between aerosols and reservoir *EF*.

Industrial metals found in the reservoirs are unlikely to be contemporaneous with the aerosol samples collected in this study. This is because industrial metals were accumulating in the surface soils during the preceding 70 years before reservoir construction. These older metals, which have been stored within the catchment, may be transported to the reservoirs at any point following their deposition. This implies the metal history of even the youngest sediments in the reservoirs could represent a mixture of historical metal deposition patterns (see Marx et al., 2010) in the Snowy Mountains. Hence some of the differences in metal enrichment in the reservoirs compared to, for example, the peat mires may be attributable to historical patterns in the atmospheric deposition of industrial metals.

Given that direct atmospheric deposition is only a minor source of industrial metal input in the reservoirs, it is unsurprising that metal *EF* patterns in the reservoirs mostly closely resemble those found in the soil samples. This is shown in Table 4.5, where the average concentration of each industrial metal in the reservoirs relative to the conservative elements (Ta, Ti, Ga and Sc) is divided by its average relative concentration to the same elements in the soils.

This general agreement in *EF* between the soil samples and the reservoir sediments further suggests that the sediment accumulating the reservoirs is largely derived from catchment top soil. If the reservoir sediment consisted of, for example, significant subsoil (which is less contaminated by industrial metals) or freshly weathered material, relative depletion of industrial metals would be expected by comparison to the top soil samples. Thus, reservoir sediments, like

the catchment soils, are generally most highly enriched in relatively enrichment sensitive metals (Mo, Cd, Sb, As and Ag). However, Table 4.5 also demonstrates possible additional enrichment (Co, Cu, Zn, As, Mo, Ag, Cd) or depletion (Cr, Sn, Pb) in metals in the reservoirs relative to the soils. These same groups of industrial metals are enriched or depleted in the reservoirs relative to their behaviour in the peat mires (with the exception of Mo and Co which are relatively enriched in reservoirs compared to the soil samples, but depleted relative to the peat mires).

The patterns in relative metal enrichment and depletion in the reservoir sediments may be attributed to differences in metal particle affinity and solubility. The partition coefficients of industrial metals in soils decrease in the order Cr >Pb >As >Ni >Sn >Zn >Cd >Ag >Cu >Sb >Co >Mo (Allison and Allison, 2005). In general, more highly particle reactive and less soluble metals, such as Pb and Cr are relatively depleted in the reservoirs, whereas less particle reactive, more mobile elements such as Zn, Cd, Ag, Cu and Mo are relatively enriched (Table 4.5). The behaviour of the metalloids, Sb and As, is more variable. Antimony is relatively mobile, however, it is enriched only in Geehi Reservoir, while As is relatively particle reactive but is enriched in the reservoirs over the soils.

Overall, however, the difference between the soils and the reservoirs implies that relatively immobile industrial metals (e.g. Pb), may be trapped within the soil matrix following deposition from the atmosphere. In contrast, more mobile metals such as Cu may be more readily transported, resulting in comparative enrichment or depletion of these elements in reservoir sediments. This assertion is supported by the soil data. Copper concentration is lower in the A1 horizon and is reduced down slope, implying it is being depleted from the soils. In addition, overall Cu is higher in the reservoirs than the catchment soils (Table 4.5). Zinc, Mo, Ag and Cd are also relatively enriched in the reservoirs; however, of these only Zn shows evidence of depletion in the soils and it is significantly less pronounced than for Cu. The uptake of Cu and Zn by vegetation (Gandois, 2010) may play a part in these patterns, as organic matter may be preferentially being transported (over mineral sediment) from the highly organic alpine soils.

Table 4.5. Industrial metal enrichment in Geehi and Guthega reservoirs relative to topsoil concentrations

	Guthega Reservoir	Geehi Reservoir
Cr	0.9	0.8
Co	1.3	1.7
Ni	1	1.1
Cu	1.2	2.1
Zn	1.2	1.3
As	1.5	2.2
Mo	1.1	1.6
Ag	1.1	1.3
Cd	1.3	1.8
Sn	0.8	0.6
Sb	0.9	1.4
Pb	0.9	0.7

The patterns in relative metal enrichment and depletion in the reservoir sediments may be attributed to differences in metal particle affinity and solubility. The partition coefficients of industrial metals in soils decrease in the order Cr >Pb >As >Ni >Sn >Zn >Cd >Ag >Cu >Sb >Co >Mo (Allison and Allison, 2005). In general, more highly particle reactive and less soluble metals, such as Pb and Cr are relatively depleted in the reservoirs, whereas less particle reactive, more mobile elements such as Zn, Cd, Ag, Cu and Mo are relatively enriched (Table 4.5). The behaviour of the metalloids, Sb and As, is more variable. Antimony is relatively mobile, however, it is enriched only in Geehi Reservoir, while As is relatively particle reactive but is enriched in the reservoirs over the soils. Overall, however, this implies that relatively immobile industrial metals (e.g. Pb), may be trapped within the soil matrix following deposition from the atmosphere. By contrast, more mobile metals such as Cu may be more readily transported, resulting in comparative enrichment or depletion of these elements in reservoir sediments. This assertion is supported by the soils data. Copper concentration is lower in the A1 horizon and is

reduced down slope, implying it is being depleted from the soils. In addition, overall Cu is higher in the reservoirs than the catchment soils (Table 4.5). Zinc, Mo, Ag and Cd are also relatively enriched in the reservoirs; however, of these only Zn shows evidence of depletion in the soils and it is significantly less pronounced than for Cu. The uptake of Cu and Zn by vegetation (Gandois, 2010) may play a part in these patterns, as organic matter may be preferentially being transported (over mineral sediment) from the highly organic alpine soils.

The differences in metal enrichment between the two reservoirs appear to be partly a function of contributing catchment area. Enrichment factors for the most enriched metals, Cd, Mo, Cu, As are higher in Geehi by 1.7, 1.4, 1.8 and 2.0 times, respectively. This is broadly equivalent to the difference in catchment area, with Geehi Reservoir 1.7 times larger than Guthega Reservoir.

4.6.7 Summary and implications

In this study, three factors appear to be of most importance in controlling metal enrichment patterns within different environmental archives in the Snowy Mountains. These are; 1) the relative contribution of atmospheric input; 2) the sensitivity of individual metals concentrations to perturbation from industrial contributions and; 3) the behaviour of individual metals. These factors are shown in Figure 4.14, where the enrichment patterns of Pb, Cu and Sb through the catchments of the Snowy Mountains are demonstrated.

Aerosols sampled in this study were enriched in industrial metals by an average of 15 times background concentrations, further confirming the widespread perturbation of industrial metals in the atmosphere. A comparison of calculated deposition flux with accumulation rates in the peat mires, the environment dominated most significantly by atmospheric deposition, implied depletion of industrial metals occurred during deposition, possibly via size fractionation, with an additional reduction in *EF* in sedimentary environments due to dilution with uncontaminated material. Despite a reduction in *EF* by 5-7 times between the aerosols and the peat mires, industrial metal enrichment was found throughout the Snowy Mountains catchments.

All else being equal, the degree of metal enrichment in the various sedimentary environments sampled (peat mires, soils, lakes and reservoirs) was a function of the *relative* contribution of atmospheric aerosol input versus that of terrestrially derived sediment. Consequently, ombrogenous peat mires and soils (particularly those closer to ridge crests), which in the Snowy Mountains are partially fed by dust, tended to record the highest enrichment in industrial metals

(Fig. 4.14). A reduction in metal *EF* therefore generally occurs down catchment (Fig. 4.14). However, geomorphically active environments (with higher sediment yields) which produce uncontaminated sediment (e.g. cirques) have reduced metal enrichment due to dilution.

The sensitivity of metals to enrichment was found to be a key influence on the *EF* patterns between industrial metals. Metal sensitivity in this context was controlled by the background concentration of the metal versus its relative degree of perturbation by industrial processes. Metals with low natural abundance (Cd, Ag, Sb and Mo) were found to be consistently enriched within all the sedimentary environments examined (for example Sb in Fig. 4.14), because relatively lower industrial input by weight is required to raise their excess contribution over their natural concentration.

The behaviour of individual metals also influences patterns of enrichment within the surficial environment. In contrast with the general behaviour of most industrial metals, which showed reduced enrichment down catchment, was the behaviour of Cu and Cd (and to a lesser degree Zn) (Fig. 4.14) which were more enriched in the reservoirs than in catchment soils. Combined with evidence of Cu loss from the soils, this implies preferential transport of the most mobile industrial metals down catchment and their subsequent accumulation (and therefore concentration) in aquatic sedimentary systems. This stands in contrast to the most particle reactive metals such as Pb, which appear to be more strongly held within the soil matrix. Metals including Pb and Cr therefore experience lower relative transport rates, at least in the alpine setting of the Snowy Mountains. They are most enriched in the atmospherically dominated environments and therefore display down catchment dilution.

The presence of enriched industrial metal in all the sampled environments demonstrates that they are widespread in this otherwise relatively pristine alpine environment and that, in the case of some metals, are mobile in the environment. Examining the implications of these metals in the Snowy Mountains is beyond the scope of this paper, however, comparing them to critical pollutant loads, i.e. the interim sediment quality guidelines (ISQG) for Australia and New Zealand (ANZECC and ARMCANZ 2000), provides an assessment of their likely impact. These guidelines provide trigger values above which metal concentrations are considered deleterious.

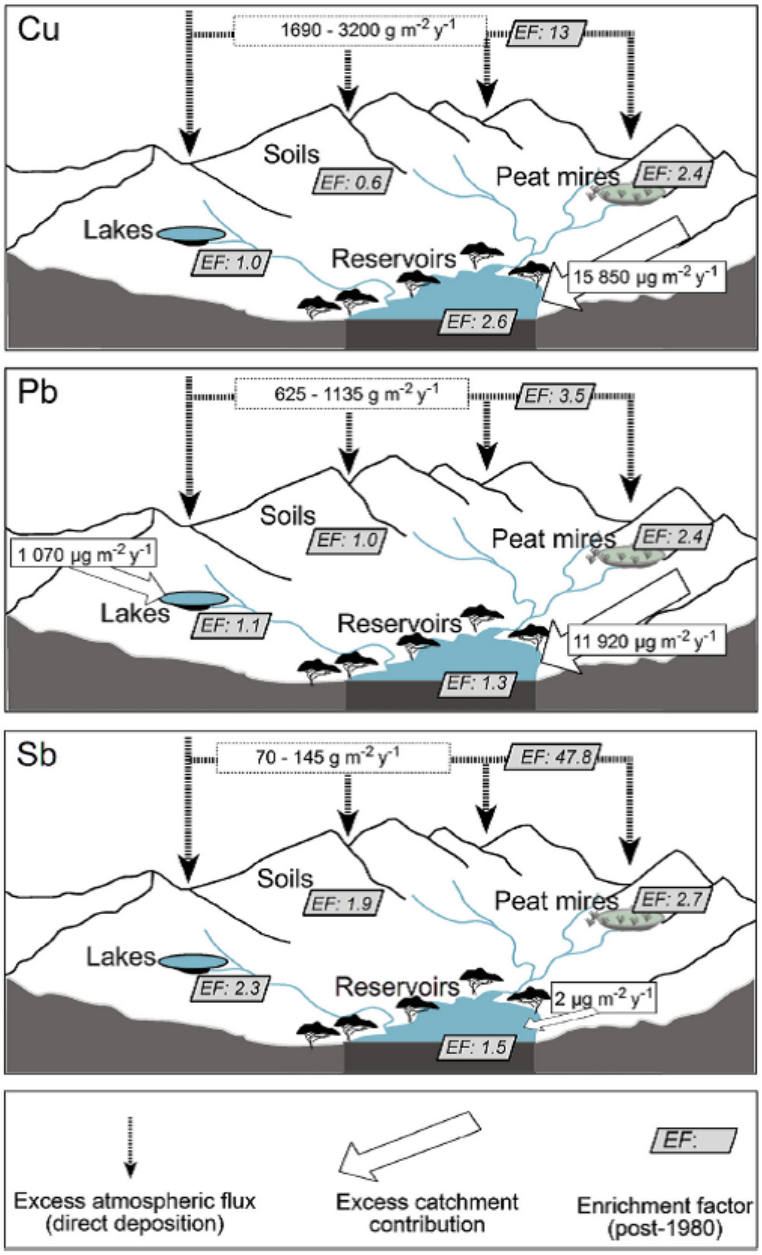

Figure 4.14. Industrial metal mass flux and metal enrichment (*EF*) patterns in the Snowy Mountains; shown for Pb (top panel), Cu (middle panel) and Sb (lower panel).

Excess industrial metal concentrations in the Snowy Mountains were generally below the ISQG trigger values (Table 4.6) in all the studied environments implying no significant ecotoxicity effect is occurring. However, Cr and Ni concentrations in Club Lake did exceed trigger values. These metals were not however found to be enriched in Club Lake. Therefore their high concentration in sediments is derived from their naturally high concentration in catchment source

rocks. In other environments Ni is close to trigger values as is Pb (Table 4.6). Industrial metals are known to be increasing in the Snowy Mountains (Fig 4.4 and 4.12), consequently, calculating the increase in industrial metal input required to reach the threshold of the ISQG trigger values provides a perspective on the sensitivity of the environment to be impacted by metal pollutants.

The required increase is calculated for each archive (peat mires, lake and reservoirs) according to equation 4.7.

$$RI = ((C_T - C_{TS}) + C_{ES})/C_{ES} \quad (4.7)$$

where RI is the required concentration increase in metal pollutant, C_T is the trigger value, C_{TS} is current concentration of the element in the sediment and C_{ES} is the excess concentration of that element in the sediment.

Table 4.6 shows the estimated additional atmospheric flux required to raise sediment metal concentrations to the trigger value levels. The required increase is variable both between different environments and for different metals. It ranges from 2 to 5 times the current rates for Ni to 13 to 74 times for Ag. Overall, metals with higher background concentrations relative to trigger values (Cu, Cr, Pb, Ni) require the lowest proportional increase in anthropogenic metal flux to reach trigger values. Considering the relatively high pre-existing flux of these elements (Table 4.3), however, this equates to a considerable additional atmospheric flux (e.g. at least 2190 ug m^2 y^{-1} in the case of Pb). Metals which are highly sensitive to enrichment (Ag, Cd and Sb) are present in low concentrations relative to trigger values. They therefore require a relatively large increase (between 6 and 74 times current the rates) in deposition flux to result in concentrations reaching deleterious levels.

Overall, atmospheric industrial metal inputs demonstrated for the Snowy Mountains can be considered broadly similar to those found outside major industrial and urban centres across the eastern seaboard of Australia and in areas similarly impacted by regional contaminant sources. However, while these metals represent a significant potential source of contamination across large areas, their surface enrichment is a function of a complex set of processes which vary across the landscape. As a result monitoring of environmental contamination by atmospheric metals and determining the threat they may pose necessitates a thorough understanding of atmospheric and surficial geochemistry and its relationship to local earth surface processes.

Table 4.6. Sensitivity of archives to enrichment (increase in industrial flux required to produce sediment concentrations equal to trigger values)

		Upper Snowy Peat Mire			Club Lake			Guthega Reservoir			Geehi Reservoir		
	Trigger value[a] (mg kg^{-1})	Current concentration[b] (mg kg^{-1})	Excess concentration (mg kg^{-1})	Required increase[c] (x)	Current concentration (mg kg^{-1})	Excess concentration (mg kg^{-1})	Required increase[c] (x)	Current concentration (mg kg^{-1})	Excess concentration (mg kg^{-1})	Required increase[c] (x)	Current concentration (mg kg^{-1})	Excess concentration (mg kg^{-1})	Required increase[c] (x)
Cr	80	25	8	8	99	d	d	48	4	10	44	2	24
Ni	21	13	6	4	35	d	d	19	0.9	5	20	2	2
Cu	65	14	9	8	25	d	d	18	0.4	7	30	20	3
Ag	1	<0.1	<0.1	74	0.1	<0.1	60	<0.1	<0.1	18	0.1	<0.1	13
Cd	1.5	0.1	0.1	15	0.2	<0.1	15	0.2	0.1	10	0.3	0.2	7
Sb	2	0.2	0.1	18	0.1	<0.1	27	0.2	<0.1	61	*0.3*	0.1	17
Pb	50	23	14	4	45	5	2	29	9	3	21	2	18

[a]Dry weight.

[b]Estimated from composition of combusted peat using organic matter content of 60% and assuming bulk density of 1 g $cm^{-3.}$

[c]Required increase is the proportional increase in anthropogenic flux to produce sediment concentrations equivalent to trigger value.

[d]Metal was not enriched meaning that required flux increase cannot be calculated.

Note required Zn flux is not calculated due to presence of Zn in filter material used to collect aerosol samples.

Supplementary material

Estimation of aerosol/metal deposition flux

Dry deposition

Size dependent deposition velocities were estimated using Stokes terminal fall speed according the procedure of Jacobson (2005). This four step process begins by estimating the deposition velocities ($V_{d,}^{iest}$ cm s^{-1}) of each particle size class according to equation (1)

$$V_{d,i}^{est} = (2r_i^2(\rho_p - p_a)g/9\eta) * G_i \quad (1)$$

where ρ_p is the density of the particle, (taken here as the density of quartz 2.65 g cm^{-3}), r is the particle radius (cm), p_a is the density of air (g cm^{-3}) determined from the mean annual temperature and elevation of the sampling sites, η is the dynamic viscosity of air and G_i is the Cunningham slip-flow correction using the values of Kasten (1968). Aerosol particle size distributions were measured for 20 randomly selected filters on a Coulter Multisizer following (McTainsh et al., 1997).

Reynold's numbers were then estimated using the estimated deposition velocities obtained from equation 2, according to equation 3.

$$Re_i^{est} = 2ri\ V_{d,i}^{est} / \upsilon_a \quad (2)$$

where υ_a is the kinematic viscosity of air determined from mean annual temperature and elevation of the sampling sites.

Following this, the Reynolds numbers were corrected according to Beard's (1976) parameterisation for either slip flow (Re <0.01) or continuum flow (0.01 < Re < 300). The final fall velocities were then recalculated according to equation 3.

$$V_{d,i} = (Re_i\ \upsilon_a)/2r_i \quad (3)$$

where $Vd,_i$ is final deposition velocity for particle size class i and Re the corresponding (corrected) Reynolds number.

Dry deposition rates were then calculated for 60 aerosol size classes using equation 4.

$$F_d = \sum_{i=1}^{n} V_{d,i} * C_i \quad (4)$$

where F_d is the dry deposition flux (g m^{-2} y^{-1}), V_d the particle size specific deposition velocity and C_i is aerosol concentration (g m^{-3}). Finally, the dry deposition flux for individual industrial metals was calculated from the total aerosol deposition rates and the individual trace metal aerosol concentrations.

Wet deposition

Precipitation deposition

Precipitation deposition was calculated by estimating the concentration of metals in precipitation from their concentration in the atmosphere using a scavenging ratio (*Z*), defined by the equation 5 (Duce et al., 1991):

$$Z = C_p/C_a \quad (5)$$

where C_p is the concentration of the metal in precipitation and C_a its concentration in the atmosphere .

Trace element flux (F_p) (ug m^{-2} y^{-1}) was estimated according to equation (6)

$$Fp = P*Z*C_a*p^{-1} \quad (6)$$

Where *P* is the annual precipitation amount (mm), *Z* is the scavenging ratio (which is dimensionless), C_a is the mean annual concentration of the element in the atmosphere (ug m^{-3}) and *p* is the density of air (taken as 1200 g m^{-3}). Precipitation depth is converted to mass of water per unit area using standard temperature and pressure.

Precipitation amount is taken as 2000 mm y^{-1} (the estimated mean annual rate for elevations above 1700 m in the Snowy Mountains)

Cloud water deposition

Cloud water deposition was estimated using equation

$$F_{i,cw} = F_{cw} * C_{i,cw} \quad (7)$$

where $F_{i,cw}$ is the annual cloud water flux of element *i*, F_{cw} is the annual cloud water hydrologic input, and $C_{i,cw}$ is the mean annual concentration of the element in cloud droplets.

Cloud water composition ($C_{i,cw}$ the concentration of each element in cloud water) was estimated using equation (8)

$$C_{i,cw} = -((E*C_a)/(E-1)) \quad (8)$$

where $C_{i,cw}$ is the air equivalent concentration of the element in cloud water (pg m-^{3}), *E* is the scavenging efficiency of cloud water drops for aerosols and C_a is the total concentration of the element in the atmosphere (cloud water + interstitial aerosols) (pg m^{-3}).

The hydrological input from cloud water was estimated using equation 9.

$$F_{\text{cw}} = LWC * V_{d,cw} * t\_ \quad (9)$$

where F_{cw} is the annual cloud water hydrological input to the catchment, *LWC* is the mean liquid water content of the clouds (g m^{-3}), V_d is the deposition velocity of cloud water droplets (m s^{-1}) and *t* is time spent below the cloud base each year.

Obtaining site-specific measurements of scavenging efficiency, liquid water content and cloud immersion time was beyond the scope of this study. Values were, therefore, estimated from previously published values for mountain environments elsewhere (*E*, *LWC*), from limited empirical data (*LWC*) and from observation (*t*). To provide an estimate of uncertainty associated with the selection of these values cloud the calculation of cloud water deposition was performed using mid, low and high estimates of *E*, *LWC* and *t*. These values are presented in Supplementary Table 4.1. These estimates were then summed with those of F_d and F_p to provide a range estimate of total deposition.

Trace element analysis

The analysis of trace elements (including heavy metals) in the aerosol samples, sediment samples extracted from the reservoirs cores, soils and samples from the Club Lake core (previously presented in Stromsoe et al., 2013) was performed by solution quadrupole ICP-MS on a Agilent 7700x instrument at the Department of Earth Sciences, University of Melbourne, Australia.

Sediment samples from the peat cores were analysed at Laurentian University, Ontario, Canada using the same approach (Marx et al., 2010).

All samples analysed for this study were dried at 60°C for 36 h to remove moisture and homogenised using an agate mortar and pestle prior to trace element analysis. Samples from the peat cores and the soil pits were additionally combusted in a high temperate oven at 450°C for 12 hours. This volatised the organic component of each subsample, while the mineral component was retained for trace element analysis. Subsamples from each aerosol filter were carefully scraped from the filter using a stainless steel spatula before their trace element composition was measured.

All samples and standards, typically about 100 mg, were digested in Teflon beakers on a hotplate at 140°C overnight using 3 ml of a 2:1 mixture of concentrated HF-HNO_3. Solutions were then evaporated to dryness and then 1 ml of 15N HNO_3 was added and evaporated to dryness twice. They were then dissolved overnight in 10ml of 3N HNO_3. A procedural blank was prepared with each batch of samples. Sample solutions were transferred to polycarbonate centrifuge tubes. For silver analyses, an aliquot of the solution was diluted to 2% HNO_3 and a dilution factor of 1000 and Rh added as an internal standard. For all other elements, solutions were diluted to 2% HNO_3 with a dilution factor of 2000.

Silver was analysed in dilution gas mode with 2.2 ml of He cell gas to minimize the level of oxide interferences on Ag. A single element Ag standard was used for calibration and 2 soil standards and one shale standard analysed as unknowns. Oxide interferences were less than 10% of the silver signal and corrected for.

Other elements were analysed in dilution gas mode without cell gas using procedures comprehensively described by Eggins et al. (1997) and Kamber (2009). The method uses a natural rock standard for calibration, internal drift correction using multi-internal standards (Li^6, Sr^{84}, Rh, Sm^{147}, Re and U^{235}), external drift monitors for drift correction and aggressive washout procedures. Two digestions of the USGS standard W-2 were used for instrument calibration. The preferred concentrations used for W-2 were mostly derived by analysing it against synthetic standards and a literature survey of isotope dilution analyses (Kamber et al., 2003, 2005).

The instrument was tuned to give Cerium oxide levels of < 0.5%. Four replicates of 100 scans per replicate were measured for each isotope. Dwell times were 10 milliseconds, except for Mo, Cd, Sb, Ta, which were 30 milliseconds. Long sample wash-out times of 6 minutes with solutions of 0.5% Triton X-100, 0.025% HF in 5% HNO_3 and 2% HNO_3 and long sample uptake times of 120 seconds were used. Drift monitors, followed by a blank were analysed every 6 – 8 samples. Concentrations of the samples were well above minimum detection limits.

Quality control was maintained by the analysis of rock and soil standards as unknowns. External precision and accuracy for soil standards (JSo-1, GSS-1), shale standard SCo-1 and basalt and andesite standards BHVO-2, JA-2 and AGV-2 are assessed in Suppl Table 3.

Supp. Table 4.1. Parameter values for cloud water deposition estimates

	LWC (g m^{-3})[a]	$V_{d,cw}$ (mm s^{-1})[b]	t (%)[c]	E (%)[d]
Moderate[1]	0.2	46 (grass) 100 (forest)	20	60
Low[2]	0.1	10 (grass) 45 (forest)	10	60
High[3]	0.3	46 (grass) 100 (forest)	30	85

[1]moderate LWC, moderate to high cloud water deposition velocity, moderate estimate for time spent below cloud base, moderate estimate for scavenging efficiency of cloud water for aerosols

[2]low LWC, low cloud water deposition velocity, moderate estimate for time spent below cloud base, low estimate for scavenging efficiency of cloud water for aerosols

[3]moderate LWC, moderate to high cloud water deposition velocity, high estimate for time spent below cloud base, high estimate for scavenging efficiency of cloud water for aerosol

[a]Reynolds et al. 1996, Kasper et al. 1998

[b]Reynolds et al 1996, Miller et al 1993

[c]Cloud immersion time is estimated from personal observation

[d]Grassbauer et ala 1994, Shumann 1991, Kasper 1998

Supp. Table 4.2. ^{210}Pb activities and CIC ages for reservoir cores

Lab code	Depth (mm)	Total ^{210}Pb activity (Bq kg^{-1})[a]	Supported ^{210}Pb activity (Bq kg^{-1})[a]	Unsupported ^{210}Pb activity (Bq kg^{-1})[a]	Calculated CIC Ages (years)
Guthega Reservoir					
N986[3]	0-10	485 ± 30	26 ± 12	463 ± 33	-
N987[2]	20-30	614 ± 26	57 ± 5	560 ± 27	-
N988[2]	40-50	553 ± 23	55 ± 5	501 ± 24	6 ± 1
N989[3]	70-80	532 ± 24	41 ± 3	495 ± 25	10 ± 1
N990[2]	90-100	462 ± 21	55 ± 5	409 ± 22	13 ± 2
N991[3]	140-150	387 ± 18	46 ± 4	344 ± 19	19 ± 2
N992	190-200	420 ± 19	45 ± 4	375 ± 19	-
Geehi Reservoir					
923	0-6	356 ± 15	47 ± 4	287 ± 14	-
924	30-34	372 ± 15	54 ± 4	296 ± 14	-
925	70-75	374 ± 15	48 ± 4	304 ± 14	-
926	95-100	429 ± 17	38 ± 3	364 ± 17	22 ± 5
927	150-155	285 ± 12	54 ± 5	215 ± 12	40 ± 6

[a]Error is counting error

Supp. Table 4.3.Trace element data of standards (mg kg^{-1})

	W-2			BHVO-2						JA-2					
				This study		Long term**		Preferred		This study		Long term**		Preferred Values*	
	Calibration Standar	Preferred Values	RS	Digestions = 3 Analyses = 3						Digestions = 3 Analyses = 6					
				Averag	RSD	Averag	RS	Average	RS	Average	RS	Averag	RS	Averag	RSD
Sc	36	35.9	2	33	1	32	0.9	32	3	19.6	2	19.6	1.4	17.4	6.9
Ti	6 356			16 725	0.9	16 481	1	16 300	12	4 018	2.3	4 037	2.4		
Cr	93	93	6	308	0.8	301	1.2	280	6.8	437.8	2.4	438.5	1.6	450	8.9
Co	45	45	4	46	0.3	46	0.9	45	7	30	1.6	30	1.1	27	7
Ni	70	72	6	121	1.1	119	0.8	119	6	141	1.5	139	0.9	134	11
Cu	103	105	3	125	0.9	126	0.7	127	6	27.6	2.8	27	1.1	27.9	1
Zn	77	77	8	101	2.5	102	1.3	103	6	64	1.3	63	2.1	65	8
Ga	17	18	6	21	0.8	21	0.6	22	9	16.5	0.9	16.5	0.7	16.5	7.3
As	1.4	1.1	9	0.4	27	0.6	15	0.632-0.92[a]		0.63	22	0.59	15	0.93[b]	4
Mo	0.42	0.44		4	12	3	6.7	4	5	0.54	1.2	0.54	1.6	0.59	3.4
Ag															
Cd	0.077	0.077		0.09	4.5	0.09	2.2	0.06	10	0.06	4.6	0.06	3	0.078	
Sn	2	2	5	1.9	4.9	2.0	6.5	1.7	12	1.69	4.6	1.71	7.5	1.56	1.6
Sb	0.71	0.77	5.2	0.08	2.3	0.08	5.9	0.13	31	0.12	1.4	0.12	5.4	0.14	7.1
Ta	0.45	0.47	8.5	1.15	0.8	1.14	0.5	1.14	5	0.6	0.7	0.6	0.7	0.7	14
Pb	7.5	7.7	8	1.6	6.6	1.4	5.2	1.6	19	18.3	0.6	18.5	1.5	19.3	4

Supp. Table 4.3 continued

	AGV-2				Jso-1			
	This study		Preferred Values***		This study		Compiled Values*	
	Digestions = 3 Analyses = 3				Digestions = 3 Analyses = 3			
	Average	RSD	Average	RSD	Average	RSD	Average	RSD
Sc	13	0	13	8	33	1		
Ti	6 070	1.4			7 014	2		
Cr	16	2.2	16	6	74	1	71	2
Co	16	1.1	16	6	35	1	32	1
Ni	18	1.4	20	5	41	1	39	2
Cu	49	1.3	53	8	167	1	169	2
Zn	89	0.8	86	9	116	6	105	2
Ga	20	0.9	20	5	20	0		
As	0.74	10.2			9.0	3.4	8.1	0.1
Mo	2	2.4			0.7	3		
Ag					0.112[c]	2		
Cd	0.069	2.800			0.275	5.689		
Sn	2.2	8.9	2.3	17	1.6	4.3		
Sb	0.40	7.00			0.31	4.24	0.38	0.02
Ta	0.83	1.1	0.87	9.2	0.19	1.76		
Pb	12.6	0.9	13.2	4	17.9	1.0	13.0	1.0

Supp. Table 4.3 continued

	GSS-1		Sco-1	
	This study	Compiled Values*	This study	Compiled Values*
	Digestions = 1 Analyses = 1		Digestions = 1 Analyses = 1	
	Values	Value	Values	Value
Sc	11		12	10.8-11
Ti	11	11	3 430	
Cr	58		69	68
Co	13		11	10.5-11
Ni	20	20	26	27
Cu	18	21	27	28.7-29
Zn	752	680	102	100-103
Ga	18	19	16	15
As	44	34	13.3	12-12.4
Mo	1.4	1.4	1.2	
Ag	0.36[d]	0.35	0.135	0.134
Cd	5		0.156	0.14
Sn	6.7	6.4	3.4	
Sb	1.01		2.11	
Ta	1.2	1.4	0.8	
Pb	97.0	98.0	30.4	31.0

*GeoRem (preferred/compiled values) (Jochum et al 2005)

**Long term Melbourne University Isotope and trace element geochemistry laboratory average

*** Imai et al 1995

[a] GeoRem compiled values

[b] GeoRem Compiled values are 0.77-0.85

[c] Digestions = 4, Analyses = 34

[d] Digestions = 4, Analyses = 34

Chapter 5

Estimates of late Holocene soil production and erosion in the Snowy Mountains

Chapter 5 is reproduced from the following manuscript, which has been submitted for publication

Stromsoe, N., Marx, S.K., Callow, N., McGowan, H.A., Heijnis, 2015. Estimates of late Holocene soil production and erosion in the Snowy Mountains, Australia. *Catena*, (submitted)

Chapter 5. Estimates of late Holocene soil production and erosion in the Snowy Mountains, Australia

Abstract

Soil production in actively uplifting or high precipitation alpine landscapes is potentially rapid. However, these same landscapes are also susceptible to erosion and can be sensitive to changes in climate and anthropogenic activity which can upset the balance between soil production and erosion. The Snowy Mountains, south-eastern Australia are a tectonically stable, low relief, moderate precipitation mountains environment. The alpine area is extensively blanketed by soil that has been subjected to more intensive episodes of erosion during past periods of anthropogenic disturbance and under cold climate conditions of the late Quaternary. In this study, rates of soil development and hillslope erosion were investigated using radiocarbon dating, fallout radionuclides and sediment cores collected from lakes and reservoirs. Estimated Holocene soil development rates were 20-220 t/km^2/y. Erosion rates determined from the radionuclides ^{137}Cs and ^{210}Pb were equivocal, due to the inherent spatial variability of radionuclide inventories relative to apparent erosion rates. Estimated average erosion rates over the past 100 years, determined from $^{210}Pb_{ex}$ inventories, were 60 t/km^2/y (95% confidence interval [10, 90]). Inventories of ^{137}Cs observed at the same site implied that more recent erosion rates (over the past 60 years) was below the detection limits of the sampling method applied here (i.e. <70 t/km^2/y). The upper estimate of 90 t/km^2/y is comparable to the mean erosion rate estimated using the radionuclide method for uncultivated sites in Australia and is significantly lower than that measured at sites where vegetation cover was disturbed by livestock grazing prior to its exclusion from the alpine area in the 1940s CE. Low erosion and high soil production rates relative to the lowland soils are explained by extensive vegetation cover which protects soils against erosion and contributes to the formation of organic alpine soils, which rapidly accumulate organic matter by comparison to other soil types.

5.1 Introduction

On a global scale, alpine landscapes are recognised as regions of relatively high geomorphic activity due to their high potential energy and climates which promote rapid physical weathering, erosion and sediment transport (Dedkov and Moszherin, 1992; Milliman and Syvitski, 1992; Vanmaercke et al., 2011; Walling and Webb, 1996). Globally, rivers draining mountain basins transport a disproportionately large mass of sediment, with an average sediment yield of 870 t/km^2/y compared to 115 t/km^2/y for the rest of the world's rivers (Milliman and Farnsworth, 2011). In tectonically active mountain ranges, erosion by either glacial, paraglacial or fluvial processes can be so rapid as to equal or exceed the rate of uplift (Brozović et al., 1997; Koppes and Montgomery, 2009; Mitchell and Montgomery, 2006).

It was historically considered that in cold mountain environments rapid erosion outpaced the processes of chemical weathering and, therefore, soil production, which is temperature inhibited (e.g. Peltier, 1950). However, in alpine regions experiencing rapid uplift and high precipitation, for example in the Southern Alps New Zealand, where rainfall may exceed 10 m/y and uplift approximates 10 mm/y, soil production rates may reach 2.5 mm/y, an order of magnitude higher than measured elsewhere (Larsen et al., 2014). The significance of chemical weathering in mountain environments is further evidenced by the existence of extensive soil mantles in a variety of alpine settings worldwide (Dixon and Thorn, 2005; Egli et al., 2014; Norton and von Blanckenburg, 2010; Riebe et al., 2004).

Despite high formation rates in some settings, alpine soils have been shown to be sensitive to changes in climate and human activity which can alter the processes of soil production and erosion (Barsch and Caine, 1984). Episodic changes in changes in climate, vegetation cover, fire frequency and human disturbance are, therefore, likely to be important controls on the balance between soil production and erosion in mountain environments (Hewawasam et al., 2003; Kirchner et al., 2001; Koppes and Montgomery, 2009; Schmidt et al., 2002).

In tectonically stable, non-glaciated, high to moderate rainfall, i.e. less than 2 m/y, alpine areas, such as the Snowy Mountains, south-eastern Australia, rates of soil production and erosion have received less attention. The Snowy Mountains have traditionally been viewed as distinct from other alpine regions (Costin, 1989; Kirkpatrick, 1994) due to their intra-plate setting and resulting tectonic stability and moderate relief (slopes) (Bishop and Goldrick, 2000). In addition, they experienced relatively limited Pleistocene glaciation (Barrows, 2001). These characteristics have facilitated the development of a relatively thick soil mantle

(60 cm - > 1 m) over almost the entire alpine area (Costin, 1989). Nevertheless, the Snowy Mountains are considered to have experienced pulses of intensified sediment transport in response to changing climate of the late Quaternary (Costin, 1972; Kemp and Rhodes, 2010; Ogden et al., 2001; Page et al., 2009) and as a result of livestock grazing between the mid-1800s and 1940s CE (Costin et al., 1959). Accounts of the state of the region during the grazing period describe the stripping of the entire depth of soil from areas of the alpine zone, especially on exposed, north facing slopes (Bryant, 1971; Costin, 1954).

The quantification of inherently spatially and temporally variable soil production and erosion rates remains a major challenge within geomorphology. Measurement of hillslope erosion has been undertaken by a variety of methods that can be broadly categorised into: plot and survey approaches (e.g. Costin et al., 1960); measurement of sediment yields by either stream gauging or by measurement of the mass of sediment accumulated in geomorphic sinks such as lakes (e.g. Neil, 1991; Tomkins et al., 2007); erosion tracer methods using fallout radionuclides (e.g. ^{137}Cs and ^{210}Pb) (Blake et al., 2009; Loughran et al., 1988; Porto et al., 2009; Ritchie and McHenry, 1990; Walling et al., 2003), and; the application of cosmogenic nuclides (e.g. Dixon and Clifford, 2014; Heimsath et al., 2002).

These methods are each limited by the challenges of upscaling point measurements in time and space in relation to the representativeness of reference sites, the spatial heterogeneity of tracer fallout and transport and the issues of sediment storage and delivery (Chappell et al., 2011b; de Vente et al., 2007; Zhang et al., 2015). In addition, all methods provide data over distinct time periods, e.g. stream gauging typically provides short term data (event to decadal scale), radionuclides provide decadal to centennial scale data, and commonly used cosmogenic nuclides integrate over millennial scales. As a result, different approaches will commonly yield very different results (e.g. Tomkins et al., 2007; Wasson et al., 1996) that are then subject to various interpretations.

The objective of this study is to quantify soil production rates versus erosion in a tectonically stable, non-glaciated mountain environment and to advance the understanding of the relative controls that changing climate and anthropogenic activities place on landscape stability and sediment budgets. In doing so the likely age of these soils is discussed. This study employs multiple methods to attempt to quantify rates of soil production, hillslope erosion and sediment transport. Hillslope erosion rates are investigated using the fallout radionuclide (^{137}Cs and $^{210}Pb_{ex}$) and by calculating sediment mass accumulation rates in alpine lakes and reservoirs. Soil production rates are examined using geomorphic and paleoclimate evidence

combined with radiocarbon analysis. These approaches overlap in time, allowing the balance between soil formation and erosion rates to be investigated. Results are placed within the context of historical data quantifying erosion under past conditions of anthropogenic and climatic change.

5.2. Regional setting

The Snowy Mountains are a high elevation plateau of moderate (undulating) relief. Despite being the highest region of Australia, they reach only 2228 m at their highest point (Mt Kosciusko) and local relief of the alpine area is usually less than 200 m. The Snowy Mountains are the erosional remnants of uplift associated with the Cretaceous breakup of Gondwana beginning 100 Ma with most intense activity centered around 55 Ma (Bishop and Goldrick, 2000). Their intraplate setting results in low denudation rates over geological timescales (2-5 m/ma (Young and McDougall, 1993). The basement rocks of the mountains are Silurian and Devonian aged granites with Ordovician meta-sediments and occasional Tertiary basalts. The Snowy Mountains contain the only peaks above 2000 m in Australia and form part of mainland Australia's limited subalpine and alpine area, which covers only 2500 km^2.

Aligned perpendicular to the prevailing westerly moisture-bearing winds, the Snowy Mountains experience a cool montane climate, with mean temperature varying from 18°C in summer to -7°C in winter with annual precipitation ~ 2000 mm (BOM, 2014b). In the alpine tract, continuous snow cover is present for up to 4 months of the year with isolated snow patches sometimes persisting through the year (Green and Pickering, 2009). Interannual variability of snow-depth and snow persistence is high and is related to the frequency of occurrence of snow bearing synoptic weather systems (Nicholls, 2005; Theobald et al., 2015; Whetton et al., 1996). Minor periglacial activity (needle ice formation and frost heave) is today confined to the alpine zone with gelifluction and frost shattering most significant above 2000 m (Barrows et al., 2001; Galloway, 1965).

In the montane zone (900-1500 m), vegetation comprises wet-sclerophyll forests dominated by alpine ash (*Eucalyptus delgatensis*) and mountain gum (*E. dalrympleana*), subalpine (above 1500 m) vegetation consists largely of snowgum (*E. pauciflora*) woodlands with a grassy (*Poa ceaspitossa*) understory. Above 1 850 m are alpine herbfields (dominated by *Celmisia and Poa spp*) with areas of heath, sod tussock grassland and fen-bog communities (*Carex-Sphagnum*). The vegetation cover is almost complete, extending to the highest peaks.

The entire alpine area has been protected from grazing and resource extraction since 1944 when it was declared a National Park.

5.3. Methods

5.3.1 Study locations

Estimates of soil development, hillslope erosion and sediment yield were undertaken within the catchment of Guthega Reservoir, located in the headwaters of the Snowy River (Fig. 5.1). Guthega catchment includes the highest peaks of the Main Divide. Sixty-five percent of the catchment lies within the alpine zone, which is characterised by both high relative precipitation and high runoff coefficients (Reinfelds et al., 2014). Much of this area is composed of high elevation plateaux surfaces or low gradient valley floors and, as a result, mean catchment slope is only 13°. Only 20% of the catchment area has a gradient greater than 20°, distinguishing it from many other alpine settings. The topography of Guthega catchment is representative of the Kosciusko alpine region in general, with the exception of the steeper western facing slopes of the range and the valleys of the major rivers.

Estimates of erosion (via ^{137}Cs and $^{210}Pb_{ex}$) and soil production were made on a hill slope in the sub-catchment of Guthega Creek (-36.367°, 148.368°, Fig. 5.1), which flows directly into Guthega Reservoir. The slope has a westerly aspect with an elevation range of 1880 m AHD at the ridge crest to 1670 m at Guthega Creek. The local treeline is located at approximately 1800 m AHD, just below the ridge crest. Snowgrass (*Poa spp)* predominates above the treeline, with open snowgum (*Eucalyptus pauciflora*), with a dense grassy understorey (*Poa and Chionachloa frigida* (Ribbony Grass)) below. Together these provide close to 100% vegetation cover. This site is considered broadly representative of alpine and subalpine zones in the Snowy Mountains in terms soil and vegetation and slope characteristics. Mean slope at the site is 16°, compared to a median of 12° for the Snowy Mountains as a whole.

Erosion measurement by ^{137}Cs and $^{210}Pb_{ex}$ was also undertaken across a second hillslope at Cootapatamba, which lies within the alpine zone, at the ridgeline of the Main Range. Site elevation is 2160 m AHD at the ridge-crest and 1910 m AHD at the valley floor. The hill slope has a northwesterly aspect. It is densely covered by alpine herbfield vegetation with a mean slope of 14°.

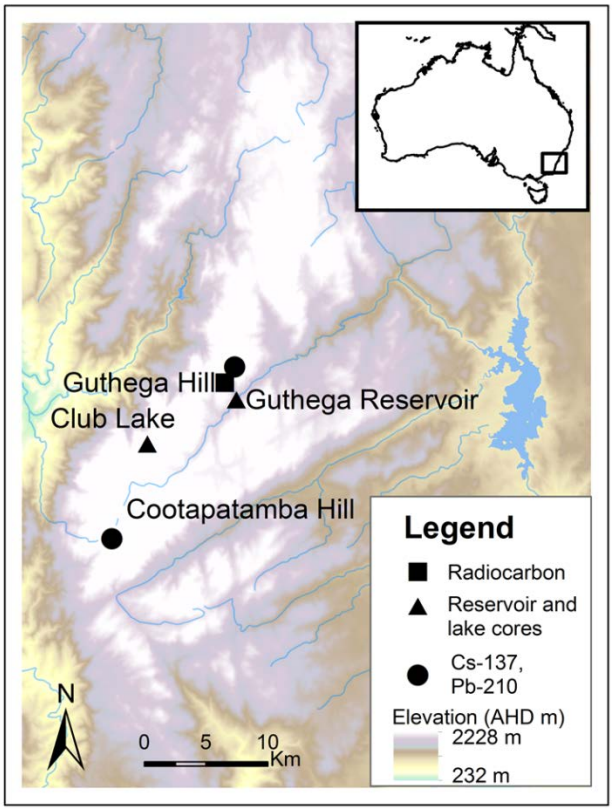

Figure 5.1 Location of soil and sediment sampling sites

Catchment sediment yield was estimated from sediment mass accumulation rates for Guthega Reservoir (-36.379, 148.371, 1 578 m) and Club Lake (-36.414, 148.291 1 950 m), a small cirque lake located within the headwaters of the reservoir catchment. Guthega Reservoir has an area of 0.26km^2 with a contributing catchment area of 91 km^2. The area of Club Lake area is 0.015 km^2 with a contributing catchment area of 0.3 km^2. Catchment soils are largely stabilised by alpine herbfield vegetation, although evidence of past instability is provided by gravel deposits buried within fen peats on the margins of the lake (Dodson et al., 1994). The phyllite bedrock is exposed on the steeper sections of the cirque walls and areas of scree are also present. The mean cirque catchment slope is 22° and 20% of the catchment has a gradient greater than 32°. Hillslope erosive potential is therefore high relative to the region in general, falling within the most erosion susceptible 20% of the land surface.

5.3.2 Measurement of soil development rates

A potential range for the rate of soil development was estimated by two separate methods. In the first approach, the likely date of onset for the development of Holocene soils was ascertained from geomorphic evidence and from previous studies describing the

reestablishment of stable conditions following the last ice age in southern Australia. Soil development rates were then estimated by dividing the depth of accumulated soil by their likely age. A second estimate was made from the radiocarbon ages of soil organic matter (SOM) at multiple depths within the soil profile (Wang et al., 2014b). These approaches were used in combination to provide a potential range rather than absolute estimate of the rate of soil development.

In this context, it is acknowledged that radiocarbon ages are typically younger than the true soil age (Wang et al., 1996). This method has received critical discussion within the radiocarbon literature, the chief identified limitation being the contaminating effect of new carbon which is incorporated into the profile during pedogenesis (Goh et al., 1977; Scharpenseel and Becker-Heidmann, 1992; Wang et al., 1996). The soils formed on the hillslopes of the Snowy Mountains alpine zone, however, display properties which suggest that they may build upwards in a manner similar to peat (further discussion of which is provided in the section 6.2 of this manuscript). Accordingly, it was considered that the variation in radiocarbon content through the depth of the soil profile could provide insight into relative rates of soil formation, within the acknowledged limitations of this method. Radiocarbon measurement was performed on the humin SOM fraction, which has been argued to be the environmentally stable SOM component and, therefore, relatively less susceptible to contamination by newly incorporated carbon (Kristiansen et al., 2003; Pessenda et al., 2001; Wang et al., 2014b). Radiocarbon ages undertaken on soil humins have been shown to reasonably estimate true age in a range of modern soils (Leavitt et al., 2007; Pessenda et al., 2001).

For the current study, samples were collected from soil profiles excavated at three locations along a transect down the slope. These were the ridge crest (-36.360, 148.366 1866 m), the mid-slope (-36.360, 148.370, 1804 m) and the toe-slope (-36.360, 148.366 1665 m). Profiles were excavated until the underlying fractured bedrock was reached (approximately 0.6 m), with samples collected at approximately 100 mm depth intervals.

Sample pre-treatment and analysis was performed by ^{14}C Accelerator Mass Spectrometry Dating (AMS) at the Waikato Radiocarbon Dating Laboratory and at the UC Irvine Keck-CCAMS facility, respectively. To remove visible organic contaminants (modern roots), soil was first disaggregated by stirring with sodium pyrophosphate on a hotplate and then was washed through a 1 mm sieve. The <1 mm fraction was retained and evaporated to dryness. The soil was then lightly homogenised in a mortar and pestle. Humins were separated from

more mobile fractions, such as fulvic and humic acids, prior to graphitisation using the acid-base-acid method (UCI KCCAMS Facility. Acid/Base/Acid sample pre-treatment protocol). Samples were washed first in hot HCl then with NaOH to remove soil humics. The NaOH insoluble fraction was washed again in hot HCl, then rinsed and dried. Radiocarbon ages were calibrated using the Oxcal programme (v 4.2) (Bronk-Ramsey, 2009) and the SHCal 13 southern hemisphere calibration curve (Hogg et al., 2013).

Soil organic content was estimated by the dry combustion method. Sub-samples from each soil depth interval were oven dried then ashed at 450°C for 12 hours.

5.3.3 Estimating hillslope erosion rates

Quantification of hillslope erosion was undertaken using the radionuclide tracers $^{210}Pb_{ex}$ and ^{137}Cs. Soil cores were collected from three transects at Guthega Hill and three transects at Cootapatamba Hill (Fig. 5.1). At each site, six cores were collected from each transect (18 cores in total) using 100 mm diameter PVC tube. Soil was collected to a depth of 15 cm or until the stone line, a feature of some Snowy Mountains soils (Brewer and Haldane, 1972), prevented further excavation. Fifteen cores were collected from the reference site(s) which were located at the ridge crests of the respective hillslopes. Samples were oven dried to constant weight, homogenised, and sieved through a 2 mm sieve. The <2mm fraction was ground in a rock mill to a fine powder, packed into petri dishes and sealed for approximately three weeks to achieve secular equilibrium between ^{226}Rn and it daughter ^{222}Rn. Samples were analysed for ^{210}Pb and ^{137}Cs by gamma spectrometry at the Institute for Environmental Research, Australian Nuclear Science and Technology Organisation (ANSTO). The activity of $^{210}Pb_{ex}$ was calculated as the difference between total measured ^{210}Pb and ^{226}Ra activity (which was derived from the activity of its granddaughter isotope ^{214}Pb). Count times were between 1 and 5 days depending on the total sample activity, resulting in mean counting errors of 6 ± 0.4% for ^{137}Cs. Mean $^{210}Pb_{ex}$ counting errors were 13 ± 2%. Activity of ^{137}Cs was decay corrected to February 2013 and all $^{210}Pb_{ex}$ activities were decay corrected to their sampling date.

To account for the intrinsic variability of radionuclide inventories and the resulting uncertainty of erosion estimates produced using the available conversion models, this study adopted the recommendations of Zhang (2014) and Kirchner (2013). These authors argue that the approach most frequently used when modelling erosion volumes from radionuclide inventories, i.e. comparing individual points at the suspected eroding site to a single value

representing the reference inventory, usually the reference site mean, is problematic in that it ignores the contribution of random spatial variability and sampling error to the deviation of any point measurement from the reference mean (Kirchner, 2013; Zhang et al., 2015). In reality, the reference mean is unlikely to accurately represent the original inventory at the point in question (Wallbrink and Murray, 1996). For this reason, prior to modelling being undertaken, a number of statistical tests (t-test, independent samples median test and independent samples Kolmogorov-Smirmov test) were applied to establish whether the observed differences between the reference and hillslope inventories were greater than that which would be expected due to random spatial variability and sampling error. Net erosion or deposition was assumed only if the deviation from the reference inventory exceeded that expected due to random spatial variability and sampling error at the 95% confidence level ($p < 0.05$). The percentage change in radionuclide inventory, representing the volume of soil lost or gained from the hillslope was taken as the difference between the mean of each hillslope and that of its respective reference site. An estimate of uncertainty in modelled erosion rates was obtained by rerunning the conversion models using the upper and lower 95% confidence limits of both the reference site and hillslope means.

The ^{137}Cs and $^{210}Pb_{ex}$ inventories were converted to erosion volumes using the theoretical diffusion and migration models of Walling et al. (2007), using their software. In the case of ^{137}Cs inventories an alternative model, the Australian Empirical Model (AEM) (Elliott et al., 1990; Loughran et al., 2004) was also used. The AEM was developed specifically for Australian conditions and is based on relationships established between ^{137}Cs and erosion plot data (Elliott et al., 1990; Loughran et al., 1988). Erosion rates estimated using the AEM have been shown to correspond well with erosion plots and sediment yield data in some areas (Martinez et al., 2009). Equally, the diffusion and migration model has produced more comparable estimates in other cases (Simms et al., 2008). Based on past studies undertaken within Australia it is possible that the AEM may underestimate and the diffusion and migration model overestimate true erosion rates for Australian soils (Martinez et al., 2009; Simms et al., 2008). Accordingly, both results are presented here.

The diffusion and migration model used here considers the time-dependent fallout and subsequent redistribution of $^{210}Pb_{ex}$ and ^{137}Cs within the soil profile. As this can be affected by factors extraneous to soil redistribution such as fallout history, radioactive decay, diffusion, leaching and bioturbation, the diffusion and migration model requires inputs describing the profile typology of radionuclide activity in soil unaffected by erosion or

deposition. In order to characterise the change in radionuclide activity with depth, three cores from the reference site were selected and sectioned into 2 cm increments on which ^{137}Cs and $^{210}Pb_{ex}$ activity was measured. Model inputs (diffusion coefficient, downward migration rate and relaxation depth factor (which describes profile shape) were estimated from these cores using the models of Walling et al. (2007) (Table 5.1). A particle size correction factor of 1.6 (Blake et al., 2009) was applied to eroding points to account for the enrichment of radionuclides in eroded material due to the preferential erosion of smaller particles with higher ^{210}Pb activity.

The different fallout histories (essentially undetectable after the 1980s for ^{137}Cs and constant for naturally derived $^{210}Pb_{ex}$) of the two radionuclides mean that they integrate the net effect of soil redistribution processes over different times spans, that is approximately 60 years for ^{137}Cs and around 100 years for $^{210}Pb_{ex}$ (^{210}Pb half-life is 22.2 years) (Walling et al., 2007).

Table 5.1 Model parameters describing radioactivity depth distribution

Site	Guthega Hill		Cootapatamba Hill	
Method	^{137}Cs	$^{210}Pb_{ex}$	^{137}Cs	$^{210}Pb_{ex}$
Relaxation depth (profile shape factor)	4	4	4	4
Diffusion coefficient ($kg^2\ m^{-4}\ y^{-1}$)	36.96	2.69	17.2	0.83
Migration rate ($kg\ m^{-2}\ y^{-1}$)	0.62	0	0.42	0

5.3.4 Estimating sedimentation rates

Sediment cores were retrieved from Guthega Reservoir and Club Lake. Collection processing and dating of the Club Lake core was previously described in Stromsoe et al. (2013) and Chapter 3, while similarly the Guthega core was described in Stromsoe et al. (2015) and Chapter 4. Both cores are described briefly here.

A 0.38 m core was collected from Club Lake using 70 mm diameter polyvinylchloride pipe, while a 0.27 m core was collected from Guthega Reservoir, using a gravity corer. Cores were extracted from approximately the centre of the lake and the reservoir.

Cores were sectioned into 2-5 mm slices. Samples from both the Guthega Reservoir (n=7) and Club Lake (n=9) cores were dated using ^{210}Pb at the Institute for Environmental

Research, Australian Nuclear Science and Technology Organisation (ANTSO). In addition, samples from Club Lake core were also dated by ^{14}C Accelerator Mass Spectrometry at Waikato Radiocarbon Dating Laboratory (n=4). Dating results and age model construction for the Club Lake and Guthega cores are discussed in Stromsoe et al. (2013) and Stromsoe et al (2014) and Chapter 3 and 4, respectively.

Mass accumulation rates (MAR) were calculated from the product of the increment volume, derived from the age model, and the corresponding dry bulk density, according to equation 5.1.

$$MAR = SAR * BD \quad (5.1)$$

where *MAR* is in g/cm^2/y, SAR is the linear sediment accumulation rate (cm/y) and BD is bulk density (g/cm^3). It is acknowledged that true sediment yields from such a large area may differ substantially or be considerably more variable than suggested by single cores extracted from a limited number of sinks. However, the specific sediment yields calculated from the Club Lake and Guthega cores are used here to provide estimated lower limit for hillslope erosion rates occurring within the catchments for comparison with the rates estimated by ^{137}Cs and $^{210}Pb_{ex}$. Area specific sediment yields (*SSY*) were calculated by dividing the mass accumulation rate by the catchment area.

5.5 Results

5.5.1 Radiocarbon ages

Soils at the study site are classed as chernic tenosols (Australian Soil Classification). These soils are formed on hillslopes throughout the alpine and subalpine zone (McKenzie et al. 2014). They are characterised by a humose A horizon of approximately 30 cm depth with an abrupt to distinct transition to a relatively shallow stony BC horizon. The BC horizon grades to the granite substrate at approximately 60 cm depth.

The A horizon, considered to be Holocene in age, is dominated by high organic inputs from the covering snowgrass accompanied by slow decomposition due cold temperatures, frequently waterlogged soils and high aluminium content (McKenzie et al., 2004). Accordingly, the A horizon, organic matter comprises 14-27% of the total soil weight. This differs markedly from the underlying chemically weathered B/C horizon which is considered to represent the truncated Pleistocene paleosol (Brewer and Haldane, 1972). It is considered that the A horizon, therefore, may undergo pedogenesis by upbuilding with organic inputs

augmented by significant dust accretion (Costin et al., 1952; Johnston, 2001; Marx et al., 2011). The density of the snow grass root mass within the upper A horizon likely provides a significant soil binding effect.

Samples from each of the three soil profiles from the Guthega catena were dated by ^{14}C AMS. The deepest sample dated, in each case, came from the base of the A horizon at its intersection with the B/C horizon, i.e. the presumed stripped Pleistocene surface (Fig. 5.2). Returned ages for A/BC horizon transition show good agreement between sites with ages for the ridge-crest ranging from 2330-2430 y. cal. BP; 2520-2750 y. cal. BP for the mid-slope and, 2150-2310 y. cal. BP in the toe-slope profile (Fig. 5.2 and Table 5.2). Minimum age differences are as small as 30 years between the ridge-crest and toe-slope and do not display a consistent downslope relationship. The maximum radiocarbon age of the organic horizon is, therefore, approximately 2150-2750 y. cal. BP, indicating the potential onset of Holocene soil development at or prior to this date. Due to the potential incorporation of new carbon at depth, this should be regarded as a minimum estimate of the true soil age (Wang et al., 1996).

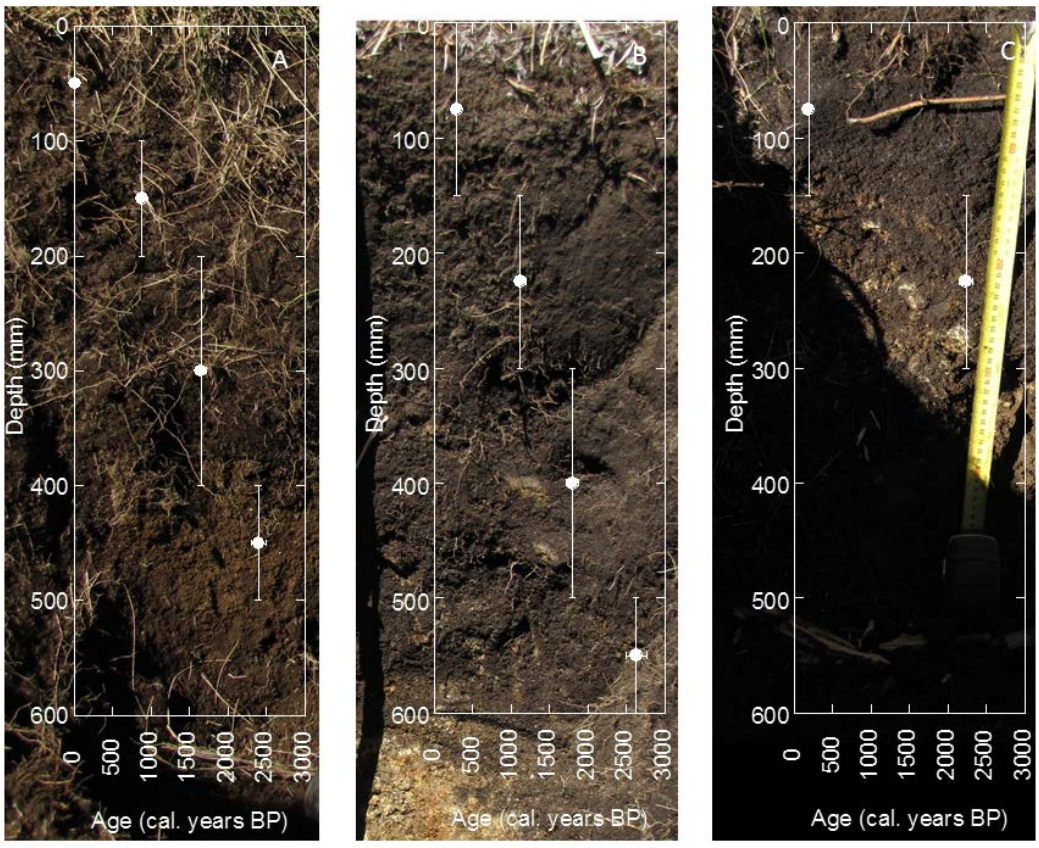

Figure 5.2 **Radiocarbon soil ages vs depth for soil pits at Guthega Hill A) ridge-crest, B) mid-slope pit, C) toe slope.**

For each of the three profiles, returned radiocarbon ages were progressively younger toward the top of the profile, as would be expected in upbuilding soils as organic matter is added to

the surface of the profile. In addition the same depths at different positions on the slope show relatively the same age. This implies that is there is no obvious mixing of carbon by mass wasting/movement processes. The lack of significant mass wasting or soil creep is also indicated by coherence of A/BC horizon ages horizon transition ages. If the former had occurred, then the toeslope ages would be expected to be appreciably older than those of farther up the catena.

Table 5.2. Radiocarbon ages for hillslope soils

Lab code	Profile	Depth (mm)	Conventional Radiocarbon Age (BP)	Error	Age years BP (calibrated)	Error[b]
Wk-39223	ridge-crest	0-100	104.5	± 0.3	7	± 0.18
Wk-39224	ridge-crest	100-200	918	± 30	880	± 65
Wk-39225	ridge-crest	200-400	1790	± 25	1650	± 70
Wk-39226	ridge-crest	400-500	2392	± 26	2400	± 90
Wk-39228	mid-slope	0-150	268	± 25	295	± 25
Wk-39229	mid-slope	150-300	1234	± 25	1120	± 70
Wk-39230	mid-slope	300-500	1905	± 25	1800	± 80
Wk-39231	mid-slope	500-600	2584	± 29	2625	± 135
Wk-39233	toe-slope	0-150	222	± 25	185	± 45
Wk-39234	toe-slope	150-300	2251	± 25	2235	± 85

[a] 1 sigma standard deviation due to counting statistics multiplied by experimentally determined laboratory error multiplier

[b] 1 sigma standard deviation

5.5.2 Hillslope erosion rates

5.5.2.1 Radionuclide reference inventories

The down -profile distribution of the radionuclide activity at the reference site was typical of that found within undisturbed soils with the peak of ^{137}Cs activity located just below the soil surface and $^{210}Pb_{ex}$ relatively more concentrated in the soil surface (Mabit et al., 2008) (Fig. 5.3). Mean ^{137}Cs reference inventories were 1010± 40 Bq/m^2 (errors are mean counting errors

only) at Guthega and 890 ± 50 Bq/m^2 at Cootapatamba (Table 5.3). The mean $^{210}Pb_{ex}$ reference inventory was 11 200 ± 500 and 6900 ± 900 Bq/m^2 (errors are mean counting errors only) at Guthega and Cootapatamba, respectively (Table 5.3).

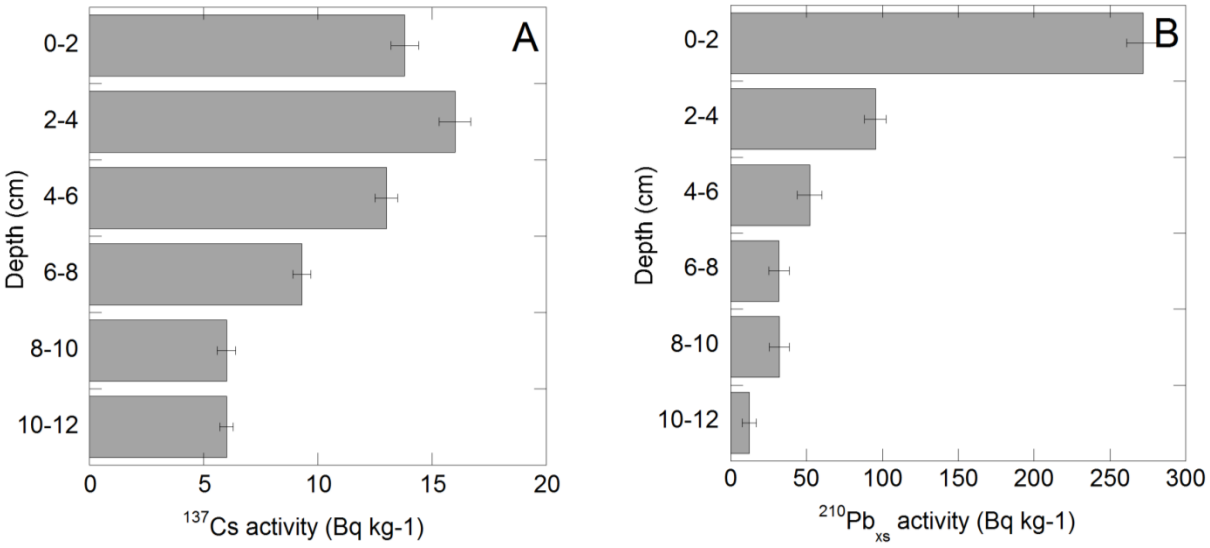

Figure 5 .3 Vertical distribution of ^{137}Cs and $^{210}Pb_{xs}$ in Snowy Mountains soil. Plots show the mean activity from 3 cores from Guthega reference site. Bars show counting error.

These reference inventories are high compared to previous measurements within Australia for both ^{137}Cs and $^{210}Pb_{ex}$. Previous measurements of ^{137}Cs fallout for south-eastern Australia are in approximate accordance with UNSCEAR estimate of 360 Bq/m^2 for the 30 to 40°S latitude band (UNSCEAR, 2000). For example, reported reference inventory values from south-eastern Australia include: 383 Bq m^{-2} (Blue Gum Creek,34.222°S, 150.492°E (Blake et al., 2009)); 425 Bq/m^2 (estimated from multiple sites in southern Australia between 30°- 40°S (Chappell et al., 2011a; Elliott, 1997)) and 540-653 Bq/m^2 (Stanley catchment, -32.092°S, 150.117°E (Martinez et al., 2009)) (all values are decay corrected to 2013 for comparison).

Table 5.3. Descriptive statistics for radionuclide inventories at Guthega and Cootapatamba (Bq/m^2)[a]

Site	Method	Site type	Range	Mean	SE	95% confidence limit of the mean		Median	1/2 IQR	95% confidence limit of the median	
						Lower	Upper			Lower	Upper
Guthega	^{137}Cs	Reference	740-1320	1008	63	883	1132	996	204	759	1209
		Hill slope	422-1447	1447	88	827	1001	1009	180	750	1209
	$^{210}Pb_{xs}$	Reference	8734-16 314	11 199	564	10 093	12 305	11 151	947	9545	11 840
		Hill slope	5591-12 400	8579	609	7385	9774	8322	918	6691	9618
Cootapatamba	^{137}Cs	Reference	356-1196	886	70	749	1023	759	226	713	1164
		Hill slope	570-1491	928	66	798	1727	874	177	713	1184
	$^{210}Pb_{xs}$	Reference	3597-20 409	7692	1042	5649	9734	7185	1400	5308	8262
		Hill slope	2455-17 385	6967	1002	1965	5002	8932	2378	3831	9297

[a] these values do not include counting error, number of significant figures do not reflect precision. Mean counting errors are 6% for ^{137}Cs and 13% for $^{210}Pb_{xs}$

The relatively high values for the Snowy Mountains is likely explained by the area's high precipitation as ^{137}Cs activity tends to increase with increasing rainfall (e.g Chappell et al., 2011a; Schuller et al., 2002). The inventory for the Snowy Mountains is broadly consistent, although still higher, than the inventory predicted from the annual precipitation amount and the rainfall-inventory relationship developed for Australian sites by Chappell et al. (2011a), i.e. 745 Bq/m^2. It is also similar to the only previous measurement from a location where annual precipitation approaches the 2000 mm/y experienced in the Snowy Mountains, i.e. 884 Bq m^{-2} at 1800 mm/y in coastal New South Wales (Chappell et al., 2011a; Elliott, 1997).

Excess ^{210}Pb reference inventories for the Snowy Mountains sites are approximately 5 times those reported for Blue Gum Creek ((34.222°S, 150.492°E, 1 923 Bq/m^2 (Blake et al., 2009)) and for Townsville (19.256°S, 146.818°E, 1600 Bq/m^2 (Pfitzner et al., 2004)). In this case, the higher inventories of the Snowy Mountains sites are likely explained by a combination of characteristics known to increase $^{210}Pb_{ex}$ fallout, including the area's relatively high precipitation rate, high rates of dust deposition (Marx et al., 2011; Stromsoe et al., 2015), and relative distance from the coast, where ^{210}Pb production is low (Garcia-Orellana et al., 2006; Preiss et al., 1996).

The spatial variability of for ^{137}Cs and $^{210}Pb_{ex}$ inventories can be described by the coefficient of variation (CV). The CV of the ^{137}Cs reference inventory was 21% at Guthega and 30% at Cootapatamba. For $^{210}Pb_{ex}$ the CV was 30% at Guthega and 50% at Cootapatamba. Radionuclide inventories tend to display high intrinsic variability due to the small-scale variability of several factors including: initial fallout, which is influenced for example, by the deposition of dust, which scavenges ^{210}Pb (Marx et al., 2005); microtopography; vegetation; as well as runoff and infiltration (Owens and Walling, 1996; Zhang, 2014). The level of natural variability demonstrated for the Snowy Mountains sites is consistent with that observed by previous studies, which is typically ~20% in the case of ^{137}Cs (Kirchner, 2013; Pennock and Appleby, 2003; Sutherland and de Jong, 1990).The intrinsic spatial variability of $^{210}Pb_{ex}$ fallout is less well known, but CVs of ~10% (Porto et al., 2009) to 115% (Mabit et al., 2009) have been previously reported. The high spatial variability of $^{210}Pb_{ex}$ relative to ^{137}Cs in the Snowy Mountains reference sites may be partly attributable to the relative imprecision of gamma spectrometry for determining ^{210}Pb activity compared to ^{137}Cs (e.g. Shakhashiro and Mabit, 2009).

5.5.2.2 Hillslope radionuclide inventories

Ceasium-137 inventories at the hill sites were similar to or only slightly higher than that measured at the reference sites (Fig. 5.4A and 5.4C and Table 5.3). The mean ^{137}Cs inventory at Guthega Hill was 1001 ± 63 Bq/m^2 (cf reference inventory 1008 ± 88 Bq/m^2). At Cootapatamba Hill the mean ^{137}Cs inventory was 928 ± 66 Bq/m^2 (cf reference inventory 886 ± 70 Bq/m^2) (these values do not include counting error). In each case, statistical tests confirmed that the mean (t-test), median (independent samples median test) and distribution (Kolmogorov-Smirmov test) of the hill sites inventories are not statistically different from the reference site (at the 95% confidence level) (Table 5.4).

In contrast to the ^{137}Cs results, the $^{210}Pb_{ex}$ hillslope inventories imply potential loss of $^{210}Pb_{ex}$ (i.e. net soil loss) at the hillslope sites (Fig. 5.4B and D and Table 5.3). The mean $^{210}Pb_{ex}$ inventory at Guthega Hill was approximately 2600 Bq/m^2 lower than the expected natural inventory (Figure 5.4B and D Table 5.3) while the $^{210}Pb_{ex}$ inventory at Cootapatamba Hill is 725 Bq/m^2 lower than the expected natural inventory. Differences between hill and reference inventories are statistically significant at Guthega Hill but not at Cootapatamba (Table 5.4).

5.5.2.3 Modelled erosion rates

For the most part, there were no statistically significant differences in the radionuclide inventories to provide convincing evidence of significant erosion at the analysed hillslopes, the exception being the $^{210}Pb_{ex}$ inventory at Guthega, which was significantly lower than the reference inventory. Based on the difference between the mean hillslope and reference inventories, the estimated erosion rate at the Guthega hillslope produced by the diffusion and migration model, i.e. the average rate occurring over the last ˜100 years, was 60 t/km^2/y. The range of potential erosion rates estimated from the upper and lower 95% confidence intervals of the reference and hillslope means was 10-90 t/km^2/y. Based on a mean soil bulk density of 0.6 g/cm^3 the 60 t/km^2/y of soil loss experienced at Guthega Hill equates to a surface lowering rate of 0.1 mm/y.

At Cootapatamba Hill, the observed loss of $^{210}Pb_{ex}$, was shown to be statistically non-significant, however, as the results imply some potential loss of $^{210}Pb_{ex}$, modelled erosion rates are provided for reference. At Cootapatamba, the estimated erosion rate produced from the diffusion and migration model based on the difference in the mean $^{210}Pb_{ex}$ inventories of the hillslope and reference site, was 20 t/km^2/y. However, as $^{210}Pb_{ex}$ loss at this site is small

relative to its natural variability, this value is relatively uncertain. The maximum difference between the 95% confidence intervals of the reference and hillslope mean inventories at Cootapatamba Hill imply a potential soil redistribution rate of between 110 t/km^2/y of erosion to 76 t/km^2/y of deposition.

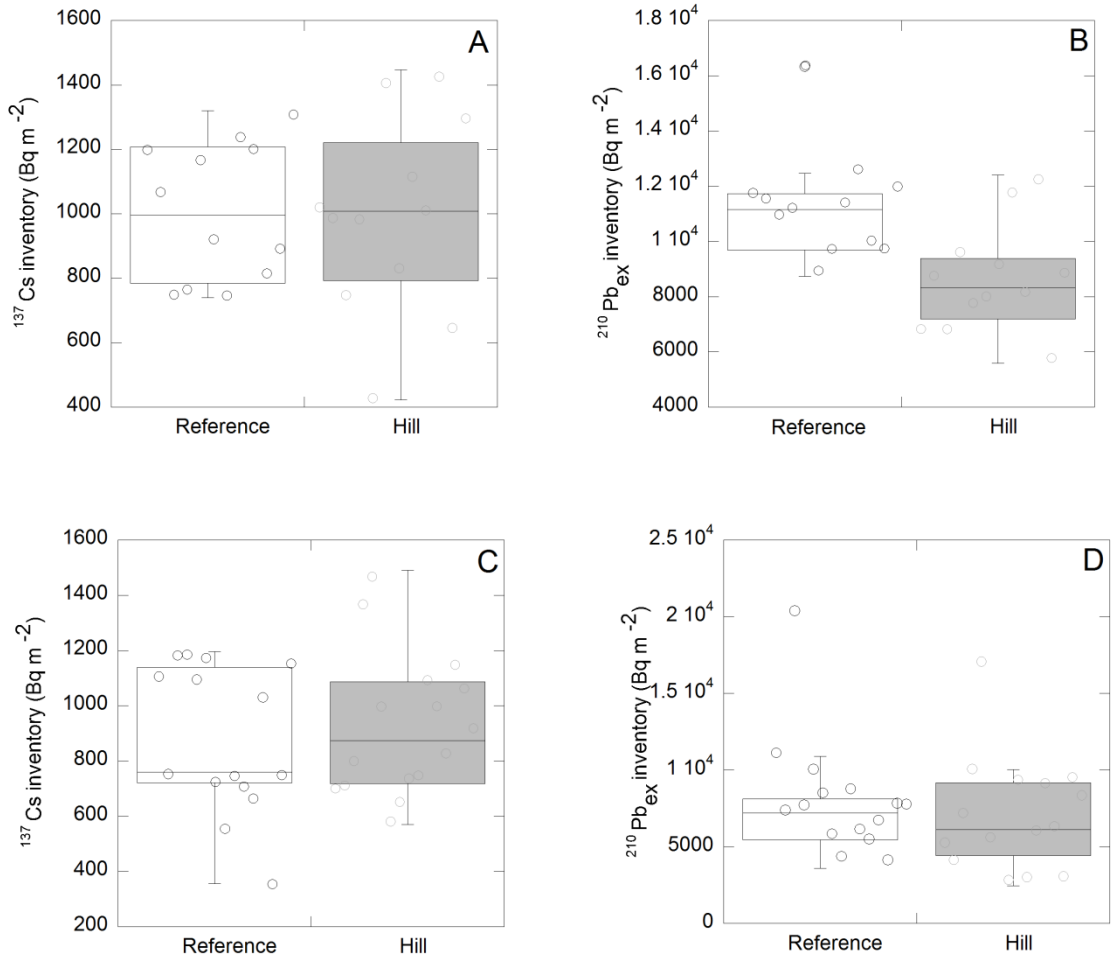

Figure 5.4 Radionuclide inventories for reference and hillslope at Guthega A) ^{137}Cs B) ^{210}Pb$_{ex}$ and Cootapatamba C) ^{137}Cs and D) ^{210}Pb$_{ex}$

Table 5.4. Statistical tests for differences in distribution, mean and median between reference and hillslope radionuclide inventories for ^{137}Cs and $^{210}Pb_{ex}$

Site	Null Hypothesis	Test	^{137}Cs		$^{210}Pb_{ex}$	
			Significance (p)	Inventories are significantly different (Y/N)	Significance (p)	Inventories are significantly different (Y/N)
Guthega	A#	t-test	0.953	N	0.004	Y
	B*	ISMT[2]	1	N	0.03	Y
	C[1]	ISKST[3]	0.996	N	0.01	Y
Cootapatamba	A#	t-test	0.664	N	0.62	N
	B*	ISMT[2]	0.862	N	0.953	N
	C[1]	ISKST[3]	0.876	N	0.925	N

#A= the mean inventory at the hillslope is the same as would be expected due to fallout and natural variability alone

*B= the median inventory at the hillslope is the same as would be expected due to fallout and natural variability alone

[1]C= the distribution of the hillslope inventory is the same as would be expected due to natural variability alone

ISMT[2] = independent samples median test

ISKST[3] = independent samples Kolmogorov Smirmov test

The ^{137}Cs hillslope inventories at both sites were essentially identical or slightly higher than their respective reference inventories, implying either that the total volume of soil lost over the past 60 years (the timespan of the ^{137}Cs method) was negligible and/or that the sampling resolution was insufficient to capture and accurately characterise the ^{137}Cs inventory at the hillslope site. While the chosen sample size (n=15) is considered as sufficient in much of the radionuclide literature (see for example the review by Pennock and Appleby, 2003) power analysis demonstrates that the erosion rates occurring on Snowy Mountains hillslopes may be near the limit of that detectable by the statistical tests applied in this study. Allowing for an 80% probability of detecting erosion or deposition if it did occur, the smallest overall ^{137}Cs loss or gain detectable by this study is 336 Bq/m^2 or approximately 33% of the mean reference inventory at Guthega and 227 Bq/m^2 or 31% of the mean reference inventory at Cootapatamba. This rate of ^{137}Cs loss converts to an erosion rate of 70 t/km^2/y using Walling's (2007) diffusion and migration model. This value is towards the mid-upper end of the erosion rates calculated using $^{210}Pb_{ex}$ (see section 5.2.3). The same ^{137}Cs values convert to an erosion rate of 24 t/km^2/y using the AEM model.

5.5.3 Sedimentation rates

Sediment mass accumulation rates (MAR) calculated using equation 5.1 for Club Lake and Guthega Reservoir were 470 t/km^2/y, and 2610 t/km^2/y respectively. These values represent the mean accumulation rates since approximately 1920 CE for Club Lake and since approximately 1955 CE for Guthega Reservoir. The MARS equate to a catchment sediment yield of 23 t/km^2/y for Club Lake and 6 t/km^2/y from Guthega.

The results from Club Lake are considered to be at the upper end of sediment yields from the Snowy Mountains in general due to the relatively small size, steepness and limited potential for sediment storage within the lake catchment, although some eroded sediment is stored within talus slopes on the cirque wall and within fens at the margins of the lake (Mooney et al., 1997). In contrast, sediment storage within Guthega may be affected by the release of sediment through the river outlet structure at the base of the dam. Accordingly, the 6 t/km^2/y value from Guthega may underestimate true sediment yields. Considering that a proportion of eroded sediment will be stored within both the lake and reservoirs catchments, the sediment yields from Club Lake and Guthega suggest that hillslope erosion rates from the Snowy Mountains may exceed 6 - 23 t/km^2/y.

5.6 Discussion

5.6.1 The age of alpine and subalpine soils in the Snowy Mountains and its implications for sediment production

It is generally accepted that late Pleistocene sediment erosion and transport rates in the highlands of Australia were greater than present (Kemp and Rhodes, 2010; Page and Nanson, 1996; Page et al., 1991). The major rivers which drain the Snowy Mountains (the Murray and Murrumbidgee Rivers) are known to have experienced markedly different channel forms and sediment characteristics, i.e. braided, low sinuosity channels transporting bedload by comparison to the current meandering high sinuosity suspended load channels (Page et al., 2009). In high altitude catchments the change to the present regime occurred at approximately 6- 10 ka and may have been driven, in part, by changing erosion rates in the Snowy Mountains (Ogden et al., 2001). The timing of the onset of soil formation in the Snowy Mountains would document the onset of an implied period of relative geomorphic stability which is considered to mark the Holocene, or in this context at least the mid to late Holocene.

While the timing of late Pleistocene glaciation and also of maximum frost shattering (and by implication the age of the underlying substrate) in the Snowy Mountains is relatively well constrained (with three glacial advances occurring between approximately 15 and 35 ka (Barrows et al., 2001)), the subsequent development of the alpine soils is comparatively unknown. The only relevant existing dates for soils in the alpine/subalpine (>1 500 m) zone come from peat mires (Costin, 1972; Kemp and Hope, 2014; Martin, 1986; Marx et al., 2011), which develop under specific topographic and hydrological conditions, and from timing of activity of solifluction terraces (Costin, 1972). The presented ^{14}C dates from Guthega hillslope are therefore the first ages for organic hillslope soils which blanket almost the entire subalpine/alpine area. Radiocarbon dating of soil organic matter (SOM) is not straightforward due to the continuous incorporation of new carbon into the soil via root decay, bioturbation and translocation of mobile organic fractions (Wang et al. 1995). Consequently, macro-carbon, such as macro-charcoal is regarded as producing more reliable ages, but was unfortunately not present in the studied soils. Humins, as were dated in this study, are considered, by some to be the SOM fraction which most closely resembles the true soil age (Pessenda et al., 2001). Although paired radiocarbon dates on the humin fraction and on macro-charcoal from the same depth have returned equivalent ages (Wang et al. 2014,

Pessenda et al. 2001), it is not possible to rule out the addition of new carbon from root material to the humin fraction in this study. Consequently, radiocarbon ages presented here are considered to represent minimum ages reflecting the mean residence time (MRT) of carbon in soil,that is the average age of all components of different ages in the soil, allowing for renewal and decomposition.

The chernic tenosols of the Australian Alps are considered to be polygenetic (Brewer and Haldane, 1972). The A horizon is dominated by organic inputs and has been ascribed a Holocene age (McKenzie et al., 2004). The underlying material, consisting of a poorly developed B/C horizon, has been interpreted as a truncated Pleistocene soil (originally termed pedoderms (Brewer et al., 1970)) developed during a period of greater chemical weathering. The presence of stone lines below the A horizon, as occurs commonly in the Snowy Mountains, has been argued to represent an erosional feature consistent with the polygenetic origin of the soils (Brewer and Haldane, 1972). While a Pleistocene origin is presumed, the age of the B/C horizon has not yet been confirmed by suitable dating methods. However, the A-B/C transition, the position of the deepest dates obtained here, marks the onset of A horizon development and the establishment of conditions favouring preservation of organic matter and soil up-building.

The radiocarbon dates performed on SOM in these humose chernic tenosols would be expected to be significantly less influenced by incorporation of new carbon than many other soils. In this mountain environment, low temperatures and humid conditions inhibit mineralisation of SOM, and may facilitate the formation of organic up-building soils. While the SOM reservoir may receive new carbon from root decay, the zone of active root growth and bioturbation will shift up with time, meaning that the radiocarbon content at different depths should reflect that date at which they formed to a greater extent than more mineral soils. This is supported by the progressive increase in radiocarbon age with depth which implies that SOM is continuously buried by younger organic matter.

The radiocarbon analyses from the A – B/C horizon transition at each the three profiles examined here returned ages of c.2 500 y. cal. BP (Table 2). These are considerably younger than previously expected ages of approximately 12-16 ka indicated by the termination of glaciation and the decline of significant frost shattering in the Snowy Mountains (Barrows et al., 2004; Barrows et al., 2001). The implication of this discrepancy is that either the soil at the A-BC transition has incorporated significant new carbon, e.g. approximately 30-40 % of the ^{14}C present at the A-B/C transition has been incorporated following initial soil formation,

or alternatively that the organic horizon has developed since 2500 y. cal. BP. In the following sections the potential ages of alpine and subalpine soils are explored using other geomorphic and palaeoclimatic evidence.

Maximum possible ages for the onset of soil development in the Snowy Mountains

The maximum likely date for the onset of the current phase of soil development at Guthega is determined by the timing of the end of glaciation in the late Pleistocene and the subsequent reestablishment of conditions suitable to the establishment of vegetation and development of the organic A horizons of the chernic tenosols. On the Australian mainland, the extent of late Pleistocene glaciation, even at the height of the Last Glacial Maximum (LGM) is believed to have been spatially limited. In the Kosciusko region, permanent ice is thought to have been restricted to small cirque glaciers above 1850 m AHD which covered a maximum area of 15 km^2 (Barrows et al., 2001). However, periglacial activity was likely to have been considerably more widespread, resulting in major slope instability possibly extending to as low 600m above current sea level (Galloway, 1965). In the Snowy Mountains, the limits of periglacial solifluction were possibly 975 m lower than today, implying summer time temperatures 9°C colder than present (Galloway, 1965). In the current alpine/subalpine zone (>1500 m AHD) periglacial slope processes were considered sufficient to initiate widespread stripping of the pre-existing soil and vegetation, producing the stony rubble which today underlies much of the alpine/subalpine zone (Costin, 1972). Thus the earliest time at which fine-grained weathering products began to accumulate on slopes above 1500 m in the Snowy Mountains must at the least post-date the latest deglaciation of the Kosciusko Massif.

On the Australian mainland, several lines of evidence place the most recent Pleistocene glaciation at ~35-16 ka, with maximum cooling at 21 ± 2 ka (Williams et al., 2009). Rivers draining the eastern highlands experienced episodic increased discharge and bed load transport centered at 30-25, 20-18 and 18-14 ka, implying increased snowpack volumes and instability in less vegetated headwater catchments at these times (Kemp and Rhodes, 2010; Page and Nanson, 1996; Page et al., 1991). On the Kosciusko Massif, cosmogenic ^{10}Be dating of glacial moraines demonstrates that the latest (Mt Tynam) and least extensive glacier advance occurred at 16.8 ± 1.4 ka (Barrows et al., 2001). A lack of recessional moraines implies that the subsequent deglaciation was likely to have been rapid (Barrows et al., 2001). Block streams and block aprons located between 1200 - 1750 m AHD in the Snowy Mountains and Victorian Alps also appear to have become inactive after ~12-17 ka (Barrows

et al., 2004), indicating a decline in the intensity of frost shattering. Basal dates for organic sediment overlying glacial till in the region's largest cirque lake suggest local establishment (i.e. to 1890 m AHD) of vegetation by as early as 15.8 ka (De Dekker and Shakau, unpublished data in (Barrows et al., 2001)). The end of the last bedload dominated phase on the Riverine Plain sometime before ~12 ka also implies increasing stability for the highlands in general (Page et al., 2009). Thus the maximum probable date for the renewed onset of soil development in the Snowy Mountains region is ~14-16 ka.

At high elevations (the current subalpine and alpine zone) there is evidence to suggest that return to suitable conditions may not have occurred until several thousand years later. At Caledonia Fen (1280 m AHD), located ~170 km SE of the Guthega site, the timing of the transition from mineral to organic sedimentation implies that the establishment of high lake levels and stable catchment slopes did not occur until ~11 ka (Kershaw et al., 2007). This change was concomitant with a dramatic increase in eucalypt abundance and the decline of cold climate vegetation (including *Asteraceae Tubiliflorea* and *Chenopodiaceae*) indicating the rise of the treeline to close, or above, 1280 m AHD at this time. This is 600 m lower than the elevation of the current tree line at Guthega Hill. Assuming a lapse rate of 0.77° C/ 100 m and a temperature increase of 1°C for each degree of latitude, the Caledonia Fen results suggest that the 11 ka B.P. temperature at the Guthega ridge-crest was ~3.6° C lower than present. By implication, mean daily temperatures at Guthega Hill may have been <- 6° C in the coldest months with maximum daily temperatures remaining below 0°C for 3-4 months of the year (at present mean maximum daily temperatures rise above freezing in all months).While this temperature estimate is imprecise, it nevertheless provides insight into the likelihood of organic soil development occurring in the alpine area at 11 ka and suggests that cold climate conditions may have limited the rate of organic soil building until after 11 ka. This is supported by pollen data from elevations of 1955-1960 m AHD surrounding Mt Kosciusko which suggest that grassland was not present in the alpine tract until 11 000 y. cal. BP, with the transition to the current alpine community occurring sometime after 9000 (Rain , 1974) to 7000 y. cal. BP (Martin, 1986).

The development of peat mires in the alpine zone would also have been inhibited until slopes stabilised sufficiently to allow the rate peat growth in low gradient areas to exceed its removal (Hope, 2003). Early ^{14}C dates from the Snowy Mountains placed the onset of peat growth above 1800 m AHD at ~11–18 ka (Costin, 1972; Martin, 1986). More recently obtained dates, however, show that peat development at many sites did not occur until ~7-9

ka (Martin, 1999; Marx et al., 2011). This suggests that summer temperatures in the current alpine zone may have remained c.≤ 10°C until 7-8 ka, after which they warmed sufficiently to permit peat growth in topographically favourable positions, or to permit more extensive development (Marx et al., 2011). This date coincides approximately with a decline in alpine pollen and rise in *Eucalpyptus* at Diggers Creek peat mire (at approx. 6 500 cal. y. BP) indicating the advance of the local treeline above ~1700 m (Martin, 1999).

The only previous estimate for the onset of hillslope soil development in the alpine zone comes from Pound Creek (at 1960 m AHD), where soil overlies 15 cm of fine granitic gravel, dated to 9000 radiocarbon years (Costin, 1972; Martin, 1986). This was interpreted as representing a period of intense periglacial activity preceding the onset of soil development. Elsewhere, soil developed on late Pleistocene substrates in the Blue Mountains (>900 m AHD, 250 km north of Guthega) and dated by optically stimulated luminescence (OSL) shows a marked discontinuity in age with depth, related to accelerated erosion above the treeline during the LGM. OSL ages jump from 32 ka at 40 cm depth to 7 ka at 30 cm, implying sediment accumulation on top of the relict erosional surface began slightly after 8 ka (Wilkinson et al., 2005). A delayed return to stable conditions in high elevation catchments is supported by the timing of the initiation of modern fluvial activity on upper Murray River and its tributaries, which at 7 -10 ka, post-dates that of the lower elevation Goulburn and mid Murray Basin by 1-10 ka (Ogden et al., 2001; Page et al., 2009; Pels, 1969).

This period of warming climate was followed by the Holocene climatic optimum, which manifested in Australia as high lake levels (Sakata and Asakura, 2007), increased river discharge (Cohen and Nanson, 2007), reduced aeolian deposition recorded in Blue Lake (Stanley and De Deckker, 2002) and a maxima in rainforest and wet scelorphyll taxa suggesting a period of enhanced rainfall and temperatures 1-2° C higher than present (Gao et al., 2003) between ~8.5-4 ka BP, centered around 6 ka (Cohen and Nanson, 2007; Gao et al., 2003). Thus, the most likely maximum age for the attainment of conditions for organic soil building in the alpine area is considered to be 7-9 ka. This is likely to have had a considerable impact on the hydrology of alpine catchments as their capacity for storage and delayed release of rainfall and snowmelt increased with the development of organic soils and peatlands.

Evidence for late Holocene onset of soil development

The 2 500 y. cal. BP basal ages for the Guthega soils obtained by this study are concomitant with the Neoglacial, a period of glacial advances and enhanced geomorphic activity across the Southern Hemisphere (Porter, 2000). Evidence for altered climate conditions during this period is derived predominately from glacial advances, onset of peat development and palynological studies from southern South America and New Zealand (Kilian and Lamy, 2012; Markgraf et al., 1992; Porter, 2000; Shulmeister et al., 2004; Stansell et al., 2013; Wanner et al., 2008) including Antarctic cooling at 5 ka (Hodell et al., 2001) and 2.3 ka (Masson-Delmotte et al., 2004). In the Southern Hemisphere, this has widely been attributed to increase in the strength/position of the southern westerly wind belt and an associated increase in precipitation (Lamy et al., 2001; Marx et al., 2011; Shulmeister et al., 2004; Strother et al., 2014). Glacial advances are typically taken as being centred around 4500 y. cal. BP., however, a series of advances occur between 5400 and 2500 y. cal. BP (Wanner et al., 2008).

The retreat of glaciers after 15 ka years in Australia means there is less obvious evidence of this event in the landscape compared with active glacial environments. However, the mid to late Holocene (after 6 ka) is associated with increased rainfall variability, including both droughts and pluvial episodes associated with the strengthening and increased frequency of the El Nino Southern Oscillation and switches the Indian Ocean Dipole (Gliganic et al., 2014; Gouramanis et al., 2013; Marx et al., 2011; Marx et al., 2009; Petherick et al., 2013). Evidence for cooler conditions is equivocal. Nevertheless, several distinct cold phases occurring throughout the mid to late Holocene in Australia are evident in $\delta^{18}O$ records from offshore records in the canyons of the Murray river at 4 300, 2 700 and 1 400 years BP (Moros et al., 2009). These cold phases are generally replicated in deuterium derived records from the EPICA ice core (Masson-Delmotte et al., 2004). In addition there is evidence of cooler conditions in the Snowy Mountains at this time (e.g. Kemp and Hope, 2014; Martin, 1999), as discussed below.

In the Snowy Mountains, Costin (1972) found evidence of episodic geomorphic instability particularly at ~2 000-4 000 years BP. This included reactivation of solifluction terraces, rubble layers in fen peats surrounding Club Lake. The timing of this activity was established using some of earliest radiocarbon dates undertaken in Australia, however, and occurred prior to advances in sample preparation to improve the removal of contamination.

More recent studies provide additional evidence of enhanced geomorphic activity and changing climate in the Australian Alps in the mid to late Holocene. Marx et al. (2011) found an increase in fluvial/colluvial sediment input to a peat mire in the headwaters of the Snowy River between 2 000-4 000 y. cal. BP and a decrease in long-range dust input, interpreted to represent increased local geomorphic activity coinciding with wetter conditions in dust source areas (the lower Murray-Darling Basin).

The sedimentological pattern in lower elevation mires displays alternating peaty silt and humic clay bands between 10 000 and 3 500 y. cal. BP. At 3 500 y. cal. BP the peats are sometimes capped by a sand layer followed by continuous and rapid peat development to the present (Hope et al., 2009). Combined this indicates potentially variable geomorphic conditions before 3500 y. cal. BP, potentially increased geomorphic activity at 3 500 yrs cal. BP, followed by lower activity or wetter conditions after this date until the present. Further evidence of geomorphic stability sometime after 3.5 ka is provided by higher elevation peat mires in the Snowy Mountains which at some sites began developing at c. 3 000 y. cal. BP, indicating the onset of favourable conditions for peat development at this time (Buck et al., 2013; Costin, 1972; Martin, 1999).

The c.3 000 y. cal. BP signal in peat mires is potentially linked to periods of increased drought or fire (Hope et al., 2009). A possible decrease in temperature during this period is implied by palynological studies from high elevation sites. These show an increase in Poaceae pollen and a eucalypt minima in the Diggers Creek peat bog from 1900-4000 y. cal. BP (Martin 1999), return to subalpine woodland or daisy rich grassland between 2700 and 900 y. cal. BP at Micalong Swamp (Kemp and Hope, 2014) and an increase of *Nothofagus* at high elevation sites in the Victorian Alps (>900 m AHD) at approximately 2 200 years BP (McKenzie, 1997), which has been interpreted as indicating cooler and/or wetter conditions.

Consequently, there is evidence that supports the onset of alpine and subalpine soil development in the Snowy Mountains at 2500 y. cal. BP. However, there is also evidence that soil formation, following the last Pleistocene glaciation, is likely to have begun at least 7 ka. If the Guthega hill slope soils have developed from 2500 y. cal. BP then it implies previous soil developed in the early to mid-Holocene has been eroded during the Neoglacial. Peat development continued through the Neoglacial period in the Snowy Mountains at high elevation sites, confirming significant biological activity. However, peat in the Snowy Mountains is confined to topographic depressions which are less likely to experience erosion. Overall, the age of soil development cannot be established unequivocally by this study;

however, the minimum dates for the stable soil carbon fraction are consistent with the palaeoclimate evidence. The timing of the onset of soil formation and associated implications relating to the stability of the landscape remains important for understanding palaeoclimate conditions and geomorphic response in the Snowy Mountains.

5.6.2 Soil production rates

The current phase of soil development in the Snowy Mountains alpine zone has thus been proceeding for between 2.5 and 12 ka, producing between 30 and 60 cm of organic soil. The soil ages estimated by the radiocarbon ages and the geomorphic evidence provide two alternative methods for calculating the rate of soil development (the net effect of soil production and erosion) in the Snowy Mountains over the early to late Holocene. In the first approach, soil development rates were estimated by dividing the accumulated soil depth by maximum soil age implied by paleoclimate and geomorphic data (7- 12 ka). An alternative estimate was obtained from the radiocarbon ages and the depth of soil accumulated between each ^{14}C dated interval.

Assuming that soil development has been continuous since deglaciation, i.e. since approximately 7- 12 ka BP (method 1), produces in a mean estimated soil development rate of approximately 0.05 - 0.09 mm/y (50 and 90 mm/ky) in the mid-slope and ridge-crest profiles and of 0.03 – 0.04 mm/yr (30-40 mm/ky) in the toe-slope profile. Assuming an average bulk density of 0.7 g/cm^3 for the A horizon, this equates to a mean mass accumulation rate of 20 – 60 t/km^2/y.

Using the second approach (i.e. estimating soil development rates from the depth of soil accumulated between each radiocarbon dated interval), soil development rates are estimated to have ranged between 0.08 - 0.26 mm/y since the late Holocene. Based on the soil bulk density for the equivalent depth interval (which ranged from 0.6 g/cm^3 near the surface to 0.9 - 1.2 g/cm^3 at the base of the A horizon) this equates to a mass accumulation rate of between 40 and 220 t/km^2/y. Thus the rate of soil development at Guthega estimated using the two methods described above ranges between a minimum of 0.05 and a maximum of 0.26 mm/y, with corresponding mass accumulation rates of 20 to 220 t/km^2/y.

Previously estimated rates for soil formation, undertaken in Australia using cosmogenic ^{10}Be nuclides, range from 10 ± 4 mm/ka on Devonian, Carboniferous and Permian aged sedimentary and metamorphic substrates in warm temperate New South Wales to 75 ± 24 mm/ka on sandstone in the tropical Northern Territory (Stockmann et al., 2014). Closer to the

Snowy Mountains at Frogs Hollow, (930 AHD, rainfall 500 mm year), production rates inferred from U-series isotopes for soils developed on Devonian granites were 10 -24 mm/ky (Suresh et al., 2013). Assuming a bulk density of 1.6 g/cm^3, this equates to a mass accumulation rate for Australian soils of 16 - 118 t/km^2/y. Thus even at the lowest estimated production rates, soil development in the Snowy Mountains is towards the upper end of values previously reported for Australian soils, despite their location in what is traditionally viewed as a low chemical weathering environment.

The production rates estimated for Guthega (20-220 t/km^2/y) are, in fact, broadly similar to those reported for Holocene aged soils on soil mantled alpine slopes elsewhere. Soil production rates estimated by the ^{10}Be method on the low relief plateau of the San Gabriel Mountains, California USA ranged from 38-196 t/km^2/y (Dixon et al., 2012). Dixon et al. (2013) considered these plateau sites to be relatively uninfluenced by tectonic uplift, making them comparable in this regard to the Snowy Mountains. With a mean annual precipitation (MAP) of 500 mm the San Gabriel Mountains are, on the other hand, considerably more arid than the Snowy Mountains, where MAP exceeds 2000 mm. The rates from both Guthega and the San Gabriel Mountains are also broadly comparable to those from the actively uplifting and relatively humid (MAP 1137 mm) Rhone Valley (60-270 t/km^2/y) (Norton and von Blanckenburg, 2010). Soils of comparable age (1.5-12 ka) to those at Guthega have been shown to develop at similar rates at various sites in the European Alps (32 -346 /km^2/y) and on the Wind River Range, Wyoming, USA (43-183 t/km^2/y) (Egli et al., 2014)). Some of the highest rates of soil development have been measured in alpine areas experiencing both rapid uplift and very high annual precipitation. In the New Zealand Southern Alps (MAP 10 000 mm), for example, soil production rates reach 2.5 mm/y, one to two orders of magnitude faster than the rates inferred for the Snowy Mountains.

The maintenance of significant soil mantles on alpine hillslopes, particular in wetter regions, has been attributed to the modulating influence of precipitation on the rate of soil production (Larsen et al., 2014). High moisture availability facilitates chemical weathering by supporting high vegetation productivity and consequently the production of chelating ligands, organic acids and increased subsurface CO_2 (Larsen et al., 2014; Riebe et al., 2004). By lowering the effective activation energy of weathering reactions these biological processes may also lessen the otherwise inhibitory effect of low alpine temperatures on chemical weathering rates (Riebe et al., 2004).

In the Snowy Mountains, the high organic content of the chernic tenosols point to an additional, more direct effect of vegetation in maintaining hillslope soil mantles. At 14-27% the organic content of these soils greatly exceeds typical values for soils within Australia where organic matter normally constitutes <5% of the total soil weight (McKenzie et al., 2004). This is likely explained by high vegetation productivity as well as inhibition of organic decomposition by low temperatures, low pH and frequent saturation of the soil profile (McKenzie et al., 2004). Together these factors support an SOM accumulation rate of between 2 and 27 t/km^2/y, representing a significant contribution to total soil production. Therefore, the high soil production rates in the Snowy Mountains, by comparison to lowland Australian landscapes may be largely a function of high rates of organic input and low rates of oxidation.

5.6.3 Erosion rates

The $^{210}Pb_{ex}$ inventories from Guthega Hill imply a hillslope erosion rate of 60 t/km^2/y with a range of 10-90 t/km^2/y over the past c.100 years. This compares to catchment-wide sediment yields of 6-23 t/km^2/y at Guthega and Club Lake. Sediment yields in this context represent minimum erosion estimates due to catchment storage and potential sediment loss from both lakes, Guthega Reservoir in particular. Sensitivity analysis (power analysis) of the ^{137}Cs inventories demonstrated that the minimum erosion rate which could be detected given the sampling strategy was 70 t/km^2/y. No net soil erosion (or gain) was detectable using ^{137}Cs, implying erosion rates at Guthega Hill are no higher than 70 t/km^2/y, which accords with upper range $^{210}Pb_{ex}$ erosion estimate. Combined these results indicate erosion rates at Guthega are likely to approximate those calculated using $^{210}Pb_{ex}$, i.e. ~60 t/km^2/y but may have be considerable lower , particularly during the past 60 years.

The Guthega erosion rate is somewhat lower than the mean erosion rate of 90 t/km^2/y rate estimated for uncultivated sites around Australia using the ^{137}Cs method (Chappell et al., 2011b; Loughran et al., 2004). By comparison, erosion rates estimated for the Southern Tablelands of Australia from sedimentation in farm dams range from 4 t/km^2/y for undisturbed sites to 90 t/km^2/y for degraded pasture (Neil, 1991). Assuming that the rates estimated from the 210Pbex and sediment yield data are representative of the mean erosion rate for the 2500 km^2 subalpine/alpine zone as a whole, the total sediment yield from the Australian Alps over the past 9 ky approximates 540 x 10^6 t, although periods of significantly increased erosion, e.g. the Neoglaical, could have resulted in considerably higher overall yields.

The $^{210}Pb_{ex}$ inventories and the lake sedimentation rates both incorporate the grazing era (mid 1800s-1940s CE), when high stocking rates for sheep and cattle lead to significant erosion in areas of the Snowy Mountains (Costin, 1954). Plot studies of soil erosion undertaken in the 1950s CE, immediately following the exclusion of grazing from the alpine area of the Snowy Mountains, found that erosion averaged around 458 ± 214 (SE) t/km^2/y in areas where the ground cover had been disturbed by stock but was essentially undetectable in areas where the vegetation cover remained intact (Costin et al., 1959) (Fig. 5.4). In the Guthega catchment soil surveys mapped a total area of 30 km^{2,} over the 90 km^2 catchment which was deemed to be slightly to severely eroded (Bryant, 1971). Notably, the hill slope studied here (Guthega Hill) was not deemed to be significantly affected. Soil surveys reported erosion depth as well as spatial extent. Combined these indicate a sediment yield of 180 t/km^2/y from affected areas. This equates to an increase in the background erosion rate (i.e. in addition to natural erosion from other parts of the catchment) of 60 t/km^2/y for the Guthega catchment (Fig. 5.5). Independent stream sediment gauging carried out at Guthega during the same period recorded a suspended sediment yield 18 t/km^2/y (Brown and Milner, 1988) (Fig. 5.5). The difference between these two estimates (18 versus 60 t/km^2/y) implies either that substantial quantities of sediment are stored within the catchment, or transported as bedload, or a combination of the two.

The $^{210}Pb_{ex}$ erosion rates presented by the current study are substantially lower than those measured during the grazing period. However, as approximately on half of the last 100 years, the time integrated by $^{210}Pb_{ex}$ erosion modelling, included grazing; the influence of grazing cannot be ruled out. The fact that the Cootapatamba Hill site recorded minimal to no net soil loss over the past 100 years does, however, imply that the effect of grazing must have been minimal on some locations, i.e. vegetated slopes as suggested by Costin et al. (1959). Overall the magnitude of the increase in the rate of erosion initiated by the grazing era reinforces the importance of the protective vegetation cover in the maintaining the hillslope soil mantle. It appears likely that high vegetation productivity in the Snowy Mountains facilitates the persistence of hillslope soils not only by contributing to rapid soil production but also through the protective effects of dense surface cover and subsurface rootmass in slowing erosion. This implies that the alpine region is sensitive to changes in climate or land conditions that can alter vegetation cover and result in increased net sediment erosion. Therefore, if cooling during the neoglacial was sufficient to reduce vegetation cover, even temporally (for

example, vegetation composition is known to have changed during this period (Martin, 1999)) then enhanced erosion (as previously discussed) seems likely.

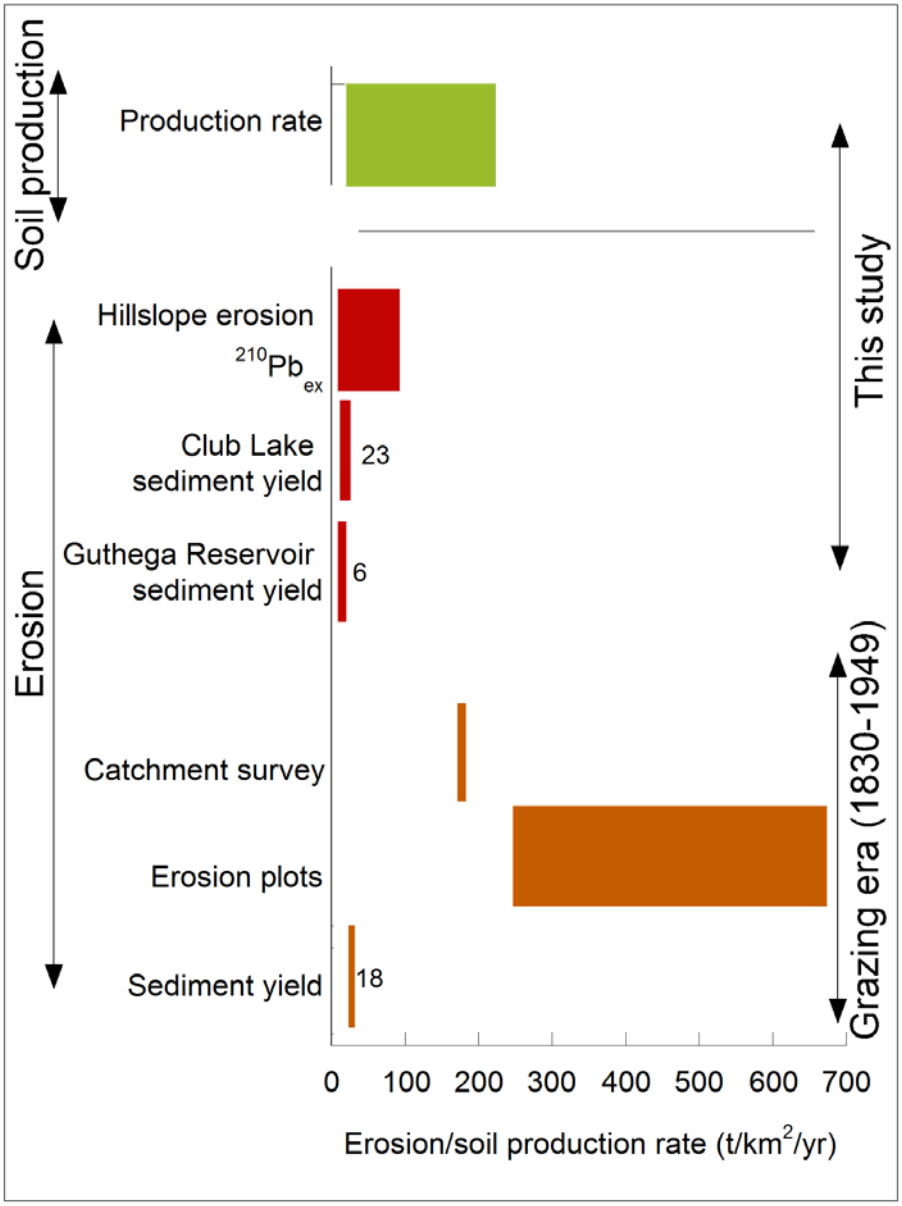

Figure 5.5 Soil production and erosion rates estimated by various methods from this study and by previous studies undertaken during the era of grazing induced erosion.

5.7. Soil development, erosion and sedimentation – Summary and implications

The results of this study imply that the Snowy Mountains experience both rapid soil development rates and slow erosion rates by comparison to lowland sites. Maximum and minimum soil production rates estimated by this study (20-220 t/km^2/y) exceed the maximum and minimum estimates of the net soil loss which has occurred over the past 100 years (10-90 t/km^2/y) (Fig. 5.5). This is consistent with the occurrence of widespread shallow alpine soils in the Snowy Mountains.

The $^{210}Pb_{ex}$ erosion rates measured by this study are, however, substantially lower than the rates of soil loss recorded during the grazing era (mid 1800s-1949), during which the opening up of the protective vegetation cover lead to soil losses of up 458 t/km^2/y (Costin et al., 1959). This dichotomy demonstrates the importance of the dense vegetation cover to the persistence of the soil mantle on alpine hillslopes. In this context, it should be noted that both the $^{210}Pb_{ex}$ and the calculated sedimentation rates presented in this study integrate over the grazing era. While, the study site was apparently not significantly affected by grazing (Bryant, 1971), it is possible that the erosion calculations could be influenced by accelerated grazing induced erosion. If so, the erosion rates calculated here would exceed both the longer term late Holocene and post grazing rates, i.e. that the presented results overestimate typical Holocene soil loss rates.

Thus the rate of soil erosion in the Snowy Mountains appears to be currently outpaced by the processes of soil production. The minimum estimated date for the onset of the current soil production phase (2500 yrs cal. BP compared with the maximum estimated age of 7-12 ka), however, would imply that soil production has exceeded erosion in only the late Holocene, and could imply that significant soil erosion occurred on hill slopes during the neo-glacial period.

Under either scenario, the production rates estimated for the highly organic soils of the Snowy Mountains alpine area are high relative to those measured for lowland Australian soils (Stockmann et al., 2014; Suresh et al., 2013). The Snowy Mountains rates are, however, comparable to production rates estimated for soil mantled hillslopes in several other alpine locations worldwide (Dixon et al., 2012; Egli et al., 2014). Rapid soil development in alpine areas has been attributed, previously, to the ready supply of fresh material in rapidly uplifting (eroding) areas and to the vegetation mediated enhancement of chemical weathering in high

rainfall mountains (Larsen et al., 2014; Riebe et al., 2004). The results presented here imply that in tectonically stable, moderate rainfall alpine areas such as the Snowy Mountains both rapid soil production and low sediment transport rates may be facilitated by the density of alpine vegetation which provides both significant material inputs for soil development and inhibits soil removal.

The following section is additional to the submitted manuscript included in the preceding chapter. In this section, the stability of hillslope metals stores is discussed in the context of the results presented in Chapter 5.

Implications of Chapter 5 for metal transport in the Snowy Mountains

Chapter 5 demonstrated that, while the alpine vegetation cover is maintained, the Snowy Mountains alpine area experiences both high soil production and low soil erosion rates, relative to lowland sites. In the context of this thesis, the aim of this chapter was to understand the stability of landscape metals stores and the potential for metals bound to soil particles to be mobilised and transported to downstream sediment sinks.

The results of Chapter 5 have implications for the storage and transport of atmospheric metal contaminants in landscape of the Snowy Mountains. Qualitatively, the upbuilding development pathway of the Snowy Mountains soils suggests that metal pollutant deposited from the atmosphere to the soil surface is likely to be incorporated into the developing soil profile/matrix. The function of hillslope soils as a sink for atmospherically derived metals is supported by the estimated soil production rates (20-220 t/km^2/y), which slightly exceed the $^{210}Pb_{ex}$ derived erosion rates (60 t/km^2/y (95% CI [10,19]). This implies that a substantial proportion of atmospherically derived metal burden is currently being locked up within accumulating hillslope soils. However, the delicate balance between soil production and erosion and the evidence for past episodes of soil stripping suggest that alpine soils are sensitive to rapid erosion if the protective vegetation cover is lost. Anthropogenic or climatic disturbance may result in a rapid switch in the function of hillslope soils from a sink to a source of anthropogenic metals.

To quantify the mobility of atmospherically derived metals in the landscape of the Snowy Mountains, Chapter 5 aimed to: 1) quantify hillslope erosion rates using ^{137}Cs and $^{210}Pb_{ex}$ inventories and erosion conversion models to estimate the rate at which atmospherically derived metals are mobilised from hillslope stores via soil erosion, and; 2) quantify the rate at which soil and, by implication, bound metals are transported downslope using U-series isotopes and chemical weathering indices to quantify soil residence time along a downslope transect. To date, it has not been possible to estimate soil residence time from the U-series data due to the variable intensity at which isotopes appear to fractionation within the soil

profile. These results are, therefore, not presented here. Allowing for uncertainty and as discussed in sections 5 and 6 of Chapter 5 we were able to estimate bulk hillslope erosion rates from the $^{210}Pb_{ex}$ inventories.

In the following section, the $^{210}Pb_{ex}$ derived erosion rates are used to provide a more quantitative estimate of the rate at which metals deposited from the atmosphere to the soil surface are mobilised by the process of sheet erosion. This was achieved by multiplying the excess (anthropogenically derived) concentration of enriched metals in the uppermost 15 cm of the soil profile, i.e. that likely to be mobilised by erosion processes measured by the $^{210}Pb_{ex}$ method, by the annual erosion rate estimated from the $^{210}Pb_{ex}$ inventories. Excess concentration ($Metal_{ex}$) was calculated according to equation 5.2.

$$Metal_{ex} = Cm-(Cm/EF) \quad (5.2)$$

where *Cm* is the total soil concentration of each metal and *EF* is the enrichment factor calculated according to equation 5.3.

$$EF = (Cm/Cc_{ex})/(Cm/Cc_{natavg}) \quad (5.3)$$

Where Cm/Cc_{ex} is the ratio, in the topsoil, of the metals whose concentration is suspected of being perturbed (*Cm*) to that of a conservative element (*Cc*) and (Cm/Cc_{natavg}) is the ratio of *Cm* to *Cc* in the BC horizon.

Metal concentrations were analysed by inductively coupled plasma mass spectrometry (ICPMS) as described in the supplementary section of Chapter 4. The choice of conservative elements and soil standard tables are provided in section 4.5.1 and in the supplementary section of Chapter 4, respectively. Estimation of soil EF by this method has associated uncertainties which arise from the potentially non-conservative behaviour of normalising elements in soils which are discussed further in section 4.5.4 of Chapter 4. This method produced the highest estimated for soil metal EF of those described in section 4.5.4 of Chapter 4 and is therefore used here to provide a upper range estimate for the mass of metal pollutant mobilised from hillslopes.

The rate of metal mobilisation was calculated using equation 5.4.

$$\text{Mobilisation rate}_{Metalex} = Metal_{ex} * \text{ER} \quad (5.4)$$

where ER is the erosion rate derived using the $^{210}Pb_{ex}$ method (60 t/km^2/y (95% CI[10,90]). The potential range of mobilisation rates is assessed by substituting the upper and lower 95% CI values for the $^{210}Pb_{ex}$ estimated erosion rates into equation 5.4. Soil metal concentrations

were undertaken on ashed samples. Ashed concentrations were corrected to total concentrations using the percentage organic content of the soil samples.

Soil excess concentration and mobilisation rates are shown in Table 5.6. As discussed in section 4.5.4, only those metals with the lowest natural concentrations (Ag, Mo, Cd, Sb) could definitively be identified as enriched in Snowy Mountains soils. While other metals were enriched in aerosol samples collected over the Snowy Mountains, it is presumed that their anthropogenic concentrations are masked by metals derived from weathering of local bedrock or that enrichment is not distinguishable due to the inherent complexities of calculating EF for soils. For these metals (Cr, Co, Ni, Cu, Zn, Sn, Pb), the anthropogenically, derived component which is mobilised from hillopes via sheetwash is not distinguishable from the general background rate of transport for metals which are naturally present in the environment.

The range of estimated mobilisation rates for excess Ag, Mo, Cd and Sb is large due to the large degree of uncertainty surrounding the estimated $^{210}Pb_{ex}$ erosion rates. However, even allowing for an erosion rate close to the upper estimate presented here (90 t/km^2/y), the mass mobilised from hillslopes is < ˜20 g/km^2/y for all enriched metals. Using these mobilisation rates the mass of anthropogenic metal delivered from catchments to downstream sediment sinks (by the transport of sediment-bound metals) can be estimated. Assuming a mean erosion rate of 60 t/km^2/yr, the estimated annual mass of anthropogenic (excess) metal delivered from the catchment (91 km^2) to Guthega Reservoir is estimated to be: Ag: 180 g, Mo: 1270 g, Cd: 460g, Sb: 360 g. This compares to natural delivery rates for lithogenic metals of Ag: 80 g, Mo: 730 g. Cd: 180 g and Sb: 460 g. Using the upper estimated erosion rate of 90 t/km^2/yr the mass anthropogenic (excess) metal delivered to Guthega Reservoir each year is Ag: 360 g, Mo: 1910 g, Cd: 730 g, and Sb: 1000 g while natural delivery rates are estimated at Ag: 330 g, Mo: 1880 g. Cd: 740 g and Sb: 490 g. The actual rate of delivery to the reservoir is most likely considerable less due to the storage of sediment and bound metals within the reservoir catchment.

Table. 5.6 Mobilisation rate via hillslope erosion for metals enriched in Snowy Mountains soils

	Soil EF	Soil concentration (mg/kg)[a]	Soil excess concentration (mg/kg)[a]	Mobilisation rate excess metal ($g/km^2/y$)[b]	Mobilisation rate excess metal Range ($g/km^2/y$)
Ag	3.9	0.06	0.04	2	0 - 4
Mo	2.8	0.3	0.23	14	2 - 21
Cd	5.1	0.16	0.09	5	1 - 8
Sb	1.9	0.16	0.06	4	1 - 11

[a]concentration in the uppermost 15 cm of the soil profile, corrected for % organic content

[b]based on hillslope erosion estimate of 60 t/km2/yr from $^{210}Pb_{ex}$ inventory

[c]derived from 95% CI of $^{210}Pb_{ex}$ derived hillslope erosion rate and the mean excess metal concentration in the uppermost 15cm of the soil

Chapter 6. Synthesis and conclusion

6.1 Introduction

The aim of this thesis was to quantify the enrichment of atmospherically derived metals in the surface environment of a remote-from-source setting, the Snowy Mountains, south-eastern Australia, to assess the variability of atmospheric metal contamination across the landscape and to understand the factors that control that variability.

This thesis has provided a detailed record of atmospheric metal enrichment across a variety of environmental archives. It has identified a range of factors which control the transport and concentration of atmospheric metals across landscapes; contributed to filling the significant data gap on metal contamination in Australia and more generally in the Southern Hemisphere, and; provided new data on the enrichment of a range of metals other than most frequently measured Pb and Hg, including Cr, Co, Ni, Cu, As, Mo, Ag, Cd, Sb.

This section presents a synthesis of the major findings of this research in relation to the objectives outlined in section 1.3. The specific research findings in relation to each objective are summarised in section 6.2. In section 6.3 the implications of these findings are discussed in context of the broader discipline and identified knowledge gaps. Limitations of the research and recommendations for further research are presented in section 6.4. An overall synthesis and conclusion is provided in section 6.5.

6.2 Research findings

6.2.1 Objective 1

Objective 1: To construct a temporal record of metal enrichment in tarn lake sediments, in order to place previous metal contamination records constructed in the Snowy Mountains in a wider landscape context. Assess the response of lake sediment metal concentrations to changing atmospheric metal deposition. Identify the processes that control the timing, magnitude and pattern of metal enrichment in the tarn.

In the Snowy Mountains, industrial metals were previously shown to be enriched in peat mires as a result of upwind mining, metal production, coal combustion and agriculture (Marx et al., 2010). The record by Marx et al. (2010) provided a detailed chronology of atmospheric metal contamination in the Snowy Mountains and was, prior to the current study, one of only

two existing records of far travelled atmospheric contaminants in Australia. At a landscape-scale, ombrogenous peat mires occupy a small fraction of the Snowy Mountains bioregion ((< 5% (Hope et al., 2012)). In addition, it was considered that atmospherically derived metals could be "locked-up" in peat mires at relatively high concentrations due to the immobility of (some) metals within the peat substrate (Novak et al., 2011) and the relative insignificance of potentially diluting terrigenous sediment inputs (Marx et al., 2011). Therefore, the degree to which the results of Marx et al., (2010) can be considered to be representative of the degree of contamination across the Snowy Mountains landscape more broadly was unknown.

Understanding the impact of increasing atmospheric metal deposition on the wider Snowy Mountains landscape was considered particularly important in the context of ongoing AgI releases during cloud seeding. An assessment of landscape-scale metal contamination risk, identified that a number of landscape features may be sensitive to atmospheric metal contamination. This included sediment sinks such as lakes and reservoirs where atmospherically derived metals mobilised from the catchment may be redeposited.

In Chapter 3 a record of metal accumulation in an alpine tarn (Club Lake) between c.110 CE to 2011 CE was presented (this chapter was also published as Stromsoe et. al. 2013). The tarn was located within 4 km of the peat mire of Marx et al. (2010). This chapter aimed to: understand how changing atmospheric metal deposition is recorded in the tarn sediments; place the previous peat mire record of Marx et al. (2010) into a wider landscape context, and; contribute to the gap in understanding of how atmospheric metal contamination varies across the landscape.

This study showed that there were clear differences in the way the proximal peat mire and tarn lake sediments recorded changes in atmospheric metal deposition. In comparison to the earlier peat records of Marx et al., (2010), enrichment of atmospherically derived metals in lake sediments was minimal, i.e. there was only minor apparent enrichment of industrial metals in sediments dating from after the industrialisation of Australia continent (which occurred in the mid to late 1800s). In addition, metal enrichment in the lake core, in contrast to the peat mire record, displayed only approximate temporal coherence with known emissions histories. Mean industrial period EFs for metals in the peat mire were Ag: 2.2, Pb: 3.3, Zn:2.1, Cu: 4.1 (Marx et al., 2010) (Fig. 3.7 of this thesis). These values are consistent with previous records from atmospherically dominated archives (peat mires and snow) from the Southern Hemisphere (New Zealand and Antarctica) (Marx et al., 2008; Wolff and Suttie,

1994). In tarn sediments, mean industrial period EFs for selected metals were lower, Ag: 1.3, Pb: 1.3, Zn: 1.1, Cu:1.2 (Fig. 3.5), implying a comparatively dampened response of tarn sediment EFs to increasing metal emissions.

Trace element signatures for sediments extracted from the tarn core show that the composition of non-anthropogenic trace elements in lake sediments was distinct from aeolian dust which acts as a carrier of pollutant metals to the mire. This implies that atmospheric deposition is not the primary source of inputs to the lake. In addition, unpolluted sediment derived from the lake catchment was found to contain high natural concentrations of Pb, Cu and Zn compared to unpolluted aeolian dust from the bottom of the peat mire core. This implies that atmospheric contaminants are masked by the fluvial input of lithogenic metals to the lake.

Metal flux to the lake is controlled primarily by the rate of sediment transport from the catchment, with atmospheric deposition accounting for only 4-8% of metal input to the lake. Thus, the lake sediments are relatively insensitive to enrichment by increasing atmospheric deposition, due to the dilution of atmospherically derived metal by catchment derived terrigenous sediments. In the context of cloud seeding, producing Ag enrichment equivalent to the 90^{th} percentile of current sediment Ag concentrations would require that cloud seeding emissions increase by at least 19 times the current rate. This implies that cloud seeding related enrichment of Ag in lakes is extremely unlikely.

Overall, this chapter demonstrated that the significance of atmospheric industrial metals varies across the landscape, depending on the relative rates of atmospheric deposition and terrestrial sediment transport, which is itself controlled by geomorphic and hydrological processes. Assessing the impact of increasing atmospheric metal emissions in complex environments requires consideration of geomorphic and hydrological processes, which vary at a landscape scale.

6.1.2 Objective 2

Objective 2: Examine the response of a variety of different surface archives to increased atmospheric metal deposition in a remote-from-source setting. Assess how the magnitude of contamination varies across the landscape. Identify the factors which control metal enrichment in different parts of the landscape.

The findings in Chapter 3 showed that the concentration of atmospherically derived metals in surface sediments varies across the landscape of the Snowy Mountains. Peat mires and lake

sediments recorded a different response to increasing atmospheric metal contamination. This was attributed to the variability of geomorphic and hydrological processes which control the flux of atmospherically derived contaminants, lithogenic metals and sediment to these archives. Therefore, Chapter 4 further explored the variability of atmospheric metal contamination across the landscape of the Snowy Mountains.

In Chapter 4, metal concentration, metal enrichment and metal flux was examined across a wider range of surface archives. These archives (soils, peat mires, tarn lakes and reservoir sediments) were identified by the conceptual model (outlined in section 2.7.4 of this thesis) as key receptors for atmospherically derived metals. In addition, examining metal concentrations in these archives allowed a range of processes which may potentially influence metal accumulation and enrichment across and alpine landscape to be explored. Aerosols were also sampled using a network of high volume samplers. Aerosols were analysed for trace elements to quantify the enrichment of metals in the atmosphere. The aerosols samples provided a snapshot estimate of atmospheric metal fluxes. This was compared to metal accumulation and enrichment in surface archives to investigate patterns of dilution and concentration across the landscape.

This chapter demonstrated that human activity has substantially increased the concentration of industrial metals in the atmosphere of the remote-from-source Snowy Mountains. In aerosols, industrial metals including Pb, Sb, Cr, and Mo were enriched by 3.5 (Pb) to 48 (Mo) times natural levels. In surface settings (peat mires, hillslope soils, tarn lake and reservoir sediments) enrichment was variable and depended on the relative rates of atmospheric deposition and terrigenous sediment input, metal sensitivity to enrichment (the natural background concentration of metals in local soils), metal behaviour and catchment area.

Only those metals with the lowest concentration in local soils (Ag, Mo, Cd, Sb) and the greatest enrichment in aerosols were enriched in all surface archives, implying that atmospheric metals are generally diluted during incorporation into the surface environment. In atmospherically dominated settings (peat mires in the upper parts of the landscape), surface metal enrichment showed the greatest fidelity with the state of the atmosphere. On, average, however, metal EFs were still 5-7 fold lower in peat mires than in aerosols (Fig. 4.8)

In the tarn lake, only those metals most sensitive to enrichment (metals which were both highly enriched in aerosols and present in low concentrations in local soil and sediments) (Mo, Cd, Sb, As and Ag) were enriched. Their EFs were 8, 19, 21, 18 and 11 fold lower than

those of the aerosols (Fig. 4.9). No other metals were enriched, indicating that atmospherically derived metals are diluted by uncontaminated sediment transported from the catchment.

Reservoirs, which have relatively large catchments, showed the lowest fidelity with atmospheric metal enrichment. Instead metal concentrations generally reflected those of previously contaminated or naturally metal-bearing catchment soils. Some metals were, however, additionally enriched or diluted in reservoir sediments depending on their relative particle affinity. Particle reactive metals (e.g. Pb) displayed minimal enrichment, implying they were retained within catchment soils. More soluble elements and less particle reactive metals (e.g. Cu and Zn) showed evidence that they were being concentrated during transport from the catchment to the reservoir.

Both landscape positon and natural background concentration determine the potential for atmospheric contaminants to reach environmental trigger values (interim sediment quality guidelines (ISQG) (ANZECC, 2000)) in different environmental sinks. For those metals which are most sensitive to enrichment (Ag, Cd, Sb), the increase in excess flux required to reach trigger value concentrations is lowest in the reservoir sediments (Ag: 13-18, Cd: 7-10 and Sb: 17-61 times the current flux) and highest in the tarn lake (Ag: 60, Cd: 15, Sb: 27 times the current flux) and the peat mire (Ag: 74, Cd: 15, Sb: 18 times the current flux). In the context of an ongoing cloud seeding program (which is only releasing Ag) this suggests that relatively large increases in the mass of Ag released to the atmosphere of the Snowy Mountains would be required to produce Ag concentrations equivalent to the ISQG environmental trigger value of 1 mg/kg.

Overall, this results of this chapter further demonstrated that the concentration of atmospherically derived metals varies across landscapes and between different archive types. It identified that the degree to which the atmospheric contamination is translated to enrichment of surface sediments depends on a range of processes that control the transport and accumulation of atmospheric metals and matrix material through surface environments. Metal enrichment in surface archives depends on the relative rates of atmospheric deposition and terrigenous sediment input, metal sensitivity to enrichment (the natural concentration of metals in local soils), catchment area and metal behaviour.

6.1.3 Objective 3

Objective 3 Quantify soil production and soil erosion rates to assess landscape stability in the Snowy Mountains over recent timescales (millennia to decades), with the aim of understanding the potential for metal contaminants to be transported through the landscape.

In Chapter 4 it was shown that atmospherically derived metals were enriched in the soils of the Snowy Mountains. Due to their spatial extent, hillslope soils in the Snowy Mountains and across the Earth's environment more generally represent a potentially important secondary source of industrial metals to downstream areas. Chapter 4 also showed that metals were enriched in downstream sediment sinks such as reservoirs, implying that they are being mobilised from hillslope stores.

Therefore, Chapter 5 aimed to assess the stability and persistence of hillslope soils and thus the potential for metals to be mobilised from hillslope stores by the processes of erosion and sediment transport. This was achieved by quantifying soil production and erosion rates to understand the balance between soil production and erosion under different forcing conditions, including anthropogenic and climatic change. Soil erosion rates determined from $^{210}Pb_{ex}$ inventories also allowed the rate at which metals are mobilised from hillslope soil stores to be quantified.

Hillslope erosion rates estimated using ^{137}Cs and $^{210}Pb_{ex}$ inventories showed that erosion rates under undisturbed conditions were relatively low by comparison to uncultivated hillslopes in other parts of Australia (Chappell et al., 2011b). On balance, the average erosion rate over the past 100 years is estimated to be 60 t/km^2/y. However, uncertainties in determining radionuclide inventories, imply this value may be as low as 10 and as high as 90 t/km^2/yr (95% CI). The erosion rates presented in this thesis are substantially lower than those estimated for past periods when the alpine grasslands of the Snowy Mountains were degraded by sheep and cattle grazing (estimated by other work at 458 t/km^2/y (Costin et al., 1959), and 180 t/km^2/y (Bryant, 1971)). This highlights the importance of vegetation cover in maintaining the stability of hillslope soils.

Soil production rates (20-220 t/km^2/y) were similar to rates estimated for alpine regions elsewhere (32-346 t/km^2/y) (Egli et al., 2014; Norton and von Blanckenburg, 2010) and were towards the upper end of rates reported for non-alpine soils within Australia (16-118 t/km^2/y) (Stockmann et al., 2014; Suresh et al., 2013). Thus, this study adds to the global data set demonstrating rapid soil production rates in alpine areas where moisture availability and

vegetation productivity is high (Riebe et al., 2004). High soil organic contents (14-27%) and radiocarbon ages which progressively increase with soil depth suggest that Snowy Mountains alpine soils may build upwards by rapid incorporation of organic matter. On balance, the results presented in Chapter 5 show that soil production rates have slightly exceeded the rate of soil erosion over the mid-late Holocene. However, soil basal ages (2500 y. cal. BP) implied a significant soil stripping event may have occurred during altered climatic conditions of the Neoglacial. This finding and historical accounts of rapid erosion during the grazing era raise important questions on the sensitivity of these rapidly developing soils to stripping following removal of vegetation by grazing or climate change.

The findings of this Chapter have implications for the function of hillslope soils as a sink for atmospheric metals. The implication that alpine soils build upwards by the incorporation of organic matter is significant because it suggests that a substantial proportion of the total atmospheric metal burden is incorporated into the developing soil profile. The demonstrated balance between soil production and erosion suggests that hillslope soils, and by implication hillslope metal stores, are relatively stable so long as the protective alpine vegetation cover is maintained.

Erosion rates derived from $^{210}Pb_{ex}$ inventories imply that anthropogenic metals (Ag, Mo, Cd, Sb) are currently mobilised from hillslopes at a rates of <20 g/km^2/y (Table 5.6). Thus, the rate at which anthropogenic metals are mobilised by soil erosion is exceeded by the rate of input by atmospheric deposition (Table 4.3). This supports the implication that hillslope soils are currently a net sink for atmospheric metal contaminants. However, evidence for past erosion events suggests that the landscape is susceptible to rapid soil stripping and sediment loss if the protective vegetation cover is lost. This is important because it implies that loss of vegetation under climatic change or anthropogenic disturbance may result in the rapid transformation of hillslope soils from a net sink to net source of metal contaminants (albeit, at concentrations which are many times less than the environmental trigger values (Chapter 4, section 4.6.7) .

It is worth noting that parts of the Australian Alps region have been shown to be sensitive to erosion following fire, including the extensive 2003 fires which burnt over 1 million ha (68%) of forested land in the Australian Alps National Parks (Lane et al., 2006; Nyman et al., 2011; Sheridan et al., 2007). This raises questions as to the role of fire in mobilising soil and atmospheric contaminants from landscape stores.

By comparison to much of the region, unplanned fires in the true alpine and much of the subalpine zones of Kosciusko National Park are infrequent (NSW NPWS, 2008). Much of the subalpine zone has only burnt once since records began in 1956 (NSW NPWS, 2008). In contrast, some lowland areas of the park have burn three times over the same period (NSW NPWS, 2008). From previous research undertaken in the Snowy Mountains, there are some indications that the subalpine woodland is, in addition, less sensitive to post-fire erosion than lower elevation forests (Nyman et al., 2011; Sheridan et al., 2007; Smith and Dragovich, 2008).

The Guthega Hillslope site was burnt during the 2003 bushfires. The current study found no evidence of a major soil stripping event associated with this fire (based on visual observation of intact soil profiles, the absence of fire-associated deposits in toeslopes or reservoir sediments, and the relatively low $^{210}Pb_{ex}$ derived erosion rates). It is possible that preservation of the subsurface alpine rootmass may bind soil against erosion following removal of the above-ground biomass. Thus, while previous instances of post-fire erosion imply that this may be a significant mechanism for the mobilisation of sediment-bound metals in areas of the Snowy Mountains, further research is required to understand the specific response of alpine/subalpine soils to erosion following fire.

6.3 Study significance

6.3.1 Introduction

This thesis began by identifying a series of key gaps in our understanding of the scale of enrichment and behaviour of atmospherically derived metals in the Earth's environment.

As outlined in Chapter 1 and discussed further in Chapter 2, these include:

1) A limited understanding of variability in atmospherically derived metal enrichment in different parts of the landscape that are affected by different geomorphic processes.
2) A correspondingly limited understanding of where atmospheric metal enrichment occurs in landscapes and how changes in atmospheric deposition are recorded in different environmental archives.
3) A historic focus on the environmental enrichment of Hg and Pb, with correspondingly limited understanding of the accumulation of other potentially deleterious metals in the landscape.

4) A paucity of metal enrichment records from the Southern Hemisphere and from Australia in particular.

In the following section the findings of this thesis are discussed in the context of the contribution of this research to (in part) addressing these identified key knowledge gaps.

6.3.2 Discussion

Metal enrichment in different landscape and geomorphic settings.

To date, few studies have directly compared the magnitude and chronology of atmospheric metal enrichment across a variety of proximal environmental archives (exceptions include Bindler et al., 1999; Brännvall et al., 2001c; Klaminder et al., 2010; Koinig et al., 2003; Liu et al., 2012; Norton and Kahl, 1987; Shotyk and Krachler, 2010; Yang et al., 2007). This constitutes a significant gap in understanding because geomorphic processes, which themselves vary across the landscape, may mobilize and transport atmospherically derived metals between landscape stores, in the process modifying the concentration of anthropogenic metals relative to matrix materials (Boyle et al., 2015). In addition, increases in metal contaminants may be masked by the supply of naturally generated metals at concentrations that are high relative to those of the excess metal (Stromsoe et al., 2013). The lack of comparative studies, therefore, constitutes a clear gap in the understanding of the scale of atmospherically derived metal contamination across the wider landscape. Moreover, the degree to which individual archives represent the state of contamination across the wider landscape is not fully understood.

This study contributed to filling these gaps by directly comparing the magnitude and chronology of atmospheric metal enrichment in a variety of surface archives in the Snowy Mountains, including soils, peat mire, tarn lake and reservoir sediments. In the process, it identified a range of key factors which control the incorporation of atmospheric metals into the environment and, consequently, the extent and magnitude of metal contamination across the wider landscape. These controlling factors included: the relative rates of atmospheric deposition and terrestrial inputs; the natural background concentration of metals in local sediments; catchment size, and; characteristics of individual metals such as their relative particle reactivity.

Atmospheric metal enrichment and how changes are recorded in different archives.

Chapter 4 of this thesis demonstrated that while metal enrichment patterns in ombrogenous peat mires of the Snowy Mountains most closely resembled that of the atmosphere, metals were additionally enriched or depleted in archives such as soils, tarn lake and reservoir sediments. These results imply that, while atmospherically dominated archives such as peat mires are important for quantifying the load of contaminants deposited to the Earth's surface, they do not necessarily represent the state of contamination across the wider landscape.

Archives which are less favoured for constructing temporal records of atmospheric deposition, such as lakes at the end of large catchments, may provide a broader assessment of the state of metal contamination at the scale of the catchment or account for processes which concentrate metals relative to those of primary sinks. In addition, sediment sinks such as lakes may provide critical habitat to sensitive ecological communities (e.g. Wolfe et al., 2003) and are, therefore, of interest with respect to the ecological impact of metals across the landscape. Thus, this study has demonstrated how geomorphic knowledge can be used to identify the value of different archive types in assessing state of environmental metal contamination at the landscape scale. Accordingly these findings have implications for the assessment, management and monitoring of atmospheric pollutant impacts.

This study applied methods from geomorphology and geoscience to quantify the stability of landscape metal stores and to assess the potential for remobilisation of anthropogenic metals from primary stores to secondary sinks elsewhere in the landscape. In the context of global metal contamination, understanding the behaviour of metals within landscape stores is critical because much of the global contaminant burden is contained within environments which are sensitive to geomorphic reactivation.

Soils and peat mires, for example, are known to be susceptible to erosion in response to anthropogenic disturbance or changing environmental conditions, such as drought or fire (Blake et al., 2009; Rothwell et al., 2008). In the Snowy Mountains and across the Earth's terrestrial environment more broadly, soils are identified as an important primary receptor and store of atmospherically derived metals (e.g. Steinnes and Friedland, 2006). Consequently, soil erosion and deposition represents a potentially major conduit of atmospherically derived metal contaminants in the Snowy Mountains and elsewhere.

In Chapter 5, the stability of hillslope soil metal stores was assessed by quantifying the balance between soil production and soil erosion using a variety of methods including fallout

radionuclides (^{137}Cs and $^{210}Pb_{ex}$), ^{14}C dating, historical accounts and geomorphic evidence. These methods provided insight into the specific development pathways of Snowy Mountains alpine soils under a range of environmental conditions. Accordingly, they have implications for the understanding the storage and transport of metals through the Snowy Mountains landscape.

The soil production and erosion rates presented in Chapter 5 imply that the soils of the Snowy Mountains alpine zone are currently a net sink for anthropogenic metals. Metals deposited from the atmosphere may be largely incorporated into soils which build upwards by rapid accumulation of organic matter. At the same time, the fine balance between soil production and erosion implies that soil stability and, consequently, the integrity of soil metal stores may be highly sensitive to vegetation loss under changing boundary conditions. Soil basal ages and historical accounts of soil stripping following anthropogenic disturbance imply that changes which negatively affect vegetation cover may result in increased soil erosion and the transformation of hillslope stores from a net sink to net source of metal contaminants. Thus, the approach presented in Chapter 5 provides an example of how geomorphic/geoscience techniques can be used to assess the stability of landscape metal stores and to predict how metals may be mobilised under changing environmental conditions, including climate change.

Common methods of quantifying the transport of metalsby soil erosion and sediment transport (which include real time stream water sampling, analysis of sediments deposited to sinks such as lakes and resampling of contaminated sites) are limited by the challenges of temporal upscaling, delayed mobilisation and intermediate catchment storage and the intensity of data and time requirements. In this thesis, a novel approach was used to estimate excess metal transport by scaling soil erosion rates calculated using ^{137}Cs and ^{210}Pb inventories.

In contrast to real time sampling methods, the radionuclide approach can provide a time-integrated estimate of soil mobilisation and soil loss over timespans of 60-100 years without the need for extended monitoring programs (Mabit et al., 2008). As the commonly employed radionuclides (^{137}Cs, $^{210}Pb_{ex}$) exhibit similar behaviour and transport pathways to particle reactive pollutant metals, this method is considered appropriate for quantifying transport rates of sediment-bound metals in the landscape.

As applied in this thesis, the radionuclide method provided support for identified function of Snowy Mountains soils as a net sink for atmospheric metal contaminants and allowed the rates at which metals are exported from hillslope stores by the processes of erosion and sediment transport to be estimated. This approach is of particular importance in areas such as the Snowy Mountains where there is an increasing load of atmospheric contaminants being supplied to surface environments (Marx et al., 2010). This nascent metal contamination represents a potential future contaminant burden which may not yet be recorded in landscape compartments lower within catchments. In these situations the radionuclide method may be used to calculate current rates of excess metal transport and, potentially, to predict the future metal contaminant burden within secondary catchment sinks.

Metals other than Pb

Historically, studies of metal enrichment in environmental archives have focussed on Pb and Hg. However, a variety of other potentially toxic metals including Cd, Sb, As, Zn and Cr have been shown to enriched in the Earth's surface environment as a result of human activity (Grahn et al., 2006; Planchon et al., 2002; Shotyk et al., 1996). Despite potentially considerable impacts to human health and ecosystems, there is, to date, a relative paucity of data quantifying both the natural background concentrations and the scale of anthropogenic enrichment of these metals (Nriagu, 1990).

This thesis demonstrated that, in addition to the commonly examined metal pollutant, Pb, a number of other potentially toxic metals including Cr, Co, Ni, Cu, As, Mo, Ag, Cd, Sb are enriched in the remote-from-source environment of the Snowy Mountains. These metals are found to be present in the atmosphere of the Snowy Mountains at concentrations which exceed natural concentrations by 2.6 (Ni) to 48 (Sb) times (that is, in comparison to the levels which existed prior the industrialisation of the Australian continent in the mid-late 1800s CE). In doing so, this study has contributed to the understanding of effects of anthropogenic activity in perturbing the concentration of these metals, supporting evidence that they are widely transported through the atmosphere and subsequently incorporated in the environment (Grahn et al., 2006; Planchon et al., 2002; Shotyk et al., 1996).

This study has demonstrated that enrichment of seldom-measured industrial metals within peat mires and reservoir sediments of the Snowy Mountains ranged from 1.4 for Cr to 6.8 for Cd. Anthropogenic enrichment of several metals (Cd, Ag, Sb, Pb and Mo) was apparent even in geomorphically active environments where atmospherically derived metals were found to

be diluted by matrix material transported from the catchment. This supports assertions (e.g. Nriagu and Pacyna, 1988) that, as demonstrated conclusively for Pb, a wide range of other industrial metals are ubiquitous in the Earth's environment.

While the consequences of environmental Pb exposure have been recognised since the 1970s CE, there is a growing concern that chronic low-level exposure to metals including As, Cd, Cr, Sb may also carry significant human health risks (Martinez-Zamudio and Ha, 2011; Nriagu, 1988; Satarug et al., 2010). However the relative lack of data means both the natural background levels and the scale of anthropogenic enrichment of these metals are poorly understood (Nriagu, 1990). Given the global distribution of atmospheric metal emissions (Fig. 2.1) and the greater scale of Pb contamination in other regions of the globe, e.g. EF=100 in Europe, the presence of these metals in the Snowy Mountains imply that the excess concentrations of these metals are likely to be present broadly, and at high enrichment levels in the global environment.

Metal enrichment records from the Southern Hemisphere

In comparison to Europe and to a lesser extent North America, there are relatively few records of atmospheric metal deposition for the Southern Hemisphere. Thus, the chronology and magnitude of metal enrichment in the Southern Hemisphere is less well constrained than for the older industrial centres of Europe and North America. This constitutes an important gap in knowledge because the focus of manufacturing, mining and metal production has recently shifted away from North America towards Asia, Australia and the developing economies of the South America and Africa (Dicken, 2011; Pacyna and Pacyna, 2001). Thus, recent increases in metal emissions have been concentrated in areas of the globe which have so far received comparatively little attention in the atmospheric metal pollution literature (Pacyna and Pacyna, 2001; Pacyna et al., 2009; Wilson et al., 2006).

Prior to the current study, only two records of long-travelled metal contamination had been undertaken in Australia (Marx et al., 2010; Smith and Hamilton, 1992). The record of Marx et al. (2010) represented the only assessment of contemporary metal enrichment relative to natural background concentrations which existed prior to the industrialisation of Australia in the mid-late 1800s CE. This record showed that the rate of atmospheric metal deposition to the peat mire had not experienced the decrease which is apparent in North America in Europe following the rise of post-industrial economies and the introduction of emission control measures in the 1970s CE (Marx et al., 2010). However, the study by Marx et al. (2010) did

not investigate metal enrichment across the wider landscape. Therefore, there was a need to quantify metal enrichment in other parts of the landscape in order to more fully understand the scale and extent of atmospheric metal contamination in Australia.

This thesis provided new data on metal enrichment in the atmosphere, soil, tarn lake and reservoir sediments of the Snowy Mountains. Through the use of multiple archives, it represents the most detailed investigation undertaken in Australia. In addition, this thesis presented, to the best my knowledge, the first direct quantification of in-situ regional atmospheric metal concentrations. The results presented in this thesis have confirmed that the metal contamination produced by Australia's resource industry extends beyond the immediate vicinity of mining and smelting towns to remote areas such as the Snowy Mountains. Accordingly, this work has improved our understanding of the impact of Australia's exploitation of coal and mineral resources on the wider environment.

While the metal enrichment factors calculated within this study are lower than those reported for Europe (e.g. Pb EF 35 in peat bogs of the Swiss Jura Mountains (Shotyk et al., 2001)) , they are nonetheless substantial considering: 1) the relative distance of the of the study setting from major emission sources (for example the Snowy Mountains are 1000 km from the major metal smelting at Port Pirie), and 2) the scale of Australia's metal and coal combustion industries (which typically account for less than 5% of global metal emissions (Pacyna and Pacyna, 2001) (Fig. 2.4, Chapter 2 of this thesis)). This study demonstrates that Australia, while historically accounting for a relatively small proportion of global metal emissions, (Pacyna and Pacyna, 2001) is nonetheless subject to substantial contamination by regional air pollution, supporting previous findings from around the globe that industrial metals are ubiquitous in the Earth's ecosystems.

As the Snowy Mountains lie within the major southeast atmospheric transport pathway (Bowler, 1976; Hesse and McTainsh, 2003; Marx et al., 2008) the atmospheric enrichment results from the Snowy Mountains are representative of concentrations available to be transported beyond the Australian continent. Thus, these results support previous research in Antarctica and New Zealand which identifies Australia as a major source of contaminants to the atmosphere of the Southern Hemisphere (Marx et al., 2008; McConnell et al., 2014).

Other emerging themes from this work

While not identified at the beginning of this thesis as explicit knowledge gaps, this work has implications beyond the context of understanding the transport and fate of atmospheric metal

contaminants. In addition to the findings outlined above, the soil production and erosion rates presented in this thesis contribute to the understanding of how the balance between soil production and erosion in alpine areas is controlled and maintained. It was traditionally assumed that soil production rates in alpine environments were temperature inhibited and were outpaced by rapid rates of erosion (e.g. Peltier, 1950). Recently however, an increasing global body of literature has shown that soil production rates in alpine areas may be more rapid than previously thought due to the higher than expected rates of chemical weathering under conditions of high rainfall and vegetation productivity (Larsen et al., 2014; Riebe et al., 2004). The soil production rates presented in this thesis (20-220 t/km^2/y) were towards the upper end of those previously reported for lowland soils within Australia (Stockmann et al., 2014; Suresh et al., 2013) (16 - 118 t/km^2/y) and were similar to rates estimated for alpine regions elsewhere (32-346 t/km^2/y) (Egli et al., 2014). Thus, the results of this study add to the global data set demonstrating high soil production rates in certain alpine areas.

Globally, there has been a focus on determining soil production in actively uplifting alpine settings where it is difficult to deconvolute the role of uplift versus that of other processes (Dixon and Thorn, 2005; Larsen et al., 2014; Riebe et al., 2004). Consequently the results of this study are of additional significance as soil production rates are report for a tectonically stable, alpine setting. They, therefore, add to the global data set on soil production rates and indicate that production rates in tectonically stable alpine regions may be similar to those reported in actively uplifting areas.

The soil production rates calculated in Chapter 5 represent the first direct estimates for the Snowy Mountains region. The results are significant beyond the context of this thesis as the Snowy Mountains and the Great Dividing range are considered as the protosource for the vast sedimentary load which has accumulated in the Murray-Darling Basin (Kemp and Rhodes, 2010; Ogden et al., 2001; Page et al., 2009). The rates of soil production estimated here constrain sediment delivery to the basin during stable interglacial conditions.

An additional significant outcome of this study was the potential finding of a major soil stripping event during the period known as the Neoglacial. Evidence for altered climate conditions during this period is primarily derived from a series of glacial advances, onset of peat development and palynological changes in occurring in New Zealand and South America 5400 to 2500 y. cal. BP (Kilian and Lamy, 2012; Markgraf et al., 1992; Porter, 2000; Shulmeister et al., 2004; Stansell et al., 2013; Wanner et al., 2008). Evidence of its effects in Australia remains equivocal. This study concluded that there is some evidence to

support a significant erosion event at one of the alpine study sites prior to 2500 years BP, suggesting that climatic change during the Neoglacial may have been sufficient to trigger increased geomorphic activity in parts of Australia.

6.4 Priorities for future research

This thesis has presented the first landscape scale assessment of long-travelled atmospheric metals in the Australian environment. This study has shown that human activities have modified the flux of industrial metals to the atmosphere to the extent that metal contaminants are present in otherwise pristine environments such as the Snowy Mountains in concentrations which substantially exceed background levels. This includes a range of metals and mettaloids for which there is limited previous enrichment data, including Cr, Co, Ni, Cu, As, Mo, Ag, Cd and Sb. In addition, it has shown that these atmospheric metals are incorporated into surface environments in varying concentrations, meaning the scale of enrichment varies across landscapes and between geomorphic process zones.

These results provide further evidence that a wide range of metals, some seldom studied, are likely enriched across large areas of the Earth's surface, especially in areas more proximal to emission sources. In addition, these metals are mobile in the environment, representing a potential future source of contamination to other landscape compartments. Therefore, there is a need for further research to more completely understand the scale, extent and fate of atmospheric metal contaminants in the surface environment.

This study has allocated effort and available resources to 1) maximising the number of different archive types, and 2) producing high resolution temporal records. In general, the confidence of conclusions relating specifically to the Snowy Mountains would be increased by increasing the number of replicate cores analysed within each archive (e.g. to n=5; Engstrom and Rose, 2013; Rippey et al., 2008). To better understand the mechanisms by which metals are transported through the environment the trace element analyses could be repeated using sequential extractions. This could provide insight into, for example, the role of dissolved organic matter and the relative importance of the dissolved and particulate phases in transporting metals from soils to lake sediments.

The use of enrichment factors to determine the anthropogenic contribution to total metal concentrations can be uncertain in settings where material which reliably represents the pre-anthropogenic concentration is not available (Hernandez et al., 2003) (e.g. the soils and reservoir sediments described in this study). Recent improvements in the analytical precision

of isotope ratios obtained by multi-collector-ICP-MS have raised the possibility that isotopic fingerprinting methods which have been instrumental in quantifying the environmental burden of contaminant Pb may be applied to other metals, such as Zn and Cd (Cloquet et al., 2008; Cloquet et al., 2006). Currently these techniques are still being developed (Cloquet et al., 2008; Cloquet et al., 2006). However, their application to determining the source of less frequently quantified metals in remote-from-source settings has the potential to further advance this technique and to improve the understanding of the scale of contamination by metals other than Pb relative to background concentrations.

As methods emerge, these isotopic fingerprinting techniques could be attempted to more definitively determine the anthropogenic contribution to the metal concentration measured in the peat mires, soils, tarn and reservoir sediments of the Snowy Mountains. For example, the total inventory of isotopically determined anthropogenic metals in ombrogenous peats could be compared to that of more geomorphically active archives, e.g. lake sediments. This could allow the relative contributions from anthropogenic sources and lithogenic catchment inputs to be more definitively quantified.

Isotopic fingerprinting techniques could also be applied to quantify the anthropogenic metal burden in surface soils. In the Snowy Mountains and more generally across the Earth's terrestrial environment, soils are identified as a diffuse but spatially extensive store of atmospherically derived metals. Potential future research which builds on the results presented here includes the quantification of anthropogenic atmospheric metal burden in soils through the use of trace elements, isotopes and fallout radionuclides to understand the importance of atmospheric deposition relative to in-situ weathering and colluvial transport. This also has potential applications in understanding the contribution of aeolian dust to alpine soil development. In areas downwind of major dust source areas, such as the Rocky Mountains of the western USA, the deposition of atmospherically transported dust is considered to have a substantial impact on the rate and pathways of alpine soil development (e.g. Dahms, 1993; Lawrence et al., 2010; Litaor, 1987). In the Snowy Mountains, dust deposition rates have been previously quantified (Johnston, 2001; Marx et al., 2011) but questions remain as to the influence on the geochemistry and development of alpine soils.

This thesis has provided a case study in how the landscape scale impact of contamination may be assessed, using, in this case, a geomorphic process framework. It is suggested that the prediction of the impact of human metal use on the wider environment may be improved by a more comprehensive assessment of landscape composition, configuration and connectivity

than examined here e.g. by combining remote sensing and metrics of landscape classification and connectivity derived from geomorphology with geochemical methods. This could be applied. for example, to exploring the role of peat lands and organic soils in sequestering contaminants within catchments by identifying patterns of landscape connectivity and targeting archives for sampling accordingly.

The enrichment of metals and mettaloids including, Cd, As, and Sb throughout the surface environments of the remote-from-source Snowy Mountains implies that they are likely substantially enriched elsewhere, i.e. in areas more proximal to industrial and coal combustion sources. The impact of anthropogenic activity on the flux of these metals in the global environment is generally not well known (e.g. Filella et al., 2002; Shotyk and Krachler, 2004).Considering the potential consequences of low level exposure to these metals (Martinez-Zamudio and Ha, 2011; Nriagu, 1988; Satarug et al., 2010), there is a need to more definitively quantify the scale of their enrichment in Australia and elsewhere.

This includes more fully understanding the impact of Australia's resource economy on areas beyond the immediate surroundings of mines and metal smelters and transport corridors. It has been demonstrated that the burden of Pb held in soils surrounding major emission sources such as mines and smelters and in inner city suburbs represents an ongoing source of exposure (Gulson et al., 1994; Laidlaw and Taylor, 2011). It is recommended this assessment be extended to quantifying the enrichment of other metals that are potentially toxic but relatively infrequently studied. This assessment could be undertaken on the soils of areas which are likely to be more substantially impacted by indirect atmospheric emissions than the Snowy Mountains but have not been the focus of previous research, such as residential areas surrounding coal fired power stations and industrial centres.

6.4 Summary

This research has provided further evidence that atmospheric metals contamination is ubiquitous in the Earth's surface environment. It has improved the understanding of atmospheric metal contamination in Australia and in the Southern Hemisphere by producing detailed records of atmospheric metal enrichment across a variety of archives, showing that industrial metals are present in the surface environments of the Snowy Mountains by up to seven times natural concentrations. This includes enrichment in a range of potentially toxic metals, including Cr, Co, Ni, Cu, As, Mo, Ag, Cd, and Sb, for which there has, to date, been a relative lack of data.

This thesis has demonstrated that the concentration of atmospherically derived metal contaminants varies across the surface environment and between archive types. It has identified a range of processes which control the incorporation of atmospheric metals into surface sediments and, consequently, the impact of mining, metal production and fossil fuel combustion on the wider environment. Factors controlling the relative concentration of industrial metals in different parts of the environment were found to include: the relative rates of atmospheric deposition and terrigenous sediment inputs; the natural background concentrations of metals in local soils and sediments; catchment area, and; characteristics of individual metals, such as their relative particle reactivity. This thesis has shown that considering metal enrichment within the context of geomorphic and hydrological processes can improve understanding of the scale and extent of atmospheric metal contamination across the wider environment.

References

Abbott, M.B., Wolfe, A.P., 2003. Intensive Pre-Incan Metallurgy Recorded by Lake Sediments from the Bolivian Andes. Science, 301, 1893-1895.

Abrahim, G.M.S., Parker, R.J., 2008. Assessment of heavy metal enrichment factors and the degree of contamination in marine sediments from Tamaki Estuary, Auckland, New Zealand. Environmental Monitoring and Assessment, 136, 227-238.

Allison, J., Allison, T., 2005. Partition coeffecients for metals in surface water, soil and waste. U.S. Environmental Protection Agency Office of Research and Development, Washington DC.

Alloway, B., 1990. Heavy Metals in Soils. Blackie, London.

Alyazichi, Y.M., Jones, B.G., McLean, E., 2015. Source identification and assessment of sediment contamination of trace metals in Kogarah Bay, NSW, Australia. Environmental Monitoring and Assessment, 187.

ANZECC/ARMCANZ, 2000. Australian and New Zealand Guidelines for Fresh and Marine Water Quality: Volume 1 - The Guidelines. Australian and New Zealand Environment and Conservation Council/Agriculture and Resource Management Council of Australia and New Zealand, Canberra.

Appleby, P.G., Oldfield, F., 1978. The calculation of 210Pb dates assuming a constant rate of supply of unsupported 210Pb to the sediment. Catena, 5, 1-8.

Arimoto, R., Duce, R.A., Ray, B.J., 1989. Concentrations, sources and air-sea exchange of trace elements in the atmosphere over the Pacific Ocean. in: Duce, R.A., Riley, J.P., Chester, J.P. (Eds.), Chemical Oceanography, SEARX: The sea/air exchange program, pp. 107-145.

Arimoto, R., Duce, R.A., Ray, B.J., Ellis, W.G., Cullen, J.D., Merrill, J.T., 1995. Trace-elements in the atmosphere over the North-Atlantic. Journal of Geophysical Research-Atmospheres, 100, 1199-1213.

Arimoto, R., Duce, R.A., Ray, B.J., Hewitt, A.D., Williams, J., 1987a. Trace-elements in the atmosphere of American Samoa: Concentrations and deposition to the tropical South-Pacific. Journal of Geophysical Research-Atmospheres, 92, 8465-8479.

Arimoto, R., Duce, R.A., Ray, B.J., Hewitt, A.D., Williams, J., 1987b. Trace elements in the atmosphere of American Samoa: Concentrations and deposition to the tropical South Pacific. Journal of Geophysical Research-Atmospheres, 92, 8465-8479.

Arimoto, R., Duce, R.A., Ray, B.J., Unni, C.K., 1985. Atmospheric trace-elements at Enewetak Atoll .2. Transport to the ocean by wet and dry Deposition. Journal of Geophysical Research-Atmospheres, 90, 2391-2408.

Arimoto, R., Ray, B.J., Duce, R.A., Hewitt, A.D., Boldi, R., Hudson, A., 1990. Concentrations, sources, and fluxes of trace-elements in the remote marine atmosphere of New Zealand. Journal of Geophysical Research-Atmospheres, 95, 22389-22405.

Augustsson, A., Peltola, P., Bergbäck, B., Saarinen, T., Haltia-Hovi, E., 2010. Trace metal and geochemical variability during 5,500 years in the sediment of Lake Lehmilampi, Finland. Journal of Paleolimnology, 44, 1025-1038.

Bacardit, M., Krachler, M., Camarero, L., 2012. Whole-catchment inventories of trace metals in soils and sediments in mountain lake catchments in the Central Pyrenees: Apportioning the anthropogenic and natural contributions. Geochimica et Cosmochimica Acta, 82, 52-67.

Balogh, S.J., Meyer, M.L., Hansen, N.C., Moncrief, J.F., Gupta, S.C., 2000. Transport of mercury from a cultivated field during snowmelt. Journal of Environmental Quality, 29, 871-874.

Barbante, C., Schwikowski, M., Döring, T., Gäggeler, H.W., Schotterer, U., Tobler, L., Van de Velde, K., Ferrari, C., Cozzi, G., Turetta, A., Rosman, K., Bolshov, M., Capodaglio, G., Cescon, P., Boutron, C., 2004. Historical record of European emissions of heavy metals to the atmosphere since the 1650s from alpine snow/cce cores drilled near Monte Rosa. Environmental Science & Technology, 38, 4085-4090.

Barbante, C., Turetta, C., Capodaglio, G., Scarponi, G., 1997. Recent decrease in the lead concentration of Antarctic snow. International Journal of Environmental Analytical Chemistry, 68, 457-477.

Barbieri, M., Sappa, G., Vitale, S., Parisse, B., Battistel, M., 2014. Soil control of trace metals concentrations in landfills: A case study of the largest landfill in Europe, Malagrotta, Rome. Journal of Geochemical Exploration, 143, 146-154.

Barrie, L.A., 1985. Scavenging ratios, wet deposition, and in-cloud oxidation: An application to the oxides of sulphur and nitrogen. Journal of Geophysical Research: Atmospheres, 90, 5789-5799.

Barrie, L.A., Barrie, M.J., 1990. Chemical components of lower tropospheric aerosols in the high arctic: Six years of observations. Journal of Atmospheric Chemistry, 11, 211-226.

Barrows, T.T., Stone, J.O., Fifield, L.K., 2004. Exposure ages for Pleistocene periglacial deposits in Australia. Quaternary Science Reviews, 23, 697-708.

Barrows, T.T., Stone, J.O., Fifield, L.K., Cresswell, R.G., 2001. Late Pleistocene glaciation of the Kosciuszko Massif, Snowy Mountains, Australia. Quaternary Research, 55, 179-189.

Barsch, D., Caine, N., 1984. The nature of mountain geomorphology. Mountain Research and Development, 4, 287-298.

Batley, G., 1987. Heavy metal speciation in waters, sediments and biota from Lake Macquarie, New South Wales. Marine and Freshwater Research, 38, 591-606.

Beard, K.V., 1976. Terminal velocity and shape of cloud and precipitation drops aloft. Journal of Atmospheric Science, 18, 1163-1170.

Berg, N.H., Gallegos, A., Dell, T., Frazier, J., Procter, T., Sickman, J., Grant, S., Blett, T., Arbaugh, M., 2005. A screening procedure for identifying acid-sensitive lakes from catchment characteristics. Environmental Monitoring and Assessment, 105, 285-307.

Biester, H., Kilian, R., Franzen, C., Woda, C., Mangini, A., Schöler, H.F., 2002. Elevated mercury accumulation in a peat bog of the Magellanic Moorlands, Chile (53°S) – an anthropogenic signal from the Southern Hemisphere. Earth and Planetary Science Letters, 201, 609-620.

Bindler, R., 2008. Comment on "The biosphere: A homogeniser of Pb-isotope signals" by C. Reimann, B. Flem, A. Arnoldussen, P. Englmaier, T.E. Finne, F. Koller and Ø. Nordgulen. Applied Geochemistry, 23, 2519-2526.

Bindler, R., 2011. Contaminated lead environments of man: reviewing the lead isotopic evidence in sediments, peat, and soils for the temporal and spatial patterns of atmospheric lead pollution in Sweden. Environmental Geochemistry and Health, 33, 311-329.

Bindler, R., Brännvall, M.-L., Renberg, I., Emteryd, O., Grip, H., 1999. Natural Lead Concentrations in Pristine Boreal Forest Soils and Past Pollution Trends: A Reference for Critical Load Models. Environmental Science & Technology, 33, 3362-3367.

Bindler, R., Renberg, I., Appleby, P.G., Anderson, N.J., Rose, N.L., 2001. Mercury accumulation rates and satial patterns in lake sediments from West Greenland: a coast to ice margin transect. Environmental Science & Technology, 35, 1736-1741.

Bindler, R., Renberg, I., Klaminder, J., 2008. Bridging the gap between ancient metal pollution and contemporary biogeochemistry. Journal of Paleolimnology, 40, 755-770.

Birch, G., Taylor, S., 1999. Source of heavy metals in sediments of the Port Jackson estuary, Australia. Science of the Total Environment, 227, 123-138.

Birch, G., Vanderhayden, M., Olmos, M., 2011. The Nature and Distribution of Metals in Soils of the Sydney Estuary Catchment, Australia. Water, Air, & Soil Pollution, 216, 581-604.

Bishop, P., Goldrick, G., 2000. Geomorphological evolution of the east Australian continental margin. in: Summerfield, M. (Ed.), Geomorphology and Global Tectonics. John Wiley and Sons, Chichester, pp. 109-134.

Blake, W.H., Wallbrink, P.J., Wilkinson, S.N., Humphreys, G.S., Doerr, S.H., Shakesby, R.A., Tomkins, K.M., 2009. Deriving hillslope sediment budgets in wildfire-affected forests using fallout radionuclide tracers. Geomorphology, 104, 105-116.

Blaser, P., Zimmermann, S., Luster, J., Shotyk, W., 2000. Critical examination of trace element enrichments and depletions in soils: As, Cr, Cu, Ni, Pb, and Zn in Swiss forest soils. Science of The Total Environment, 249, 257-280.

Boës, X., Rydberg, J., Martinez-Cortizas, A., Bindler, R., Renberg, I., 2011. Evaluation of conservative lithogenic elements (Ti, Zr, Al, and Rb) to study anthropogenic element enrichments in lake sediments. Journal of Paleolimnology, 46, 75-87.

BOM, 2012. Climate Data Online. Bureau of Meteorology, 10/9/12.

BOM, 2014. Climate Statistics Charlotte Pass. 21/6/14, 27/6/14.

Boutron, C.F., Candelone, J.-P., Hong, S., 1994. Past and recent changes in the large-scale tropospheric cycles of lead and other heavy metals as documented in Antarctic and Greenland snow and ice: A review. Geochimica et Cosmochimica Acta, 58, 3217-3225.

Boutron, C.F., Gorlach, U., Candelone, J.-P., Bolshov, M.A., Delmas, R.J., 1991. Decrease in anthropogenic lead, cadmium and zinc in Greenland snows since the late 1960s. Nature, 353, 153-156.

Boutron, C.F., Patterson, C.C., 1983. The occurrence of lead in Antarctic recent snow, firn deposited over the last two centuries and prehistoric ice. Geochimica et Cosmochimica Acta, 47, 1355-1368.

Boutron, C.F., Vandal, G.M., Fitzgerald, W.F., Ferrari, C.P., 1998. A forty year record of Mercury in central Greenland snow. Geophysical Research Letters, 25, 3315-3318.

Bowler, J.M., 1976. Aridity in Australia: Age, origins and expression in aeolian landforms and sediments. Earth-Science Reviews, 12, 279-310.

Boyle, J., Chiverrell, R., Schillereff, D., 2015. Lacustrine archives of metals from mining and other industrial activities—a geochemical approach. in: Blais, J.M., Rosen, M.R., Smol, J.P. (Eds.), Environmental Contaminants. Springer Netherlands, pp. 121-159.

Boyle, J.F., Rose, N.L., Appleby, P.G., Birks, H.J.B., 2004. Recent environmental change and human impact on Svalbard: the lake-sediment geochemical record. Journal of Paleolimnology, 31, 515-530.

Brännvall, M.-L., Bindler, R., Renberg, I., Emteryd, O., Bartnicki, J., Billström, K., 1999. The medieval metal industry was the cradle of modern large-scale atmospheric lead pollution in Northern Europe. Environmental Science & Technology, 33, 4391-4395.

Brännvall, M.L., Bindler, R., Emteryd, O., Nilsson, M., Renberg, I., 1997. Stable Isotope and Concentration Records of Atmospheric Lead Pollution in Peat and Lake Sediments in Sweden. Water, Air, and Soil Pollution, 100, 243-252.

Brännvall, M.L., Bindler, R., Emteryd, O., Renberg, I., 2001a. Four thousand years of atmospheric lead pollution in northern Europe: a summary from Swedish lake sediments. Journal of Paleolimnology, 25, 421-435.

Brännvall, M.L., Bindler, R., Emteryd, O., Renberg, I., 2001b. Vertical distribution of atmospheric pollution lead in Swedish boreal forest soils. Water, Air and Soil Pollution: Focus, 1, 357-370.

Brännvall, M.L., Kurkkio, H., Bindler, R., Emteryd, O., Renberg, I., 2001c. The role of pollution versus natural geological sources for lead enrichment in recent lake sediments and surface forest soils. Environmental Geology, 40, 1057-1065.

BREE, 2014. Energy in Australia. Bureau of Resources and Energy Economics, Australian Government, last updated: 2014, accessed: 21/06/2015.

Brewer, R., Crook, K.A.W., Speight, J.G., 1970. Proposal for soilstratigraphic units in the Australian Stratigraphic Code. Journal of the Geological Society of Australia 17, 103-111.

Brewer, R., Haldane, A., 1972. Some aspects of the genesis of an alpine humus soil. Australian Journal of Soil Research, 11, 1-11.

Bridges, K.S., Jickells, T.D., Davies, T.D., Zeman, Z., Hunova, I., 2002. Aerosol, precipitation and cloud water chemistry observations on the Czech Krusne Hory plateau adjacent to a heavily industrialised valley. Atmospheric Environment, 36, 353-360.

Bronk-Ramsey, C., 2009. Bayesian Analysis of Radiocarbon Dates. Radiocarbon, 51, 337-360.

Brown, J., Milner, F., 1988. Aspects of the meteorology and hydrology of the Australian Alps. in: Good, R. (Ed.), The Scientific Signficance of the Australian Alps. Australian Academy of Science, Canberra, pp. 300.

Brozović, N., Burbank, D.W., Meigs, A.J., 1997. Climatic limits on landscape development in the northwestern Himalaya. Science, 276, 571-574.

Bryant, 1971. Deterioration of vegetation and erosion in the Guthega catchment area, Snowy Mountains. N.S.W Soil Conservation Journal, 27, 62-82.

Buck, C.S., Landing, W.M., Resing, J., 2013. Pacific Ocean aerosols: Deposition and solubility of iron, aluminum, and other trace elements. Marine Chemistry, 157, 117-130.

Bureau of Meterology, 2014. Archive: Twelve-monthly rainfall deciles for Australia. 27/03/2014, 1/07/2014.

Bureau of Resources and Energy Economics, 2013. Resources and Energy Statistics - Silver. Bureau of Resources and Energy Economics, Canberra.

Burn-Nunes, L.J., Vallelonga, P., Loss, R.D., Burton, G.R., Moy, A., Curran, M., Hong, S., Smith, A.M., Edwards, R., Morgan, V.I., Rosman, K.J.R., 2011. Seasonal variability in the input of lead, barium and indium to Law Dome, Antarctica. Geochimica et Cosmochimica Acta, 75, 1-20.

Camarero, L., Botev, I., Muri, G., Psenner, R., Rose, N., Stuchlik, E., 2009. Trace elements in alpine and arctic lake sediments as a record of diffuse atmospheric contamination across Europe. Freshwater Biology, 54, 2518-2532.

Candelone, J.-P., Hong, S., Pellone, C., Boutron, C.F., 1995. Post-Industrial Revolution changes in large-scale atmospheric pollution of the northern hemisphere by heavy metals as documented in central Greenland snow and ice. Journal of Geophysical Research: Atmospheres, 100, 16605-16616.

Cartwright, B., Merry, R.H., Tiller, K.G., 1977. Heavy metal contamination of soils around a lead smelter at Port Pirie, South Australia. Australian Journal of Soil Research, 15, 69-81.

Cattle, S.R., McTainsh, G.H., Elias, S., 2009. Æolian dust deposition rates, particle-sizes and contributions to soils along a transect in semi-arid New South Wales, Australia. Sedimentology, 56, 765-783.

Chappell, A., Hancock, G., Viscarra Rossel, R.A., Loughran, R., 2011a. Spatial uncertainty of the 137Cs reference inventory for Australian soil. Journal of Geophysical Research: Earth Surface, 116, F04014.

Chappell, A., Viscarra Rossel, R.A., Loughran, R., 2011b. Spatial uncertainty of 137Cs-derived net (1950s–1990) soil redistribution for Australia. Journal of Geophysical Research: Earth Surface, 116, F04015.

Chenhall, B.E., 2004. Trace Metals in sediments from Lake Illawarra, New South Wales, Australia. Wetlands (Australia), 21, 198-208.

Chenhall, B.E., Yassini, I., Depers, A.M., Caitcheon, G., Jones, B.G., Batley, G.E., Ohmsen, G.S., 1995. Anthropogenic marker evidence for accelerated sedimentation in Lake Illawarra, New South Wales, Australia. Environmental Geology, 26, 124-135.

Chester, R., Nimmo, M., Preston, M.R., 1999. The trace metal chemistry of atmospheric dry deposition samples collected at Cap Ferrat: a coastal site in the Western Mediterranean. Marine Chemistry, 68, 15-30.

Chiaradia, M., Chenhall, B.E., Depers, A.M., Gulson, B.L., Jones, B.G., 1997. Identification of historical lead sources in roof dusts and recent lake sediments from an industrialized area: Indications from lead isotopes. Science of the Total Environment, 205, 107-128.

Chow, T.J., Patterson, C.C., 1962. The occurrence and significance of lead isotopes in pelagic sediments. Geochimica et Cosmochimica Acta, 26, 263-308.

Chow, T.J., Snyder, C.B., Earl, J.L., 1975. Isotope ratios of lead as pollutant source indicators.

Chrastný, V., Čadková, E., Vaněk, A., Teper, L., Cabala, J., Komárek, M., 2015. Cadmium isotope fractionation within the soil profile complicates source identification in relation to Pb-Zn mining and smelting processes. Chemical Geology, 405, 1-9.

Chubb, T.H., Siems, S.T., Manton, M.J., 2011. On the Decline of Wintertime Precipitation in the Snowy Mountains of Southeastern Australia. Journal of Hydrometeorology, 12, 1483-1497.

Cloquet, C., Carignan, J., Lehmann, M., Vanhaecke, F., 2008. Variation in the isotopic composition of zinc in the natural environment and the use of zinc isotopes in biogeosciences: a review. Analytical and Bioanalytical Chemistry, 390, 451-463.

Cloquet, C., Carignan, J., Libourel, G., Sterckeman, T., Perdrix, E., 2006. Tracing source pollution in soils using cadmium and lead isotopes. Environmental Science & Technology, 40, 2525-2530.

Cloy, J.M., Farmer, J.G., Graham, M.C., MacKenzie, A.B., Cook, G.T., 2008. Historical records of atmospheric Pb deposition in four Scottish ombrotrophic peat bogs: An isotopic comparison with other records from western Europe and Greenland. Global Biogeochemical Cycles, 22, GB2016.

Cohen, T.J., Nanson, G.C., 2007. Mind the gap: an absence of valley-fill deposits identifying the Holocene hypsithermal period of enhanced flow regime in southeastern Australia. The Holocene, 17, 411-418.

Connor, S.E., Thomas, I., 2003. Sediments as Archives of Industrialisation: Evidence of Atmospheric Pollution in Coastal Wetlands of Southern Sydney, Australia. Water, Air, & Soil Pollution, 149, 189-210.

Cooke, C.A., Abbott, M.B., Wolfe, A.P., 2007. Late-Holocene atmospheric lead deposition in the Peruvain and Bolivian Andes. Holocene, 18, 353-359.

Cooke, C.A., Balcom, P.H., Biester, H., Wolfe, A.P., 2009. Over three millennia of mercury pollution in the Peruvian Andes. Proceedings of the National Academy of Sciences of the United States of America, 106, 8830-8834.

Cooper, C.F., Jolly, W.C., 1970. Ecological effects of silver iodide and other weather modification agents: A review. Water Resoures Research, 6, 88-98.

Costin, A., Kerr, D., Wimbush, D., 1960. Studies in catchment hydrology in the Australian Alps. CSIRO, Melbourne.

Costin, A.B., 1954. A study of the ecosystems of the Monaro region of New South Wales with special reference to soil erosion. Soil Conservation Service of New South Wales, Sydney.

Costin, A.B., 1972. Carbon-14 dates from the Snowy Mountains area, southeastern Australia, and their interpretation. Quaternary Research, 2, 579-590.

Costin, A.B., 1989. The Alps in a global perspective. in: Good, R. (Ed.), The Scientific Signficance of the Australian Alps. Australian Alps Liason Commitee, Canberra, pp. 7-20.

Costin, A.B., Hallsworth, E.G., Woof, M., 1952. Studies in pedogenesis in New South Wales III. The alpine humus soils. Journal of Soil Science, 3, 190-218.

Costin, A.B., Wimbush, D.J., Kerr, D., Gay, L.W., 1959. Studies in Cathment Hydrology in the Australian Alps I. Trends in Soils and Vegetation. Commonwealth Scientific and Industrial Research Organisation, Melbourne.

Dahms, D.E., 1993. Mineralogical evidence for eolian contribution to soils of late Quaternary moraines, Wind River Mountains, Wyoming, USA. Geoderma, 59, 175-196.

Davis, B.S., Birch, G.F., 2011. Spatial distribution of bulk atmospheric deposition of heavy metals in metropolitan Sydney, Australia. Water, Air, & Soil Pollution, 214, 147-162.

de Vente, J., Poesen, J., Arabkhedri, M., Verstraeten, G., 2007. The sediment delivery problem revisited. Progress in Physical Geography, 31, 155-178.

De Vleeschouwer, F., Vanneste, H., Mauquoy, D., Piotrowska, N., Torrejón, F., Roland, T., Stein, A., Le Roux, G., 2014. Emissions from pre-Hispanic Metallurgy in the South American atmosphere. PLoS ONE, 9, e111315.

Dedkov, A.P., Moszherin, V.I., 1992. Erosion and sediment yield in mountain regions of the world, pp. 29-36.

Dick, A.L., 1991. Concentrations and sources of metals in the Antarctic Peninsula aerosol. Geochimica et Cosmochimica Acta, 55, 1827-1836.

Dicken, P., 2011. Global Shift: Mapping the Changing Contours of the World Economy. Guilford Publications, New York.

Dietz, R., Riget, F., Cleemann, M., Aarkrog, A., Johansen, P., Hansen, J.C., 2000. Comparison of contaminants from different trophic levels and ecosystems. Science of The Total Environment, 245, 221-231.

Dillon, P.J., Evans, R.D., 1982. Whole-lake lead burdens in sediments of lakes in southern Ontario, Canada. Hydrobiologia, 91-92, 121-130.

Dixon, J.C., Thorn, C.E., 2005. Chemical weathering and landscape development in mid-latitude alpine environments. Geomorphology, 67, 127-145.

Dixon, J.L., Hartshorn, A.S., Heimsath, A.M., DiBiase, R.A., Whipple, K.X., 2012. Chemical weathering response to tectonic forcing: A soils perspective from the San Gabriel Mountains, California. Earth and Planetary Science Letters, 323–324, 40-49.

Dixon, L.J., Clifford, R.S., 2014. Tracing and pacing soil across slopes. Elements, 10, 363-368.

Dodson, J.R., De Salis, T., Myers, C.A., Sharp, A.J., 1994. A thousand years of environmental change and human impact in the alpine zone at Mt Kosciusko, New South Wales. Australian Geographer, 25, 77-87.

Duce, R.A., Hoffman, G.L., Zoller, W.H., 1975. Atmospheric trace metals at remote Northern and Southern Hemisphere sites: pollution or natural? Science, 187, 59-61.

Duce, R.A., Liss, P.S., Merrill, J.T., Atlas, E.L., Buat-Menard, P., Hicks, B.B., Miller, J.M., Prospero, J.M., Arimoto, R., Church, T.M., Ellis, W., Galloway, J.N., Hansen, L., Jickells, T.D., Knap, A.H., Reinhardt, K.H., Schneider, B., Soudine, A., Tokos, J.J., Tsunogai, S., Wollast, R., Zhou, M., 1991. The atmospheric input of trace species to the world ocean. Global Biogeochemical Cycles, 5, 193-259.

Eggins, S.M., Woodhead, J.D., Kinsley, L.P.J., Mortimer, G.E., Sylvester, P., McCulloch, M.T., Hergt, J.M., Handler, M.R., 1997. A simple method for the precise determination of ≥ 40 trace elements in geological samples by ICPMS using enriched isotope internal standardisation. Chemical Geology, 134, 311-326.

Egli, M., Dahms, D., Norton, K., 2014. Soil formation rates on silicate parent material in alpine environments: Different approaches–different results? Geoderma, 213, 320-333.

Elliott, G.L., 1997. A National Reconnaissance Survey of Soil Erosion of Australia, New South Wales. University of Newcastle, Newcastle, Australia.

Elliott, G.L., Campbell, B.L., Loughran, R.J., 1990. Correlation of erosion measurements and soil caesium-137 content. International Journal of Radiation Applications and Instrumentation. Part A. Applied Radiation and Isotopes, 41, 713-717.

Engstrom, D., Rose, N., 2013. A whole-basin, mass-balance approach to paleolimnology. Journal of Paleolimnology, 49, 333-347.

Erel, Y., Kalderon-Asael, B., Dayan, U., Sandler, A., 2007. European atmospheric pollution imported by cooler air masses to the Eastern Mediterranean during the summer. Environmental Science & Technology, 41, 5198-5203.

Erel, Y., Patterson, C.C., 1994. Leakage of industrial lead into the hydrocycle. Geochimica et Cosmochimica Acta, 58, 3289-3296.

Erel, Y., Veron, A., Halicz, L., 1997. Tracing the transport of anthropogenic lead in the atmosphere and in soils using isotopic ratios. Geochimica et Cosmochimica Acta, 61, 4495-4505.

Evans, R.D., 1986. Sources of mercury contamination in the sediments of small headwater lakes in south-central Ontario, Canada. Archives of Environmental Contamination and Toxicology, 15, 505-512.

Fekiacova, Z., Cornu, S., Pichat, S., 2015. Tracing contamination sources in soils with Cu and Zn isotopic ratios. Science of the Total Environment, 517, 96-105.

Ferrari, C.P., Clotteau, T., Thompson, L.G., Barbante, C., Cozzi, G., Cescon, P., Hong, S., Maurice-Bourgoin, L., Francou, B., Boutron, C.F., 2001. Heavy metals in ancient tropical ice: initial results. Atmospheric Environment, 35, 5809-5815.

Filella, M., Belzile, N., Chen, Y.-W., 2002. Antimony in the environment: a review focused on natural waters: I. Occurrence. Earth-Science Reviews, 57, 125-176.

Flegal, A.R., Maring, H., Niemeyer, S., 1993. Anthropogenic lead in Antarctic sea water. Nature, 365, 242-244.

Foster, I., Charlesworth, S., Dearing, J., Keen, D., Dalgleish, H., 1991. Lake sediments: a surrogate measure of sediment associated heavy metal transport in fluvial systems?, Sediment and Stream Water Quality in a changing Environment: Trends and Explanation. IAHS, Vienna, pp. 321-327.

Foster, I.D.L., Charlesworth, S.M., 1996. Heavy metals in the hydrological cycle: trends and explanation. Hydrological Processes, 10, 227-261.

Friedland, A., Johnson, A., Siccama, T., 1984. Trace metal content of the forest floor in the green mountains of Vermont: Spatial and temporal patterns. Water, Air, and Soil Pollution, 21, 161-170.

Friedland, A.J., Craig, B.W., Miller, E.K., Herrick, G.T., Siccama, T.G., Johnson, A.H., 1992. Decreasing Lead Levels in the Forest Floor of the Northeastern USA. Ambio, 21, 400-403.

Fujikawa, Y., Fukui, M., Kudo, A., 2000. Vertical distributions of trace Mmetals in natural soil horizons from Japan. Part 1. effect of soil types. Water, Air, and Soil Pollution, 124, 1-21.

Gaillardet, J., Dupré, B., Allègre, C.J., 1999. Geochemistry of large river suspended sediments: silicate weathering or recycling tracer? Geochimica et Cosmochimica Acta, 63, 4037-4051.

Galloway, R.W., 1965. Late Quaternary climates in Australia. The Journal of Geology, 73, 603-618.

Gandois, L., Nicolas, M., VanderHeijden, G., Probst, A., 2010. The importance of biomass net uptake for a trace metal budget in a forest stand in north-eastern France. Science of The Total Environment, 408, 5870-5877.

Gantner, N., Muir, D.C., Power, M., Iqaluk, D., Reist, J.D., Babaluk, J.A., Meili, M., Borg, H., Hammar, J., Michaud, W., Dempson, B., Solomon, K.R., 2010. Mercury concentrations in landlocked Arctic char (Salvelinus alpinus) from the Canadian Arctic. Part II: Influence of lake biotic and abiotic characteristics on geographic trends in 27 populations. Environmental Toxicology and Chemistry, 29, 633-643.

Gao, Y., Fan, S.-M., Sarmiento, J.L., 2003. Aeolian iron input to the ocean through precipitation scavenging: A modeling perspective and its implication for natural iron fertilization in the ocean. Journal of Geophysical Research: Atmospheres, 108, 4221.

García-Alix, A., Jimenez-Espejo, F.J., Lozano, J.A., Jiménez-Moreno, G., Martinez-Ruiz, F., García Sanjuán, L., Aranda Jiménez, G., García Alfonso, E., Ruiz-Puertas, G., Anderson, R.S., 2013. Anthropogenic impact and lead pollution throughout the Holocene in Southern Iberia. Science of The Total Environment, 449, 451-460.

Garcia-Orellana, J., Sanchez-Cabeza, J.A., Masqué, P., Àvila, A., Costa, E., Loÿe-Pilot, M.D., Bruach-Menchén, J.M., 2006. Atmospheric fluxes of 210Pb to the western Mediterranean Sea and the Saharan dust influence. Journal of Geophysical Research: Atmospheres, 111.

Gillis, A.C., Birch, G.F., 2006. Investigation of anthropogenic trace metals in sediments of Lake Illawarra, New South Wales. Australian Journal of Earth Sciences, 53, 523-539.

Gliganic, L.A., Cohen, T.J., May, J.-H., Jansen, J.D., Nanson, G.C., Dosseto, A., Larsen, J.R., Aubert, M., 2014. Late-Holocene climatic variability indicated by three natural archives in arid southern Australia. The Holocene, 24, 104-117.

Glooschenko, W.A., Holloway, L., Arafat, N., 1986. The use of mires in monitoring the atmospheric deposition of heavy metals. Aquatic Botany, 25, 179-190.

Goh, K.M., Molloy, B.P.J., Rafter, T.A., 1977. Radiocarbon dating of quaternary loess deposits, Banks Peninsula, Canterbury, New Zealand. Quaternary Research, 7, 177-196.

Gouramanis, C., De Deckker, P., Switzer, A.D., Wilkins, D., 2013. Cross-continent comparison of high-resolution Holocene climate records from southern Australia — Deciphering the impacts of far-field teleconnections. Earth-Science Reviews, 121, 55-72.

Grahn, E., Karlsson, S., Karlsson, U., Duker, A., 2006. Historical pollution of seldom monitored trace elements in Sweden-Part B: Sediment analysis of silver, antimony, thallium and indium. Journal of Environmental Monitoring, 8, 732-744.

Green, K., Pickering, C., 2009. Vegetation, microclimate and soils associated with the latest-lying snowpatches in Australia. Plant Ecology & Diversity, 2, 289-300.

Gulson, B.L., Mizon, K.J., Law, A.J., Korsch, M.J., Davis, J.J., Howarth, D., 1994. Source and pathways of lead in humans from the Broken Hill mining community; an alternative use of exploration methods. Economic Geology, 89, 889-908.

Gulson, B.L., Tiller, K.G., Mizon, K.J., Merry, R.H., 1981. Use of lead isotopes in soils to identify the source of lead contamination near Adelaide, South Australia. Environmental Science & Technology, 15, 691-696.

Gundermann, D.G., Hutchinson, T.C., 1995. Changes in soil chemistry 20 years after the closure of a nickel-copper smelter near Sudbury, Ontario, Canada. Journal of Geochemical Exploration, 52, 231-236.

Guzmán, G., Quinton, J., Nearing, M., Mabit, L., Gómez, J., 2013. Sediment tracers in water erosion studies: current approaches and challenges. Journal of Soils and Sediments, 13, 816-833.

Hamelin, B., Ferrand, J.L., Alleman, L., Nicolas, E., Veron, A., 1997. Isotopic evidence of pollutant lead transport from North America to the subtropical North Atlantic gyre. Geochimica et Cosmochimica Acta, 61, 4423-4428.

Han, J.S., Moon, K.J., Ahn, J.Y., Hong, Y.D., Kim, Y.J., Ryu, S.Y., Cliff, S.S., Cahill, T.A., 2004. Characteristics of ion components and trace elements of fine particles at Gosan, Korea in spring time from 2001 to 2002. Environmental Monitoring and Assessment, 92, 73-93.

Han, Y., Jin, Z., Cao, J., Posmentier, E., An, Z., 2007. Atmospheric Cu and Pb Deposition and Transport in Lake Sediments in a Remote Mountain Area, Northern China. Water, Air, and Soil Pollution, 179, 167-181.

Hansmann, W., Köppel, V., 2000. Lead-isotopes as tracers of pollutants in soils. Chemical Geology, 171, 123-144.

Harmens, H., Norris, D.A., Koerber, G.R., Buse, A., Steinnes, E., Rühling, Å., 2007. Temporal trends in the concentration of arsenic, chromium, copper, iron, nickel, vanadium and zinc in mosses across Europe between 1990 and 2000. Atmospheric Environment, 41, 6673-6687.

Harmens, H., Norris, D.A., Koerber, G.R., Buse, A., Steinnes, E., Rühling, Å., 2008. Temporal trends (1990–2000) in the concentration of cadmium, lead and mercury in mosses across Europe. Environmental Pollution, 151, 368-376.

Harrison, J., Heijnis, H., Caprarelli, G., 2003. Historical pollution variability from abandoned mine sites, Greater Blue Mountains World Heritage Area, New South Wales, Australia. Environmental Geology, 43, 680-687.

Heimsath, A.M., Chappell, J., Spooner, N.A., Questiaux, D.G., 2002. Creeping soil. Geology, 30, 111-114.

Heiri, O., Lotter, A., Lemcke, G., 2001. Loss on ignition as a method for estimating organic and carbonate content in sediments: reproducibility and comparability of results. Journal of Paleolimnology, 25, 101-110.

Herckes, P., Mirabel, P., Wortham, H., 2002. Cloud water deposition at a high-elevation site in the Vosges Mountains (France). Science of The Total Environment, 296, 59-75.

Hermanson, M.H., 1991. Chronology and sources of anthropogenic trace metals in sediments from small, shallow Arctic lakes. Environmental Science & Technology, 25, 2059-2064.

Hernandez, L., Probst, A., Probst, J.L., Ulrich, E., 2003. Heavy metal distribution in some French forest soils: evidence for atmospheric contamination. Science of The Total Environment, 312, 195-219.

Hesse, P.P., McTainsh, G.H., 2003. Australian dust deposits: modern processes and the Quaternary record. Quaternary Science Reviews, 22, 2007-2035.

Hewawasam, T., von Blanckenburg, F., Schaller, M., Kubik, P., 2003. Increase of human over natural erosion rates in tropical highlands constrained by cosmogenic nuclides. Geology, 31, 597-600.

Hodell, D.A., Kanfoush, S.L., Shemesh, A., Crosta, X., Charles, C.D., Guilderson, T.P., 2001. Abrupt cooling of Antarctic surface waters and sea ice expansion in the South Atlantic sector of the Southern Ocean at 5000 cal yr B.P. Quaternary Research, 56, 191-198.

Hogg, A.G., Hua, Q., Blackwell, P.G., Niu, M., Buck, C.E., Guilderson, T.P., Heaton, T.J., Palmer, J.G., Reimer, P.J., Reimer, R.W., Turney, C.S.M., Zimmerman, S.R.H., 2013. SHCal13 Southern Hemisphere Calibration, 0–50,000 Years cal BP.

Hollins, S.E., Harrison, J.J., Jones, B.G., Zawadzki, A., Heijnis, H., Hankin, S., 2011. Reconstructing recent sedimentation in two urbanised coastal lagoons (NSW, Australia) using radioisotopes and geochemistry. Journal of Paleolimnology, 46, 579-596.

Hong, S., Barbante, C., Boutron, C., Gabrielli, P., Gaspari, V., Cescon, P., Thompson, L., Ferrari, C., Francou, B., Maurice-Bourgoin, L., 2004a. Atmospheric heavy metals in tropical South America during the past 22 000 years recorded in a high altitude ice core from Sajama, Bolivia. Journal of Environmental Monitoring, 6, 322-326.

Hong, S., Candelone, J.-P., Patterson, C.C., Boutron, C.F., 1994. Greenland ice evidence of hemispheric lead pollution two millennia ago by Greek and Roman civilizations. Science, 265, 1841-1843.

Hong, S., Candelone, J.-P., Patterson, C.C., Boutron, C.F., 1996. History of ancient copper smelting pollution during Roman and medieval times recorded in Greenland ice. Science, 272, 246-249.

Hong, S.M., Barbante, C., Boutron, C., Gabrielli, P., Gaspari, V., Cescon, P., Thompson, L., Ferrari, C., Francou, B., Maurice-Bourgoin, L., 2004b. Atmospheric heavy metals in tropical South America during the past 22000 years recorded in a high altitude ice core from Sajama, Bolivia. Journal of Environmental Monitoring, 6, 322-326.

Hope, G., 2003. The mountain mires of southern New South Wales and the Australian Capital Territory: their history and future. in: Janet Mackay and Associates (Ed.), Proceedings of an International Years of Mountains Conference. Austraian Alps Liaison Committee, Jindabyne, pp. 67-79.

Hope, G., Nanson, R., Flett, I., 2009. The peat-forming mires of the Australian Capital Territory. Territory and Municipal Services, Canberra.

Hope, G., Nanson, R., Jones, P., 2012. Peat-forming bogs and fens of the Snowy Mountains of New South Wales. New South Wales Office of Environment and Heritage, Sydney.

Howe, P., Dobson, S., 2002. Silver and Silver Compounds: Environmental Aspects, Concise International Chemical Assesment Document 44, Geneva.

Huang, S., Arimoto, R., Rahn, K.A., 2001. Sources and source variations for aerosol at Mace Head, Ireland. Atmospheric Environment, 35, 1421-1437.

Imai, N., Terashima, S., Itoh, S., Ando, A., 1995. 1994 Compilation of analytical data for minor and trace elements in seventeen GSJ geochemical reference samples, igneous rock series. Geostandards Newsletter, 19, 135-213.

Jacobson, M.Z., 2005. Fundamentals of Atmospheric Modelling. Cambridge University Press, New York.

Jaffe, D., Anderson, T., Kotchenruther, R., Trost, B., Danielson, J., Simpson, W., Brentsen, T., Karlsdottir, S., Blake, D., Harris, J.M., Carmichael, G., Uno, I., 1999. Transport of Asian air pollution to North America. Geophysical Research Letters, 26, 711-714.

Jickells, T.D., Spokes, L.J., 2001. Atmospheric iron inputs to the ocean. in: Turner, D., Hunter, K.A. (Eds.), Biogeochemistry of Iron in Seawater. John Wiley, New York, pp. 8-21.

Johnson, C.E., Siccama, T.G., Driscoll, C.T., Likens, G.E., Moeller, R.E., 1995. Changes in lead biogeochemistry in response to decreasing atmospheric inputs. Ecological Applications, 5, 813-822.

Johnston, S.W., 2001. The influence of aeolian dust deposits on alpine soils in south-eastern Australia. Australian Journal of Soil Research, 39, 81-88.

Jones, K.C., Davies, B.E., Peterson, P.J., 1986. Silver in Welsh soils: Physical and chemical distribution studies. Geoderma, 37, 157-174.

Kabata-Pendias, A., Mukherjee, A., 2007. Trace Elements from Soil to Human. Springer, Berlin, Germany.

Kabata-Pendias, A., Pendias, H., 2001. Trace Elements in Soils and Plants. CRC Press, Boca Raton, Florida.

Kachenko, A., Singh, B., 2006. Heavy metals contamination in vegetables grown in urban and metal smelter contaminated sites in Australia. Water, Air, and Soil Pollution, 169, 101-123.

Kamber, B.S., 2009. Geochemical fingerprinting: 40 years of analytical development and real world applications. Applied Geochemistry, 24, 1074-1086.

Kamber, B.S., Greig, A., Collerson, K.D., 2005. A new estimate for the composition of weathered young upper continental crust from alluvial sediments, Queensland, Australia. Geochimica et Cosmochimica Acta, 69, 1041-1058.

Kamber, B.S., Marx, S.K., McGowan, H., A.,, 2010. Comment on: "Lead isotopic evidence for an Australian source of aeolian dust to Antarctic at times over the last 170,000 years". Palaeogeography Palaeoclimatology Palaeoecology, Submitted.

Kane, M.M., Rendell, A.R., Jickells, T.D., 1994. Atmospheric scavenging processes over the North Sea. Atmospheric Environment, 28, 2523-2530.

Kasten, F., 1968. Falling speed of aerosol particles. Journal of Applied Meteorology and Climatology, 7, 944-7.

Kearns, A., 2003. Assessment of Snowy Alpine Ecosystem Dynamics in Response to Cloud Seeding, Expert Panel Assessment Snowy Precipitation Enhancement Trial (SPET)

Kemp, A.L.W., Thomas, R.L., 1976. Impact of man's activities on the chemical composition in the sediments of Lakes Ontario, Erie and Huron. Water, Air, and Soil Pollution, 5, 469-490.

Kemp, J., Hope, G., 2014. Vegetation and environments since the Last Glacial Maximum in the Southern Tablelands, New South Wales. Journal of Quaternary Science, 29, 778-788.

Kemp, J., Rhodes, E.J., 2010. Episodic fluvial activity of inland rivers in southeastern Australia: Palaeochannel systems and terraces of the Lachlan River. Quaternary Science Reviews, 29, 732-752.

Kemp, K., Kownacka, L., 1987. Collection efficiency for ambient aerosols on coarse pored nuclepore filters. Nuclear Instruments and Methods in Physics Research Section B: Beam Interactions with Materials and Atoms, 22, 340-343.

Kershaw, A.P., McKenzie, G.M., Porch, N., Roberts, R.G., Brown, J., Heijnis, H., Orr, M.L., Jacobsen, G., Newall, P.R., 2007. A high-resolution record of vegetation and climate through the last glacial cycle from Caledonia Fen, southeastern highlands of Australia. Journal of Quaternary Science, 22, 481-500.

Kilby, G.W., Batley, G.E., 1993. Chemical indicators of sediment chronology. Australian Journal of Marine and Freshwater Research, 44, 635-647.

Kilian, R., Lamy, F., 2012. A review of Glacial and Holocene paleoclimate records from southernmost Patagonia (49-55°S). Quaternary Science Reviews, 53, 1-23.

Kirchner, G., 2013. Establishing reference inventories of 137Cs for soil erosion studies: Methodological aspects. Geoderma, 211–212, 107-115.

Kirchner, J.W., Finkel, R.C., Riebe, C.S., Granger, D.E., Clayton, J.L., King, J.G., Megahan, W.F., 2001. Mountain erosion over 10 yr, 10 k.y., and 10 m.y. time scales. Geology, 29, 591-594.

Kirkpatrick, J., 1994. The International Signficance of the Natural Values of the Australian Alps. Department of Geography and Environmental Studies, University of Tasmania, Hobart.

Klaminder, J., Bindler, R., Emteryd, O., Appleby, P., Grip, H., 2006a. Estimating the mean residence time of lead in the organic horizon of boreal forest soils using lead-210, stable lead and a soil chronosequence. Biogeochemistry, 78, 31-49.

Klaminder, J., Bindler, R., Laudon, H., Bishop, K., Emteryd, O., Renberg, I., 2006b. Flux rates of atmospheric lead pollution within soils of a small catchment in northern Sweden and their implications for future stream water quality. Environmental Science & Technology, 40, 4639-4645.

Klaminder, J., Bindler, R., Rydberg, J., Renberg, I., 2008. Is there a chronological record of atmospheric mercury and lead deposition preserved in the mor layer (O-horizon) of boreal forest soils? Geochimica et Cosmochimica Acta, 72, 703-712.

Klaminder, J., Hammarlund, D., Kokfelt, U., Vonk, J.E., Bigler, C., 2010. Lead contamination of subarctic lakes and its response to reduced atmospheric gallout: can the recovery process be counteracted by the ongoing climate change? Environmental Science & Technology, 44, 2335-2340.

Klaminder, J., Renberg, I., Bindler, R., Emteryd, O., 2003. Isotopic trends and background fluxes of atmospheric lead in northern Europe: Analyses of three ombrotrophic bogs from south Sweden. Global Biogeochemical Cycles, 17.

Kober, B., Wessels, M., Bollhöfer, A., Mangini, A., 1999. Pb isotopes in sediments of Lake Constance, Central Europe constrain the heavy metal pathways and the pollution history of the catchment, the lake and the regional atmosphere. Geochimica et Cosmochimica Acta, 63, 1293-1303.

Koinig, K.A., Shotyk, W., Lotter, A.F., Ohlendorf, C., Sturm, M., 2003. 9000 years of geochemical evolution of lithogenic major and trace elements in the sediment of an alpine lake – the role of climate, vegetation, and land-use history. Journal of Paleolimnology, 30, 307-320.

Koppes, M.N., Montgomery, D.R., 2009. The relative efficacy of fluvial and glacial erosion over modern to orogenic timescales. Nature Geoscience, 2, 644-647.

Kristiansen, S.M., Dalsgaard, K., Holst, M.K., Aaby, B., Heinemeier, J., 2003. Dating of prehistoric burial mounds by (super 14) C analysis of soil organic matter fractions. Radiocarbon, 45, 101-112.

Kylander, M.E., Weiss, D.J., Kober, B., 2009. Two high resolution terrestrial records of atmospheric Pb deposition from New Brunswick, Canada, and Loch Laxford, Scotland. Science of The Total Environment, 407, 1644-1657.

Lafrenière, M.J., Sinclair, K.E., 2011. Snowpack and precipitation chemistry at a high altitude site in the Canadian Rocky Mountains. Journal of Hydrology, 409, 737-748.

Laidlaw, M.A.S., Taylor, M.P., 2011. Potential for childhood lead poisoning in the inner cities of Australia due to exposure to lead in soil dust. Environmental Pollution, 159, 1-9.

Lamy, F., Hebbeln, D., Röhl, U., Wefer, G., 2001. Holocene rainfall variability in southern Chile: a marine record of latitudinal shifts of the Southern Westerlies. Earth and Planetary Science Letters, 185, 369-382.

Landre, A., Watmough, S., Dillon, P., 2010. Metal pools, fluxes, and budgets in an acidified forested catchment on the Precambrian Shield, Central Ontario, Canada. Water, Air, & Soil Pollution, 209, 209-228.

Lane, P.N.J., Sheridan, G.J., Noske, P.J., 2006. Changes in sediment loads and discharge from small mountain catchments following wildfire in south eastern Australia. Journal of Hydrology, 331, 495-510.

Larsen, I.J., Almond, P.C., Eger, A., Stone, J.O., Montgomery, D.R., Malcolm, B., 2014. Rapid Soil Production and Weathering in the Southern Alps, New Zealand. Science, 343, 637-640.

Lawrence, C.R., Neff, J.C., 2009. The contemporary physical and chemical flux of aeolian dust: A synthesis of direct measurements of dust deposition. Chemical Geology, 267, 46-63.

Lawrence, C.R., Painter, T., Landry, C., Neff, J., 2010. Contemporary geochemical composition and flux of aeolian dust to the San Juan Mountains, Colorado, United States. Journal of Geophysical Research: Biogeosciences (2005–2012), 115.

Le Roux, G., Aubert, D., Stille, P., Krachler, M., Kober, B., Cheburkin, A., Bonani, G., Shotyk, W., 2005. Recent atmospheric Pb deposition at a rural site in southern Germany assessed using a peat core and snowpack, and comparison with other archives. Atmospheric Environment, 39, 6790-6801.

Le Roux, G., Fagel, N., De Vleeschouwer, F., Krachler, M., Debaille, V., Stille, P., Mattielli, N., van der Knaap, W.O., van Leeuwen, J.F., Shotyk, W., 2012. Volcano- and climate-driven changes in atmospheric dust sources and fluxes since the late glacial in Central Europe. Geology, 40, 335-338.

Le Roux, G., Weiss, D., Grattan, J., Givelet, N., Krachler, M., Cheburkin, A., Rausch, N., Kober, B., Shotyk, W., 2004. Identifying the sources and timing of ancient and medieval atmospheric lead pollution in England using a peat profile from Lindow bog, Manchester. Journal of Environmental Monitoring, 6, 502-510.

Leavitt, S.W., Follett, R.F., Kimble, J.M., Pruessner, E.G., 2007. Radiocarbon and δ13C depth profiles of soil organic carbon in the U.S. Great Plains: A possible spatial record of paleoenvironment and paleovegetation. Quaternary International, 162–163, 21-34.

Lee, C.S.L., Qi, S.H., Zhang, G., Luo, C.L., Zhao, L.Y.L., Li, X.D., 2008. Seven thousand years of records on the mining and utilization of metals from lake sediments in central China. Environmental Science and Technology, 42, 4732-4738.

Lee, J.A., Tallis, J.H., 1973. Regional and Historical Aspects of Lead Pollution in Britain. Nature, 245, 216-218.

Lee, K., Hur, S.D., Hou, S., Burn-Nunes, L.J., Hong, S., Barbante, C., Boutron, C.F., Rosman, K.J.R., 2011. Isotopic signatures for natural versus anthropogenic Pb in high-altitude Mt. Everest ice cores during the past 800 years. Science of The Total Environment, 412–413, 194-202.

Lidman, F., Köhler, S.J., Mörth, C.-M., Laudon, H., 2014. Metal Transport in the Boreal Landscape—The Role of Wetlands and the Affinity for Organic Matter. Environmental Science & Technology, 48, 3783-3790.

Lindberg, S.E., Turner, R.R., 1988. Factors influencing atmospheric deposition, stream export, and landscape accumulation of trace metals in forested watersheds. Water, Air, and Soil Pollution, 39, 123-156.

Lindqvist, O., 1991. Mercury in the swedish environment: recent research on causes, consequences and corrective methods, . Water Air Soil Pollution, 55, 1-261.

Litaor, M.I., 1987. The Influence of Eolian Dust on the Genesis of Alpine Soils in the Front Range, Colorado. Soil Science Society of America Journal, 51, 142-147.

Liu, X., Jiang, S., Zhang, P., Xu, L., 2012. Effect of recent climate change on Arctic Pb pollution: A comparative study of historical records in lake and peat sediments. Environmental Pollution, 160, 161-168.

Livett, E.A., Lee, J.A., Tallis, J.H., 1979. Lead, zinc and copper analyses of British blanket peats. Journal of Ecology, 67, 865-891.

Loughran, R.J., Campbell, B.L., Elliott, G.L., 1988. Determination of erosion and accretion rates using caesium-137. Fluvial geomorphology of Australia, 87-103.

Loughran, R.J., Elliott, G.L., McFarlane, D.J., Campbell, B.L., 2004. A survey of soil erosion in Australia using caesium-137. Australian Geographical Studies, 42, 221-233.

Mabit, L., Benmansour, M., Walling, D.E., 2008. Comparative advantages and limitations of the fallout radionuclides 137Cs, 210Pbex and 7Be for assessing soil erosion and sedimentation. Journal of Environmental Radioactivity, 99, 1799-1807.

Mabit, L., Klik, A., Benmansour, M., Toloza, A., Geisler, A., Gerstmann, U.C., 2009. Assessment of erosion and deposition rates within an Austrian agricultural watershed by combining 137Cs, 210Pbex and conventional measurements. Geoderma, 150, 231-239.

Macdonald, R.W., Barrie, L.A., Bidleman, T.F., Diamond, M.L., Gregor, D.J., Semkin, R.G., Strachan, W.M.J., Li, Y.F., Wania, F., Alaee, M., Alexeeva, L.B., Backus, S.M., Bailey, R., Bewers, J.M., Gobeil, C., Halsall, C.J., Harner, T., Hoff, J.T., Jantunen, L.M.M., Lockhart, W.L., Mackay, D., Muir, D.C.G., Pudykiewicz, J., Reimer, K.J., Smith, J.N., Stern, G.A., Schroeder, W.H., Wagemann, R., Yunker, M.B.,

2000. Contaminants in the Canadian Arctic: 5 years of progress in understanding sources, occurrence and pathways. Science of The Total Environment, 254, 93-234.

MacKenzie, A.B., Farmer, J.G., Sugden, C.L., 1997. Isotopic evidence of the relative retention and mobility of lead and radiocaesium in Scottish ombrotrophic peats. Science of The Total Environment, 203, 115-127.

Manning, M., Meilhuish, W., 1994. $^{14}CO_2$ records from Wellington. in: Boden, T., Kaiser, D., Sepanski, R., Stoss, F. (Eds.), A Compendium of Data on Global Change and Online Updates. Carbond Dioxide Information Analysis Center, Oak Ridge National Laboratory, Oak Ridge, TN, USA, pp. 143-202.

Manton, M., Warren, L., Kenyon, S., Peace, A., Bilish, S., Kelmsley, K., 2011. A confirmatory snowfall enhancement project in the Snowy Mountains Australia Part 1: Project design and response variables. Journal of Meteorology and Climatology.

Markgraf, V., Dodson, J.R., Kershaw, A.P., McGlone, M.S., Nicholls, N., 1992. Evolution of late Pleistocene and Holocene climates in the circum-south Pacific land areas. Climate Dynamics, 6, 193-211.

Martin, A.R.H., 1986. Late glacial and holocene alpine pollen diagrams from the Kosciusko National Park, New South Wales, Australia. Review of Palaeobotany and Palynology, 47, 367-409.

Martin, A.R.H., 1999. Pollen analysis of Diggers's Creek Bog, Kosciuszko National Park: vegetation history and tree-line change. Australian Journal of Botany, 47, 725-744.

Martínez-Cortizas, A., Pontevedra-Pombal, X., Muñoz, J.C.N., García-Rodeja, E., 1997a. Four Thousand Years of Atmospheric Pb, Cd and Zn Deposition Recorded by the Ombrotrophic Peat Bog of Penido Vello (Northwestern Spain). Water, Air, and Soil Pollution, 100, 387-403.

Martínez-Cortizas, A., Pontevedra-Pombal, X., Nóvoa Muñoz, J.C., García-Rodeja, E., 1997b. Four thousand years of atmospheric Pb, Cd and Zn deposition recorded by the ombrotrophic peat bog of Penido Vello (Northwestern Spain). Water, Air, and Soil Pollution, 100, 387-403.

Martinez-Zamudio, R., Ha, H.C., 2011. Environmental epigenetics in metal exposure. Epigenetics, 6, 820-827.

Martinez, C., Hancock, G.R., Kalma, J.D., 2009. Comparison of fallout radionuclide (caesium-137) and modelling approaches for the assessment of soil erosion rates for an uncultivated site in south-eastern Australia. Geoderma, 151, 128-140.

Martínez Cortizas, A., García-Rodeja, E., Pontevedra Pombal, X., Nóvoa Muñoz, J.C., Weiss, D., Cheburkin, A., 2002a. Atmospheric Pb deposition in Spain during the last 4600 years recorded by two ombrotrophic peat bogs and implications for the use of peat as archive. Science of The Total Environment, 292, 33-44.

Martínez Cortizas, A., García-Rodeja Gayoso, E., Weiss, D., 2002b. Peat bog archives of atmospheric metal deposition. Science of The Total Environment, 292, 1-5.

Martínez Cortizas, A., Peiteado Varela, E., Bindler, R., Biester, H., Cheburkin, A., 2012. Reconstructing historical Pb and Hg pollution in NW Spain using multiple cores from the Chao de Lamoso bog (Xistral Mountains). Geochimica et Cosmochimica Acta, 82, 68-78.

Martley, E., Gulson, B.L., Pfeifer, H.R., 2004. Metal concentrations in soils around the copper smelter and surrounding industrial complex of Port Kembla, NSW, Australia. Science of The Total Environment, 325, 113-127.

Marx, S., McGowan, H., 2011. Long-Distance Transport of Urban and Industrial Metals and Their Incorporation into the Environment: Sources, Transport Pathways and Historical Trends. in: Zereini, F., Wiseman, C.L.S. (Eds.), Urban Airborne Particulate Matter. Springer Berlin Heidelberg, pp. 103-124.

Marx, S.K., Kamber, B.S., McGowan, H., A.,, Denholm, J., 2011. Holocene dust deposition rates in Australia's Murray-Darling Basin record the interplay between aridity and the position of the mid-latitude westerlies. Quaternary Science Reviews, 30, 3290-3305.

Marx, S.K., Kamber, B.S., McGowan, H.A., 2005. Estimates of Australian dust flux into New Zealand: Quantifying the eastern Australian dust plume pathway using trace element calibrated ^{210}Pb as a monitor. Earth and Planetary Science Letters, 239, 336-351.

Marx, S.K., Kamber, B.S., McGowan, H.A., 2008. Scavenging of trace metal pollutants by mineral dust: Inter-regional transport of trace metal pollution to New Zealand. Atmospheric Environment, 42, 2460-2478.

Marx, S.K., Kamber, B.S., McGowan, H.A., Zawadzki, A., 2010. Atmospheric pollutants in alpine peat bogs record a detailed chronology of industrial and agricultural development on the Australian continent. Environmental Pollution, 158, 1615-1628.

Marx, S.K., Lavin, K.S., Hageman, K.J., Kamber, B.S., O'Loingsigh, T., McTainsh, G.H., 2014a. Trace elements and metal pollution in aerosols at an alpine site, New Zealand: Sources, concentrations and implications. Atmospheric Environment, 82, 206-217.

Marx, S.K., McGowan, H., A., Kamber, B.S., Knight, J., Denholm, J., Zawadzki, A., 2014b. Unprecedented wind erosion and perturbation of surface geochemistry marks the Anthropocene in Australia. Journal of Geophysical Research-Earth Surface, 119, 45-61.

Marx, S.K., McGowan, H.A., Kamber, B.S., 2009. Long-range dust transport from eastern Australia: a proxy for Holocene aridity and ENSO-induced climate variability. Earth and Planetary Science Letters, 282, 167-177.

Mason, R., 2013. Trace Metals in Aquatic Systems. John Wiley and Sons, Hoboken, New Jersey.

Masson-Delmotte, V., Stenni, B., Jouzel, J., 2004. Common millennial-scale variability of Antarctic and Southern Ocean temperatures during the past 5000 years reconstructed from the EPICA Dome C ice core. The Holocene, 14, 145-151.

Matschullat, J., 2011. The global arsenic cycle revisited, Arsenic. CRC Press, pp. 3-26.

McConnell, J.R., 2002. A 250-year high-resolution record of Pb flux and crustal enrichment in central Greenland. Geophysical Research Letters, 29.

McConnell, J.R., Edwards, R., 2008. Coal burning leaves toxic heavy metal legacy in the Arctic. Proceedings of the National Academy of Sciences of the United States of America, 105, 12140-12144.

McConnell, J.R., Lamorey, G.W., Hutterli, M.A., 2002. A 250-year high-resolution record of Pb flux and crustal enrichment in central Greenland. Geophysical Research Letters, 29, 451-454.

McConnell, J.R., Maselli, O.J., Sigl, M., Vallelonga, P., Neumann, T., Anschütz, H., Bales, R.C., Curran, M.A.J., Das, S.B., Edwards, R., Kipfstuhl, S., Layman, L., Thomas, E.R., 2014. Antarctic-wide array of high-resolution ice core records reveals pervasive lead pollution began in 1889 and persists today. Sci. Rep., 4.

McCormac, F., Hogg, A., Blackwell, P., Buck, C., Higham, T., Reimer, P., 2004. SHCal04 Southern Hemisphere calibration, 0-11.0 cal kyr BP. Radiocarbon, 46, 1087-1092.

McKee, J.D., Wilson, T.P., Long, D.T., Owen, R.M., 1989. Pore water profiles and early diagenesis of Mn, Cu, and Pb in sediments from large lakes. Journal of Great Lakes Research, 15, 68-83.

McKenzie, G.M., 1997. The late Quaternary vegetation history of the south-central highlands of Victoria, Australia. I. Sites above 900 m. Australian Journal of Ecology, 22, 19-36.

McKenzie, N., Jacquier, D., Isbell, R., Brown, K., 2004. Australian soils and landscapes: An illustrated compendium. CSIRO, Collingwood.

McTainsh, G.H., 1989. Quaternary aeolian dust processes and sediments in the Australian region. Quaternary Science Reviews, 8, 235-253.

McTainsh, G.H., Burgess, R., Pitblado, J.R., 1989. Aridity, drought and dust storms in Australia (1960-84). Journal of Arid Environments, 16, 11-22.

McTainsh, G.H., Lynch, A.W., 1996. Quantitative estimates of the effect of climate change on dust storm activity in Australia during the Last Glacial Maximum. Geomorphology, 17, 263-271.

McTainsh, G.H., Lynch, A.W., Hales, R., 1997. Particle-size analysis of aeolian dusts, soils and sediments in very small quantities using a Coulter Multisizer. Earth Surface Processes and Landforms, 22, 1207-1216.

McTainsh, G.H., Lynch, A.W., Tews, E.K., 1998. Climatic controls upon dust storm occurrence in eastern Australia. Journal of Arid Environments, 39, 457-466.

Meili, M., Bishop, K., Bringmark, L., Johansson, K., Munthe, J., Sverdrup, H., de Vries, W., 2003. Critical levels of atmospheric pollution: criteria and concepts for operational modelling of mercury in forest and lake ecosystems. Science of The Total Environment, 304, 83-106.

Mighall, T.M., Timberlake, S., Foster, I.D.L., Krupp, E., Singh, S., 2009. Ancient copper and lead pollution records from a raised bog complex in Central Wales, UK. Journal of Archaeological Science, 36, 1504-1515.

Miller, E.K., Friedland, A.J., 1994. Lead migration in forest soils: response to changing atmospheric inputs. Environmental Science & Technology, 28, 662-669.

Milliman, J.D., Farnsworth, K.L., 2011. River Discharge to the Coastal Ocean : A Global Synthesis. Cambridge University Press, Cambridge.

Milliman, J.D., Syvitski, J.P.M., 1992. Geomorphic/Tectonic Control of Sediment Discharge to the Ocean: The Importance of Small Mountainous Rivers. The Journal of Geology, 100, 525-544.

Mitchell, S.G., Montgomery, D.R., 2006. Influence of a glacial buzzsaw on the height and morphology of the Cascade Range in central Washington State, USA. Quaternary Research, 65, 96-107.

Monna, F., Galop, D., Carozza, L., Tual, M., Beyrie, A., Marembert, F., Chateau, C., Dominik, J., Grousset, F.E., 2004. Environmental impact of early Basque mining and smelting recorded in a high ash minerogenic peat deposit. Science of The Total Environment, 327, 197-214.

Mooney, S.D., Watson, J.R., Dodson, J.R., 1997. Late holocene environmental change in an upper Montane area of the snowy mountains, New South Wales. Australian Geographer, 28, 185-200.

Moros, M., De Deckker, P., Jansen, E., Perner, K., Telford, R.J., 2009. Holocene climate variability in the Southern Ocean recorded in a deep-sea sediment core off South Australia. Quaternary Science Reviews, 28, 1932-1940.

Mudd, G.M., 2007. An analysis of historic production trends in Australian base metal mining. Ore Geology Reviews, 32, 227-261.

Murozumi, M., Chow, T.J., Patterson, C., 1969. Chemical concentrations of pollutant lead aerosols, terrestrial dusts and sea salts in Greenland and Antarctic snow strata. Geochimica et Cosmochimica Acta, 33, 1247-1294.

Natural Resources Commission, 2010. Mid-term review of the Snowy Mountains Cloud seeding trial. Natural Resources Commission, Sydney.

Neil, D.T., 1991. Land use and sediment yield on the Southern Tablelands of New South Wales. Australian Journal of Soil and Water Conservation, 4, 33-39.

Nicholls, N., 2005. Climate variability, climate change and the Australian snow season. Australian Meteorological Magazine, 54, 177-185.

Nickel, S., Hertel, A., Pesch, R., Schröder, W., Steinnes, E., Uggerud, H., 2015. Correlating concentrations of heavy metals in atmospheric deposition with respective accumulation in moss and natural surface soil for ecological land classes in Norway between 1990 and 2010. Environmental Science and Pollution Research, 22, 8488-8498.

Norton, K.P., von Blanckenburg, F., 2010. Silicate weathering of soil-mantled slopes in an active Alpine landscape. Geochimica et Cosmochimica Acta, 74, 5243-5258.

Norton, S.A., Kahl, J.S., 1987. A comparison of lake sediments and ombrotrophic peat deposits as long term monitors of atmospheric pollution. in: Boyle, T. (Ed.), New Approaches to Monitoring Aquatic Ecosystems. ASTM, Philadelphia, pp. 40-57.

Novák, M., Emmanuel, S., Vile, M.A., Erel, Y., Véron, A., Pačes, T., Wieder, R.K., Vaněček, M., Štěpánová, M., Bízová, E., Hovorka, J., 2003. Origin of Lead in Eight Central European Peat Bogs Determined from Isotope Ratios, Strengths, and Operation Times of Regional Pollution Sources. Environmental Science & Technology, 37, 437-445.

Novak, M., Zemanova, L., Voldrichova, P., Stepanova, M., Adamova, M., Pacherova, P., Komarek, A., Krachler, M., Prechova, E., 2011. Experimental Evidence for Mobility/Immobility of Metals in Peat. Environmental Science & Technology, 45, 7180-7187.

NPI, 2014. Total industry emission: lead and compounds from all sources. Department of the Environment, Australian Government, last updated: 2014, accessed: 3 July 2015.

NPWS, 2008. Kosciuszko National Park Fire Managment Strategy 2008-2013. Department of Environment and Climate Change, New South Wales Government, Jindabyne.

Nriagu, J., Pacyna, J., 1988. Quantitative assessment of worldwide contamination of air, water and soils by trace metals. Nature, 333, 134-139.

Nriagu, J.O., 1983. Lead and Lead Poisoning in Antiquity. John Wiley and Sons, New York.

Nriagu, J.O., 1988. A silent epidemic of environmental metal poisoning? Environmental Pollution, 50, 139-161.

Nriagu, J.O., 1989. A global assessment of natural sources of atmospheric trace metals. Nature, 338, 47-49.

Nriagu, J.O., 1990. Global metal pollution: poisoning the biosphere? Environment: Science and Policy for Sustainable Development, 32, 7-33.

Nyman, P., Sheridan, G.J., Smith, H.G., Lane, P.N.J., 2011. Evidence of debris flow occurrence after wildfire in upland catchments of south-east Australia. Geomorphology, 125, 383-401.

Nyrstar, 2013. Annual report 2013, Zurich.

Ogden, R., Spooner, N., Reid, M., Head, J., 2001. Sediment dates with implications for the age of the conversion from palaeochannel to modern fluvial activity on the Murray River and tributaries. Quaternary International, 83-85, 195-209.

Olid, C., Diego, D., Garcia-Orellana, J., Cortizas, A.M., Klaminder, J., 2016. Modeling the downward transport of 210Pb in Peatlands: Initial Penetration-Constant Rate of Supply (IP-CRS) model. Science of The Total Environment, 541, 1222-1231.

Osterberg, E., Mayewski, P., Kreutz, K., Fisher, D., Handley, M., Sneed, S., Zdanowicz, C., Zheng, J., Demuth, M., Waskiewicz, M., Bourgeois, J., 2008. Ice core record of rising lead pollution in the North Pacific atmosphere. Geophysical Research Letters, 35, L05810.

Outridge, P.M., Hermanson, M.H., Lockhart, W.L., 2002. Regional variations in atmospheric deposition and sources of anthropogenic lead in lake sediments across the Canadian Arctic. Geochimica et Cosmochimica Acta, 66, 3521-3531.

Outridge, P.M., Stern, G.A., Hamilton, P.B., Percival, J.B., McNeely, R., Lockhart, W.L., 2005. Trace metal profiles in the varved sediment of an Arctic lake. Geochimica et Cosmochimica Acta, 69, 4881-4894.

Owens, P.N., Walling, D.E., 1996. Spatial variability of caesium-137 inventories at reference sites: an example from two contrasting sites in England and Zimbabwe. Applied Radiation and Isotopes, 47, 699-707.

Pacyna, J.M., Pacyna, E.G., 2001. An assessment of global and regional emissions of trace metals to the atmosphere from anthropogenic sources worldwide. Environmental Reviews, 9, 269-298.

Pacyna, J.M., Pacyna, E.G., Aas, W., 2009. Changes of emissions and atmospheric deposition of mercury, lead, and cadmium. Atmospheric Environment, 43, 117-127.

Page, K.J., Kemp, J., Nanson, G.C., 2009. Late Quaternary evolution of Riverine Plain paleochannels, southeastern Australia. Australian Journal of Earth Sciences, 56, S19-S33.

Page, K.J., Nanson, G.C., 1996. Stratigraphic architecture resulting from Late Quaternary evolution of the Riverine Plain, south-eastern Australia. Sedimentology, 43, 927-945.

Page, K.J., Nanson, G.C., Price, D.M., 1991. Thermoluminescence chronology of late quaternary deposition on the riverine plain of South-Eastern Australia. Australian Geographer, 22, 14-23.

Patterson, C.C., 1965. Contaminated and natural lead environments of man. Archives of Environmental Health: An International Journal, 11, 344-360.

Patterson, C.C., Settle, D.M., 1987. Review of data on eolian fluxes of industrial and natural lead to the lands and seas in remote regions on a global scale. Marine Chemistry, 22, 137-162.

Pels, S., 1969. Radio-carbon datings of ancestral river sediments on the Riverine Plain of southeastern Australia and their interpretation. Journal and Proceedings, Royal Society of New South Wales, 102, 189-195.

Peltier, L.C., 1950. The Geographic Cycle in Periglacial Regions as it is Related to Climatic Geomorphology. Annals of the Association of American Geographers, 40, 214-236.

Pennock, D.J., Appleby, P.G., 2003. Site Selection and Sampling Design. in: Zapata, F. (Ed.), Handbook for the Assessment of Soil Erosion and Sedimentation Using Environmental Radionuclides. Springer Netherlands, pp. 15-40.

Pessenda, L., Gouveia, S., Aravena, R., 2001. Radiocarbon dating of total soil organic matter and soil humin fraction and its comparision with C-14 ages of fossil charcoal. Radiocarbon, 43, 595-601.

Petherick, L., Bostock, H., Cohen, T.J., Fitzsimmons, K., Tibby, J., Fletcher, M.S., Moss, P., Reeves, J., Mooney, S., Barrows, T., Kemp, J., Jansen, J., Nanson, G., Dosseto, A., 2013. Climatic records over the past 30 ka from temperate Australia – a synthesis from the Oz-INTIMATE workgroup. Quaternary Science Reviews, 74, 58-77.

Pfitzner, J., Brunskill, G., Zagorskis, I., 2004. 137Cs and excess 210Pb deposition patterns in estuarine and marine sediment in the central region of the Great Barrier Reef Lagoon, north-eastern Australia. Journal of Environmental Radioactivity, 76, 81-102.

Planchon, F.A.M., Boutron, C.F., Barbante, C., Cozzi, G., Gaspari, V., Wolff, E.W., Ferrari, C.P., Cescon, P., 2002. Changes in heavy metals in Antarctic snow from Coats Land since the mid-19th to the late-20th century. Earth and Planetary Science Letters, 200, 207-222.

Planchon, F.A.M., van de Velde, K., Rosman, K.J.R., Wolff, E.W., Ferrari, C.P., Boutron, C.F., 2003. One hundred fifty–year record of lead isotopes in Antarctic snow from Coats Land. Geochimica et Cosmochimica Acta, 67, 693-708.

Pompeani, D.P., Abbott, M.B., Steinman, B.A., Bain, D.J., 2013. Lake Sediments Record Prehistoric Lead Pollution Related to Early Copper Production in North America. Environmental Science & Technology, 47, 5545-5552.

Porter, S.C., 2000. Onset of neoglaciation in the Southern Hemisphere Quaternary Science Reviews, 15, 395.

Porto, P., Walling, D.E., Callegari, G., Capra, A., 2009. Using caesium-137 and unsupported lead-210 measurements to explore the relationship between sediment mobilisation, sediment delivery and sediment yield for a Calabrian catchment. Marine and Freshwater Research, 60, 680-689.

Pratte, S., Mucci, A., Garneau, M., 2013. Historical records of atmospheric metal deposition along the St. Lawrence Valley (eastern Canada) based on peat bog cores. Atmospheric Environment, 79, 831-840.

Preiss, N., Mélières, M.-A., Pourchet, M., 1996. A compilation of data on lead 210 concentration in surface air and fluxes at the air-surface and water-sediment interfaces. Journal of Geophysical Research: Atmospheres, 101, 28847-28862.

Purcell, T.W., Peters, J.J., 1998. Sources of silver in the environment. Environmental Toxicology and Chemistry, 17, 539-546.

Rasmussen, P.E., 1998. Long-range atmospheric transport of trace metals: the need for geoscience perspectives. Environmental Geology, 33, 96-108.

Rauch, J.N., Pacyna, J.M., 2009. Earth's global Ag, Al, Cr, Cu, Fe, Ni, Pb, and Zn cycles. Global Biogeochemical Cycles, 23, GB2001.

Raupach, M.R., McTainsh, G.H., Leys, J.F., 1994. Estimates of dust mass in recent major Australian dust storms. Australian Journal of Soil and Water Conservation, 7, 20-24.

Reiners, W.A., Marks, R.H., Vitousek, P.M., 1975. Heavy Metals in Subalpine and Alpine Soils of New Hampshire. Oikos, 26, 264-275.

Reinfelds, I., Swanson, E., Cohen, T., Larsen, J., Nolan, A., 2014. Hydrospatial assessment of streamflow yields and effects of climate change: Snowy Mountains, Australia. Journal of Hydrology, 512, 206-220.

Renberg, I., Brännvall, M.-L., Bindler, R., Emteryd, O., 2000. Atmospheric Lead Pollution History during Four Millennia (2000 BC to 2000 AD) in Sweden. AMBIO: A Journal of the Human Environment, 29, 150-156.

Renberg, I., Brännvall, M.L., Bindler, R., Emteryd, O., 2002. Stable lead isotopes and lake sediments—a useful combination for the study of atmospheric lead pollution history. Science of The Total Environment, 292, 45-54.

Renberg, I., Persson, M.W., Emteryd, O., 1994. Pre-industrial atmospheric lead contamination detected in Swedish lake sediments. Nature, 368, 323-326.

Riebe, C.S., Kirchner, J.W., Finkel, R.C., 2004. Erosional and climatic effects on long-term chemical weathering rates in granitic landscapes spanning diverse climate regimes. Earth and Planetary Science Letters, 224, 547-562.

Rippey, B., Anderson, N.J., Renberg, I., Korsman, T., 2008. The accuracy of methods used to estimate the whole-lake accumulation rate of organic carbon, major cations, phosphorus and heavy metals in sediment. Journal of Paleolimnology, 39, 83-99.

Ritchie, J.C., McHenry, J.R., 1990. Application of radioactive fallout cesium-137 for measuring soil erosion and sediment accumulation rates and patterns: a review. Journal of Environmental Quality, 19, 215-233.

Ritchie, J.C., Spraberry, J.A., McHenry, J.R., 1974. Estimating Soil Erosion from the Redistribution of Fallout 137Cs. Soil Science Society of America Journal, 38, 137-139.

Roach, A.C., 2005. Assessment of metals in sediments from Lake Macquarie, New South Wales, Australia, using normalisation models and sediment quality guidelines. Marine Environmental Research, 59, 453-472.

Robbins, J.A., Edgington, D.N., 1975. Determination of recent sedimentation rates in Lake Michigan using Pb-210 and Cs-137. Geochimica et Cosmochimica Acta, 39, 285-304.

Rose, N., Morley, D., Appleby, P., Battarbee, R., Alliksaar, T., Guilizzoni, P., Jeppesen, E., Korhola, A., Punning, J.-M., 2011. Sediment accumulation rates in European lakes since AD 1850: trends, reference conditions and exceedence. Journal of Paleolimnology, 45, 447-468.

Rose, N.L., Yang, H., Turner, S.D., Simpson, G.L., 2012. An assessment of the mechanisms for the transfer of lead and mercury from atmospherically contaminated organic soils to lake sediments with particular reference to Scotland, UK. Geochimica et Cosmochimica Acta, 82, 113-135.

Rosman, K.J.R., Chisholm, W., Boutron, C.F., Candelone, J.P., Hong, S., 1994. Isotopic evidence to account for changes in the concentration of lead in Greenland snow between 1960 and 1988. Geochimica et Cosmochimica Acta, 58, 3265-3269.

Rosman, K.J.R., Chisholm, W., Boutron, C.F., Hong, S., Edwards, R., Morgan, V., Sedwick, P.N., 1998. Lead isotopes and selected metals in ice from Law Dome, Antarctica. Annals of Glaciology, 27, 349-354.

Rosman, K.J.R., Chisholm, W., Hong, S., Candelone, J.-P., Boutron, C.F., 1997. Lead from Carthaginian and Roman Spanish mines isotopically identified in Greenland ice dated from 600 B.C. to 300 A.D. Environmental Science & Technology, 31, 3413-3416.

Rothwell, J.J., Evans, M.G., Daniels, S.M., Allott, T.E.H., 2008. Peat soils as a source of lead contamination to upland fluvial systems. Environmental Pollution, 153, 582-589.

Sakata, M., Asakura, K., 2007. Estimating contribution of precipitation scavenging of atmospheric particulate mercury to mercury wet deposition in Japan. Atmospheric Environment, 41, 1669-1680.

Salomons, W., Förstner, U., 1984a. Interactions with ligands, particulate matter and organisms. in: Salomons, W., Förstner, U. (Eds.), Metals in the Hydrocycle. Springer Berlin Heidelberg, pp. 5-62.

Salomons, W., Förstner, U., 1984b. Sediments and the transport of metals. in: Salomons, W., Förstner, U. (Eds.), Metals in the Hydrocycle. Springer Berlin Heidelberg, pp. 63-98.

Satarug, S., Garrett, S.H., Sens, M.A., Sens, D.A., 2010. Cadmium, environmental exposure, and health outcomes. Environmental Health Perspectives, 118, 182-190.

Scharpenseel, H., Becker-Heidmann, P., 1992. Twenty-five years of radiocarbon dating soils: a paradigm of erring and learning. Radiocarbon, 34541-549, 238.

Schmidt, R., Koinig, K.A., Thompson, R., Kamenik, C., 2002. A multi proxy core study of the last 7000 years of climate and alpine land-use impacts on an Austrian mountain lake (Unterer Landschitzsee, Niedere Tauern). Palaeogeography, Palaeoclimatology, Palaeoecology, 187, 101-120.

Schneider, L., Maher, W., Potts, J., Batley, G., Taylor, A., Krikowa, F., Chariton, A., Zawadzki, A., Heijnis, H., Gruber, B., 2015. History of metal contamination in Lake Illawarra, NSW, Australia. Chemosphere, 119, 377-386.

Schuller, P., Voigt, G., Handl, J., Ellies, A., Oliva, L., 2002. Global weapons' fallout 137Cs in soils and transfer to vegetation in south-central Chile. Journal of Environmental Radioactivity, 62, 181-193.

Schütz, L., Rahn, K.A., 1982. Trace-element concentrations in erodible soils. Atmospheric Environment (1967), 16, 171-176.

Settle, D.M., Patterson, C.C., 1980. Lead in Albacore: guide to lead pollution in Americans. Science, 207, 1167-1176.

Settle, D.M., Patterson, C.C., 1982. Magnitudes and sources of precipitation and dry deposition fluxes of indestrial and natural leads to the North Pacific at Enewetak. Journal of Geophysical Research: Oceans, 87, 8857-8869.

Shakhashiro, A., Mabit, L., 2009. Results of an IAEA inter-comparison exercise to assess 137Cs and total 210Pb analytical performance in soil. Applied Radiation and Isotopes, 67, 139-146.

Shao, Y., Wyrwoll, K.-H., Chappell, A., Huang, J., Lin, Z., McTainsh, G.H., Mikami, M., Tanaka, T.Y., Wang, X., Yoon, S., 2011. Dust cycle: An emerging core theme in Earth system science. Aeolian Research, 2, 181-204.

Shen, G.T., Boyle, E.A., 1987. Lead in corals: reconstruction of historical industrial fluxes to the surface ocean. Earth and Planetary Science Letters, 82, 289-304.

Sheridan, G.J., Lane, P.N.J., Noske, P.J., 2007. Quantification of hillslope runoff and erosion processes before and after wildfire in a wet Eucalyptus forest. Journal of Hydrology, 343, 12-28.

Shirahata, H., Elias, R.W., Patterson, C.C., Koide, M., 1980. Chronological variations in concentrations and isotopic compositions of anthropogenic atmospheric lead in sediments of a remote subalpine pond. Geochimica et Cosmochimica Acta, 44, 149-162.

Shotyk, W., 1996a. Natural and anthropogenic enrichments of As, Cu, Pb, Sb, and Zn in ombrotrophic versus minerotrophic peat bog profiles, Jura Mountains, Switzerland. Water, Air, & Soil Pollution, 90, 375-405.

Shotyk, W., 1996b. Peat bog archives of atmospheric metal deposition: geochemical evaluation of peat profiles, natural variations in metal concentrations, and metal enrichment factors. Environmental Reviews, 4, 149-183.

Shotyk, W., 2002. The chronology of anthropogenic, atmospheric Pb deposition recorded by peat cores in three minerogenic peat deposits from Switzerland. Science of the Total Environment, 292, 19-31.

Shotyk, W., Cheburkin, A.K., Appleby, P.G., Fankhauser, A., Kramers, J.D., 1996. Two thousand years of atmospheric arsenic, antimony, and lead deposition recorded in an ombrotrophic peat bog profile, Jura Mountains, Switzerland. Earth and Planetary Science Letters, 145, E1-E7.

Shotyk, W., Goodsite, M.E., Roos-Barraclough, F., Givelet, N., Le Roux, G., Weiss, D., Cheburkin, A.K., Knudsen, K., Heinemeier, J., van Der Knaap, W.O., Norton, S.A., Lohse, C., 2005a. Accumulation rates and predominant atmospheric sources of natural and anthropogenic Hg and Pb on the Faroe Islands. Geochimica et Cosmochimica Acta, 69, 1-17.

Shotyk, W., Krachler, M., 2004. Atmospheric deposition of silver and thallium since 12 370 14C years BP recorded by a Swiss peat bog profile, and comparison with lead and cadmium. Journal of Environmental Monitoring, 6, 427-433.

Shotyk, W., Krachler, M., 2010. The isotopic evolution of atmospheric Pb in central Ontario since AD 1800, and its impacts on the soils, waters, and sediments of a forested watershed, Kawagama Lake. Geochimica et Cosmochimica Acta, 74, 1963-1981.

Shotyk, W., Krachler, M., Martinez-Cortizas, A., Cheburkin, A.K., Emons, H., 2002. A peat bog record of natural, pre-anthropogenic enrichments of trace elements in atmospheric aerosols since 12 370 C-14 yr BP, and their variation with Holocene climate change. Earth and Planetary Science Letters, 199, 21-37.

Shotyk, W., Weiss, D., Appleby, P.G., Cheburkin, A.K., et al., 1998. History of atmospheric lead deposition since 12,370 14C yr BP from a peat bog, Jura Mountains, Switzerland. Science, 281, 1635.

Shotyk, W., Weiss, D., Kramers, J.D., Frei, R., Cheburkin, A.K., Gloor, M., Reese, S., 2001. Geochemistry of the peat bog at Etang de la Gruère, Jura Mountains, Switzerland, and its record of atmospheric Pb and lithogenic trace metals (Sc, Ti, Y, Zr, and REE) since 12,370 14C yr BP. Geochimica et Cosmochimica Acta, 65, 2337-2360.

Shotyk, W., Zheng, J., Krachler, M., Zdanowicz, C., Koerner, R., Fisher, D., 2005b. Predominance of industrial Pb in recent snow (1994–2004) and ice (1842–1996) from Devon Island, Arctic Canada. Geophysical Research Letters, 32, n/a-n/a.

Shulmeister, J., Goodwin, I., Renwick, J.A., Harle, K., Armand, L., McGlone, M.S., Cook, E., Dodson, J., Hesse, P.P., Mayewski, P., Curran, M., 2004. The Southern Hemisphere westerlies in the Australasian sector over the last glacial cycle: a synthesis. Quaternary International, 118-119, 23-53.

Siccama, T.G., Smith, W.H., 1978. Lead accumulation in a northern hardwood forest. Environmental Science & Technology, 12, 593-594.

Simms, A.D., Woodroffe, C., Jones, B.G., Heijnis, H., Harrison, J., Mann, R.A., 2008. Assessing soil remobilisation in catchments using a 137 Cs-sediment hillslope model. Australian Geographer, 39, 445-465.

Sinex, S.A., Helz, G.R., 1981. Regional geochemistry of trace elements in Chesapeake Bay sediments. Environmental Geology, 3, 315-323.

Smith, E.J., Adderley, E.E., Walsh, D.T., 1963. A cloud-seeding experiment in the Snowy Mountains, Australia. Journal of Applied Meteorology, 2, 324-332.

Smith, H.G., Dragovich, D., 2008. Post-fire hillslope erosion response in a sub-alpine environment, south-eastern Australia. CATENA, 73, 274-285.

Smith, I., Carson, B., 1977. Trace Metals in the Environment, Volume 2 - Silver. Ann Arbour Science, Ann Arbour.

Smith, J.D., Hamilton, T.F., 1992. Trace metal fluxes to lake sediments in south-eastern Australia. Science of The Total Environment, 125, 227-233.

Snowy Hydro Ltd, 2011. Snowy Precipitation Enhancement Research Project Annual Report 2010. Cooma.

Stankwitz, C., Kaste, J.M., Friedland, A.J., 2012. Threshold increases in soil lead and mercury from tropospheric deposition across an elevational gradient. Environmental Science and Technology, 46, 8061-8068.

Stanley, S., De Deckker, P., 2002. A Holocene record of allochthonous, aeolian mineral grains in an Australian alpine lake; implications for the history of climate change in southeastern Australia. Journal of Paleolimnology, 27, 207-219.

Stansell, N.D., Rodbell, D.T., Abbott, M.B., Mark, B.G., 2013. Proglacial lake sediment records of Holocene climate change in the western Cordillera of Peru. Quaternary Science Reviews, 70, 1-14.

Starr, M., Lindroos, A.-J., Ukonmaanaho, L., Tarvainen, T., Tanskanen, H., 2003. Weathering release of heavy metals from soil in comparison to deposition, litterfall and leaching fluxes in a remote, boreal coniferous forest. Applied Geochemistry, 18, 607-613.

Steinnes, E., Allen, R.O., Petersen, H.M., Rambæk, J.P., Varskog, P., 1997. Evidence of large scale heavy-metal contamination of natural surface soils in Norway from long-range atmospheric transport. Science of The Total Environment, 205, 255-266.

Steinnes, E., Friedland, A.J., 2006. Metal contamination of natural surface soils from long-range atmospheric transport: Existing and missing knowledge. Environmental Reviews, 14, 169-186.

Steinnes, E., Njastad, O., 1995. Enrichment of metals in the organic surface layer of natural soil: identification of contributions from different sources. Analyst, 120, 1479-1483.

Stockmann, U., Minasny, B., McBratney, A.B., 2014. How fast does soil grow? Geoderma, 216, 48-61.

Stromsoe, N., Callow, J.N., McGowan, H.A., Marx, S.K., 2013. Attribution of sources to metal accumulation in an alpine tarn, the Snowy Mountains, Australia. Environmental Pollution, 181, 133-143.

Stromsoe, N., Marx, S.K., McGowan, H.A., Callow, N., Heijnis, H., Zawadzki, A., 2015. A landscape-scale approach to examining the fate of atmospherically derived industrial metals in the surficial environment. Science of The Total Environment, 505, 962-980.

Strother, S.L., Salzmann, U., Roberts, S.J., Hodgson, D.A., Woodward, J., Van Nieuwenhuyze, W., Verleyen, E., Vyverman, W., Moreton, S.G., 2014. Changes in Holocene climate and the intensity of Southern Hemisphere Westerly Winds based on a high-resolution palynological record from sub-Antarctic South Georgia. The Holocene.

Suresh, P.O., Dosseto, A., Hesse, P.P., Handley, H.K., 2013. Soil formation rates determined from Uranium-series isotope disequilibria in soil profiles from the southeastern Australian highlands. Earth and Planetary Science Letters, 379, 26-37.

Survey, U.S.G., 2015. Mineral Commodity Summaries. U.S. Deparment ofthe Interior, U.S Geological Survey, last updated: accessed: 4/4/15.

Sutherland, R.A., 2000. Bed sediment-associated trace metals in an urban stream, Oahu, Hawaii. Environmental Geology, 39, 611-627.

Sutherland, R.A., de Jong, E., 1990. Statistical analysis of gamma-emitting radionuclide concentrations for three fields in southern Saskatchewan, Canada. Health physics, 58, 417.

Swain, E.B., Engstrom, D.R., Brigham, M.E., Henning, T.A., Brezonik, P.L., 1992. Increasing rates of atmospheric mercury deposition in midcontinental North America. Science, 257, 784-787.

Taylor, M.P., 2007. Distribution and storage of sediment-associated heavy metals downstream of the remediated Rum Jungle Mine on the East Branch of the Finniss River, Northern Territory, Australia. Journal of Geochemical Exploration, 92, 55-72.

Taylor, M.P., Mackay, A.K., Hudson-Edwards, K.A., Holz, E., 2010. Soil Cd, Cu, Pb and Zn contaminants around Mount Isa city, Queensland, Australia: Potential sources and risks to human health. Applied Geochemistry, 25, 841-855.

Terashima, S., Imai, N., Taniguchi, M., Okai, T., Nishimura, A., 2002. The preparation and preliminary characterisation of four new Geological Survey of Japan geochemical reference materials: soils, JSO-1 and JSO-2; and marine sediments, JMS-1 and JMS-2. Geostandards Newsletter, 26, 85-94.

Tex, E., 1955. Complex and imitation tectonites from the Kosciusko Pluton, Snowy Mountains. Journal of the Geological Society of Australia, 3, 33-54.

Theobald, A., McGowan, H., Speirs, J., Callow, N., 2015. A synoptic classification of inflow-generating precipitation in the Snowy Mountains, Australia. Journal of Applied Meteorology and Climatology.

Thevenon, F., Guédron, S., Chiaradia, M., Loizeau, J.-L., Poté, J., 2011. (Pre-) historic changes in natural and anthropogenic heavy metals deposition inferred from two contrasting Swiss Alpine lakes. Quaternary Science Reviews, 30, 224-233.

Tian, H., Zhou, J., Zhu, C., Zhao, D., Gao, J., Hao, J., He, M., Liu, K., Wang, K., Hua, S., 2014. A Comprehensive Global Inventory of Atmospheric Antimony Emissions from Anthropogenic Activities, 1995–2010. Environmental Science & Technology, 48, 10235-10241.

Tomkins, K.M., Humphreys, G.S., Wilkinson, M.T., Fink, D., Hesse, P.P., Doerr, S.H., Shakesby, R.A., Wallbrink, P.J., Blake, W.H., 2007. Contemporary versus long-term denudation along a passive plate margin: the role of extreme events. Earth Surface Processes and Landforms, 32, 1013-1031.

Tornimbeni, O., Rogora, M., 2012. An evaluation of trace metals in high-altitude lakes of the central Alps. Water, Air, & Soil Pollution, 223, 1895-1909.

Toscano, G., Gambaro, A., Moret, I., Capodaglio, G., Turetta, C., Cescon, P., 2005. Trace metals in aerosol at Terra Nova Bay, Antarctica. Journal of Environmental Monitoring, 7, 1275-1280.

Tsiouris, S., Aravanopoulos, F.A., Papadoyannis, I.N., Sofoniou, M.K., Samanidou, V.F., Zachariadis, G.A., Constantinidou, H.I.A., 2003. Soil silver mobility in areas subjected to cloud seeding with AGI. FRESENIUS ENVIRONMENTAL BULLETIN, 12.

Uglietti, C., Gabrielli, P., Cooke, C.A., Vallelonga, P., Thompson, L.G., 2015. Widespread pollution of the South American atmosphere predates the industrial revolution by 240 y. Proceedings of the National Academy of Sciences, 112, 2349-2354.

United States Geological Survey, 2001. Mineral Commodity Summary - Silver. United States Geological Survey, last updated: accessed: 14/1/2015.

UNSCEAR, 2000. Annex C: Exposures from man-made sources of radiation, Sources and Effects of Ionizing Radiation, Volume 1: Sources. United Nations Scientific Committee on the Effects of Atomic Radiation, New York.

Vallelonga, P., Van de Velde, K., Candelone, J.P., Morgan, V.I., Boutron, C.F., Rosman, K.J.R., 2002. The lead pollution history of Law Dome, Antarctica, from isotopic measurements on ice cores: 1500 AD to 1989 AD. Earth and Planetary Science Letters, 204, 291-306.

Van Oostdam, J., Donaldson, S.G., Feeley, M., Arnold, D., Ayotte, P., Bondy, G., Chan, L., Dewaily, É., Furgal, C.M., Kuhnlein, H., Loring, E., Muckle, G., Myles, E., Receveur, O., Tracy, B., Gill, U., Kalhok, S., 2005. Human health implications of environmental contaminants in Arctic Canada: A review. Science of The Total Environment, 351–352, 165-246.

Vandergoes, M., Prior, C., 2003. AMS dating of pollen concentrates - a methodological study of late Quaternary sediments from South Westland, New Zealand. Radiocarbon, 45, 479-491.

Vanmaercke, M., Poesen, J., Verstraeten, G., de Vente, J., Ocakoglu, F., 2011. Sediment yield in Europe: Spatial patterns and scale dependency. Geomorphology, 130, 142-161.

Wallbrink, P.J., Murray, A.S., 1996. Determining soil loss using the inventory ratio of excess lead-210 to cesium-137. Soil Science Society of America Journal, 60, 1201.

Walling, D., 2003. Using environmental radionuclides as tracers in sediment budget investigations, Erosion and Sediment Transport Measurement in Rivers: Technological and Methodological Advances (Proceedings of the Oslo Workshop, June 2002), IAHS Publ. 283. 2003. IAHS, Oslo, pp. 57-78.

Walling, D.E., Collins, A.L., Sichingabula, H.M., 2003. Using unsupported lead-210 measurements to investigate soil erosion and sediment delivery in a small Zambian catchment. Geomorphology, 52, 193-213.

Walling, D.E., Webb, B., 1996. Erosion and sediment yield: a global overview. Erosion and Sediment Yield: Global and Regional Perspectives (Proceedings of the Exeter Symposium, July 1996), IAHS Publ. no 236, 3-19.

Walling, D.E., Zhang, Y., He, Q., 2007. Models for Converting Measurements of Environmental Radionuclide Inventories (137Cs, Excess 210Pb and 7Be to Estimates of Soil Erosion and Deposition Rates (Including Software for Model Implementation). Department of Geography, University of Exeter, Exeter.

Wang, X., Zhang, L., Moran, M.D., 2014a. Development of a new semi-empirical parameterisation for below-cloud scavenging of size-resolved aerosol particles by both rain and snow. Geoscientific Model Development, 7, 799-819.

Wang, Y., Amundson, R., Trumbore, S., 1996. Radiocarbon Dating of Soil Organic Matter. Quaternary Research, 45, 282-288.

Wang, Z., Zhao, H., Dong, G., Zhou, A., Liu, J., Zhang, D., 2014b. Reliability of radiocarbon dating on various fractions of loess-soil sequence for Dadiwan section in the western Chinese Loess Plateau. Frontiers of Earth Science, 8, 540-546.

Wanner, H., Beer, J., Bütikofer, J., Crowley, T.J., Cubasch, U., Flückiger, J., Goosse, H., Grosjean, M., Joos, F., Kaplan, J.O., Küttel, M., Müller, S.A., Prentice, I.C., Solomina, O., Stocker, T.F., Tarasov, P., Wagner, M., Widmann, M., 2008. Mid- to Late Holocene climate change: an overview. Quaternary Science Reviews, 27, 1791-1828.

Wasson, R.J., Olive, L.J., Rosewell, C.J., 1996. Rates of erosion and sediment transport in Australia. Erosion and Sediment Yield: Global and Regional Perspectives (Proceedings of the Exeter Symposium, July 1996), IAHS Publ. no. 236, 139-148.

Watmough, S., Dillon, P., 2007. Lead biogeochemistry in a central Ontario Forested watershed. Biogeochemistry, 84, 143-159.

Wedepohl, H.K., 1995. The composition of the continental crust. Geochimica et Cosmochimica Acta, 59, 1217-1232.

Weiss, D., Shotyk, W., Cheburkin, A.K., Gloor, M., Reese, S., 1997. Atmospheric Lead Deposition from 12,400 to ca. 2,000 yrs BP in a Peat Bog Profile, Jura Mountains, Switzerland. Water, Air, and Soil Pollution, 100, 311-324.

Weiss, D., Shotyk, W., Rieley, J., Page, S., Gloor, M., Reese, S., Martinez-Cortizas, A., 2002. The geochemistry of major and selected trace elements in a forested peat bog, Kalimantan, SE Asia, and its implications for past atmospheric dust deposition. Geochimica Et Cosmochimica Acta, 66, 2307-2323.

Whetton, P., Haylock, M., Galloway, R., 1996. Climate change and snow-cover duration in the Australian Alps. Climatic Change, 32, 447-479.

Wiener, J.G., Knights, B.C., Sandheinrich, M.B., Jeremiason, J.D., Brigham, M.E., Engstrom, D.R., Woodruff, L.G., Cannon, W.F., Balogh, S.J., 2006. Mercury in Soils, Lakes, and Fish in Voyageurs National Park (Minnesota): Importance of Atmospheric Deposition and Ecosystem Factors. Environmental Science & Technology, 40, 6261-6268.

Wilkinson, M.T., Chappell, J., Humphreys, G.S., Fifield, K., Smith, B., Hesse, P., 2005. Soil production in heath and forest, Blue Mountains, Australia: influence of lithology and palaeoclimate. Earth Surface Processes and Landforms, 30, 923-934.

Williams, M., Cook, E., van der Kaars, S., Barrows, T., Shulmeister, J., Kershaw, P., 2009. Glacial and deglacial climatic patterns in Australia and surrounding regions from 35 000 to 10 000 years ago reconstructed from terrestrial and near-shore proxy data. Quaternary Science Reviews, 28, 2398-2419.

Wilson, S., 1998a. Data compilation and statistical analysis of intralaboratory results for AGV-2. United States Geological Survey, Denver, Colorado.

Wilson, S., 1998b. Data compilation for USGS reference material BHVO-2, Hawaiiann Basalt. United States Geological Survey, Denver, Colorado.

Wilson, S.J., Steenhuisen, F., Pacyna, J.M., Pacyna, E.G., 2006. Mapping the spatial distribution of global anthropogenic mercury atmospheric emission inventories. Atmospheric Environment, 40, 4621-4632.

Witt, M., Baker, A.R., Jickells, T.D., 2006. Atmospheric trace metals over the Atlantic and South Indian Oceans: Investigation of metal concentrations and lead isotope ratios in coastal and remote marine aerosols. Atmospheric Environment, 40, 5435-5451.

Wolfe, A.P., Van Gorp, A.C., Baron, J.S., 2003. Recent ecological and biogeochemical changes in alpine lakes of Rocky Mountain National Park (Colorado, USA): a response to anthropogenic nitrogen deposition. Geobiology, 1, 153-168.

Wolff, E., Peel, D.A., 1988. Concentrations of cadmium, copper, lead and zinc in snow from near Dye 3 in south Greenland. Annals of Glaciology, 10, 193-197.

Wolff, E.W., Suttie, E.D., 1994. Antarctic snow record of southern hemisphere lead pollution. Geophysical Research Letters, 21, 781-784.

Wolff, W.W., Suttie, E.D., Peel, D.A., 1999. Antarctic snow record of cadmium, copper and zinc content during the twentieth century. Atmospheric Environment, 33, 1535-1541.

Wong, H.K.T., Nriagu, J.O., Coker, R.D., 1984. Atmospheric input of heavy metals chronicled in lake sediments of the Algonquin Provincial Park, Ontario, Canada. Chemical Geology, 44, 187-201.

Xie, X., Yan, M., Wang, C., Li, L., Shen, H., 1989. Geochemical standard reference samples GSD 9–12, GSS 1–8 AND GSR 1–6. Geostandards Newsletter, 13, 83-179.

Yamamoto, N., Fujii, M., Kumagai, K., Yanagisawa, Y., 2004. Time course shift in particle penetration characteristics through capillary pore membrane filters. Journal of Aerosol Science, 35, 731-741.

Yang, H., Linge, K., Rose, N., 2007. The Pb pollution fingerprint at Lochnagar: The historical record and current status of Pb isotopes. Environmental Pollution, 145, 723-729.

Yang, H., Rose, N., 2005. Trace element pollution records in some UK lake sediments, their history, influence factors and regional differences. Environment International, 31, 63-75.

Yang, H., Rose, N.L., Battarbee, R.W., Boyle, J.F., 2002. Mercury and lead budgets for Lochnagar, a Scottish mountain lake and its catchment. Environmental Science & Technology, 36, 1383-1388.

Young, R., McDougall, I., 1993. Long-term landscape evolution: early Miocene and modern rivers in southern New South Wales, Australia. The Journal of Geology, 101, 35-49.

Young, S., 2013. Chemistry of Heavy Metals and Metalloids in Soils. in: Alloway, B.J. (Ed.), Heavy Metals in Soils. Springer Netherlands, pp. 51-95.

Yu, B., Neil, D., 1994. Temporal and spatial variation of sediment yield in the Snowy Mountains region, Australia. Variability in stream erosion and sediment transport. Proc. symposium, Canberra, 1994, 281-289.

Zhang, X.C., Zhang, G.H., Wei, X., 2015. How to make 137Cs erosion estimation more useful: An uncertainty perspective. Geoderma, 239–240, 186-194.

Zhang, X.C.J., 2014. New insights into using fallout radionuclides to estimate soil redistribution rates. Soil Science Society of America journal.

Zheng, J., Shotyk, W., Krachler, M., Fisher, D.A., 2007. A 15,800-year record of atmospheric lead deposition on the Devon Island Ice Cap, Nunavut, Canada: Natural and anthropogenic enrichments, isotopic composition, and predominant sources. Global Biogeochemical Cycles, 21, GB2027.

Zoller, W.H., Gladney, E.S., Duce, R.A., 1974. Atmospheric Concentrations and Sources of Trace Metals at the South Pole. Science, 183, 198-200.

Appendix 1. Trace element concentration of samples

Supplementary Table 1.Trace element concentration of samples (ppb)

Geehi Reservoir

Name	Geehi 1-0	Geehi 1-4	Geehi 1-10	Geehi 1-20	Geehi 1-30	Geehi 1-40	Geehi 1-50	Geehi 1-60
Lat	-36.379°	-36.379°	-36.379°	-36.379°	-36.379°	-36.379°	-36.379°	-36.379°
Long	148.371°	148.371°	148.371°	148.371°	148.371°	148.371°	148.371°	148.371°
Depth (mm)	1	4	10	20	30	40	50	60
Li	19213	20095	20458	20997	21280	22339	21454	19238
Sc	11884	12353	12407	12313	12544	13034	12782	11688
Ti	3232318	3273855	3270804	3223256	3374121	3432431	3393392	3046140
Cr	42812	43556	42995	44656	44422	45385	44483	38905
Co	14901	15187	16051	16066	16432	16853	15920	14483
Ni	18709	19403	19128	19620	19550	20358	19546	17308
Cu	29122	30212	31131	29750	30132	30412	30972	26847
Zn	90307	90239	92434	92296	94621	98650	95704	87501
Ga	15498	16024	16076	16178	16529	17183	16921	15492
As	9440	9496	7848	8473	8199	8423	8032	7051
Rb	78321	81135	81191	84432	85685	87954	88087	80951
Sr	106009	110484	117035	99351	98901	96124	97530	98519
Zr	79760	81098	78439	74793	86699	81140	84278	75151
Nb	9188	9556	9491	9788	9869	10296	10194	9106
Mo	637	624	596	609	616	684	631	610
Ag	96	117	93	98	95	99	101	88
Cd	272	265	253	265	273	286	275	248
In	53	54	56	57	55	57	56	51
Sn	3769	3877	3835	4045	4061	4214	4195	3926
Sb	248	258	264	244	239	249	252	230
Ba	408062	420205	418792	405770	413989	416730	420561	404897
La	37478	37639	39185	39685	39396	40196	38905	38202
Pr	9077	9076	9408	9661	9576	9711	9382	9188
Nd	34121	34262	35646	36203	35786	36354	35351	34598
Tm	481	490	483	487	500	505	497	496
Lu	417	421	413	416	422	429	422	426
Ta	811	841	835	881	883	921	916	809
W	2370	2395	2436	2532	2630	2799	2786	2401
Pb	18218	19047	18772	19940	19800	20543	20394	19820

Supplementary Table 1.Trace element concentration of samples (ppb)

Geehi Reservoir

Name	Geehi 1-70	Geehi 1-100	Geehi 1-115	Geehi 1-130	Geehi 1-145	Geehi 1-160	Geehi 1-175	Geehi 1-190
Lat	-36.379°	-36.379°	-36.379°	-36.379°	-36.379°	-36.379°	-36.379°	-36.379°
Long	148.371°	148.371°	148.371°	148.371°	148.371°	148.371°	148.371°	148.371°
Depth (mm)	70	100	115	130	145	160	175	190
Li	22395	21440	22670	22744	24510	25245	25672	24801
Sc	12875	13028	12654	12515	13461	14227	15225	15392
Ti	3424332	3524878	3266043	3211073	3414815	3617952	3589055	3692085
Cr	45355	41515	42388	41925	45731	46280	48369	47126
Co	15895	14947	14842	14919	16463	17212	18247	17940
Ni	20021	18200	18529	18794	20646	21294	22306	21936
Cu	29374	27377	26457	30680	30359	31187	32941	32691
Zn	99384	94294	89396	92118	101697	106794	107840	103792
Ga	17026	15675	16678	16464	17452	18250	19084	19212
As	6657	6979	6781	8017	6850	7681	7692	6093
Rb	91012	84770	86081	84581	88406	89976	89465	86972
Sr	95326	95355	105266	105638	96145	95342	93327	96868
Zr	84309	67078	74674	75704	78525	67567	76166	73740
Nb	10280	9363	9767	9579	10192	10474	10408	10226
Mo	667	755	584	549	593	680	747	759
Ag	95	93	91	96	102	106	107	98
Cd	277	242	253	263	272	280	264	253
In	57	52	52	54	56	57	58	57
Sn	4285	3712	4004	4015	4161	4340	4267	4145
Sb	253	259	234	271	257	253	256	252
Ba	432553	393324	393710	414572	423221	436423	436473	441478
La	39535	38159	39317	38716	41294	40197	39956	44329
Pr	9583	9244	9573	9482	10085	9887	9884	10972
Nd	36007	34916	35933	35624	37922	37068	37098	41163
Tm	478	467	487	495	504	502	512	509
Lu	407	395	413	423	432	431	440	443
Ta	920	822	879	850	922	942	933	898
W	2785	2365	2577	3154	2952	3035	3092	2967
Pb	20832	19416	20055	20867	22144	22604	22724	21886

Supplementary Table 1.Trace element concentration of samples (ppb)

	Geehi Reservoir				Guthega Reservoir			
Name	Geehi 1-205	Geehi 1-220	Geehi 1-235	Geehi 1-260	G-1	Gu 1-2	Gu 1-4	Gu 1-6
Lat	-36.379°	-36.379°	-36.379°	-36.379°	-36.305°	-36.305°	-36.305°	-36.305°
Long	148.371°	148.371°	148.371°	148.371°	148.316°	148.316°	148.316°	148.316°
Depth (mm)	205	220	235	260	0	2	4	6
Li	21811	24595	23529	21409	19213	26272	25912	28914
Sc	14032	13677	16147	16867	11185	11115	10908	11834
Ti	3705600	3542657	3987200	3751957	3275830	3273563	3353148	3593818
Cr	41623	45638	46042	45051	44224	42897	43366	46937
Co	16040	16319	17470	16546	11775	12477	12123	12658
Ni	18506	20284	21136	21204	17950	17361	17378	18656
Cu	28750	30846	30753	29946	14404	15425	15795	17497
Zn	101129	106485	107293	101410	85723	82044	85108	91443
Ga	16747	18304	21007	21582	16301	15883	15891	17292
As	8416	9113	4787	5616	16301	25249	25262	27490
Rb	81078	94806	87039	84769	99559	99252	98790	108471
Sr	98355	102419	93708	101320			54712	55872
Zr	77601	79417	62995	63272			96572	101751
Nb	9431	10820	10598	10064	10043	10608	10522	11949
Mo	1104	1256	1491	1904	522	486	503	502
Ag	98	114	90	71	71	72	77	73
Cd	226	271	209	169	173	176	179	184
In	54	58	63	63	54	55	56	62
Sn	3900	4718	4377	4198	4932	4500	4410	4912
Sb	247	275	254	300	159	158	214	184
Ba	407656	432831	467546	512756			360817	384221
La	39811	40972	38305	37560	36822	35686	42671	43670
Pr	9813	10051	9587	9430	8943	8867	10255	10616
Nd	36742	37479	35838	35441	33071	32776	37328	39231
Tm	508	525	495	495	320	343	364	398
Lu	436	450	432	438	282	313	321	348
Ta	834	981	930	869	876	952	965	1067
W	2831	3203	3034	2884	2486	2523	2596	2734
Pb	21843	24308	22061	20442	25360	25725	26288	27976

Supplementary Table 1.Trace element concentration of samples (ppb)

Guthega Reservoir

Name	Gu 1-8	Gu 1-20	G-2	Gu 1-38	Gu 1-43	Gu 1-46	G-3	Gu 1-64
Lat	-36.305°	-36.305°	-36.305°	-36.305°	-36.305°	-36.305°	-36.305°	-36.305°
Long	148.316°	148.316°	148.316°	148.316°	148.316°	148.316°	148.316°	148.316°
Depth (mm)	8	20	30	38	43	46	60	64
Li	29714	30692	30878	28974	26899	30789	31845	31691
Sc	12101	12181	12673	11805	10840	12264	12839	12807
Ti	3648518	3738109	3559978	3684343	3255802	3468355	3603506	3636548
Cr	46978	48102	47746	47747	43581	47214	48034	48642
Co	12746	13553	13537	12590	11388	12351	13865	12638
Ni	18753	19918	20076	19396	17259	18431	20353	18748
Cu	17587	19037	17062	18394	15801	16456	18283	17065
Zn	93023	102055	103897	94392	83201	93988	105319	101343
Ga	17530	18273	18430	17581	15429	16920	18583	17475
As	27868	29049	29298	27949	24529	26899	18583	27781
Rb	110072	112419	111073	108420	101791	114886	111443	118983
Sr	55117	57499		55619	53512	52548		52873
Zr	119476	85737		101781	90787	76518		82473
Nb	12010	12382	10835	11990	10801	11063	10972	11973
Mo	505	544	532	510	446	467	590	483
Ag	73	84	73	78	64	66	85	68
Cd	184	210	202	193	157	164	236	180
In	61	60	60	60	54	59	60	60
Sn	4993	5128	5516	4986	4521	4877	5640	5148
Sb	185	196	188	188	164	182	196	169
Ba	388133	388534		378605	350301	378669		405821
La	42901	41171	38663	38374	35342	39119	40046	38959
Pr	10470	10042	9424	9294	8561	9447	9690	9565
Nd	38874	37167	34982	34429	31807	34879	35902	35266
Tm	401	378	363	385	342	332	369	339
Lu	359	333	315	341	303	291	315	298
Ta	1075	1121	940	1078	969	999	954	1064
W	2762	2930	3047	2789	2503	2521	2664	2631
Pb	28137	29110	28625	28102	25407	26381	29892	27589

Supplementary Table 1.Trace element concentration of samples (ppb)

Guthega Reservoir

Name	G-4	Gu 1-80	Gu 1-86	G-5	Gu 1-110	G-6	Gu 1-142	Gu 1-146
Lat	-36.305°	-36.305°	-36.305°	-36.305°	-36.305°	-36.305°	-36.305°	-36.305°
Long	148.316°	148.316°	148.316°	148.316°	148.316°	148.316°	148.316°	148.316°
Depth (mm)	70	80	86	90	110	120	142	146
Li	32657	32936	25233	30560	30599	30711	28377	24793
Sc	13410	12880	10217	12686	12541	12986	11960	10506
Ti	3745377	3980583	2997445	3510677	3784409	3618478	3593272	2951059
Cr	49311	50206	40812	47840	49421	49457	48022	39946
Co	13623	13512	11233	12799	12625	12522	11633	9560
Ni	20413	20297	15818	19053	19652	19930	18828	14936
Cu	17577	20734	16206	16232	19572	17534	19031	13551
Zn	113002	112943	89779	105629	103330	100186	96584	77340
Ga	19224	19190	14043	17918	18758	18890	18011	14223
As	19224	30507	22325	17918	29820	18890	28632	22611
Rb	118645	118550	93077	112940	115793	114218	114119	106940
Sr		54418	50266		55033		54964	52071
Zr		89435	68436		86066		74611	94371
Nb	11363	13072	9903	10721	12218	11043	11374	9800
Mo	584	639	583	534	563	601	548	345
Ag	79	89	74	76	88	82	82	48
Cd	219	233	172	206	212	212	205	130
In	60	66	48	59	64	60	61	50
Sn	5893	5483	4118	5566	5421	5773	5388	4222
Sb	190	213	171	184	200	186	186	127
Ba		393695	332749		406206		392421	400451
La	40270	50711	31318	35582	42155	40234	39446	28287
Pr	9654	12404	7580	8618	10259	9713	9627	6745
Nd	35930	45689	28181	32066	37945	35894	35439	25028
Tm	356	411	314	330	387	357	354	280
Lu	305	350	272	288	331	307	297	259
Ta	994	1174	906	945	1130	970	1027	907
W	2785	2963	2412	2496	2834	2566	2637	2098
Pb	30253	31259	25849	28290	30994	29997	29845	23630

Supplementary Table 1.Trace element concentration of samples (ppb)

Guthega Reservoir

Name	G-7	Gu 1-174	Gu 1-176	G-8	Gu 1-194	G-9	G-10	Gu 1-250
Lat	-36.305°	-36.305°	-36.305°	-36.305°	-36.305°	-36.305°	-36.305°	-36.305°
Long	148.316°	148.316°	148.316°	148.316°	148.316°	148.316°	148.316°	148.316°
Depth (mm)	154	174	176	180	194	210	230	250
Li	30385	30515	32472	31514	30841	32469	31713	29771
Sc	12865	12570	12813	13253	12696	13425	13298	12494
Ti	3620902	3823635	3751255	3616716	3879999	3823219	3782894	3798473
Cr	48052	49548	52187	50732	49454	51166	50188	49160
Co	12444	12586	12456	12487	12261	13206	12502	11702
Ni	19279	19990	19208	19586	19573	20634	20103	19050
Cu	18082	21909	17586	15617	19088	18206	17399	18330
Zn	116761	117133	102011	100543	100100	107407	98469	95598
Ga	18288	18479	16146	18277	18720	19628	19541	18276
As	18288	29376	25667	18277	29760	19628	19541	29055
Rb	118512	113703	121427	118922	115170	117290	117425	113923
Sr		54174	48543		53865			52225
Zr		79959	60896		103931			88382
Nb	10950	12424	11934	11294	12818	11584	11571	12519
Mo	561	634	474	560	557	690	577	546
Ag	72	104	72	80	87	101	92	85
Cd	222	218	166	190	198	231	212	183
In	59	62	57	61	63	63	61	62
Sn	5795	5220	5023	5945	5413	5921	5858	5358
Sb	182	212	157	169	195	196	195	188
Ba		385488	428392		397763	390744		386753
La	37817	41346	30573	38357	43866	39715	40345	43141
Pr	9102	10114	7452	9241	10741	9585	9750	10544
Nd	33771	37363	27837	34487	39485	35673	36164	38810
Tm	331	384	303	349	404	383	375	381
Lu	287	325	258	294	347	321	319	324
Ta	978	1108	1063	988	1160	1018	1019	1121
W	2501	2737	2244	2537	2828	2653	2578	2647
Pb	29423	31520	26585	29125	31118	32021	31640	31211

Supplementary Table 1.Trace element concentration of samples (ppb)

	Guthega Reservoir			Club Lake				
Name	Gu 1-264	Gu 1-266	Gu 1-272	CL3-0	CL3-2	CL3-4	CL3-6	CL3-8
Lat	-36.305°	-36.305°	-36.305°	-36.414°	-36.414°	-36.414°	-36.414°	-36.414°
Long	148.316°	148.316°	148.316°	148.291°	148.291°	148.291°	148.291°	148.291°
Depth (mm)	264	266	272	0	2	4	6	8
Li	31528	30844	35930	15149	14307	14735	14537	15270
Sc	12980	12740	14188	13428	13018	13559	13703	14598
Ti	4066032	3925854	4270077	3953774	3848797	3957413	4026078	4217187
Cr	51482	50192	55806	90792	89234	93996	94564	102260
Co	11886	11514	12420	9797	9478	9950	10060	11013
Ni	20127	19446	20707	34884	33250	34236	33540	35971
Cu	19666	18897	19523	25773	24542	25171	24715	25936
Zn	98628	94592	101935	128306	118098	118394	120309	124808
Ga	19553	18782	20282	18350	18024	18833	19033	20242
As	31084	29859	32244	3348	2765	2904	2412	2994
Rb	121430	119858	137986	139710	137870	143119	145283	153667
Sr	55252	54102	54483	46630	44142	45070	44561	46992
Zr	105110	88408	95711	122322	132480	127898	139576	132422
Nb	13187	12850	13714	13626	13884	13874	14582	14858
Mo	561	544	514	514	430	414	347	347
Ag	102	97	104	137	137	129	139	137
Cd	191	196	175	398	380	318	339	335
In	65	63	68	93	94	92	96	96
Sn	5625	5529	5912	6952	6504	7336	6949	8048
Sb	215	204	180	185	145	136	129	126
Ba	406360	396640	433009	569643	577030	594353	617286	650642
La	41077	41442	44548	52265	50786	51668	52079	56034
Pr	10056	10150	10887	12117	11940	12050	12241	12985
Nd	36831	37200	39803	44718	43693	44538	44945	47818
Tm	392	374	361	484	483	479	500	501
Lu	350	326	320	424	426	420	446	439
Ta	1201	1161	1251	1039	1087	1065	1147	1142
W	2893	2807	2823	2949	3002	2948	3201	3188
Pb	32929	32327	32877	45026	42554	43260	42650	46082

Supplementary Table 1.Trace element concentration of samples (ppb)

Club Lake

Name	CL3-10	CL3-12	CL3-14	CL3-16	CL3-18	CL3-20	CL3-26	CL3-34
Lat	-36.414°	-36.414°	-36.414°	-36.414°	-36.414°	-36.414°	-36.414°	-36.414°
Long	148.291°	148.291°	148.291°	148.291°	148.291°	148.291°	148.291°	148.291°
Depth (mm)	10	12	14	16	18	20	26	34
Li	15011	14710	14743	15342	14994	15539	16028	18687
Sc	14515	14348	14017	14784	14293	14998	15810	18180
Ti	4074483	4188739	4146105	4207801	4214932	4262282	4546529	4967320
Cr	101087	99861	97810	104189	99996	107064	110818	127173
Co	11057	11086	10882	11749	11370	11982	12580	14182
Ni	35505	34796	34204	36342	34944	36524	37499	43043
Cu	25530	24631	24489	25166	25034	26277	27917	33279
Zn	123388	120414	122425	123845	123257	124030	123181	135009
Ga	20165	19834	19647	20558	19938	20835	21814	25140
As	2851	2663	2352	2668	2343	2623	2457	3722
Rb	152433	149202	149451	154373	151598	155983	162892	187992
Sr	46730	46117	45926	47470	46160	47045	46872	53034
Zr	128658	135536	143880	134614	148317	133150	151622	151205
Nb	14416	14668	15142	14894	15450	15167	16135	17444
Mo	327	304	284	299	282	293	296	388
Ag	137	131	140	130	137	129	132	139
Cd	322	303	299	267	282	225	229	226
In	97	95	97	100	100	99	107	113
Sn	7934	7803	7296	8170	7275	8144	8161	8871
Sb	120	120	119	144	133	140	156	188
Ba	649566	641980	646024	663112	656608	672896	700440	780289
La	54871	54141	52126	54693	52567	55574	53678	59610
Pr	12798	12591	12314	12704	12347	12939	12365	13593
Nd	46899	46360	45176	46640	45277	47468	45408	49685
Tm	491	490	494	497	509	492	492	509
Lu	436	431	447	434	457	433	450	452
Ta	1087	1124	1187	1123	1199	1142	1215	1300
W	3364	3234	3401	3269	3305	3307	3276	3703
Pb	46033	44272	43823	45503	44798	46322	45521	50639

Supplementary Table 1.Trace element concentration of samples (ppb)

Club Lake

Name	CL3-40	CL3-42	CL3-44	CL3-46	CL3-48	CL3-52	CL3-64	CL3-66
Lat	-36.414°	-36.414°	-36.414°	-36.414°	-36.414°	-36.414°	-36.414°	-36.414°
Long	148.291°	148.291°	148.291°	148.291°	148.291°	148.291°	148.291°	148.291°
Depth (mm)	40	42	44	46	48	52	64	66
Li	17593	17835	17237	16457	18864	17247	19134	17598
Sc	17261	17200	17249	15930	18616	17334	18565	17305
Ti	4916530	4911668	4913978	4588102	5152279	4969290	5069207	4861147
Cr	122645	121928	122062	113928	131840	123095	129416	119740
Co	13221	13135	12809	12730	13624	12797	13180	12444
Ni	40150	40457	39957	38035	42599	39717	42701	39837
Cu	33101	33211	32964	30328	35489	33525	34399	32497
Zn	133518	133805	130734	129019	138001	134745	126985	116126
Ga	24145	24584	24177	22767	26056	24208	25716	23971
As	3272	3509	3073	4855	3279	2035	4256	3233
Rb	180647	186588	182825	175039	197644	183286	192538	177000
Sr	50101	50617	49032	49091	52964	48758	55614	52991
Zr	161625	160618	156621	149111	155300	166268	148758	157097
Nb	17367	18074	17520	17141	18393	17731	17737	16850
Mo	362	364	344	367	400	341	384	369
Ag	139	141	178	129	136	138	141	147
Cd	218	213	192	113	172	199	185	318
In	114	116	115	110	120	116	112	110
Sn	8576	8287	8807	7975	9701	9028	8742	7952
Sb	177	184	166	172	188	171	191	181
Ba	751886	781221	760045	734414	816480	764878	789319	733826
La	57327	56629	56218	55145	60974	57835	57451	53389
Pr	13090	13206	12879	13018	13925	13234	13085	12132
Nd	48091	48119	47169	47376	51004	48605	47783	44426
Tm	501	515	501	504	525	520	501	477
Lu	462	468	459	454	467	471	446	439
Ta	1307	1396	1325	1321	1373	1342	1328	1273
W	3516	3878	3585	3676	3961	3698	3728	3331
Pb	47673	49417	47055	47675	51618	48439	49706	44588

Supplementary Table 1.Trace element concentration of samples (ppb)

Club Lake

Name	CL3-70	CL3-80	CL3-88	CL3-94	CL3-102	CL3-106	CL3-108	CL3-112
Lat	-36.414°	-36.414°	-36.414°	-36.414°	-36.414°	-36.414°	-36.414°	-36.414°
Long	148.291°	148.291°	148.291°	148.291°	148.291°	148.291°	148.291°	148.291°
Depth (mm)	70	80	88	94	102	106	108	112
Li	18783	19235	17362	17562	13287	15797	16844	15975
Sc	18006	18245	16716	16962	11771	15108	16208	15332
Ti	4952642	4858637	4773176	4827179	3910837	4453645	4716396	4465265
Cr	124755	126735	117778	120781	82008	105209	113971	106035
Co	13577	14115	12913	13493	10214	12008	12959	11970
Ni	42116	43549	40770	42371	33214	37839	40657	37552
Cu	33296	33706	31699	32040	25574	27607	29119	27172
Zn	124597	132875	131145	143666	125482	130345	139680	144189
Ga	24831	25214	23144	23502	16347	20942	22272	21088
As	3537	4111	3127	4354	2811	3471	4021	2642
Rb	182681	188209	176198	182166	131766	160299	172127	160609
Sr	57127	58789	54277	56706	44751	52035	55806	52494
Zr	145473	143333	158317	146830	150575	154146	152800	150221
Nb	17047	16779	16841	17351	13373	15755	16626	15715
Mo	408	416	313	304	227	253	269	257
Ag	144	145	138	146	**114**	132	137	131
Cd	530	274	292	341	264	245	241	268
In	112	113	110	109	**78**	107	107	106
Sn	8282	8498	8414	9095	5608	8110	8789	8054
Sb	210	181	158	240	119	137	146	138
Ba	754076	777985	743091	760604	500110	676246	718727	677601
La	55978	58772	59262	63118	46676	55216	59693	56500
Pr	12725	13282	13519	14449	10670	12717	13800	13039
Nd	46471	48646	49618	53002	39169	46903	50799	47969
Tm	488	495	510	535	460	496	529	499
Lu	432	434	462	463	417	444	465	449
Ta	1277	1229	1260	1322	1089	1199	1261	1196
W	3500	3537	3339	3631	2597	3536	3460	3450
Pb	48612	49325	48186	53878	45045	48568	52868	47777

Supplementary Table 1.Trace element concentration of samples (ppb)

Club Lake

Name	CL3-118	CL3-124	CL3-134	CL3-140	CL3-148	CL3-154	CL3-168	CL3-170
Lat	-36.414°	-36.414°	-36.414°	-36.414°	-36.414°	-36.414°	-36.414°	-36.414°
Long	148.291°	148.291°	148.291°	148.291°	148.291°	148.291°	148.291°	148.291°
Depth (mm)	118	124	134	140	148	154	168	170
Li	15699	16108	14021	14517	13889	14927	14186	15190
Sc	15320	16294	14974	15580	14849	15866	15308	16339
Ti	4381450	4613531	4282596	4363954	4218450	4299387	4328573	4519553
Cr	106373	115964	107388	113955	108049	114420	109926	118665
Co	12063	13219	11976	12559	11844	12859	12004	12957
Ni	37658	40910	37905	40435	38259	40708	38464	41072
Cu	26911	29452	26690	27271	26313	27832	27962	29554
Zn	136555	148531	136061	138658	135041	150540	134555	146494
Ga	21082	22518	21020	21665	20837	22226	21476	22794
As	3172	3096	1638	2370	1963	2300	1890	2262
Rb	161034	174445	163791	169987	161521	172686	167399	179082
Sr	52246	53721	48052	49983	47677	51980	48528	51557
Zr	145013	146862	147497	141997	146853	134897	147032	146453
Nb	15555	16528	15504	15822	15389	15712	15820	16599
Mo	254	268	218	240	237	237	227	256
Ag	130	136	121	120	120	128	130	134
Cd	293	254	227	278	308	243	203	209
In	106	109	104	103	102	111	108	113
Sn	8096	8854	8160	8489	7915	8881	8330	9043
Sb	141	119	54	55	54	56	51	55
Ba	686338	738351	706453	727592	694944	744095	725330	770773
La	56086	60040	54924	56553	54323	57672	57584	62132
Pr	12897	13762	12580	12992	12439	13310	13202	14241
Nd	47324	50759	46167	47831	45714	48913	48600	52506
Tm	493	527	473	499	472	510	502	536
Lu	439	466	425	441	425	440	447	467
Ta	1177	1262	1178	1211	1186	1183	1203	1260
W	4196	3482	3112	3365	3092	3475	3308	3666
Pb	45765	47141	37737	40136	37831	41657	38806	43122

Supplementary Table 1.Trace element concentration of samples (ppb)

Club Lake

Name	CL3-172	CL3-178	CL3-180	CL3-184	CL3-214	CL3-244	CL3-272	CL3-304
Lat	-36.414°	-36.414°	-36.414°	-36.414°	-36.414°	-36.414°	-36.414°	-36.414°
Long	148.291°	148.291°	148.291°	148.291°	148.291°	148.291°	148.291°	148.291°
Depth (mm)	172	178	180	184	214	244	272	304
Li	14354	14299	15273	15262	15575	15076	14845	14935
Sc	15478	15579	16367	16464	17112	16131	16889	15963
Ti	4390359	4386037	4516925	4596988	4606448	4359185	4632871	4507224
Cr	111578	112377	119362	119464	125651	117678	125894	120314
Co	12179	12141	12960	12986	13009	12644	12265	12472
Ni	38985	38739	41521	41590	42306	41121	39600	41330
Cu	28252	28472	30041	30004	31885	28113	28370	29396
Zn	138641	138871	147519	147325	145158	147380	128418	146493
Ga	21763	21990	23071	23103	24037	22544	23493	22646
As	1928	1818	2197	2344	2475	2191	2417	2144
Rb	169398	171152	181838	181167	190595	177334	181709	183833
Sr	48981	49112	51798	51520	50801	48646	49408	47608
Zr	147223	154201	141112	148971	145988	135978	148400	147608
Nb	16032	16115	16804	16944	17257	15950	17015	16689
Mo	240	234	245	260	261	236	258	226
Ag	128	127	131	131	131	135	137	141
Cd	230	232	220	215	186	220	170	257
In	109	111	113	112	113	110	109	109
Sn	8460	8476	9105	9093	9377	8995	8800	9244
Sb	51	51	58	58	59	54	63	53
Ba	736105	743038	778045	782716	815036	760224	799127	765594
La	58394	58239	62217	61891	61881	58842	57149	62374
Pr	13414	13375	14260	14162	14178	13544	13131	14285
Nd	49212	49175	52674	52368	52233	50093	48456	52744
Tm	504	506	536	538	540	513	514	540
Lu	445	454	462	466	472	444	456	467
Ta	1219	1215	1262	1286	1296	1203	1301	1284
W	3368	3345	3685	3680	3834	3564	3660	3750
Pb	40241	40175	44271	44634	46254	42448	40353	46760

Supplementary Table 1.Trace element concentration of samples (ppb)

Club Lake

Name	CL3-335	CL3-352	CL3-362	CL3-374	CL3-382
Lat	-36.414°	-36.414°	-36.414°	-36.414°	-36.414°
Long	148.291°	148.291°	148.291°	148.291°	148.291°
Depth (mm)	335	352	362	374	382
Li	15511	14095	14726	13958	15086
Sc	16605	15080	15722	14937	15975
Ti	4536443	4351960	4463602	4221089	4482073
Cr	123244	109572	114435	113338	122204
Co	12873	11976	12485	11679	12498
Ni	41927	38761	40392	37776	40969
Cu	29891	27129	27921	25337	28092
Zn	151501	137104	148380	137446	145960
Ga	23420	21222	22116	21020	22540
As	2080	1458	2089	1664	2130
Rb	188071	166056	173034	161730	176686
Sr	49006	46001	49583	46915	49745
Zr	147144	153583	158694	157036	151536
Nb	16807	15852	16330	15297	16305
Mo	273	198	191	188	240
Ag	140	133	147	127	132
Cd	343	249	218	201	374
In	111	107	110	105	107
Sn	9446	8203	8849	8040	8742
Sb	59	47	49	45	55
Ba	795433	705912	739444	704229	750563
La	65238	55976	58457	53070	59412
Pr	14860	12848	13322	12186	13556
Nd	55000	47000	49091	44831	50069
Tm	553	490	523	481	515
Lu	479	449	465	440	455
Ta	1289	1227	1272	1180	1262
W	3877	3208	3516	3183	3581
Pb	45844	38420	41658	37112	42320

Supplementary Table 1.Trace element concentration of samples (ppb)

Guthega Hill

Name	Gu P1A 0-10	Gu P1A 10-20	Gu P1A 20-40	Gu P1A 40-50	Gu P1A 50-60	Gu P2 0-15	Gu P2 15-30	Gu P2 30-50	Gu P2 50-60
Lat	-36.360°	-36.360°	-36.360°	-36.360°	-36.360°	-36.360°,	-36.360°,	-36.360°,	-36.360°,
Long	148.373°	148.373°	148.373°	148.373°	148.373°	148.370°	148.370°	148.370°	148.370°
Li	34,676	39,938	22,588	26,950	31,827	34,903	27,301	17,485	30,679
Sc	14,768	16,546	9,141	9,982	9,939	14,713	11,027	6,393	10,806
Ti	4,682,786	5,380,521	2,666,771	3,153,992	2,620,853	5,025,900	3,606,935	1,775,652	3,000,305
Cr	58,871	67,172	34,097	47,177	35,615	55,894	43,471	23,697	43,190
Co	11,977	13,906	8,670	7,763	9,671	9,582	6,754	4,127	8,026
Ni	21,807	24,568	12,843	13,032	14,850	18,818	14,091	8,435	15,318
Cu	19,590	20,073	11,108	12,913	13,974	14,435	10,061	6,702	11,265
Zn	102,859	99,009	48,066	48,915	54,812	80,031	55,718	31,265	53,426
Ga	22,022	24,980	13,722	12,938	13,974	22,872	17,153	9,555	14,484
As	2,267	2,449	1,031	1,050	1,102	1,838	1,065	840	1,473
Rb	155,315	169,284	93,868	102,299	106,011	146,175	112,826	65,871	103,873
Sr	62,811	63,911	38,795	53,376	75,674	65,809	45,497	35,296	45,483
Zr	81,999	90,637	117,790	42,802	36,734	98,302	60,094	27,232	46,082
Nb	14,098	16,498	8,544	10,069	8,395	15,364	11,265	5,712	9,628
Mo	459	540	239	136	81	659	431	170	262
Ag	79	91	41	17	14	80	50	14	40
Cd	215	151	39	23	35	131	49	15	22
In	70	80	45	40	45	73	55	30	52
Sn	6,452	7,272	4,443	3,801	4,257	6,967	5,275	3,038	4,695
Sb	219	234	146	128	93	188	117	67	84
Ba	460,296	477,058	307,078	348,066	394,136	457,424	367,598	267,566	335,785
La	34,357	35,999	39,029	25,485	17,608	46,826	25,540	17,334	28,404
Pr	7,915	8,249	9,224	5,877	4,217	10,874	5,886	4,101	6,777
Nd	28,615	29,813	33,770	21,154	15,315	39,328	21,345	15,055	25,007
Tm	244	287	232	128	155	255	167	90	161
Lu	223	257	223	115	142	235	153	82	145
Ta	1,260	1,483	873	970	796	1,388	1,056	542	864
W	2,345	2,735	1,781	1,572	1,682	4,953	3,558	2,329	3,289
Pb	32,342	33,692	20,015	17,316	20,508	31,208	23,010	13,827	18,377

Supplementary Table 1.Trace element concentration of samples (ppb)

	Guthega Hill				Aerosol				
Name	Gu P2 60-67	Gu P3 0-15	Gu P3 15-30	Gu P3 30-46	D45	D46	D48	D49	D50
Lat	-36.360°,	-36.360°	-36.360°	-36.360°	-36.394°	-36.394°	-35.583°	-35.583°	-35.583°
Long	148.370°	148.366°	148.366°	148.366°	148.394°	148.394°	148.293°	148.293°	148.293°
Li	48,072	10,749	26,228	49,620	21,220	28,762	14,971	14,302	17,655
Sc	16,282	7,462	10,286	12,872	8,643	12,447	7,573	7,343	8,432
Ti	4,206,802	2,569,364	2,943,471	3,533,613	2,726,389	3,851,413	2,530,356	2,521,235	2,928,647
Cr	59,513	25,091	44,204	58,060	61,675	80,811	56,025	53,942	58,942
Co	14,025	2,907	6,384	10,228	60,794	59,935	65,279	91,238	63,116
Ni	23,177	6,326	12,632	19,322	7,077	10,724	7,446	7,566	7,654
Cu	25,664	4,621	5,931	10,122	27,011	27,398	30,132	50,902	21,809
Zn	97,681	29,949	48,722	73,082	72,117	51,152	43,167	49,396	29,928
Ga	20,099	11,715	13,958	18,112	538,275	208,885	226,308	207,234	207,434
As	1,869	1,031	948	1,150	11,286	15,553	9,336	9,114	10,309
Rb	169,868	60,090	97,756	153,408	17,942	24,726	14,842	14,489	16,389
Sr	72,923	42,470	33,498	50,670	81,612	104,803	99,234	72,693	71,465
Zr	56,093	73,052	55,381	43,035	75,000	89,276	69,193	63,176	68,662
Nb	13,986	7,857	9,625	11,316	9,446	12,933	9,901	9,491	9,879
Mo	204	219	143	156	1,811	1,336	1,959	1,995	1,301
Ag	19	42	22	13	161	126	270	105	132
Cd	44	101	24	16	565	425	6,774	392	438
In	70	38	47	76	57	67	42	41	43
Sn	6,488	3,893	4,733	7,259	5,659	6,383	5,897	4,233	4,196
Sb	85	117	77	70	4,603	1,715	3,957	2,576	2,054
Ba	524,246	336,054	365,155	512,867	342,958	412,942	297,935	276,998	292,544
La	37,678	35,551	16,909	27,022	22,702	31,102	24,000	20,537	23,376
Pr	8,861	8,286	4,020	6,571	5,336	7,494	5,484	4,841	5,314
Nd	32,752	30,303	14,939	23,964	19,739	27,858	20,318	17,871	19,778
Tm	301	123	121	166	257	310	234	220	236
Lu	265	119	121	153	240	287	217	204	221
Ta	1,309	706	871	1,034	815	1,119	770	746	820
W	8,087	1,614	1,596	3,943	2,019	2,539	1,867	1,614	1,661
Pb	31,951	19,187	14,457	22,132	35,208	32,261	28,218	23,293	21,173

Supplementary Table 1.Trace element concentration of samples (ppb)

Aerosol

Name	D51	D52	D54	D56	D57	D58	D59	D60	D61
Lat	-35.583°	-35.583°	-36.394°	-36.394°	-36.394°	-36.394°	-36.394°	-35.939°,	-35.939°,
Long	148.293°	148.293°	148.394°	148.394°	148.394°	148.394°	148.394°	148.379°	148.379°
Li	16,148	20,146	24,550	24,023	22,915	25,725	25,902	16,647	19,625
Sc	8,327	9,400	9,963	10,320	9,899	10,430	11,091	7,923	8,303
Ti	2,919,464	3,553,413	3,182,577	3,608,288	3,411,925	3,891,116	3,759,119	2,603,875	2,695,876
Cr	59,590	67,799	69,380	71,304	67,587	73,385	73,215	56,223	60,145
Co	70,260	84,082	55,928	70,817	55,801	75,633	111,932	74,639	71,327
Ni	7,528	8,332	8,676	8,603	8,495	8,312	9,148	7,439	8,329
Cu	25,044	22,514	23,702	24,971	23,819	28,584	28,047	43,097	33,404
Zn	40,374	36,285	34,293	39,538	30,765	40,150	41,857	48,710	44,991
Ga	229,782	157,286	271,711	157,043	171,633	184,756	198,015	439,163	725,808
As	10,195	11,750	12,986	13,046	12,192	13,412	13,943	10,007	10,588
Rb	16,207	18,680	20,645	20,740	19,382	21,322	22,165	15,908	16,832
Sr	80,046	68,518	88,428	66,658	82,882	77,753	80,803	113,709	109,410
Zr	69,233	86,354	73,382	84,689	80,979	97,358	88,494	73,551	76,789
Nb	10,017	12,152	11,039	12,167	11,551	13,422	12,078	8,962	9,446
Mo	1,405	1,224	1,372	1,301	1,187	1,659	1,248	1,611	1,649
Ag	98	90	119	123	118	94	84	160	168
Cd	655	391	361	264	285	242	271	494	679
In	42	50	55	54	51	58	56	43	50
Sn	4,604	4,515	5,252	5,167	5,022	5,462	5,540	8,541	12,058
Sb	2,121	1,893	1,558	1,560	1,399	1,575	984	2,327	3,274
Ba	308,292	332,387	358,692	336,723	319,959	361,383	337,624	285,528	324,358
La	23,487	26,002	26,159	26,119	24,816	28,543	26,277	22,319	23,923
Pr	5,491	6,184	6,287	6,219	5,993	6,696	6,381	5,273	5,654
Nd	20,332	22,859	23,380	23,086	22,313	24,670	23,848	19,543	21,281
Tm	250	292	265	280	277	328	293	235	258
Lu	229	268	247	258	254	308	278	221	236
Ta	824	1,001	949	1,037	1,010	1,179	1,024	734	772
W	1,676	1,958	2,304	2,049	2,106	2,280	2,110	1,921	2,046
Pb	25,349	23,361	26,487	25,123	24,945	25,855	25,319	26,911	33,162

Supplementary Table 1.Trace element concentration of samples (ppb)

Aerosol

Name	D62	D63	D64	D66	D67	D69	D71	D73	D74
Lat	-35.939°,	-35.939°,	-35.939°,	-35.939°,	-36.394°	-36.394°	-36.394°	-35.939°,	-35.583°
Long	148.379°	148.379°	148.379°	148.379°	148.394°	148.394°	148.394°	148.379°	148.293°
Li	20,431	19,510	17,377	12,963	30,010	20,528	25,616	21,763	18,698
Sc	9,231	8,384	7,003	7,690	12,967	9,276	12,898	9,566	11,886
Ti	3,133,475	2,788,462	2,441,131	3,113,711	4,088,547	3,137,537	4,207,921	3,534,930	5,039,229
Cr	64,658	60,474	52,266	43,432	86,850	62,110	84,557	68,379	80,316
Co	159,060	97,168	52,623	93,082	606,685	92,653	250,675	96,826	64,950
Ni	8,803	8,556	6,482	6,597	21,654	7,733	12,498	8,239	9,511
Cu	39,845	60,763	22,977	33,330	682,813	61,196	167,010	28,292	20,985
Zn	49,478	39,556	35,001	28,823	80,996	44,083	102,015	44,378	20,725
Ga	620,289	487,952	394,990	948,760	335,120	329,024	1,919,736	697,685	681,981
As	11,815	10,465	8,839	8,281	14,771	12,006	15,274	12,178	14,521
Rb	18,783	16,636	14,052	13,164	23,482	19,086	24,281	19,361	23,085
Sr	76,909	73,119	58,898	71,991	120,294	109,243	92,420	88,708	75,410
Zr	84,950	72,591	63,606	91,232	91,129	73,259	95,334	92,071	86,813
Nb	10,823	9,707	8,463	10,228	10,974	11,671	14,137	12,241	15,876
Mo	1,635	1,753	1,359	844	5,246	1,595	2,840	2,162	981
Ag	135	155	110	90	114	149	184	107	52
Cd	537	379	337	429	526	647	561	350	198
In	50	46	39	53	59	50	68	53	57
Sn	10,843	10,329	97,577	8,739	5,119	7,007	8,612	15,917	4,682
Sb	2,240	2,354	1,945	1,112	1,288	1,835	1,901	2,318	1,017
Ba	324,227	304,223	254,440	283,354	320,583	341,317	407,113	346,013	412,984
La	25,523	23,950	19,189	33,008	26,453	24,144	31,298	27,520	29,832
Pr	6,181	5,627	4,501	7,590	6,397	5,611	7,346	6,605	6,677
Nd	22,963	20,833	16,658	28,126	23,808	20,499	26,951	24,616	24,255
Tm	273	245	212	200	294	259	323	299	306
Lu	251	225	195	178	278	242	302	280	290
Ta	884	817	702	728	890	971	1,180	1,032	1,335
W	2,086	1,993	1,511	2,210	2,688	2,599	2,955	2,565	2,445
Pb	34,188	25,222	18,776	20,453	32,649	28,856	39,821	34,059	18,140

Supplementary Table 1.Trace element concentration of samples (ppb)

Aerosol

Name	D75	D76	D77	D79	D82	D84	D87	D88	D89
Lat	-35.583°	-35.583°	-35.939°,	-35.583°	-36.394°	-35.939°,	-35.583°	-35.583°	-35.583°
Long	148.293°	148.293°	148.379°	148.293°	148.394°	148.379°	148.293°	148.293°	148.293°
Li	18,792	5,807	18,870	18,756	17,460	13,224	28,539	13,548	16,337
Sc	9,558	2,736	7,658	9,336	7,843	6,665	10,947	6,971	7,903
Ti	3,628,289	1,112,620	2,471,693	3,443,952	4,446,032	2,308,176	3,469,530	2,377,889	2,787,069
Cr	66,111	21,896	54,641	68,214	45,984	48,151	72,311	50,854	56,256
Co	152,924	59,494	342,611	61,002	210,906	452,162	115,416	276,802	80,318
Ni	7,811	2,636	ro	8,000	9,189	16,363	10,655	6,227	7,406
Cu	24,506	27,427	92,948	22,951	184,769	656,307	39,517	22,769	24,339
Zn	41,657	27,414	104,694	39,440	372,836	140,061	36,867	46,030	38,908
Ga	141,198	224,392	1,047,628	149,286	17,345,773	889,350	152,752	235,823	233,900
As	11,699	3,487	9,857	11,611	9,534	7,237	13,012	8,604	9,842
Rb	18,598	5,544	15,671	18,459	15,156	11,506	20,686	13,678	15,646
Sr	73,535	55,510	84,240	71,644	81,261	89,107	149,472	69,737	73,901
Zr	89,016	30,311	65,315	80,333	114,956	58,838	87,635	57,094	69,100
Nb	11,918	4,152	8,936	11,851	6,933	6,144	10,082	8,754	9,814
Mo	1,132	1,235	2,907	1,652	6,152	3,890	1,212	1,877	1,376
Ag	78	91	200	102	839	701	89	134	105
Cd	238	415	645	515	787	1,170	609	662	1,164
In	48	16	45	48	72	37	54	40	48
Sn	4,215	2,281	47,955	6,134	14,112	13,041	5,391	7,556	8,267
Sb	1,558	1,369	3,669	2,669	5,934	2,310	1,554	3,014	3,881
Ba	308,214	113,894	301,400	331,551	379,626	209,491	282,053	288,977	295,507
La	24,983	7,671	21,244	25,030	25,956	12,532	26,789	19,405	21,832
Pr	5,945	1,733	4,905	5,854	4,472	2,922	6,648	4,373	5,139
Nd	22,253	6,459	18,086	21,691	15,945	10,926	25,201	16,144	19,156
Tm	285	86	214	266	182	142	308	213	244
Lu	270	81	198	246	168	136	287	197	223
Ta	961	325	737	955	543	445	777	688	795
W	1,738	898	2,228	1,841	2,302	1,694	1,356	1,674	1,503
Pb	19,694	8,744	45,751	25,498	213,795	33,105	27,383	17,980	42,909

Supplementary Table 1.Trace element concentration of samples (ppb)

Aerosol

Name	D90	D91	D93	D95	D96	D98	D99	D100	D101
Lat	-35.939°,	-35.583°	-35.583°	-36.394°	-36.394°	-35.583°	-35.583°	-35.583°	-35.583°
Long	148.379°	148.293°	148.293°	148.394°	148.394°	148.293°	148.293°	148.293°	148.293°
Li	7,964	19,099	11,235	20,542	18,369	14,953	5,647	3,754	5,935
Sc	3,833	8,675	5,902	7,819	8,534	10,021	2,483	2,034	3,454
Ti	1,448,805	2,782,189	2,076,329	3,117,339	2,772,709	4,498,857	29,072,776	833,021	1,257,704
Cr	31,852	58,684	44,825	56,477	59,552	68,528	16,837	18,941	29,723
Co	105,600	85,340	197,266	131,650	93,094	93,796	61,717	58,861	239,814
Ni	6,687	8,929	8,479	8,567	8,267	8,451	86,716	3,059	8,488
Cu	186,717	73,902	204,722	51,515	42,369	19,265	47,370	56,494	307,199
Zn	70,084	45,220	72,176	497,582	179,179	33,132	60,218	104,153	84,589
Ga	500,411	830,969	317,889	14,155,305	1,851,321	921,514	590,609	677,265	740,544
As	4,712	10,622	7,188	9,446	10,602	12,236	2,585	2,669	4,126
Rb	7,491	16,886	11,427	15,017	16,855	19,451	4,109	4,243	6,559
Sr	115,705	112,595	93,310	72,745	81,022	73,811	63,454	32,460	75,645
Zr	44,055	96,439	53,956	185,909	71,230	74,151	638,094	26,905	38,438
Nb	6,880	9,043	8,069	6,416	7,951	14,372	4,202	4,200	6,187
Mo	2,663	1,475	3,125	5,418	1,777	1,179	2,926	2,403	3,947
Ag	273	89	147	2,748	264	66	279	209	297
Cd	1,076	256	720	431	1,469	528	2,626	2,957	2,301
In	28	44	34	47	54	56	19	17	23
Sn	5,552	15,196	4,875	10,518	4,805	6,377	13,861	8,071	6,652
Sb	4,679	1,635	3,370	3,579	2,640	1,885	4,169	6,754	6,438
Ba	185,662	283,912	212,639	354,450	267,834	384,798	143,600	131,310	164,718
La	11,417	24,339	15,734	9,416	18,189	25,718	7,016	6,215	9,987
Pr	2,399	5,835	3,560	1,939	4,261	5,721	1,351	1,218	2,089
Nd	8,951	21,820	13,164	7,741	15,886	20,740	4,963	4,505	7,634
Tm	111	260	165	135	208	257	61	62	94
Lu	103	247	155	113	196	244	58	56	88
Ta	465	721	598	561	629	1,179	259	283	413
W	2,546	3,013	1,280	-161	1,806	2,315	1,135	935	1,738
Pb	44,614	22,366	44,392	162,194	59,697	21,903	78,196	27,597	95,627

Supplementary Table 1.Trace element concentration of samples (ppb)

Aerosol

Name	D102	D104	D105
Lat	-35.583°	-35.939°,	-35.939°,
Long	148.293°	148.379°	148.379°
Li	12,175	15,064	14,441
Sc	6,063	6,892	7,683
Ti	2,147,344	2,248,507	2,609,544
Cr	42,363	49,121	55,467
Co	153,013	80,941	90,092
Ni	8,688	7,063	8,014
Cu	207,657	61,465	73,201
Zn	46,421	45,419	55,322
Ga	274,952	308,097	262,990
As	7,060	8,758	9,494
Rb	11,224	13,923	15,093
Sr	79,472	89,664	92,707
Zr	55,420	68,729	85,925
Nb	7,090	7,096	9,586
Mo	2,021	1,590	1,705
Ag	132	137	95
Cd	412	459	355
In	31	40	41
Sn	3,203	6,366	4,356
Sb	1,579	1,876	2,732
Ba	210,889	239,894	294,576
La	16,052	17,344	20,879
Pr	3,818	4,088	4,812
Nd	14,123	15,217	17,724
Tm	169	202	200
Lu	161	192	194
Ta	553	567	730
W	1,347	1,287	13,340
Pb	25,103	24,222	26,545